

London South Bank
University

**OPTIMISATION OF INTER-SEASONAL GROUND SOURCE HEAT
PUMPS WITH PREDICTIVE BEHAVIOURAL CONTROL**

by

METKEL YEBIYO

A thesis submitted in partial fulfilment of the
requirements of London South Bank University
for the degree of Doctor of Philosophy

June 2016

The School of the Built Environment & Architecture
London South Bank University

Supervisors

Prof. Graeme Maidment, Dr Alex Paurine & Prof. Tony Day.

Abstract

In practice, heat pumps (HP) often do not perform as expected. This is due to many factors such as how well the system and the ground loop are designed, installed and subsequently maintained and how well they are operated and controlled in the field. Improving overall system design and demonstrating increased HP performance and higher reliability are core objectives for this research. Performance instability and variations in ground source heat pump (GSHP) system output has been observed previously and this indicates that detailed research is required for example (i) to identify the relationship between dynamic performance and seasonal ground temperature patterns, (ii) to address the operation, installation and control opportunities that arise from (i). This project investigates all of these issues.

This thesis focuses on the monitoring of the long-term operation of a 500 kW installed GSHP system with the aim of understanding and establishing the current trend performance characteristics of the installation. The research involved combination of experimental measurements and analysis, mathematical simulation and the development of an empirical transient model that could be generally applied.

Despite the importance of the effect of ground temperatures on performance, relatively little data has been published on the effect of disturbed underground temperature distributions. The author has therefore developed a novel mathematical model for the analysis of disturbed ground temperatures over time. The novel mathematical model developed has been used to predict the disturbed seasonal underground temperatures based on daily fluid and air temperature data and has been validated against real historical data.

It was concluded from the critical literature review that the dynamic long term performance investigation of GSHP systems using transient models is not well understood. Therefore the work described in this thesis has focused on the development of a generic empirical transient system model of a GSHP system. This model has been developed using TRNSYS 17

software. This has permitted investigation of the effects of different control strategies using a dry air cooler (DAC) for heat rejection, energy consumption of the HP, the overall performance of the system and ground temperature variations.

The main novelty and contributions to science from this work is:

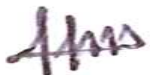
- The better understanding of the effect of ground temperature variation over time and its effect on the system's performance.
- The development of new measurement methods for assessing system performance.
- The use of ground temperature in the prediction and control of system performance, together with an analysis of the effects of specific interventions or control methodologies.
- The development of a novel mathematical model for predicting disturbed ground temperature.
- The development of a novel GSHP model using TRNSYS.
- The development and investigation of novel control strategies using DAC.

DECLARATION

I declare that the research described in this thesis is the original work of the author except where otherwise specified, or where acknowledgement is made by reference.

The work was carried out at the School of the Built Environment & Architecture, London South Bank University, under the supervision of Prof. Graeme Maidment, Dr Alex Paurine & Prof. Tony Day.

This work has not been submitted for another degree or award to any other academic or professional institution during the research program.



Metkel Yebiyo

ACKNOWLEDGEMENTS

The success and final outcome of this project required considerable amount of guidance and assistance from many people and I am extremely fortunate to have received this through the completion of my project work. I wish to express my grateful thanks to Prof. Graeme Maidment, Dr Alex Paurine & Prof. Tony Day, who have provided much valued help, guidance, encouragement and advice during this research project.

I would also like to say thanks to Dr Issa Chaer and Dr Gareth Davies for their time, support, valuable comments and suggestions in my thesis. Thanks to all my colleagues from T615 for making the office a nice environment where smiles never lack.

I would like to dedicate this thesis to my Family, Saray, Ghenet, Russom, Yordanos, Mihret, Samuel, Senait, Filmon, Aman, Thomas, Nebay, Basgana and last but not least my wife to be Solena, for their patience, infinite support and comprehension.

Thank you all for your POSITIVE SPIRIT.

The research was financially sponsored by UK Energy Research Centre (UKERC) and Engineering and Physical Sciences Research Council (EPSRC); their sponsorship is gratefully acknowledged.

Contents

Abstract.....	i
DECLARATION	iii
ACKNOWLEDGEMENTS	iv
Chapter 1	1
Introduction.....	1
Chapter 2.....	4
Critical Literature Review.....	4
2.1 Introduction.....	4
2.1.1 Sources Searched For Relevant Literature	5
2.2 Why Ground Source Heating and Cooling	6
2.3 The Heat Pump Market	7
2.3.1 Heat Pumps in the UK	8
2.4 GSHP Systems and Technology	9
2.4.1 The GSHP System	10
2.4.2 The Ground Source Circuit	10
2.4.3 The Heat Pump	13
2.4.4 The Primary Circuit	15
2.4.5 The Dry Air Cooler – DAC.....	15
2.5 Current Carbon and Energy Savings from Heat Pumps.....	16
2.5.1 Performance Metrics	16
2.5.2 CO ₂ and Energy Savings of GSHP	17
2.5.3 Methods for calculating CO ₂ saving	19
2.6 Heat Pump Performance	20

2.6.1 Projected HP Performance	20
2.6.2 HP Performance in Practice	20
2.7 Factors Affecting COP.....	23
2.7.1 Variation in Delivery Temperature	24
2.7.2 Variation in Heat Sink Temperature	25
2.7.2.1 Soil Type and Thermal Properties.....	26
2.7.2.2 Groundwater	27
2.7.3 The Impact of Ground Temperature	28
2.8 Models for Predicting Underground Temperature Distribution and Investigating Performance of GSHP	29
2.8.1 Predicting Ground Temperature Distribution	30
2.8.2 Models for Investigating Performance of a GSHP	33
2.9 Control Strategies of GSHP Systems.....	35
2.10 Conclusions.....	38
Chapter 3.....	40
Proposition	40
Chapter 4.....	42
CEREB Life Laboratory Experiment.....	42
4.1 Introduction.....	42
4.2 Description of K2 and CEREB	43
4.3 Design and Construction of K2 Building.....	44
4.4 Description of GSHP System.....	46
4.4.1 Heat Pumps	47
4.4.2 Energy Piles	48
4.4.3 Dry Air Cooler	49
4.4.4 Circulating Pumps.....	50
4.5 Current Control Strategies	52
4.5.1 GSHP System Control of Cooling Mode.....	52
4.5.2 GSHP System Control of Heating Mode.....	52

4.5.3 GSHP System Dead band Mode	53
4.5.4 Heat Pump Control.....	53
4.6 Instrumentation and Monitoring System.....	54
4.6.1 Data Logging System.....	54
4.6.2 Weather Station.....	54
4.6.3 Temperature Measurement	55
4.6.4 Ground Temperature Measurement	56
4.6.5 Flow Measurement.....	56
4.6.6 Electricity Consumption Measurement.....	57
4.7 Conclusions.....	58
Chapter 5.....	59
Commissioning of Apparatus & Investigation of Initial Results	59
5.1 Introduction.....	59
5.2 Initial Results and Commissioning	60
5.2.1 Wrong Types of Heat Meter	60
5.2.2 Heating Fluid Properties	61
5.2.3 Temperature Sensors.....	62
5.3 Quantification of Identified Errors.....	64
5.3.1 Calculated Theoretical Error	64
5.3.2 Temperature Sensors Installation.....	65
5.4 Investigation of the Performance of a Typical GSHP System	67
5.4.1 Experimental Data Validation.....	67
5.4.2 System Performance Measurement.....	69
5.4.3 Ground Temperature Variation	72
5.4.4 CO ₂ Saving by the GSHP.....	74
5.5 Conclusions.....	75
Chapter 6.....	77
Development of a Mathematical Model for Predicting Underground Temperature Distribution.....	77
6.1 Introduction.....	77

6.2 Ground Temperature Prediction.....	78
6.2.1 Methods for Previous Models and Equations	79
6.2.2 Undisturbed Ground Temperature Variations with Time and Depth.....	79
6.2.3 Assumptions.....	79
6.2.4 Our Contribution.....	81
6.3 Development of Mathematical Model for Disturbed Underground.....	83
Temperature Distribution.....	83
6.3.1 Methodology and Assumptions	83
6.4 Ground Temperature Measurement	88
6.5 Model Validation	90
6.6 Optimisation Based Control Strategy	92
6.7 Conclusion	95
Chapter 7.....	96
Development of an Empirical TRNSYS Model of a GSHP System	96
7.1 Introduction.....	96
7.2 Description of the System and Its Operation	97
7.3 The Simulation Setup.....	98
7.3.1 Ground Heat Exchanger.....	99
7.3.2 Heat Pump Model	100
7.3.3 Circulation Pumps.....	101
7.3.4 Load imposed on a liquid stream	101
7.3.5 DAC.....	101
7.3.6 Tempering valve	102
7.3.7 Tee piece	102
7.4 Model Validation	102
7.4.1 Sensitivity Analysis.....	105
7.5 Investigating New Control Strategies Using DAC	106
7.5.1 Control Strategy 1	109
7.5.1.1 Effect of DAC on COP	110

7.5.1.2 Effect of DAC on Ground Temperature.....	111
7.5.1.3 Fan, Pump & Heat Pump Running Frequency of Operation.....	112
7.5.1.4 Effect of DAC on Heat Pump Energy Consumption	113
7.5.1.5 Monthly Fan Energy Consumption.....	114
7.5.1.6 Proportion of Energy Utilisation.....	115
7.5.1.7 Economics of The Control Strategy 1	116
7.5.2 Control Strategy 2	117
7.5.2.1 Effect of DAC on COP	118
7.5.2.2 Effect of DAC on Ground Temperature.....	119
7.5.2.3 Fan, Pump & Heat Pump Running Frequency of Operation.....	120
7.5.2.4 Effect of DAC on Heat Pump Energy Consumption	121
7.5.2.5 Monthly Fan Energy Consumption.....	122
7.5.2.6 Economics of The Control Strategy 2.....	123
7.6 Conclusion	125
Chapter 8.....	126
Conclusions & Scope for Further Work	126
8.1 Introduction.....	126
8.2 Conclusions from the Literature Review	126
8.3 Conclusions from the CEREB Life Laboratory Experiment	127
8.4 Conclusions from the Commissioning of Apparatus and Investigation of Initial Results	128
8.5 Conclusions from the Development of a Mathematical Model for Predicting Underground Temperature Distribution.....	129
8.6 Conclusions from the Development of an Empirical TRNSYS Model of a GSHP System	130
8.7 Scope for Further Work	131
8.7.1 Development of Theoretical Model for Estimating Seasonal Heat Energy	131
(Petrol tank/ ground charging and discharging).....	131
8.7.2 Optimisation of Ground Source Heat Pumps with Predictive Behavioural	131
Control	131
8.7.3 Control Strategy Based on DAC.....	132

8.7.4 Investigating Heat Transfer Enhancement of Energy Piles using PCM	132
8.8 Novelty and Contribution to Science	133
References.....	134
Appendix A.....	144
TRNSYS Deck File.....	144
Introduction.....	144
Appendix B	154
Experimental Uncertainty and Error Analysis	154
Introduction.....	154
B.1 Error Approximation Method	154
B.2 Experimental Error Evaluation	156
B.2.1 Systematic Errors	156
Appendix C.....	160
Experimental Against Manufacturer’s Data Validation.....	160
Introduction.....	160
Appendix D.....	170
Ground Temperature Prediction.....	170
Introduction.....	170

List of Figures

Figure 2.1 <i>Cost and CO₂ emissions comparison (UK Committee on Climate Change, 2011)</i> ..	6
Figure 2.2 <i>Greenhouse gas emissions saved by 2013 heat pump stock, by country</i>	7
Figure 2.3 <i>Heat pumps sales in Europe from year 2005 - 2013</i>	8
Figure 2.4 <i>Projected domestic HP installation (Ecuity Consulting LLP, 2012)</i>	9
Figure 2.5 <i>Major Components of a GSHP System</i>	10
Figure 2.6 <i>Main types of GSHP (Geothermal International, 2013)</i>	11
Figure 2.7 <i>Representation of a heat pump vapour compression cycle</i>	14
Figure 2.8 <i>Vapour compression cycle on pressure–enthalpy chart</i>	15
Figure 2.9 <i>System boundaries for calculations of SPF (Nordman, 2012)</i>	17
Figure 2.10 <i>Carbon emissions from gas and HP heating systems, UK, 2008</i>	18
Figure 2.11 <i>Results of EST HP field trial phase 1 (Energy Saving Trust, 2010)</i>	21
Figure 2.12 <i>Results of EST HP field trial Phase 2 (Energy Saving Trust, 2013)</i>	22
Figure 2.13 <i>Maximum theoretical COP with temperature difference between load and source</i>	25
Figure 2.14 <i>Mean daily outdoor air temperature in the UK</i>	29
Figure 2.15 <i>Temperature around an energy pile utilised for heating or cooling</i>	31
Figure 4.1 <i>K2 building with its thermopile foundation</i>	43
Figure 4.2 <i>Concept layout of the GSHP System</i>	46
Figure 4.3 <i>Four WaterFurnace EKW130 HPs installed at K2</i>	47
Figure 4.4 (a) <i>3D visualization of the thermopile arrays and (b) Top View of the thermopile cage before being filled with concrete</i>	48
Figure 4.5 <i>Dry Air Cooler AlfaBlue BDDT902D</i>	49

Figure 4.6 Detailed Schematic of the GSHP System.....	51
Figure 4.7 Diagram of the control mechanisms of GSHP in cooling and heating modes.....	53
Figure 4.8 Schematic layout of the GSHP System with the location of sensors	55
Figure 4.9 Krohne OPTIFLUX 4100 Electromagnetic Flowmeter	57
Figure 4.10 Aidon 6000-series electricity meter.....	57
Figure 5.1 Comparison of load and source side heat energy	60
Figure 5.2 Old and new types of heat meters used at K2.....	61
Figure 5.3 Inserted and strapped temperature sensors	63
Figure 5.4 A photographic image of short thermocouple pocket.....	63
Figure 5.5 Temperature measurement at different points of pipe.....	66
Figure 5.6 Errors due to incorrectly installed temperature probes compared to fully inserted	67
Figure 5.7 Manufacturer and experimental COP correlation for heating	68
Figure 5.8 Relationship of HP heat output to external weather conditions	68
Figure 5.9 Daily building heat load profile	69
Figure 5.10 Daily heating COP	70
Figure 5.11 Daily cooling COP	70
Figure 5.12 Vapour compression cycle on pressure–enthalpy chart.....	71
Figure 5.13 Daily electricity use by HPs	71
Figure 5.14 Number of running hours per day	72
Figure 5.15 Daily COP and underground temperature variation at 3m, 14m and 26m	73
Figure 5.16 Daily COP and underground temperature variation at 3m, 14m and 26m	74
Figure 6.1 Flow diagram undisturbed and disturbed ground temperature pattern	79
Figure 6.2 Undisturbed underground temperature distributions at different times	82
Figure 6.3 Depths against damping factor of the ground.....	82

Figure 6.4 <i>Physical model of the ground temperature change due to GSHP</i>	84
Figure 6.5 <i>Flowchart of the model methodology of disturbed ground temperature</i>	87
Figure 6.6 <i>Monthly predicted disturbed underground temperature distribution at 26 m</i>	88
Figure 6.7 <i>Mean daily outdoor air temperature variation in London</i>	89
Figure 6.8 <i>Seasonal ground temperature variations during HP operation</i>	89
Figure 6.9 <i>Comparison of model predicted and measured disturbed ground temperature at 26m</i>	92
Figure 6.10 <i>Control Strategy based on the ground temperature.</i>	94
Figure 7.1 <i>Schematic of the system simulated.</i>	98
Figure 7.2 <i>Schematics of the DAC simulation setup connected to GSHP system</i>	99
Figure 7.3 <i>Comparison of actual and predicted COP</i>	103
Figure 7.4 <i>Comparison of model prediction and experimental data of energy input</i>	104
Figure 7.5 <i>Comparison of model prediction and experimental data of heat output</i>	104
Figure 7.6 <i>Comparison of model prediction and experimental data of heat rejection</i>	105
Figure 7.7 <i>Flow diagram of the control strategies</i>	108
Figure 7.8 <i>Weekly control signal to the GSHP</i>	109
Figure 7.9 <i>Schematic of the GSHP system model for Control Strategy I</i>	110
Figure 7.10 <i>Average monthly system COP CSI</i>	111
Figure 7.11 <i>Monthly ground temperature variations CSI</i>	112
Figure 7.12 <i>Annual fan, pump and HP running frequency of operation CSI</i>	113
Figure 7.13 <i>Monthly HP energy consumption CSI</i>	114
Figure 7.14 <i>Monthly fan energy consumption CSI</i>	115
Figure 7.15 <i>Proportion of energy utilisation of HP, circulation pump and fan CSI</i>	115
Figure 7.16 <i>Monthly CO2 emission savings from different control strategy CSI</i>	116
Figure 7.17 <i>Monthly cost savings from different control strategy CSI</i>	117

Figure 7.18 <i>Schematics of the GSHP system model for CS2</i>	118
Figure 7.19 <i>Average monthly system COP CS2</i>	119
Figure 7.20 <i>Monthly ground temperature variations CS2</i>	120
Figure 7.21 <i>Annual fan, pump and HP running frequency of operation CS2</i>	121
Figure 7.22 <i>Monthly HP energy consumption CS2</i>	122
Figure 7.23 <i>Monthly fan energy consumption CS2</i>	122
Figure 7.24 <i>Monthly CO2 emission savings from different control strategy CS2</i>	123
Figure 7.25 <i>Monthly cost savings from different control strategy CS2</i>	124
Figure 7.26 <i>Comparisons of CS1 and CS2</i>	124
Figure B.1 <i>Thermocouple calibration test</i>	157
Figure B.2 <i>Average experimental temperature difference error</i>	158
Figure D.1 <i>Comparison of model predicted and measured underground temperature at 26 m</i>	172
Figure D.2 <i>Comparison of model predicted and measured underground temperature at 3 m</i>	172
Figure D.3 <i>Measured daily underground temperature distribution across 3 Levels</i>	173
Figure D.4 <i>Measured monthly underground temperature distribution across 3 Levels</i>	173

List of Tables

Table 2.1 <i>Variation of COP with inlet and delivery temperature</i>	24
Table 4.1 <i>Annual Energy Demands (kWh) for K2</i>	45
Table 4.2 <i>Site CO₂ Emissions (kg and tonnes) for K2</i>	45
Table 4.3 <i>Heat pump rating details</i>	47
Table 4.4 <i>DAC BDDT902D rating details</i>	49
Table 4.5 <i>Technical Data for Krohne OPTIFLUX 4000 Electromagnetic Flowmeter</i>	56
Table 5.1 <i>Properties of Propylene Glycol and Thermox FXC2</i>	64
Table 6.1 <i>Control strategies based on predicted ground temperature</i>	94
Table 7.1 <i>Summary of primary sources of uncertainties</i>	105
Table 7.2 <i>Different control strategy approaches using DAC</i>	106
Table 7.3 <i>Zone Occupancy Period</i>	107
Table 7.4 <i>List of model inputs and assumptions</i>	109
Table B.1 <i>Summary of propagated errors for the GSHP system</i>	159
Table C.1 <i>Manufacturer's Performance Data for EKW130</i>	161
Table D.1 <i>Disturbed underground temperature distribution data</i>	171
Table D.2 <i>Measured Monthly underground temperature data</i>	174

NOMENCLATURE

Symbol	Stands for	Units
A	Area	m ²
A ₀	Amplitude of the daily mean air temperatures	°C
A _z	Amplitude of the temperature wave at depth z	°C
C _p	Specific heat of water	kJ / kg K
COP	Coefficient of Performance	-
Carnot COP	Maximum Coefficient of Performance	-
CCE	Conventional CO ₂ Emission	kgCO _{2e}
CS	Carbon Saving	kgCO _{2e}
d	Damping depth	m
e	Exponential function	-
ED	Energy Demand	kW
ELT	Entering Load Temperature from building to HP	°C
EWT	Entering Water Temperature to GSHP	°C
F	Function	-
GCE	Geothermal CO ₂ Emission	kgCO _{2e}
h	Heat transfer coefficient from ground to air	W / m ² K
Δh	Change of Enthalpy	kJ / kg
H _{e/i}	Heat extracted or injected	kW
HD	Heating Demand	kW
k	Hydraulic conductivity; permeability coefficient	-
LLT	Leaving Load Temperature from HP to building	°C
LMTD	Logarithm Mean Temperature Difference	K
LN	Natural Logarithm	-
LTHW	Low Temperature Hot Water	°C
LWT	Leaving water temperature from GSHP	°C
m	Mass flow rate	l / s
m _{source}	Mass flow rate in the source side	l / s
m _{load}	Mass flow rate in the load side	l / s
n	number	-

OAT	Outside Air Temperature	°C
P	Period	days
Q_{absorbed}	The amount of heat absorbed	W
Q_{rejected}	The amount of heat rejected	W
Q_{HP}	Heat pump heat output	W
\dot{Q}	Heat transfer rate	W
\dot{Q}_0	Initial heat transfer rate	W
q	Heat flux of density	W / m ²
R_{soil}	Conduction resistance of soil per unit length	m / W
SPF	Seasonal Performance Factor	-
SDGTP	Seasonal Disturbed Ground Temperature Prediction	°C
t	Time	Sec
ΔT	Temperature difference	K
T(z, t)	Soil temperature at depth z at time t	°C
T_0	Initial Ground Temperature	°C
T_d	Predicted ground temperature	°C
T_F	Fluid Temperature	°C
T_m	Annual mean air temperature	°C
T_N	New Temperature due to Fluid Circulation	°C
T_s	Final Ground Temperature	°C
T_U	Undisturbed Ground Temperature	°C
$T_{\text{Source,in}}$	Inlet Temperature on source side	°C
$T_{\text{Source,out}}$	Outlet Temperature on source side	°C
T_{load}	Load Temperature	°C
$T_{\text{load,out}}$	Outlet Temperature on load side	°C
$T_{\text{load,in}}$	Inlet Temperature on load side	°C
V	Volumetric flow rate of water	m ³ / s
$W_{\text{backup heater}}$	Electricity input to backup heaters	W
$W_{\text{Circ pumps/fan}}$	Electricity input to circulation pumps and fans	W
W_{HP}	Heat pump electricity input	W
$W_{\text{HP heating}}$	Heat pump electricity input in heating mode	W
z	Depth	m

Greek Letters

Symbol	Stands for	Units
α	Thermal diffusivity	m^2 / day
γ	Inverse of damping depth	m^{-1}
λ	Thermal Conductivity	$\text{W} / \text{m K}$
θ	Temperature difference	K
θ_U	Undisturbed Temperature	$^{\circ}\text{C}$
θ_0	Outside Temperature	$^{\circ}\text{C}$
η	Similarity variable	-
ρ	Density	Kg / m^3
ε	Time lag	days
ω	Angular frequency	radians per second
∞	Infinity	-

Glossary of Abbreviations

Abbreviations	Stands for
AECOM	Architecture, Engineering, Consulting, Operations, and Maintenance
AHU	Air Handling Unit
ASHRAE	American Society of Heating, Refrigerating and Air-conditioning Engineering
ASHP	Air Source Heat Pump
BACNet	Building Automation and Control Networks
BMS	Building Management System
BEMS	Building Energy Management System
BRE	Building Research Establishment
BREDEM	Building Research Establishment Domestic Energy Model
BSRIA	Building Services Research and Information Association
CEREB	Centre for Efficient Renewable Energy in Buildings
CHW	Chilled Water
CDEM	Community Domestic Energy Model

DAC	Dry Air Cooler
DECC	Department of Energy & Climate Change
DEFRA	Department for Environment, Food & Rural Affairs
DHW	Domestic Hot Water
EHPA	European Heat Pump Association
ERF	Error Function
EPA	Environmental Protection Agency
EST	Energy Saving Trust
EU	European Union
GCHP	Ground Coupled Heat Pump
GEMIS	Global Emission Model for Integrated Systems
GFB	Gas Fired Boilers
GHEADS	Ground Heat Exchanger Analysis Design and Simulation
GHX	Ground Heat Exchanger
GHG	Greenhouse Gas
GIS	Geographic Information System
GSHP	Ground Source Heat Pump
GLHX	Ground Loop Heat Exchanger
GSHPA	Ground Source Heat Pump Association
HDPE	Hard Density Poly Ethylene
HEFCE	Higher Education Funding Council for England
HP	Heat Pump
HVAC	Heating, Ventilation, and Air Conditioning
HWS	Hot Water Services
HX	Heat Exchanger
IHS	Information Handling Services
IEA	International Energy Agency
IES	Integrated Environmental Solutions
ISE	Institute for Sustainable Energy
KTP	Knowledge Transfer Partnership
LCA	Life Cycle Analysis
LDA	London Development Agency
LPHW	Low Pressure Hot Water

LP	Low Pressure
LSBU	London South Bank University
MIS	Management Information System
Mt	Mega Tonnes
NERA	National Economic Research Associates
PCM	Phase Change Material
PE	Polyethylene
PID	Proportional Integral Derivative
Pt	Platinum thermometer
PV	Photovoltaic
PVC	Polyvinyl Chloride
RACHP	Refrigeration, Air Conditioning and Heat Pumps
RHI	Renewable Heat Incentive
SAP	Standard Assessment Procedure
TRNSYS	Transient System Simulation
TRT	Thermal Response Test
TRV	Thermostatic Radiator Valve
UK	United Kingdom
VGHX	Vertical Ground Heat Exchanger
WFT	Workplace Footprint Tracker

Published Papers from this Research

Yebiyo, M., Maidment, G., Paurine, A., & Day, A. (2015). A Novel Dry Air Ground Source (DAGS) System for Heating and Cooling Buildings. In *CIB Conference Nov 2015*. London: London South Bank University.

Yebiyo, M., Day, A., & Maidment, G. (2012). The Performance of Efficient and Renewable Energy in Buildings. In *April 2012, Proc.Inst. R.2011-12.7-1*. UK: The Institution of Refrigeration.

Yebiyo, M., Chaer, I., Shatha, H., Ye, Z., & Dunn, A. (2016, March 24). UK Centre for Efficient and Renewable Energy in Buildings (CEREB)- Lessons Learned After 5 Years of Running. In *9th International Conference on Thermal Engineering: Theory and Applications*. Abu Dhabi, UAE.

Yebiyo, M., Maidment, G., Paurine, A., & Day, A. (2017). Monitoring of a large scale ground source heat pump (GSHP) system. To be presented at ASHRAE winter Conference, Chicago, USA, January 2017.

Personal Awards

Won BEST PAPER AWARD for

Yebiyo, M., Maidment, G., Paurine, A., & Day, A. (2015). A Novel Dry Air Ground Source (DAGS) System for Heating and Cooling Buildings. In *CIB Conference Nov 2015*. London: London South Bank University.

Won 2013/2014 Faculty PhD Presentation Completion

Chapter 1

Introduction

Adopting new methods of reducing energy use in buildings such as utilising a range of efficient low carbon technologies has huge potential for providing environmental and economical benefits. One such technology is the GSHP which is an environmentally friendly, economical and renewable energy technology. These systems can significantly reduce energy consumption and with it carbon emissions associated with heating and cooling a building, compared with traditional systems. HPs can provide heating with lower carbon emissions, low energy bills, as well as attracting incentives.

The UK Government's "Medium Abatement" scenario of the 4th Carbon Budget projects the deployment of 0.6 million domestic HPs by 2020, rising to 2.6 million by 2025 and 6.8 million by 2030. However the current deployment is weak with around 18,480 HPs installed in the UK during year 2010 (Ecuity Consulting, 2012).

In practice, HPs often do not perform as expected and this is due to many factors such as how well the system and the ground loop is actually designed, installed and subsequently maintained, operated and controlled in the field. Improving and demonstrating increased HP performance and reliability are core objectives of the current research. Performance instability and variations in GSHP system output indicates that detailed research is required, (i) to show the relationship between dynamic performance and seasonal ground temperature patterns, (ii) to address operation, installation and control opportunities that arise from (i). This project tackles all of these issues.

Chapter 1 introduces the investigation that is the subject of this thesis. Chapter 2 provides a critical literature review evaluating the research in this area undertaken to date and showing

the need for this research to be undertaken. The reduction of CO₂ emissions resulting from the use of GSHPs in comparison to conventional commercial and domestic heating and/or cooling alternatives has been evaluated and reviewed. The chapter also reviews current HP installations and market trends around Europe and other countries. It also gives a comprehensive review of performance assessment methods, expected HP performance and how the systems perform in reality. State of the art GSHP technology and theory, types of GSHP systems and the different parameters affecting performance of GSHP system are discussed. On-going efforts by the HP industry undertaken to improve and further demonstrate the performance and reliability of HPs are investigated. It also describes a range of different models used for investigating performance of GSHPs, interaction and prediction of ground temperature variation as well as control strategies based on seasonal and daily underground temperature variations.

Chapter 3 provides the proposition for the main area of work to be carried out in the study and Chapter 4, describes the experimental facilities used for the study. Some of the special design features for promoting energy efficiency and reducing carbon emissions for the specific building are also discussed. A detailed description of the GSHP system installed, the major components of the system i.e. heat pumps, energy piles, dry air cooler (DAC) and associated services are given. In addition the control strategy used for the GSHP system and its instrumentation and monitoring systems are also discussed.

Chapter 5 describes the commissioning of the facilities used in the study and investigation of initial results. It describes a range of installation challenges relating to the flow meters, temperature sensors and calculator units. In addition, Chapter 5 describes the process taken to overcome the difficulties and quantifies the associated errors. Also it presents an in depth analysis and evaluation of the monitored performance data in comparison with manufacturer's data. Subsequently, the reasons for differences between the expected HP performance and the actual system performance have been identified.

Chapter 6 discusses and describes the development and derivation of a generic temperature model for estimating the annual variation of the daily average undisturbed ground temperature at different depths including the effect of geothermal heat at depths beyond 100 m deep. It also presents the development of a new model for predicting the seasonal

disturbed underground temperature variation resulting from the operation of the GSHP system, as it extracts and dissipates heat into the ground. The model utilized easily accessible data such as the annual daily average air temperatures and fluid temperature to predict seasonal underground temperatures in relation to depth and the time of year. In addition Chapter 6 provides validation of the mathematical model using long term historical underground temperature data obtained from the experimental apparatus. It introduces a concept of a new optimisation control strategy based on the seasonal ground temperature variation.

Chapters 7, describes the development of a GSHP TRNSYS model. A model has been developed in order to simulate the experimental system facility using the TRNSYS 17 simulation software. This chapter also provides validation of the TRNSYS model using historical data obtained from the LSBU experimental facility. This TRNSYS model has been used to investigate control algorithms that use a DAC to identify the most appropriate control strategies to enhance the operation and efficiency of the overall GSHP system. In addition Chapter 7 describes the investigation and development of new control strategies using the DAC. It includes an investigation of the effect of using the DAC on: (i) heat rejection, (ii) energy input to the GSHP system, (iii) fan and circulation pumps, (iv) COP and (v) finally the ground temperature.

Chapter 8 draws together conclusions from the research. The conclusions from literature review, experimental work and mathematical modelling are presented. Finally, the chapter suggests further work that could be carried out using the work described in this thesis.

Chapter 2

Critical Literature Review

2.1 Introduction

Ground source heat pump (GSHP) systems have significant potential to provide low carbon heating and cooling and produce significant emission reductions. Unfortunately often GSHP systems are prohibitively expensive in terms of capital expenditure mainly due to the cost of harnessing the energy from the ground. This literature focusses specifically on low cost GSHPs using the energy piles. These piles which are concrete foundations for supporting the building incorporate a low cost heat exchanging configuration for accessing ground energy. GSHP technology incorporating energy piles as relatively new technology in the UK and are undergoing extensive research and this is the subject of this thesis.

The literature review begins by looking at the drivers for low carbon heating and cooling strategies. It describes current HP installations and market trends around Europe and other countries. In addition this chapter gives a description of the technological background of state of the art energy piles, theory, energy pile materials and types of systems. The Chapter gives a comprehensive review of performance assessment methods, and the reduction of CO₂ emissions resulting from the use of GSHPs in comparison to conventional commercial and domestic heating and/or cooling alternatives.

In theory, GSHP can work efficiently if properly designed. However, in practice the performance of these systems is dependent on a range of different parameters and issues such as how well the system and the ground loop is designed, installed, maintained, operated and controlled. There has been very little published data on the performance of installed HPs in the UK until recently. Expected HP performance and how the systems perform in reality have also been reviewed. On-going efforts undertaken by the HP industry to improve and further

demonstrate the performance and reliability of HPs are investigated. It identified how GSHPs perform in practice using a range of recently published monitored system data.

Identifying and understanding the relevant dynamics of ground temperature variation, climate conditions, site history, complex ground thermal properties, have a big effect on the performance of the energy piles and the GSHP system. The different components and parameters affecting the performance of the system are investigated. Also a range of different models used for (i) investigating and maximising performance of GSHPs, (ii) interaction and prediction of ground temperature variation as well as (iii) control strategies based on seasonal or daily underground temperature are described.

2.1.1 Sources Searched For Relevant Literature

Sources searched for relevant literature are listed below.

- ASHRAE
- BSRIA
- IHS
- London South Bank University Library including the use of inter-Library loans
- SCOPUS Research Database

These sources have been searched with the following keywords:- Energy Piles, Multi-dimensional heat transfer, Control strategy of GSHP, Energy Storage, GSHP CO₂ savings, GSHP Market, Optimisation of GSHP, Renewable Heat Incentives (RHI), Underground temperature distribution, Cooling, Geothermal.

To allow ease of cross reference, each paper was categorised in one of the following subject areas as listed below:

Fractional Uncertainty	Optimisation of GSHP	GSHP Market
Modelling	Performance Analysis of GSHP	Energy storage
Building Control Strategy	3D multidimensional	RHI
Energy Meters	Underground Temperature Distribution	GSHP
Energy Piles	Seasonal Temperature Variation	TRNSYS
GSHP CO₂ Savings	Underground Temperature Prediction	Heat transfer

2.2 Why Ground Source Heating and Cooling

It is widely accepted that the climate change is predominantly due to the emissions of greenhouse gases (GHG), 75 % of which are CO₂ (Pachauri and Reisinger, 2007). In the UK, 47 % of CO₂ emissions are due to the production of heat with a significant contributor to the total emissions from heat generation in the domestic sector (Karl, 2008; UK Office of Climate Change, 2007). One method of reducing CO₂ emissions is to make greater use of renewable energy technologies, both in the production of electricity and heat. As part of its contribution to the EU 2020 renewables targets, the UK is aiming for 12 % of its heat to be generated from renewable energy sources (UK HM Government, 2009), with 22 % of this being contributed by the domestic sector. Studies conducted to support the Government's analysis estimated that by 2020, 7.1 % i.e (4.7 TWh per annum) of domestic renewable heat could be delivered by HPs of which 4.7 % from ASHP and 2.4 % from GSHP (DECC, 2009). A report published in 2011 extrapolated models to 2030 and predicted that HPs in the residential sector would account for 55 % – 75 % of all installations by 2030 (UK Committee on Climate Change, 2011).

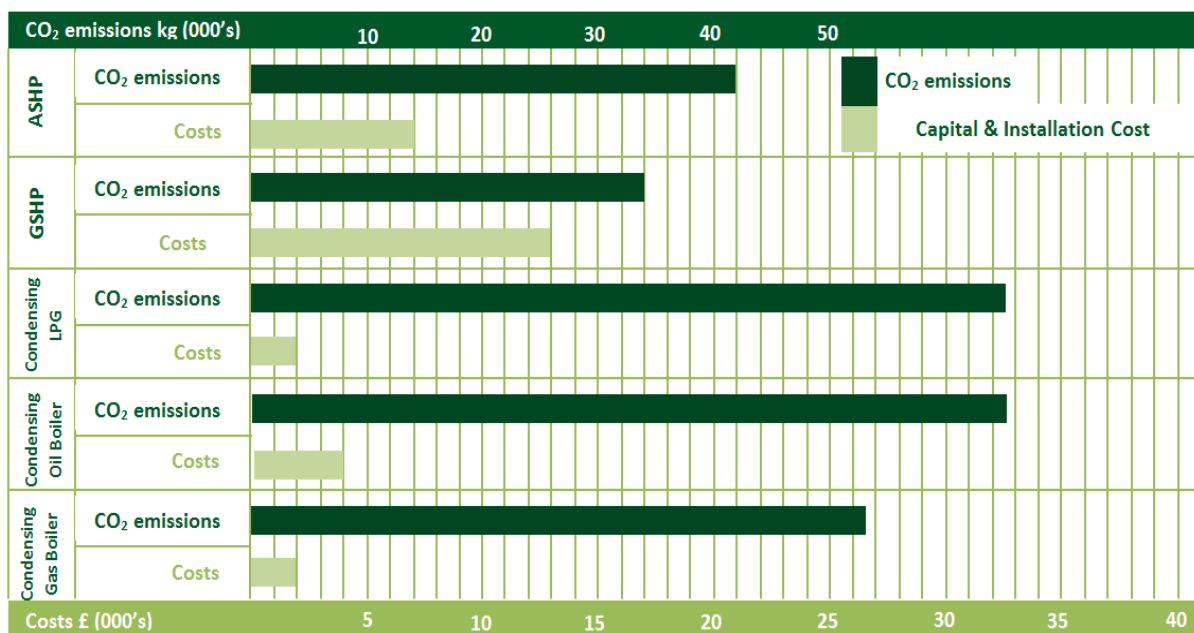


Figure 2.1 Cost and CO₂ emissions comparison (UK Committee on Climate Change, 2011)

Figure 2.1 shows cost and CO₂ emissions comparisons for different heating systems. This shows that HPs are clearly a less carbon intensive method of producing heat, compared to alternative heating systems. In most countries including the UK, due to its high cost direct electrical heating is only used by a minority and the relevant comparison is likely to be with another fossil fuel usually gas or oil. Whether a HP generates carbon savings compared with

conventional alternatives depends critically on its efficiency as well as the local carbon intensity of the fuel used. This varies widely across the EU, from a low of 0.55 kgCO₂/kWh in Sweden to 0.86 kgCO₂/kWh in Greece, with the EU - 27 2006 five year rolling average of 0.39 kgCO₂/kWh (DEFRA and DECC, 2010).

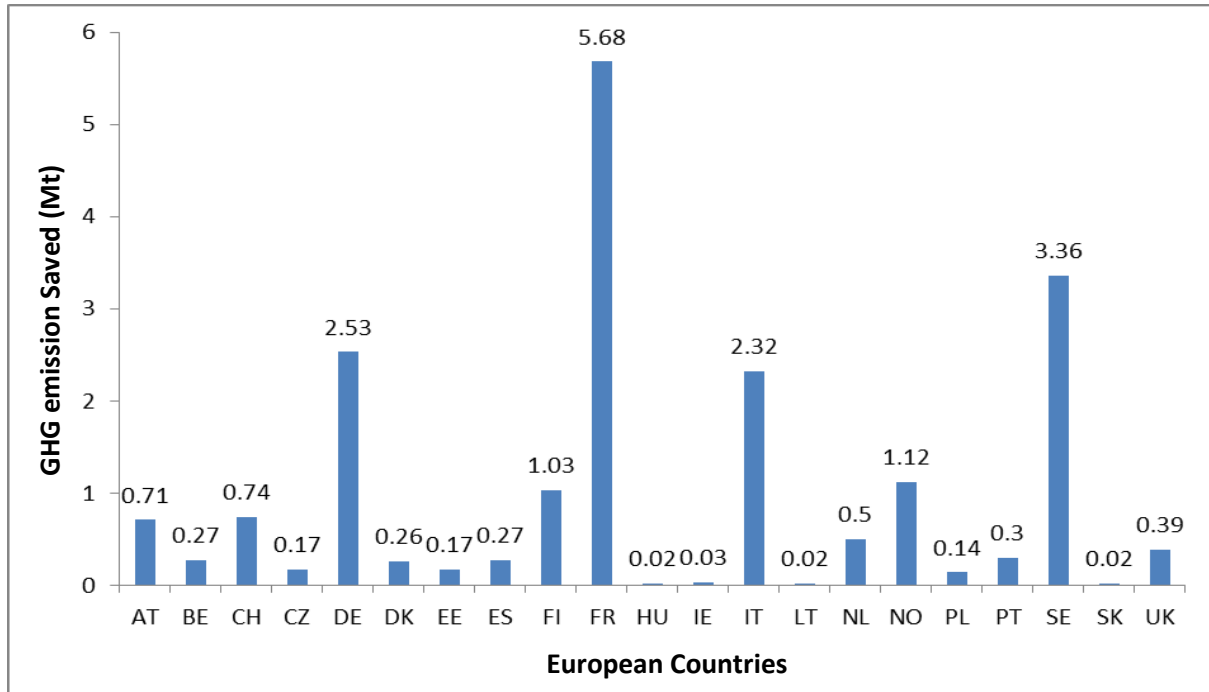


Figure 2.2 Greenhouse gas emissions saved by 2013 heat pump stock, by country

The heat pump stock in 2013 contributed to 20 Mt of GHG emission savings see Figure 2.2. Between 2005 and 2013, the European installed base of HPs produced 35 TWh of renewable energy from the air, water and the ground and is responsible for the abatement of 8 Mt of CO₂ per annum (European Heat Pump Association and Delta Energy and Environment, 2013). France produced the most renewable energy, followed by Sweden. They belong to a group of only six countries (France, Sweden, Germany, Italy, Norway and Finland) that produce 62 TWh or more than 80 % of the total renewable energy production from HP technology since 1994.

2.3 The Heat Pump Market

HP technology is not new and it has proved in many countries to be a reliable, cost effective and environmentally friendly alternative to conventional heating systems. More than 769, 879 HP systems were sold in the 21 European countries in 2013, and a total of approximately 6.7 million systems have been deployed since 2005 (European Heat Pump Association and Delta Energy and Environment, 2013) see Figure 2.3.

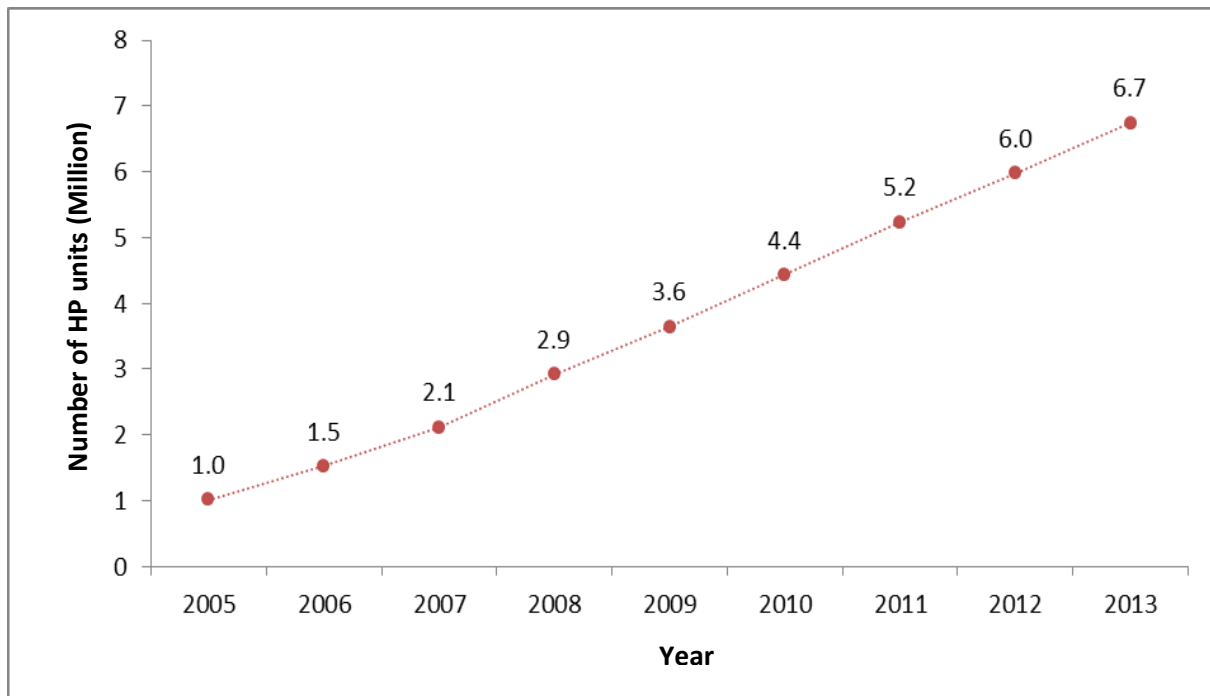


Figure 2.3 Heat pumps sales in Europe from year 2005 - 2013

Ecofys (2013) underlined that, HPs are performing well but there is still a potential for providing more benefits to the society. Looking at the above six countries with most important markets, the analysis concluded that an ambitious HP scenario would lead to a 47 % decrease of GHG emissions in the building sector compared to current levels by 2030. With the large scale carbon savings that can be achieved, significant market potential for residential HPs exists in Sweden, Switzerland and parts of Austria. In other countries the market share of HPs remain small, and the HP is not considered a first choice when installing or replacing heating and hot water equipment (IEA, 2010).

2.3.1 Heat Pumps in the UK

The IEA (2014) reported that the UK HP market grew from 2005 - 2010 but has been relatively flat since then. This dampening of the market was a result of a combination of factors including the economic downturn, and the fact that many were waiting for the introduction of the RHI which was started in 2014 but was originally planned for 2012. The total installed HP capacity in the UK is expected to rise from its 2012 level of 9.14 - 9.24 MWth, to approximately 5.4 - 5.6 GWth by 2020. Growth will be driven by, the commencement of the RHI, the tightening of building regulations, the engagement of utilities in the HP market, the emergence of more new competitive products in the UK market, and continued stable growth in the social housing and self-build sectors. The HP market in the

UK is currently dominated by air-to-water HPs, underpinned by a small base of ground source installations. It was expected that the introduction of the domestic RHI was going to revive the market from 2014 onwards and fuel a significant growth over the coming years. From 2014 onwards it was also expected to see a stronger uptake of hybrid and bivalent solutions in the on-gas sector, mainly driven by the RHI and the introduction of more competitive products from some of the major market players in the UK. The UK's climate strategy, through a series of carbon budgets and the recently published Carbon Plan, ascribes a prominent long-term role to domestic HPs. The UK Government's "Medium Abatement" scenario of the 4th Carbon Budget, projects the deployment of 0.6 million domestic HPs by 2020, rising to 2.6 million by 2025 and 6.8 million by 2030 (Ecuity Consulting LLP, 2012). These projections are shown in Figure 2.4 below.

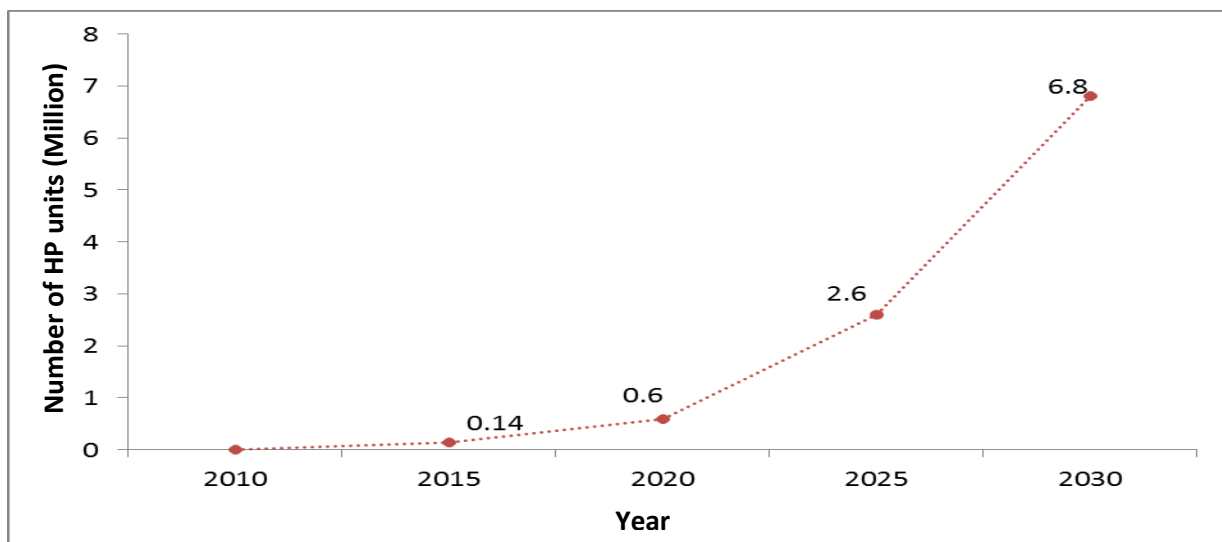


Figure 2.4 Projected domestic HP installation in UK (Ecuity Consulting LLP, 2012)

2.4 GSHP Systems and Technology

In this section, the main technology used in GSHPs and its sub-components, the different types of GSHP systems, the energy pile materials used and the absorber pipe material options are reviewed. This technology can provide cooling and heating for buildings that is independent of fossil fuels and contributes to climate protection and to the fulfilment of international obligations on emission reduction e.g. the Kyoto Protocol (Adam and Markiewicz; 2009). Furthermore, the application of GSHPs results in a positive public image for infrastructure projects because of the more efficient and innovative image of GSHP facilities. GSHP systems utilise thermal energy from within the ground as a ground energy source. Shallow ground energy is based on the principle that the subsoil can be employed as a thermal energy source by using its natural capacity for thermal storage (De Moel et al., 2010).

2.4.1 The GSHP System

As agreed conventionally by many (Brandl, 2006; Adam and Markiewicz, 2009) the system is divided into 4 major components, as shown in Figure 2.5 below.

- The ground source circuit (ground heat exchanger GHX), but not all systems are closed loop
- The heat pump
- The secondary circuit (pipework for heating/cooling of the receiving infrastructure)
- DAC

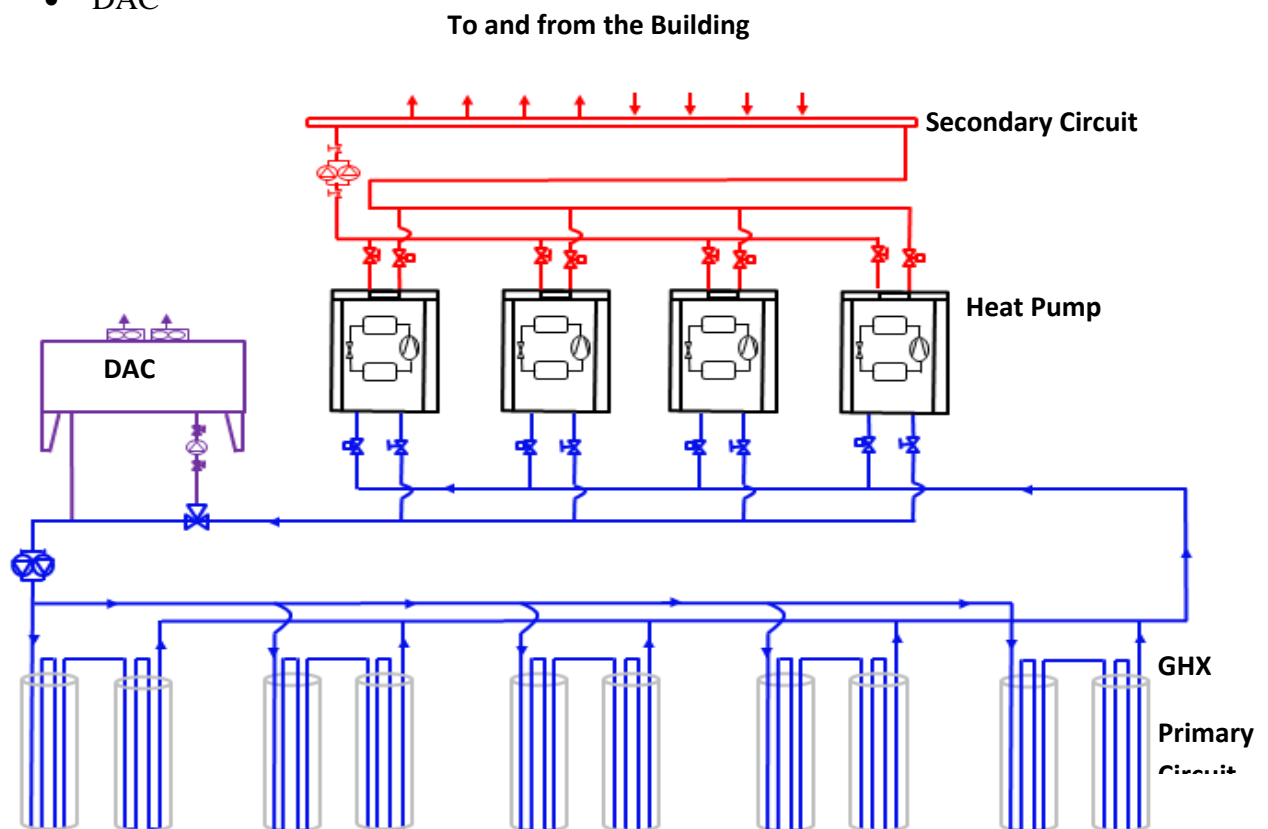


Figure 2.5 Major Components of a GSHP System.

2.4.2 The Ground Source Circuit

GSHPs can be categorised into two types, namely open-loop and closed-loop depending on the type of GHX used. In open-loop systems water is pumped from the ground to the surface, this ground water then passes through a heat exchanger, before being returned either to waste sewers or by re-injecting back into the ground at a different temperature. Sanaye and Niroomand (2009), highlighted that open-loop GSHPs have higher COP and lower initial costs than closed loop systems; however these systems require a significant water source as well as requiring a regular maintenance of water wells and equipment.

In contrast closed-loop systems are located under the ground either in horizontal, vertical or oblique configurations. This type of system does not pump ground water, instead it circulates a fluid through a loop of pipes (GHX) buried in the ground. The circulating fluid passes through a heat exchanger at the surface to extract the heat and the fluid is then re-circulated back through the buried ground loop, to absorb more heat from the surrounding soil. The vertical GHX needs the lowest heat transfer surface area and piping length due to being in contact with the soil at deeper ground levels which have a relatively constant and higher temperature for a substantial period of the year. Figure 2.6 below shows the main types of GSHP systems.

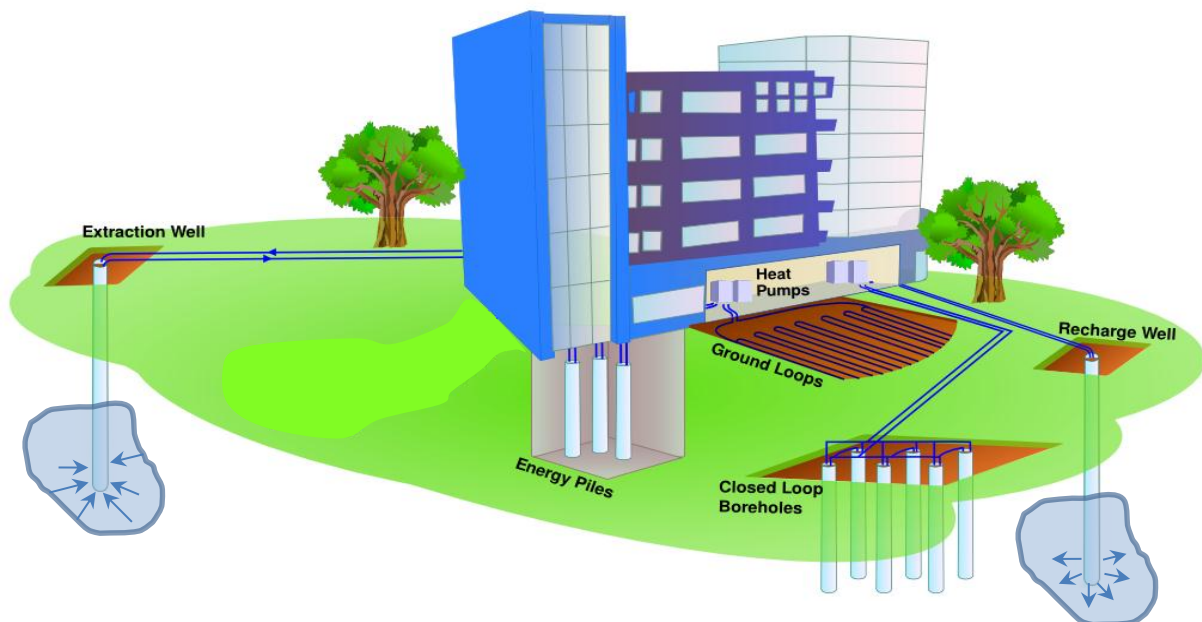


Figure 2.6 Main types of GSHP (Geothermal International, 2013)

The use of energy piles or making use of a building's foundation structure to harness the readily available heat in the shallow ground to heat or cool residential or commercial buildings was first started in the early 1980's in Austria and Switzerland (Brandl, 2006). Energy pile foundations are a closed loop GHX which contain closed coils of plastic piping through which a heat carrier fluid is pumped that exchanges energy from a building with the ground. The energy systems therefore have dual function which serves as structural building foundation and at the same time as heat exchanger.

The primary circuit contains closed pipework in contact with the ground through piles, diaphragm walls, columns and base slabs through which a heat carrier fluid is pumped and exchanges energy between the building and the ground. The heat carrier fluid is a heat transfer medium consisting of either water or water with antifreeze (glycol) or a saline solution. Glycol–water mixtures have generally proved most suitable, and also contain inhibitors to prevent corrosion in the header block, valves and HP. Once cast, the piping within the underground concrete elements are individually joined to a header or manifold block.

Pile foundations of buildings are classified into either bearing or friction type piles depending on the bearing capacity mechanism. The main materials used in the construction of bearing or friction piles that have been used to date include precast or cast in situ reinforced concrete and driven steel tube (Gao, 2008a; Brandl, 1998; Morino and Oka, 1994; Nagano, 2007).

According to Allan and Philippacopoulos (1999) grout is used to promote heat transfer between the heat exchanger and surrounding soil environment and at the same time it can be used to protect ground water. Esen and Inalli (2009) suggested that grout impact on thermal performance could be minimised by reducing the borehole diameter or by the use of clips to push the U-tube elements apart, holding them against the borehole walls.

Morino and Oka (1994) employed a 20 m deep steel pile which was used for both the building foundations and as a heat exchanger with the soil. They conducted a short experiment in the summer and winter of 1987 for around 10 days and reported experimental results for heat release and absorption when hot or cold water was circulated in the steel pile buried in the ground. A calculation type model was also developed for designing a soil heat utilization system using steel piles, and this model was verified by comparison with the experimental results obtained.

GHXs are usually composed of double U-shaped high density polyethylene (HDPE) pipes (Rawlings and Sykulski, 1999), although polyvinyl chloride (PVC) has also been trialled in the past (Tarnawski et al., 2009; Gao, 2008a; Morino and Oka, 1994; Esen and Inalli, 2009). For concrete piles, the pipes are fixed to the reinforcement cage. Prior to adding the concrete, the pipes are pressurised to prevent collapse. This pressure is maintained in order to resist the external wall pressures imposed by the wet concrete and released only when the concrete has

hardened after few days (Brandl, 2006). Their length depends on several factors including the pile depth and on performance requirements. The installed pipes adopt the form of continuous loops of particular configurations. The choice of shape will affect the overall COP of the system. Common configurations featured in several studies (Florides and Kalogirou, 2007; Gao, 2008a; Michopoulos et al., 2007) are:

- Single, double and triple U-shaped pipes and
- W-shaped pipes

Gao (2008a) highlighted a large amount of research on the GHX and the HP systems however, there are few practical examples concerning the evaluation of pile-foundation GHX and the underground field performance, especially for large-scale applications. Single U-shaped pipes were featured in Florides and Kalogirou (2007) and Hamada et al. (2007) and were regarded as the most efficient choice from an economic standpoint and in terms of workability (Hamada et al., 2007).

In Shanghai the numerical and experimental thermal performance of energy piles was investigated by adopting different U and W-shaped heat exchanger configuration and different flow rates. The study indicated that the double U-shaped heat exchanger appeared to be more thermally efficient choice from an economic standpoint and in terms of workability. Experimental testing and numerical simulation results reported by Gao (2008a) concluded that W-shaped loops were more effective than U-shaped loops, but their performance is offset by higher cost.

2.4.3 The Heat Pump

Usually, the primary and ground source circuits are connected via the HP which increases the temperature level, typically from 10 °C to 15 °C to a level between 25 °C and 35 °C. The most widely adopted type utilises the vapour compression cycle, with one or more electrically powered compressors. Gas engine driven compressor heat pumps that take advantage of additional engine waste heat are also available.

The vapour compression cycle is the most commonly used method of raising the temperature of low grade heat to a level where it can provide useful heating. Heat is put into a refrigerant fluid at the lower temperature and pressure, thus providing the latent heat to make it vaporise. The vapour is then mechanically compressed to a higher pressure and a corresponding saturation temperature at which its latent heat can be rejected so that it changes into a liquid

state giving up its latent heat as useful heat. The liquid then expands through a valve causing a drop in pressure and partial vaporisation before re-entering the evaporator for the cycle to be repeated. The cycle is shown in Figure 2.7. Heat is transferred from the working fluid during the de-superheating and condensation process and this results in a change in enthalpy between the vapour entering and the liquid leaving the condenser.

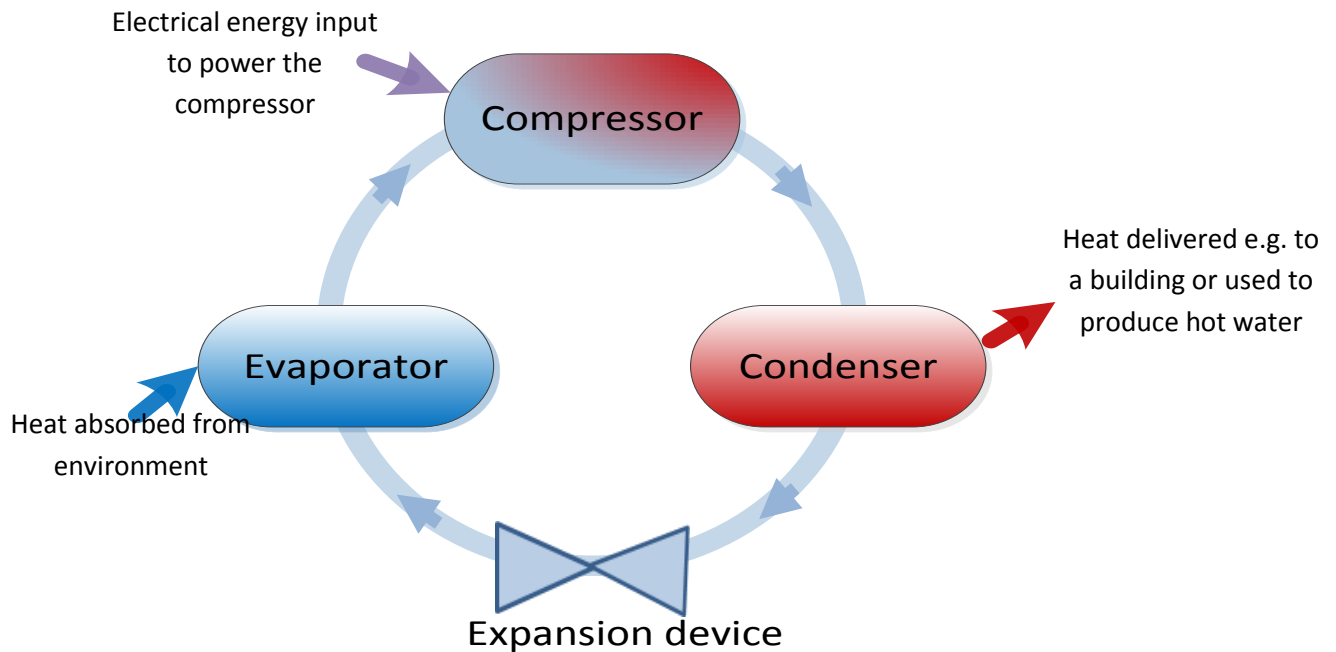


Figure 2.7 Representation of a heat pump vapour compression cycle

The corresponding pressure–enthalpy (P–h) diagram is shown in Figure 2.8. This diagram is a useful way of describing the liquid and gas phases of the refrigerant. On the vertical axis is pressure (P) and on the horizontal, enthalpy (h). The saturation curve defines the boundary of pure liquid and pure gas, or vapour. In the region marked vapour, the fluid is superheated vapour. In the region marked liquid, it is subcooled liquid. At pressures above the top of the curve, there is no distinction between liquid and vapour. Above this pressure the gas cannot be liquefied and this is called the critical pressure. In the region beneath the curve, there is a mixture of liquid and vapour.

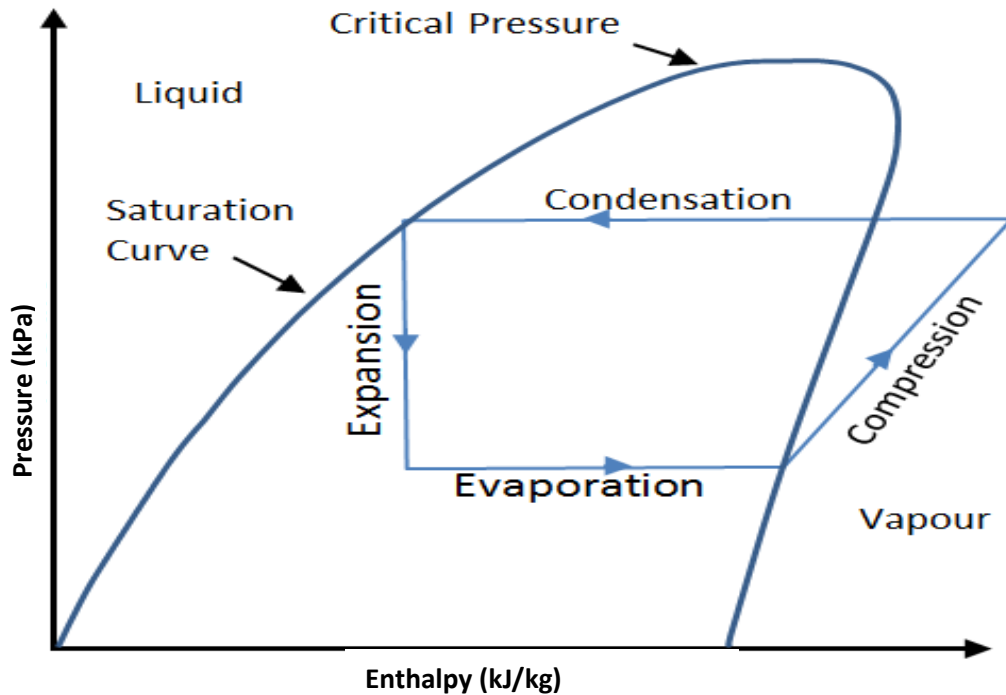


Figure 2.8 Vapour compression cycle on pressure–enthalpy chart

2.4.4 The Primary Circuit

The primary circuit is a closed fluid-based building heating or cooling network (secondary pipework) embedded in the floors and walls of the structure as shown in Figure 2.5.

2.4.5 The Dry Air Cooler – DAC

Many GSHP installations include a DAC. The conventional purpose of the DAC is to reject heat to atmosphere in adverse conditions of high ambient dry bulb temperatures. Alternatively the DAC can also be used to reject heat or cold to the ground to provide balance between heating and cooling load. The capacity of the ground to store thermal energy between heating and cooling systems can lead to a significant increase in COP, in both winter and summer operation, leading to shorter payback of capital investment and reduced CO₂ emissions. This is achieved by reducing the temperature lift in both winter and summer. It is not reported anywhere that the DAC can be used as part of an active control system to selectively reject heat or cold to the ground depending on measured weather, system and performance parameters.

2.5 Current Carbon and Energy Savings from Heat Pumps

This section describes how GSHP systems can be best applied to deliver the savings in CO₂ emissions resulting from the use of GSHPs in comparison to conventional commercial and domestic heating and/or cooling alternatives.

2.5.1 Performance Metrics

In the context of GSHPs, traditionally the most important metrics of system efficiency is the COP and seasonal performance factor (SPF) which is defined by equations 2.1 – 2.5. The COP indicates the heat output by the HP per unit input of electrical energy. Some designers often aim for COP values between 2 and 4, although Tarnawski et al. (2009) suggests closed-loop systems to generally offer COPs between 3 and 5. As stated in section 2.2, critical to the performance of a GSHP is the system COP and this directly affects the relative carbon efficiency associated with the electricity used as well as the heating fuel displaced. For systems with an additional heating system other than an electrical back up heater (e.g. oil, gas or biomass) the quantity of heat and the energy content of the fuel demand have to be determined in order to calculate the SPF in accordance to the system boundaries.

$$\text{COP} = \frac{Q_{\text{HP}}}{W_{\text{HP}}} \quad (2.1)$$

According to Nordman (2012), there are four types of SPF which are defined as:

SPF₁ includes only the HP unit itself. SPF₁ is effectively the average COP for the measured period.

$$\text{SPF}_1 = \frac{Q_{\text{HP}}}{W_{\text{HP}}} \quad (2.2)$$

SPF₂ includes the HP unit and accounts for the additional equipment needed to make the heat source available to the HP.

$$\text{SPF}_2 = \frac{Q_{\text{HP}}}{W_{\text{HP}} + W_{\text{Circ_pumps/fan}}} \quad (2.3)$$

SPF₃ includes the HP and the heat source circulation pump as in SPF₂, but also the backup heater.

$$\text{SPF}_3 = \frac{Q_{\text{HP}} + Q_{\text{backup heater}}}{W_{\text{HP}} + W_{\text{Circ_pumps/fan}} + W_{\text{backup heater}}} \quad (2.4)$$

SPF₄ includes all of the factors related to SPF₃, but also includes the work required for distribution of the heat.

$$\text{SPF}_4 = \frac{Q_{\text{HP}} + Q_{\text{backup heater}}}{W_{\text{HP}} + W_{\text{Circ pumps/fan}} + W_{\text{backup heater}} + W_{\text{Circ pumps/fan}}} \quad (2.5)$$

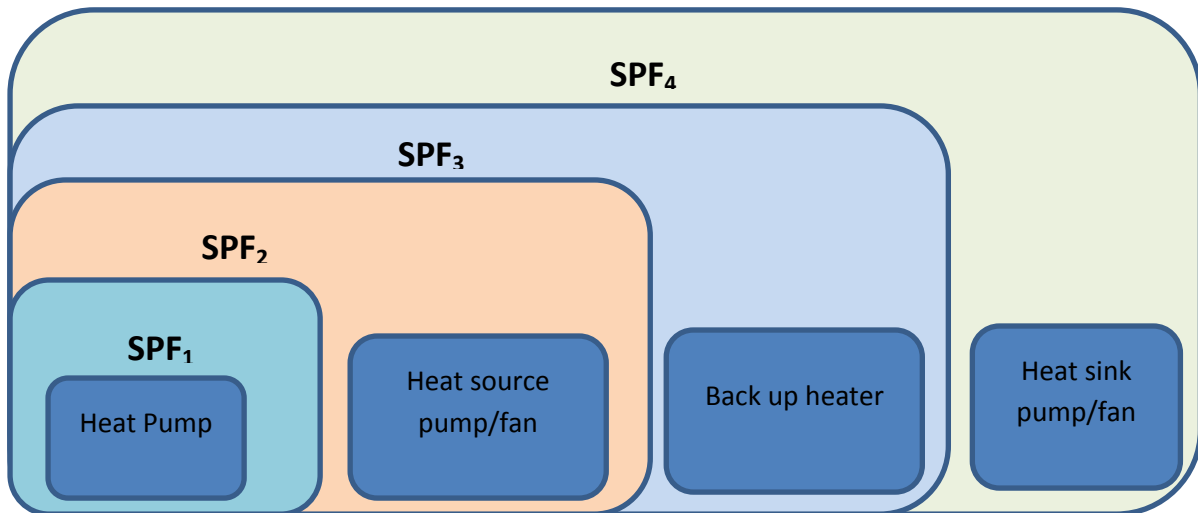


Figure 2.9 System boundaries for calculations of SPF (Nordman, 2012)

Figure 2.9 shows a summary of the system boundaries for calculating the SPF. Each individual component of the system has an effect on the overall COP value and thus consideration of the design of each individual component is important. The selection of the GSHP has a significant impact on overall system COP and consequentially the COP (Hepbasli et al., 2003; Hepbasli, 2002 and Yari, 2007).

2.5.2 CO₂ and Energy Savings of GSHP

In the UK, HPs have a higher hurdle to jump than in many other countries in order to make carbon savings compared with conventional heating alternatives. This is because the UK has higher than average carbon emissions from its electricity grid i.e. the five year rolling average figure for 2008 was 0.55 kgCO₂/kWh, and the competitor heating fuel used by more than 80 % of the population is natural gas which is the least carbon-intensive fossil fuel. Figure 2.10 shows that a HP has to achieve a COP of greater than 2.6 in order to attain lower carbon emissions than those for a new, efficient gas boiler.

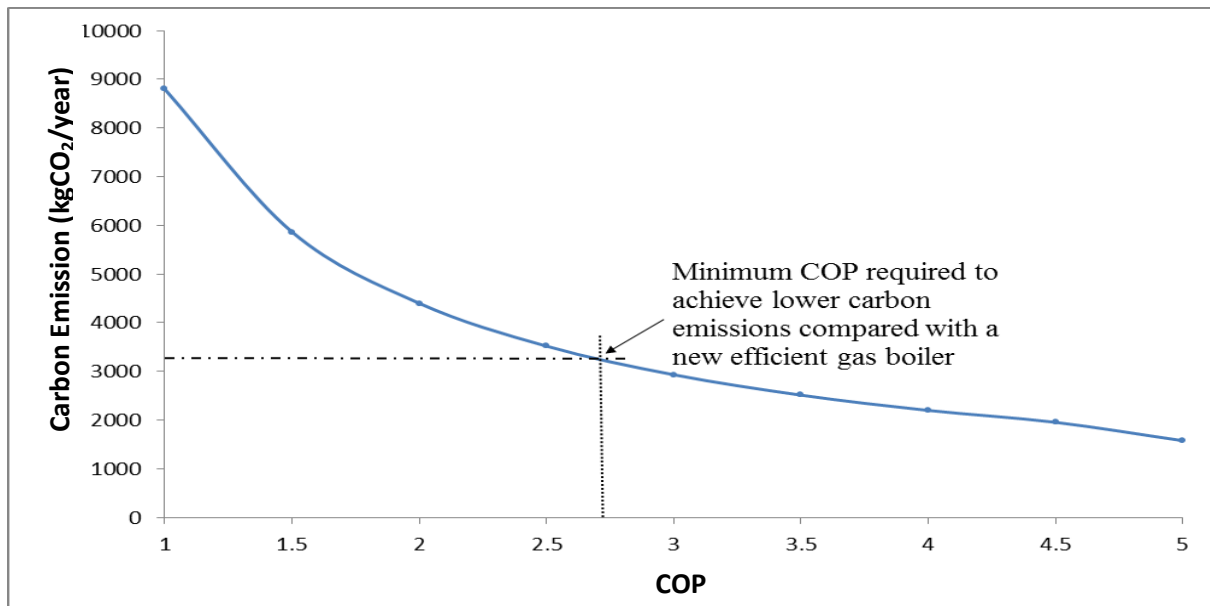


Figure 2.10 Carbon emissions from gas and HP heating systems, UK, 2008.

The calculations were based on delivering 16,000 kWh of heating and hot water energy per year (Ofgem, 2011) using current carbon intensity figures for gas and electricity (DEFRA and DECC, 2010). It was also assumed that a gas condensing boiler has a seasonal energy efficiency of 88 %. If system COP of 3.0 was achieved, a HP would save 13 % carbon emissions compared with a gas fired boiler.

Due to the generally high COP of a HP together with the utilisation of solar and ground energy stored in the subsurface, GSHP systems are capable of high COPs and therefore additional reductions in CO₂ emissions as compared with conventional heating methods such as gas-fired heating. Thus, the use of GSHP for heating and cooling of residential and commercial buildings can significantly reduce the emissions of global GHGs. A study by the US EPA (1997), demonstrated that residential fossil fuel heating systems in the US produced between 1.2 and 36 times the CO₂ emissions of GSHP systems. A European study using an average CO₂ emission factor for electricity production of 0.550 kg CO₂/kWh suggested that electrically driven HPs could save up to 45 % of CO₂ emissions compared with an oil fired boiler and up to 33 % compared with a gas fired boiler (Hohmeyer and Trittin, 2008).

2.5.3 Methods for calculating CO₂ saving

This sub section provides the methods used for calculating the potential CO₂ emissions that would result from using GSHPs as compared to the use of conventional heating methods

conventional CO₂ emission (CCE). An average of 2000 operating hours per year and a COP of 4 were assumed for the GSHP for determination of the geothermal CO₂ emissions (GCE) values, which were calculated as follows:

$$GCE \left[\frac{\text{kg}}{\text{year}} \right] = ED[\text{kW}] \times 2000 \left[\frac{\text{hours}}{\text{year}} \right] \times 0.594 \left[\frac{\text{kgCO}_2}{\text{kWh}} \right] \quad (2.6)$$

Where ED is the energy demand of the GSHP system. The calculated CO₂ emissions for a typical energy mix for conventional heating was 0.229 kgCO₂/kWh, which is approximately equal to the CO₂ equivalent for heating using only natural gas of 0.228 kgCO₂/kWh (Fritsche and Schmidt, 2007). Assuming an equivalent heating demand (HD), the conventional CO₂ emissions (CCE) were determined using the following equation.

$$CCE \left[\frac{\text{kg}}{\text{year}} \right] = HD[\text{kW}] \times 2000 \left[\frac{\text{hours}}{\text{year}} \right] \times 0.229 \left[\frac{\text{kgCO}_2}{\text{kWh}} \right] \quad (2.7)$$

Using equations 2.6 and 2.7 CO₂ savings (CS) for a GSHP per year, operated with electricity, for 2000 operating hours per year and a COP of 4, were calculated as follows:

$$CS \left[\frac{\text{kg}}{\text{year}} \right] = GCE \left[\frac{\text{kg}}{\text{year}} \right] - CCE \left[\frac{\text{kg}}{\text{year}} \right] \quad (2.8)$$

Equation (2.8) provides an appropriate average estimation of CO₂ savings as a result of using a GSHP instead of conventional heating systems. Thus using a GSHP system, CO₂ emissions savings of 35 % or 72 % respectively can be achieved depending on the supplied electricity mix for the GSHP. These results highlight the importance of the COP value, in delivering carbon savings.

2.6 Heat Pump Performance

2.6.1 Projected HP Performance

UK projections are predicted on the assumption that ASHP and GSHPs perform at COP levels of 2.5 - 2.75 and 3.15 - 3.85 respectively (UK Committee on Climate Change, 2011). These levels of performance are consistent with the assumptions in widely used domestic energy models published by BRE, e.g., BREDEM (Anderson et al., 2008). The Government's own energy performance measure of dwellings, the Standard Assessment Procedure (SAP) (UK Standard Assessment Procedure, 2005) SAP itself being a simplified BREDEM model with values of 2.50 for ASHPs and 3.20 for GSHPs.

Manufacturers tend to present more optimistic performance levels for ASHPs of up to 3.50 and up to 4.20 for GSHPs (Mitsubishi, 2013). Across all sectors (*i.e.*, residential and non-residential) a predicted total of 66 TWh of heat could be generated from renewable sources by 2020 with 18 Mt of CO₂ abated as a result (UK Committee on Climate Change, 2011). This projection gives no breakdown of the CO₂ abatement contribution from HPs, however, ASHPs are projected to contribute 40 % of the total CO₂ abatement by 2030 in the residential sector, for the “Medium Abatement Scenario” (UK Committee on Climate Change, 2011). With 85 % of heating installations currently being natural gas central heating (Department for Communities and Local Government, 2010), and given the 2030 installation levels being considered, HPs will need to displace significant amounts of gas central heating.

2.6.2 HP Performance in Practice

Until recently, there has been only limited publicly available data on the performance of HPs in the UK. In a comprehensive literature review, Singh et al. (2010), found only two studies reporting data. They concluded that very few installations have been subjected to monitoring to establish their effectiveness and running costs. However, in 2010 the EST published results on the first phase of the first comprehensive field trial of these technologies undertaken in the UK, which studied HPs at 83 sites (54 GSHP and 29 ASHP). The trial began in early 2009 and monitored both technical performance and customers’ experiences for a full 12 month period.

Monitored system COP data was presented for 47 GSHPs and 22 ASHPs, and is shown in Figure 2.11. The average system efficiency of the GSHPs was 2.3, and the average for the ASHPs was 1.9. At the most efficient end of the distribution, there were 9 GSHPs with system efficiencies of 3.0 and 3.2, and 1 ASHP with a system efficiency of 3.0. At the least efficient end, there were 9 GSHPs and 10 ASHPs with system efficiencies of less than 2.0.

These results compare badly with experiences reported in other European countries. The Fraunhofer Institute for Sustainable Energy (ISE) published a survey of HP installations in Germany. They found that ASHPs in new buildings achieved an average COP of 3.0, while those retrofitted to existing buildings had an average COP of 2.6 (Centre for Alternative Technology, 2010).

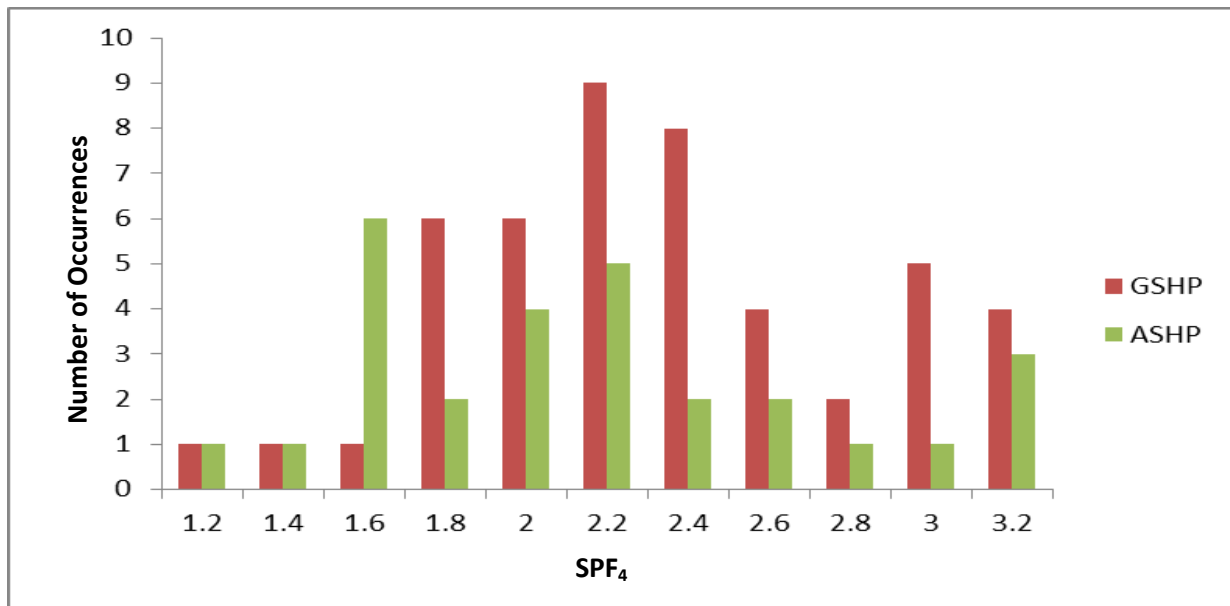


Figure 2.11 Results of EST HP field trial phase 1 (Energy Saving Trust, 2010).

EST presented the results in a positive light, for example stating that “results show that a number of HP installations performed very well, achieving an overall system COP rating of three and above”, but also noted that “some installations performed as well as HPs studied in European field trials, but many failed to meet these levels” (Energy Saving Trust, 2010). EST has used the findings to give detailed advice to customers and installers on how to ensure they achieve a high quality HP installation.

Earlier research reported that some householders experienced problems with their GSHP installations. Roy et al. (2008) carried out a survey of GSHP adopters. Their results showed that nearly 90 % of those adopting GSHP technology were very happy with their system, and that the system had raised their energy awareness in 70 % of cases, but only 40 % reported the cost savings that they expected. Key problems identified were centred around the complex controls designed to make the most efficient use of electricity and how to achieve comfortable room temperatures. Only 40 % found the controls easy to use and 20 % had great difficulty. A quarter of users complained about the slow response times of the system and/or its inability to heat rooms to the required temperature.

Phase 2 of the EST study was completed, between 2010 and 2013 (Energy Saving Trust, 2013). This included a comprehensive study of 44 HPs to investigate the variation in performance shown in phase 1. The results suggested that over-complicated system designs and poor understanding of heating controls by both installers and householders contributed to

the inadequate performance reported in phase 1. However the findings from the phase 2 study provided useful insights into the impact of a number of interventions, including how an updated installation method and improved control can improve the performance of both ASHP and GSHP systems. Figure 2.12 shows comparison of ASHP and GSHP performances for phase 2.

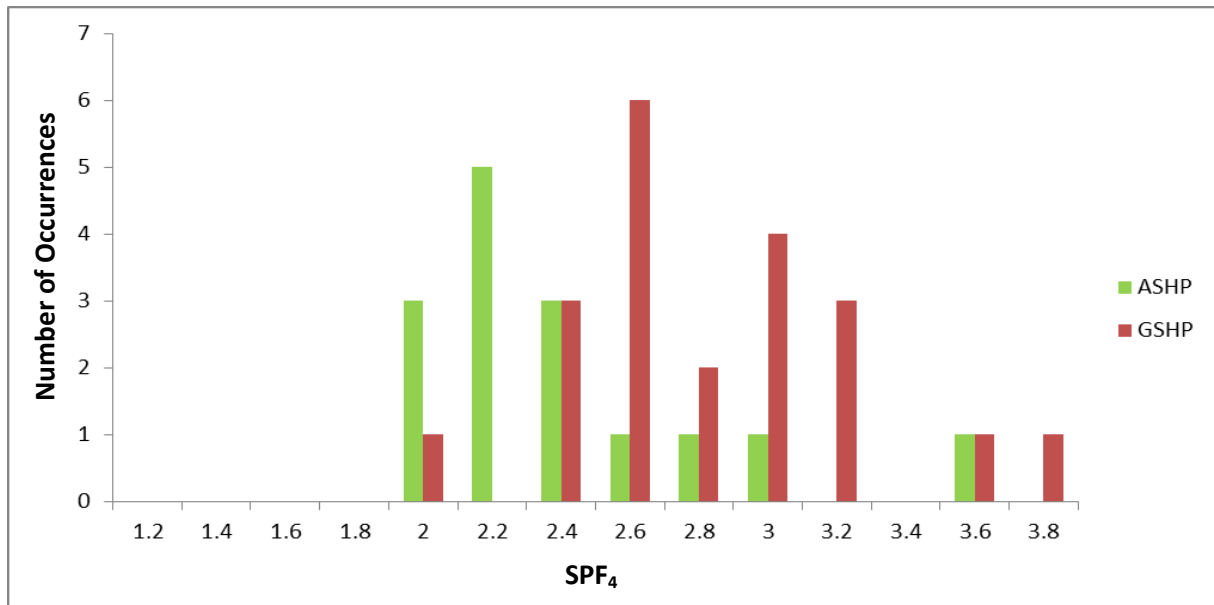


Figure 2.12 Results of EST HP field trial Phase 2 (Energy Saving Trust, 2013)

The average system COP for GSHPs was 2.82 compared to that in phase 1 where an average COP of 2.3 was found, and the average for ASHP was 2.45 compared to a phase 1 COP 1.9. A study in New Zealand by Pollard (2010), which has a similar climate to the UK, investigated the energy performance of ASHP water heaters (*i.e.* no space heating) using both real - world installations and corresponding models, and confirmed that COP can drop to as low as 1 - 1.50, for water heated to 60 °C and for an ambient temperature of 5 °C. This observation is consistent with other ASHP water heater studies e.g. Morrison et al. (2004) that compared performance with an increasing difference between ambient air temperature and water output temperature.

2.7 Factors Affecting COP

The energy performance of a GSHP system can be influenced by three primary factors:

1. The heat pump
2. The circulating pump and
3. The thermal process in the ground with its GHX.

HPs are generally characterised by the strong dependency of their COP on the primary circuit temperature (Michopoulos et al., 2007). The design and performance of the ground element of HPs depends on key parameters such as the initial ground temperature, its thermal conductivity and specific heat capacity. However the cost of obtaining site-specific thermal parameters may be substantial and can be a significant proportion of the overall capital cost for the installation (Preene and Powrie, 2009). Over a given period of time, any difference between the heat input and the heat extracted from the control volume will result in a change in the temperature of the ground, which will also depend on the specific heat capacities of the ground or rock and the heat carrier fluid. Changes in the ground temperature could cause the system to become gradually less effective over a period of several years, until it reaches a serviceability limit state in which it can no longer fulfil the function for which it was designed (Preene and Powrie, 2009; Wang and Qi, 2008).

The maximum theoretical COP of a HP in terms of the useful temperatures of the warm condenser ($T_{load,in}$) and the cool evaporator ($T_{source,in}$) is:

$$\text{Carnot COP}_{\max} = \frac{T_{load,in}}{(T_{load,in} - T_{source,in})} \quad (2.9)$$

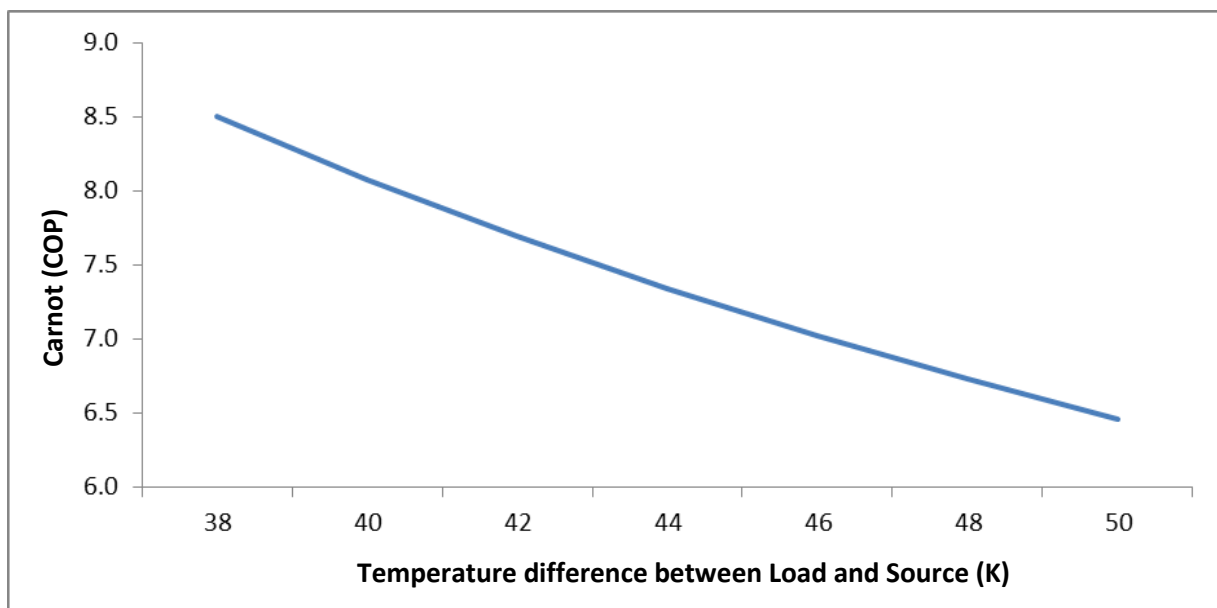
The theoretical maximum COP which can be achieved to deliver heat at 35 °C when the outside temperature is 2 °C is 9.3. However, in real life, such high efficiencies are not achieved. The COP equation 2.9 shows that a HP operates most efficiently when the temperature gap between the heat source and the heat demand is minimised (Karl, 2008), this is also illustrated in Figure 2.13 below. In practice, this means that HPs operate efficiently when lower rather than higher temperature heat is required in heating mode. The equation also shows that the higher the input heat temperature $T_{source,in}$, the higher the COP that can be achieved. A reduction in condensing temperature of 1 K or an increase in the evaporating temperature of 1 K reduces energy use by 2 % – 4 %. For an example of how these factors affect the performance of real HPs, see Table 2.1, which shows how COP varies with both input $T_{source,in}$ and output $T_{load,in}$ temperatures for 7 kW and 9.5 kW Worcester Bosch ASHPs.

Table 2.1 Variation of COP with inlet and delivery temperature.

Inlet Temperature (°C)	Delivery Temperature (°C)	HP COP	
		7 kW	9.5 kW
-7	35	2.3	2.5
2	35	3.0	3.3
7	35	3.4	3.8
7	45	2.8	3.0

2.7.1 Variation in Delivery Temperature

The temperature at which the heat is delivered is therefore very important with a lower temperature distribution producing higher COP values. In practice, this makes well insulated new build properties which can be designed with low temperature heat distribution systems more suitable for HPs than properties that currently use high temperature systems. The maximum temperature for underfloor heating is typically 50 °C and sometimes as low as 35 °C, compared with traditional UK radiator systems which use heat at 70 °C to 80 °C. Oversized radiators can use water at more moderate temperatures, say, 40 °C to 50 °C and hot water in stored systems is typically heated to 55 °C to 60 °C. A HP system will therefore work best with an underfloor heating system. The HP system design needs to balance the heat requirements of users, the COP (which can be achieved at different heat delivery temperatures) and therefore running costs, and capital costs.

**Figure 2.13** Maximum theoretical COP with temperature difference between load and source

2.7.2 Variation in Heat Sink Temperature

In the same way that the distribution temperature is important the heat sink temperature is also critical to COP and this is very much controlled by the ground source that is being used as the sink. The ground temperature and heat transfer between the GSHP systems and their surrounding environment (of soil and rock) involves a very complex collection of processes, which require a thorough understanding if efficient design is to be achieved. In practice, the system is likely to penetrate several geologic strata each exhibiting different thermal properties and ground heat potential. The ability of a vertical GHX to operate with the ground depends on local geology, hydrogeology and other conditions that impact on the feasibility and economics of the system. Furthermore, ground temperature distribution, soil moisture content and its thermal properties, ground water movement and possible freezing and thawing in the ground are some of the main factors as reported by Diao, Li and Fang (2004) that influence the performance of the GHX and therefore COP. As a result, understanding the relevant, complex ground thermal properties, site history, climate conditions, groundwater effects, spatial and temporal variations is critical for an efficient GSHP system design.

The heat sink and delivery temperatures are mainly affected by the heat transfer in the ground, soil type and thermal properties and ground water movement. Hepbasli et al. (2003), reported that the transfer of heat between the GHX and the surrounding soil is primarily by heat conduction and to a certain degree by a moisture migration. Rees et al. (2000) and Thomas and Rees (2009), explain that the transport of heat in porous ground media may be induced by several mechanisms. The three most influential mechanisms are conduction, convection and the transfer of heat due to water phase change, also known as latent heat of vaporisation. Radiation is often assumed to be negligible and excluded from formulations as its effect in sand is less than 1 % of the overall heat transfer at normal atmospheric temperatures. Brandl (2006) confirms that these are all relevant processes, and adds to this list by also including condensation, ion exchange and freezing-thawing cycles.

Most studies agree that, under normal circumstances, conduction is the most significant process to consider (Brandl, 2006; Rees, 2000; Thomas and Rees, 2009; Yari and Javani, 2007). Heat conduction is the process whereby heat is transferred from one region of the medium e.g. ground to another, without visible motion (Rees et al., 2000). In this case the heat energy is passed from molecule to molecule; Thomas and Rees (2009) explain that heat

conduction is mainly dependent on the degree of saturation of the soil. Clarke et al. (2008) report that thermal conductivity and specific heat capacity of the soil mass are also influential factors.

2.7.2.1 Soil Type and Thermal Properties

The soil type surrounding the ground heat exchanger is of paramount importance in terms of performance efficiency for a shallow GSHP system. Saturated soils will generally conduct heat at a much faster rate than unsaturated material (Rees et al., 2000). Loose dry soil traps air and is less effective for heat transfer, while damp materials have been found to exhibit the most desirable heat transfer rates (Sanaye and Niroomand, 2009). Soil, which is rich in clay or organic material (shale or coal), has low thermal conductivity and heat will travel slowly through the surrounding subsurface towards the energy piles. In contrast, a high quartz content geology (e.g. sandstone) has high thermal conductivity.

Allan and Philippacopoulos (1999) highlighted that a decrease in soil moisture content associated with heat rejection and subsequent soil shrinkage may result in loss of bonding to the pile and consequently reduce the effectiveness of the GSHP. The temperature of the ground at a given depth is not only dependent on the average ambient temperature and the annual ground temperature swing but also is greatly affected by the type of soil (Hepbasli et al., 2003).

Thermal conductivity for soil and rock varies as a function of density and moisture content. Thus knowing the soil / rock type alone is insufficient to determine the thermal conductivity, the single most important element in GHX design. In-situ conductivity testing is the most reliable method by which thermal conductivity can be measured accurately. This accurate measurement allows the designer to avoid over sizing the ground loop to cover potential variations in conductivity on any particular site. The conductivity test also provides an accurate measurement of the undisturbed ground temperature which is also important to HP design (Esen and Inalli, 2009; Jones, 2002).

The concept of the in-situ thermal conductivity testing is to drill a bore hole at the location of the proposed ground loop, install an individual loop and grout it, connect a constant heat source to the water being circulated through the loop and measure the energy input and inlet and outlet temperatures. With these values a line source equation model can be applied to the

data to determine the thermal conductivity. It is known that increasing quartz content will improve thermal conductivity of the soil (Tarnawski, 2009).

2.7.2.2 Groundwater

Groundwater flow can have a significant impact on the performance of a GHX potentially complicating the heat transfer process between the subsoil and the GHX. Diao, Li and Fang (2004) point out the process of water advection in porous medium. This may significantly alter the conductive temperature distribution, as it will result in lower temperature rises and eventually lead to a steady condition. Rates of groundwater flow can vary significantly based on specific strata types and the height of the water table. Diao, Li and Fang (2004) and Rees et al. (2000) both caution that if these ground flows are significant, an adverse effect on the system may result because of potential heat transfer, significant distances away from the structure. This is because heat transfer rates in water are at least 20 times greater than that of air (Thomas and Rees, 2009). Many soils commonly exhibit low permeability and thus groundwater flow rates are low and the process of convection in regards to groundwater is minimal (Rees et al., 2000; Thomas and Rees, 2009). Groundwater flow is generally beneficial to the thermal performance of the GHX since there is a moderating effect on fluid temperatures in both heating and cooling modes.

A variety of circumstances can lead to changes in groundwater behaviour which may affect the ongoing performance of the system. Examples include precipitation, evaporation, transpiration, vegetation changes, ground works or construction and groundwater abstraction (Rees et al., 2000). Brandl (2006) also found that the hydraulic, physicochemical and biological properties of groundwater could significantly vary and should be considered (Thomas and Rees, 2009). In the UK, the depth of the water table can vary spatially, depending on local conditions (soil profile, surface topography, cover, run off/on) and can vary seasonally, depending on climatic condition.

2.7.3 The Impact of Ground Temperature

Florides and Kalogirou (2007) suggested that the ground temperatures below 100 m of the surface and below the zone of seasonal influence are relatively constant with depth. This is due to the high thermal inertia of the soil, for example in the UK the ground temperature increases by only 1 °C – 2 °C for every 100 m depth as a result of the Earth's crust. Ground

temperature in this zone reflects the mean annual air temperature at a site, in the UK for instance $10\text{ }^{\circ}\text{C} - 14\text{ }^{\circ}\text{C}$. In the Tropics the constant ground temperature at a depth of more than 10 m – 15 m below the surface varies between $20\text{ }^{\circ}\text{C}$ and $25\text{ }^{\circ}\text{C}$ which is a useful temperature for cooling of buildings. This stable temperature means that in summer the mean outside air temperature will be higher than the ground temperature, therefore heat can be rejected to the ground, and this is illustrated by Time Zone B in Figure 2.14. Conversely in winter the ground temperature is higher than the outside air temperature therefore heat can be extracted from the ground, as illustrated in Time Zone A and C in Figure 2.14, (Preene and Powrie, 2009; Brandl, 2006; Adam and Markiewicz, 2009).

In operation stage, environmental factors can also affect the system performance. Michopoulos et al. (2007) for example explained that injecting heat into an already high temperature ground may saturate the ground resulting in a lower COP. Wang and Qi (2008) stated that the ground temperature distribution is affected by the structure and the physical properties of the ground, ground surface cover (e.g. bare ground, lawn, snow), climate interaction determined by ambient air temperature, wind, solar radiation, relative humidity and rainfall.

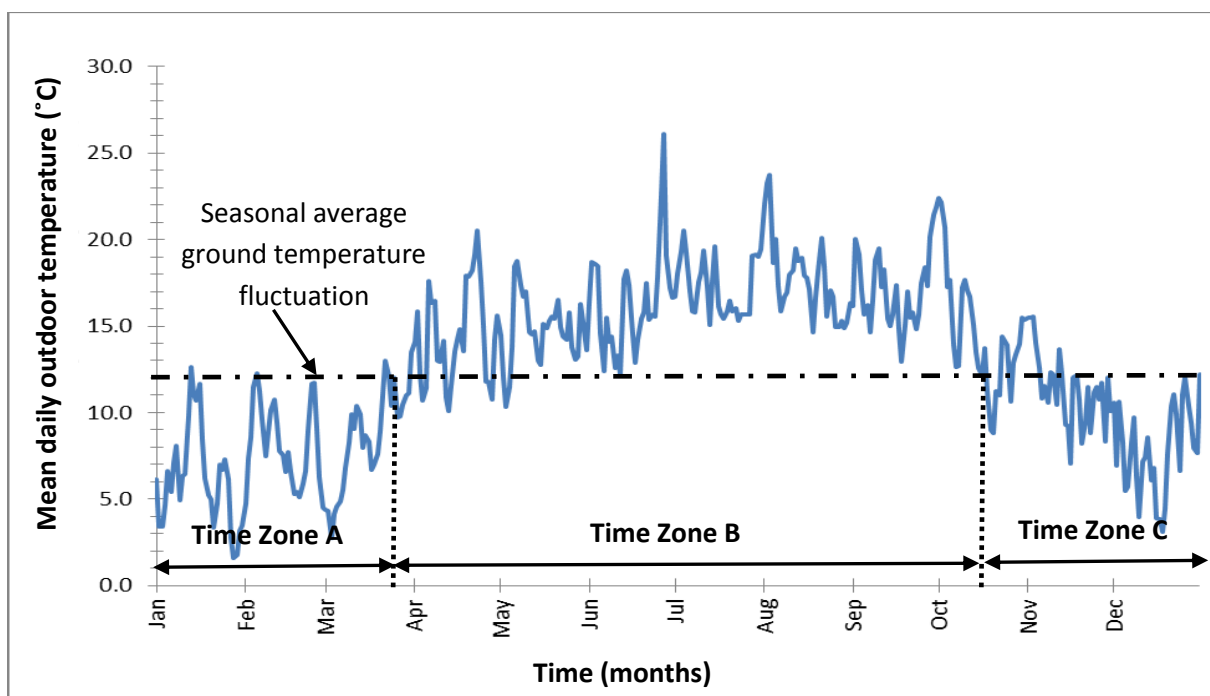


Figure 2.14 Mean daily outdoor air temperature in the UK

Popiel et al. (2001) and Wang and Qi (2008) described the temperature depth relationship using three main ground zones:

- Surface zone: Significant fluctuations in temperatures occur due to short-term ambient variations, spanning to depths of up to approximately 1 m below the ground surface.
- Shallow zone: Temperatures are less sensitive, but still influenced by seasonal changes throughout the year, ranges in depths highly dependent on soil type and saturation levels between approximately 1 m and 8 m.
- Deep zone: Temperatures in this region are stable throughout the year; depths are generally greater than about 8 m. Sanner (2001) indicates that a gradual increase in temperature beyond these depths can occur due to the Earth's core, on average, 3 K for each additional 100 m.

2.8 Models for Predicting Underground Temperature Distribution and Investigating Performance of GSHP

In this section a review of the literature on the currently available models for investigating performance of GSHP systems and simulation tools for predicting ground temperature variation yields a multitude of design approaches that range from crude rule-of-thumb approximations to detailed analytical and/or numerical techniques. Whilst rules of thumb exist in design, their use for larger scale systems is not recommended (Boennec, 2008).

2.8.1 Predicting Ground Temperature Distribution

Most models are based on cylindrical heat sources and the line source methods. Brandl (2006) developed a formula for predicting the daily or seasonal temperature variation in the ground; first this included harmonic temperature oscillation on the surface due to heat transfer between the soil and air. Secondly a time lag is needed to represent the delay between outside air and ground. This time delay depends on the depth and may even cause an anti-cyclic behaviour in the seasonal variation of the mean annual air temperature (T_m). Furthermore, the formula is based on the solution for transient heat conduction in a semi-infinite solid, where the temperature of the exposed surface is varying periodically with time. Under these conditions the soil temperature fluctuates according to the mean annual air temperature T_m , if radiation effects and ground temperature gradient are neglected. However, the amplitudes decrease with depth owing to the thermal inertia of the soil. The formula adapted has a form:

$$T(z, t) = T_m + A_z \eta e^{\frac{-z}{d}} \cos \left[\omega(t - \varepsilon) - \frac{z}{d} \right] \quad (2.10)$$

Where

$$d = \sqrt{\frac{2\alpha}{\omega}} \quad (2.11)$$

$$\eta = \frac{1}{\sqrt{1+2k+2k^2}} \quad (2.12)$$

$$\varepsilon = \arctan \frac{k}{k+1} \quad (2.13)$$

$$k = \frac{\lambda}{hd} \quad (2.14)$$

$T(z, t)$ (°C) is the ground temperature at time t and depth z .

T_m (°C) is the mean surface temperature.

ε (days) is the time lag needed for the surface ground temperature to reach T_m .

A_z (°C) is the amplitude of temperature wave at depth z .

d (m) is the damping depth.

t (s) is the period duration of temperature oscillation.

h (W / m² K) is the heat transfer coefficient from ground to air.

k is the hydraulic conductivity; permeability coefficient.

α (m² / s) is the thermal diffusivity.

ω is angular frequency of temperature oscillation

η is the amplitude factor of the surface temperature.

On the surface ($z = 0$) the solution reduces to:

$$T(0, t) = T_m + A_z \eta \cos \omega(t - \varepsilon) \quad (2.15)$$

It is evident that the amplitude of the surface temperature decreases by a factor $\eta < 1$ in relation to the air temperature and, moreover, undergoes a time lag of ε .

The undisturbed ground temperature is a critical parameter for sizing the GHX, especially for vertical boreholes. Calculation of the temperature distribution in the ground due to energy foundations is increasingly being demanded by local authorities for environmental risk assessment. This refers mainly to possible influences on adjacent ground properties and on the groundwater by the long-term operation of thermo-active deep foundations (De Moel et al., 2010). The mathematics of heat transfer in GHX are generally based on cylindrical heat source theory (Wang and Qi, 2008; Ingersoll and Plass, 1948; Bourne-Webb, 2009). Heat transfer along the GHX is described as radial and relatively constant. Many heat transfer

models are based on this particular theory, for example that used in TRNSYS (Wang and Qi, 2008). Figure 2.15 shows the temperature variation around energy piles.

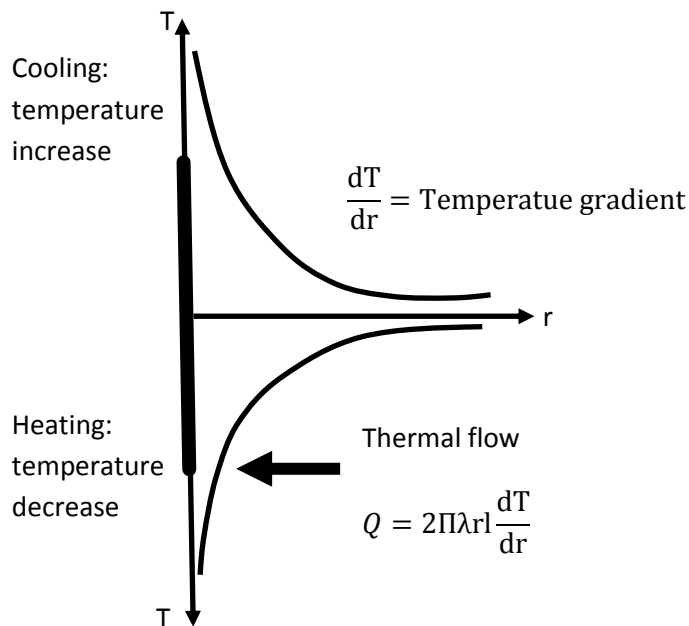


Figure 2.15 Temperature around an energy pile utilised for heating or cooling

Mohamed et al. (2014) stated that it is obvious that direct measurement gives accurate values. Often, for large buildings with relatively high cooling and heating loads, one well is drilled to perform thermal response tests (TRTs). In addition to the thermal properties of the ground (conductivity and diffusivity) and the borehole thermal resistance, the TRT gives the undisturbed ground temperature. However, this test results in an additional cost for the GSHP system. Another way to obtain the value of the undisturbed ground temperature is by using theoretical predictions based on the meteorological data and the thermal properties of the ground. Most of the design and simulation programs require monthly building loads and provide monthly average ground loop entering and exiting temperatures of the heat transfer fluid. Some models take a slightly more detailed approach by requiring the input of peak loads. This allows for the calculation of peak loop entering and exiting temperatures during a month, but determining exactly when they occur during the given month is not possible.

A good number of the analytical design approaches are based on Kelvin's line source theory or its derivations by Ingersoll et al. (1954). The line source approach approximates the ground loop borehole with the U-tube pipe as an infinitely long line with radial heat flow. The short time-step system behaviour cannot be modeled directly since the approach is exact

only for a true line source and can be applied to cylindrical heat sources with acceptable error only after several hours of system operation. The cylinder source method as developed by Carslaw and Jaeger (1947) and derivative methods such as that of Deerman and Kavanaugh (1991) are widely used and considered to be more accurate than the line source approach. In the cylinder source models, an analytical solution is developed for a region bounded internally by a cylinder of a constant radius.

Hellstrom (1989, 1991a, 1991b) developed a simulation model for vertical ground heat stores, which are densely packed GHX used for seasonal thermal energy storage. The model represents the total change in the initial ground temperature for a time step first by the spatial superposition of three parts: a so-called “global” temperature difference due to heat conduction between the bulk of the heat store volume with multiple boreholes and the far field, a temperature difference from the local solution immediately around the heat store volume, and a temperature difference from the local steady-flux part. The average ground temperature at any subsequent time is determined by decomposing the time-varying heat transfer profile into a series of individual step heat pulses and then superimposing the resulting responses in time. Hellstrom’s model is not ideal for determining long time-step system responses for GSHP systems since the geometry of the borehole field is assumed to be densely packed, with a minimum surface area to volume ratio, as is typical for heat stores.

In addition Mohamed et al. (2014) described that two of the earliest analytical models were developed by Van Wijk (1963) & Kasuda and Achenbach (1965). Both models were based on Fourier analysis of multi-year measured data. The correlation proposed by Kasuda and Achenbach (1965) is commonly used in several commercial softwares such as TRNSYS (2005) and RETScreen (2005). It gives the ground temperature as a function of the time of the year and the depth below the ground surface. Among the input data for this correlation is the annual average surface ground temperature which is not often accessible. For this reason, this parameter is often substituted by the annual average air temperature. Such a simplification appears to be rather inaccurate in the design and prediction of GSHP performance systems. By introducing a correction for the daily amplitude of the ground temperature by a sinusoidal function of time rather than a constant value, Elias et al. (2004) and Smerdon et al. (2006) have improved the model proposed by Van Wijk (1963).

2.8.2 Models for Investigating Performance of a GSHP

GSHP systems use the ground whose temperature is not heavily dependent on the outside temperature. Ground temperature can, however, increase or decrease over long periods of time because of the energy imbalance between the building's heating and cooling loads that can degrade the GSHP COP. The long-term thermal performance of a GSHP system can be investigated using multi-year integrated computer simulations that can analyse both the HP and the GHX.

A number of simulation tools that can carry out integrated computer simulations are available. The most widespread are EnergyPlus (2013) and TRNSYS (2005), and both can simulate several HVAC systems. EnergyPlus uses long and short-time g-functions to handle simulations of borehole GHX. TRNSYS software includes three main models to simulate borehole GHX. The first, an approach proposed by Hellstrom (1989, 1991a, 1991b) (Type 557), considers axial heat conduction but ignores borehole thermal capacitance. The second one, proposed by Huber and Wetter (1997) for double U-tube GHX (Type 451), does not include axial heat conduction. The last one implements the long-time g-functions method developed by Eskilson (1987) (Type 281) but does not consider the contribution of the borehole thermal capacitance. None of the approaches takes into consideration heat transfer via convection and radiation along the ground surface.

Thornton et al. (1997) used Hellstrom's approach as part of a detailed component-based simulation model of a GSHP system. The model was implemented in TRNSYS (Klein, 1996). It was calibrated to monitored data from a family housing unit by adjusting input parameters such as the far-field temperature and the soil thermal properties. When calibrated, the model was able to accurately match measured entering water temperatures.

Parisch et al. (2015) used the three models included in TRNSYS software to compare measurements and numerical simulations over a short time period using a commercial finite element software considering a common U-tube borehole heat exchanger; according to their study, the simulation results underestimated the injected heat load by 50 % when the borehole thermal capacitance was not modelled. Montagud et al. (2013) used TRNSYS to analyse an entire GSHP system consisting of six vertical boreholes containing a single U-tube and compared simulation results with experimental measurements for one day in the cooling mode of a reversible water-to-water HP with nominal heating and cooling capacities equal to

18 kW and 14 kW, respectively. Wu et al. (2014) used TRNSYS (Type 557) to investigate the effect of borehole free cooling of ground source absorption heat pumps in three cities in China; the results of their simulations showed that additional cooling reduced the deterioration of the system's energy performance caused by the thermal imbalance of the building load profiles.

Tarnawski et al. (2009) applied energy analysis, considering the various components of energy consumption in GSHP system within an energy balance equation, which was applied to three years' worth of monitoring data in Japan. Energy analysis is also taken into consideration by the computer software package "GHX Analysis, Design and Simulation" (GHEADS), which provides outputs of the daily average COP, energy consumption, ground temperature distributions and volumetric soil moisture concentration near to the GHX based on meteorological data, house heating requirements and cooling load data inputs (Tarnawski et al., 2009). This was not the first model of its kind, as a report by the same author from more than a decade previously, considered a model that coupled surface and subsurface climatology with ground-source GHX operation (Tarnawski and Leong, 1993). There is still, however, an important need for existing models to be refined or coupled with other algorithms to obtain better accuracy. Sanaye and Niroomand (2009); Esen and Inalli (2009), have both implemented a way of optimizing the GSHP system by defining an objective function and using two different optimization techniques by Nelder-Mead method and generic algorithm method to find the optimum design (Tarnawski et al., 2009). Because of the massive design computations and time consuming optimization process of a GSHP, a computer program was developed in Visual Basic 6 based on the presented model using Nelder-Mead mathematical optimization method to obtain the optimized values of independent parameters in GSHP design.

Montagud et al. (2013) evaluated performance of a GSHP system installed in an office building in Spain. The system performance has been analysed based on the experimental measurement since 2005. In addition, this system has also been examined using a numerical model developed by GLHEPRO software. The numerical results have been validated and compared with the experimental measurements. This study indicated that the ground has a stronger recovery capability in practice as compared to the numerical results obtained using GLHEPRO.

2.9 Control Strategies of GSHP Systems

Appropriately commissioned controls are essential to maintain the desired levels of performance and safety with good energy efficiency. As is discussed in section 2.7, the single biggest design factor in determining the COP of the GSHP system is the distribution system and the temperatures used in it. Controls also have a major bearing on the eventual system COP. Assuming the control system is well designed and installed, and that the design temperatures have been chosen so as to maximise the COP of the system, this will contribute in reducing the carbon emission and energy use in buildings.

According to the BSRIA (1999) technical guide for GSHPs, there are different methods of control strategy of GSHP systems for improved energy savings and to utilise and optimise the operation. The developments include the use of fuzzy logic control and of control algorithms based on sophisticated parameters for relating physical conditions and comfort such as predicted percentage of dissatisfied (PPD) and predicted mean vote (PMV) (Rawlings, 1999).

Research detailing the predictive controllers for thermal comfort optimisation and energy savings outlines that as far as thermal comfort optimisation is concerned; there are other parameters that should be considered in order to provide thermal satisfaction to the occupants. It further highlights that thermal comfort in buildings is a concept which is difficult to define, however over the last decades or so a large number of comfort indices have been established, a well disseminated one is the PMV (Hanqing, 2006).

Weather compensated control is the most efficient means of operation since it ensures that the HP never works harder than necessary through utilising a sensor for gauging the outside air temperature. This data can then be plotted on a curve of ambient air temperature and required output temperature. The compressor is then controlled in response to the water return temperature in the distribution system i.e. output will be lowered as the ambient temperature increases.

CIBSE (2005), states that the inclusion of a building management system provides the designer with a number of additional ways to maximise the operating efficiency of the GSHP system by precise control of the plant items to exactly match the system requirements. One such example is the ability to vary the chilled water flow temperature to match exactly the cooling requirements of the system, rather than allowing the plant to control to a single set-

point temperature. In order that the benefits of the controls system are maximised, it is important that the control system communicates correctly with the refrigeration plant and vice versa. Failure to address this at the design stage can result in problems with final commissioning onsite or, at worst, the controls system failing to control the refrigeration plant to the level specified by the designer.

Kizilkan and Dincer (2015) conducted an energy and exergy analysis of a GSHP system located in Ontario (Canada); they concluded that the system's performance was slightly improved in the heating mode when the fluid temperature entering the HP was higher. Some studies have extensively investigated the performance of a GSHP from the HP point of view. Zhao et al. (2003) presented a theoretical and experimental analysis in order to investigate the effects on the energy efficiency of the HP of several capacity control strategies (turning on/off compressor, controlling intake and discharge valves' on/off times, concentration ratios of the refrigerant mixture and compressor's speed); in their study, the ground loop was considered making use of a water tank. Lee (2010) analysed the part-load performance of a GSHP system equipped with a double U-tube borehole heat exchanger that was simulated with a three-dimensional implicit finite difference model; the analysis focused on the variable-speed compressor. Madani et al. (2013) used variable and single speed compressors to carry out an in-depth study of capacity control in GSHP systems based on a comparative analysis of on/off controlled and variable capacity systems. Del Col et al. (2014) evaluated the performance of a GSHP of an office building consisting of four 80 m long vertical boreholes (two with single U-tube and two with double U-tube) during the heating season; they presented experimental data and developed a numerical model based on lookup tables of the main components of the system. The work of Del Col et al. (2014) focused on how the performance of the HP was affected in partial loads, analysing the effect of the variable speed; in their study, the thermal behaviour of borehole GHX was simulated separately from the HP by means of a commercial software. The above overall publications demonstrated that the current models are too complicated, and requires a range of different parameters, and this shows the need for developing tools that require easily attainable parameters.

A novel design and performance prediction tool for a GSHP system has been developed in Japan Katsunori (2006); the authors have developed a novel tool to predict design and performance for GSHP systems, which includes life cycle analysis (LCA).

As covered in section 2.7.3, the performance of GSHP systems is intrinsically related to the ground and load temperatures, it is unavoidable that ground temperatures will change to some degree in response to extraction of heat from, or rejection of heat to, the ground. However, it is important to recognise that the ground is not an infinite source or sink of energy, and that excessively large net rates of extraction or rejection of heat to the ground must be avoided. If excessive rates of heat extraction from, or rejection to, the ground are allowed for prolonged periods, then it is likely that significant changes in ground temperature will occur; such ground temperature changes can have significant detrimental impact on overall system COP, as well as large environmental impact. Zoi and Constantinos (2012) proposed three control strategies to minimise this significant change in ground temperature by using simpler heat rejection or ‘free cooling’ strategies. The first one determines set point at which a cooling tower starts its operation according to the fluid temperature exiting HP and ambient air wet bulb temperature exceeds a given set point. The second one activates the cooling tower when the fluid temperature exiting GHX is greater than a certain value. The third one sets cooling tower on when the fluid temperature exiting HP is greater than a given value.

Opportunities exist to control the performance of GSHP system by selectively rejecting heat to air using a DAC. This can be controlled using predicted seasonal or daily ground temperature as well as predicted/available energy demand of the building. However these control systems are not reported in the literature.

2.10 Summaries

Developments in HP technology have resulted in well proven technologies in many countries that are efficient, reliable, environmentally beneficial, cost effective and socially acceptable. The literature review has shown that GSHP systems have been found to have great potential as an aid in tackling climate challenges and meeting legislation requirements by facilitating the abatement of additional CO₂ emissions resulting from the use of GSHP systems in comparison to conventional commercial and domestic heating and/or cooling alternatives.

In theory, GSHP systems can work efficiently if properly designed and operated. However, in practice the performance of these systems is dependent on a range of different parameters and issues. There has been very little published data on the performance of installed GSHP systems in the UK until recently. The literature review has given a comprehensive description of expected HP performance and performance metrics. It identified how GSHP systems

performs in practice using a range of recently published monitored system COP data such as the EST field trial phase 1 and 2 reports.

The literature review has investigated the different components and parameters affecting the performance of the system. It covered an extensive collection of literature, looking at the design parameters affecting system's performance and operational experiences of GSHP systems. Identifying and understanding the relevant dynamics of groundwater effects and impact of ground temperature variation, control, climate conditions, site history, complex ground thermal properties, have huge effect on the vital energy piles and the GSHP performance.

Furthermore the literature review has shown that there are concerns that the use of GSHPs for extracting heat for a longer period could lead to a reduction of COP over time, and other complications. Opportunities exist to address the effect of seasonal imbalances of heat extracted versus heat returned to the ground by the GSHP system. The literature review has shown that by developing models for investigating performance of GSHP systems based on seasonal or daily underground temperature variations as well as predicting energy demand of the building it is possible to optimise the performance of the system.

Chapter 3

Proposition

It was concluded from the critical literature review that GSHP systems can work efficiently if properly designed and have significant potential to reduce carbon emissions in the UK. In practice however, critical studies have found that many GSHP systems do not perform as expected. Although there have been considerable efforts to improve the design of GSHP systems, there have been relatively few studies reported on their operation in practice, and specifically with respect to control of the system for optimum performance. The EST has recently published the first large-scale HP field trial study in the UK to determine how HPs perform in real-life conditions. The results demonstrated significant performance variation among installations and were generally lower than similar European trials, such as those carried out regularly by the Swedish Energy Agency. According to the EST report, the majority of poorly performing HP installations were either not properly installed or not optimally operated and controlled. Opportunities exist to improve the seasonal performance with improved controls.

Therefore the first aim of this research is to focus on the monitoring of the long-term operation of an installed GSHP system to understand and establish the current trend performance characteristics of the installation. This will provide a base case performance and thus enabling the optimisation of seasonal performance using an advanced control mechanisms.

The critical literature review has also shown that the performance of GSHP systems is highly dependent upon its interaction with the underground temperature distribution, and specifically the rate of heat extraction from and heat injection to the ground and other different parameters. There has been little work carried out to determine the relationship between the seasonal underground temperature variation and the performance of the GSHP

system. Despite the importance of ground temperatures on a GSHP system performance relatively little data has been published on disturbed underground temperature distributions. This is due to lack of experimental data and suitable mathematical models designed to enable investigation of disturbed ground temperature. Consequently the second aim of this research is to establish and develop a novel mathematical model for the analysis of the disturbed ground temperature over time. This aim feeds into the first aim as knowledge of the ground temperature will enable the prediction and control of system performance. In addition the model will allow the analysis of specific interventions or control methodologies to optimise the GSHP system performance.

The novel mathematical model will be used to predict the disturbed seasonal underground temperatures from daily fluid and air temperature data and is validated against real historical data. It can then be used to provide guidelines for engineering calculations. More specifically, a comparison will be made between long-term measured experimental data and novel predicted results to determine if the new undisturbed underground temperature model developed can be used to predict seasonal ground temperature profiles. This will enable accurate energy saving prediction for ground source heating and cooling applications.

In addition the critical literature review has also shown that the dynamic long term performance investigation of GSHP systems using transient models is not well understood. The third aim of this research is therefore using TRNSYS to build and establish a generic empirical transient system model. This will allow the construction of a GSHP system simulator to investigate the effects of different control strategy approaches using a DAC for heat rejection, energy consumption of the HP, the performance of the system and ground temperature variations.

The research will be combination of experimental measurements and analysis, mathematical simulation, and the development of a generic empirical transient model. The experimental results will be used to validate both the mathematical model and the empirical TRNSYS modelling methodologies developed during the research. This work is specific to GSHPs and ground temperature evaluation particularly with regard to prediction and control of the practical performance of GSHP systems and temperature regulation using DAC through sustainable methods but the principles developed have wide application throughout the building services engineering.

Chapter 4

CEREB Life Laboratory Experiment

4.1 Introduction

Almost 50 % of the energy consumption and carbon emissions in the UK relate to buildings. In the UK, planning regulations, financial incentives and building regulations are all combining to drive the building sector towards using more renewable technologies. For example, currently many local authorities require at least a 10 % on-site renewable energy contribution before planning is granted (20 % in London). Also, the UK Government has announced that all new homes will be zero carbon from 2016 and is working towards a similar commitment for non-domestic new buildings from 2019.

The literature review has highlighted that many building technologies such as GSHP systems are reported to underperform, and the reason for this is that the majority of poorly performing GSHP systems were either not properly designed or are not being optimally controlled and operated.

It is clear, that the practical performance of GSHP systems are little understood in both the building design and in-use operational sectors. This project involves detailed strategy of a GSHP system to investigate design and control. The 500 kW_{th} GSHP system being investigated during the present research study is one of the many different low carbon technologies installed at LSBU K2 building and the Centre for Efficient and Renewable Energy in Buildings (CEREB).

This chapter specifically provides a detailed background and description of the K2 building and CEREB which provided the opportunity to acquire detailed knowledge about the real operation of a GSHP installation and range of different ways of how to optimise it. The results of this study should provide significant benefits for both the construction industry and future users of these systems.

In addition this chapter presents detailed description of the GSHP system, control strategy of the system and finally the instrumentation and monitoring systems used to collect data in real time from working equipment in order to carry out this study.

4.2 Description of K2 and CEREB

There are a small number of existing renewable energy centres in the UK. However, these are generally in rural settings where there is plenty of space, flexibility and opportunity for the installation of renewable technologies which offer significant space requirements. K2 is located one mile from the centre of London and is set in an urban context on a tight London university campus. The K2 building is the newest development on campus (8500 m² floor area) completed in June 2009 and is shown in Figure 4.1 below. CEREB is part of K2 and is a new £3m research and teaching energy technology centre at LSBU, funded by Higher Education Funding Council for England (HEFCE) and the London Development Agency (LDA).



Figure 4.16 K2 building with its thermopile foundation

The building K2 is eight storeys high with a central atrium that rises to the fourth floor level.

The southern wing of the building, which comprises around a quarter of the building footprint area is five storeys high and has a roof level terrace. Most of the building's services are located in the plant room on the roof however some of the plant is on the ground floor. The building consists mainly of offices and laboratories, and some teaching space. The facility is used by all the Schools at the university.

- Ground Floor: Lecture theatres, toilets, offices, services and café.
- First: Lecture theatre, classrooms, toilets and offices.
- Second Floor: Classrooms, laboratories, offices and toilets.
- Third Floor: Classrooms, laboratories, offices, operating theatre and toilets.
- Fourth Floor: laboratories, meeting rooms and toilets.
- Fifth, Sixth and Seventh Floor: Offices and toilets.
- Eighth Floor: Roof Services.

The building was designed with 55 % lower carbon emissions than the prevailing UK building regulations. It includes a range of features to reduce carbon emissions including technologies such as solar thermal cooling, phase change materials with night time ventilation, solar fibre-optic lighting, solar photovoltaics and GSHP system for heating and cooling.

4.3 Design and Construction of K2 Building

The K2 building was designed to be energy efficient. Its built form means that it benefits from good daylight, reducing the need for artificial lighting. Overheating is prevented by treatment of the south west facade with an external solar shading system, which reduces demand for cooling in the summer. A large proportion of the concrete structure is exposed and can be utilised along with the ventilation system as part of a night cooling strategy aimed at reducing the cooling system energy requirement. In addition a number of features have been included to reduce the heating energy requirements. These include:

- An underfloor heating system, which delivers heat directly within the occupied zone. In high ceiling areas such as the atria, this provides an effective method of heating. Since underfloor heating systems operate at lower temperatures than most conventional heat emitters (e.g. flow and return of 50 °C / 40 °C), they allow the GSHP system to work at higher efficiencies. Hence no supplementary e.g. gas fired heating is necessary.

- All trench heaters and radiators have TRV control to limit wastage by providing more precise control. Separate primary circuits are proposed for the two main blocks. This zoning of the heating system reduces unnecessary overheating of the building. The ventilation system also includes a number of features which serve to reduce energy demand. These include:
- Thermal wheel heat recovery with high operating efficiencies within all main air handling units (AHU's). This significantly reduces the heating required to warm up incoming fresh air in winter. The thermal wheels used are of the hygroscopic type, which also recover latent heat.
- WC extract fans operate on a variable volume basis and are provided with inverter control driven off occupancy sensors. The cooling system's energy requirements have been reduced by using the main AHUs at night during warm weather conditions, to cool the buildings structure utilising free night cooling.
- The majority of lights used are high efficiency T5 fluorescent luminaries, with movement detection and daylight control.
- Both heating and cooling demand of the K2 building is provided for by the GSHP system and domestic hot water (DHW) provided for by solar hot water heating system.

The building energy demand was calculated by a consultant. Tables 4.1 and 4.2 below provide a summary of the energy consumption (kWh) and site CO₂ emission for the K2 development.

Table 4.2 *Annual Energy Demands (kWh) for K2*

	Rooms Heating Energy (kWh)	Mechanical Ventilation Heating Energy (kWh)	Total Heating Energy (kWh)	Mechanical Ventilation Cooling Energy (kWh)	DHW (kWh)	Total Electrical Energy (kWh)
	117,833	202,656	320,489	113,953	496,522	459,754

Table 4.3 *Site CO₂ Emissions (kg and tonnes) for K2*

		Total Heating	Total Cooling	DHW	Electrical Energy	Total
Site CO₂ Emissions	(kg)	75,911	20,197	79,785	194,016	369,909
	(tonnes)	76	20	80	194	370

4.4 Description of GSHP System

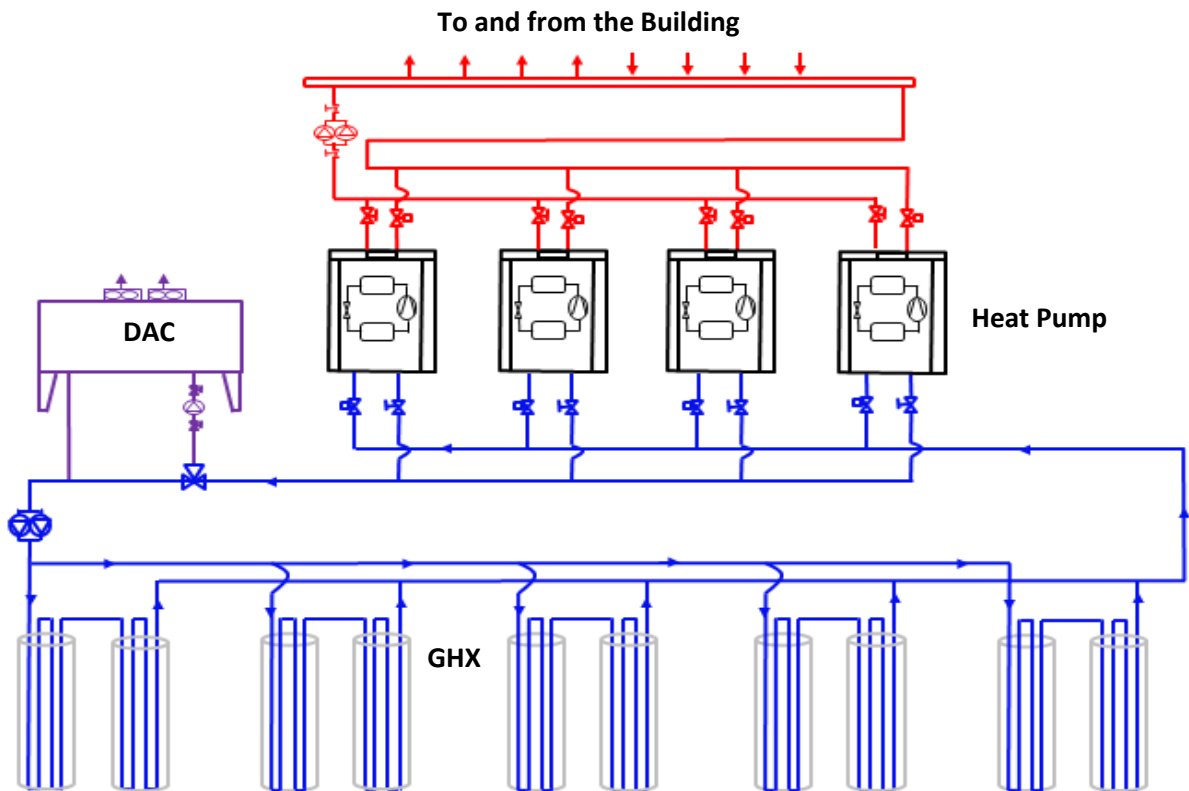


Figure 4.17 Concept layout of the GSHP System

The building's heating and cooling generation is fully provided for by the GSHP system, as shown in Figure 4.2. The detailed schematic of the system is shown in Figure 4.6. This includes heat pump, the energy piles or GHX and DAC. The GSHP system within the K2 building at LSBU uses four WaterFurnace EKW130 reversible HP units. Each has a nominal capacity of 120 kW for heating and 125 kW for cooling and is located within the roof plant room. The source-side of the system consists of energy piles and header pipes to which the HPs add or extract heat using a heat transfer fluid, which is pumped and exchanges energy between the building and the ground. There are four pumped secondary circuits fed from the primary GSHP low loss header, which provide either heating or cooling water to the building services systems. It should be noted that, there are no simultaneous demand requirements for both heating and cooling allowed for within the design. All four circuits are Constant Temperature / Variable Volume systems. Heating circuits are based on a 50 °C flow and a 40 °C return temperature. Cooling circuits are based on a 12 °C flow and an 18 °C return temperature. The heat carrier fluid is a heat transfer medium mixed with 32 % of glycol

concentration (i.e. CoolFlow FXC2 water antifreeze), which is based on a proprietary blend of refined vegetable extracts and has a very low oral toxicity.

4.4.1 Heat Pumps



Figure 4.18 Four WaterFurnace EKW130 HPs installed at K2

The system has four Water Furnace model number EKW130 HPs which are two stage reversible devices each incorporating two scroll compressors and plate heat exchangers. The rating point data from the manufacturer's catalogue for the EKW130 HPs are shown in Table 4.3.

Table 4.4 Heat pump rating details

Model	Capacity	Load Liquid Flow (l/s)	Source Liquid Flow (l/s)	Cooling		Load Liquid Flow (l/s)	Source Liquid Flow (l/s)	Heating	
				LLT18 °C LST 35 °C				LLT35 °C LST -3 °C	
				Capacity kW	COP			Capacity kW	COP
EKW130	Full	8.50	6.80	172.3	5.4	6.80	8.50	126.6	4.9
	Part	8.50	6.80	85.7	5.4	6.80	8.50	65.2	4.9

LLT – Leaving Load Temperature
LST – Leaving Source Temperature

4.4.2 Energy Piles

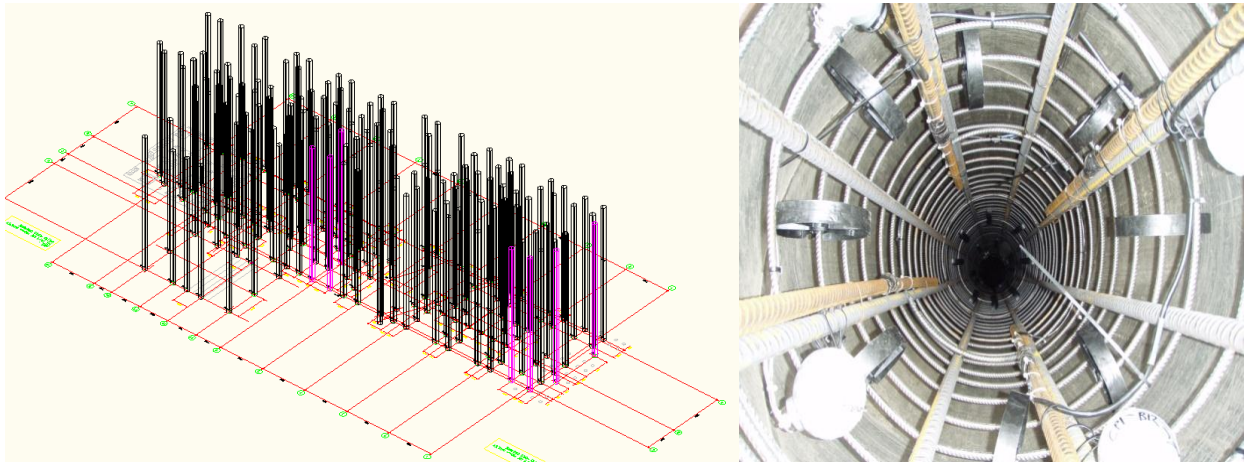


Figure 4.19 (a) 3D visualization of the thermopile arrays and (b) Top View of the thermopile cage before being filled with concrete

The heat is transferred from and to the ground through a closed loop system with the aid of 159 vertical energy piles which are built into the foundations of the structure and bored into the London clay as illustrated in Figure 4.1. Figure 4.4 shows a 3D visualization of the thermopile arrays and the top view of one of the thermopiles, before the thermopile cage was filled with concrete. The ground loop is comprised of a total of 318 U - tubes placed in 159 foundation piles. Each one contains two 32 mm OD PE100 U-tubes attached to the pile's metallic cage with an average active loop length of 28 m. The thermal conductivity of concrete is approximately 1.38 W / m K while the thermal conductivity of the ground has been calculated through an onsite thermal response test performed on both structural and non-structural elements. Results from the test show a thermal conductivity for the ground of approximately 1.3 W / m K. Applying the calculated conductivity with a tabulated data for density of 1.2 kg / m³ and specific heat capacity of 0.190 kJ / kg K for London clay the overall thermal diffusivity has been determined to be 0.049 m² / day. These values for conductivity and diffusivity showed good correlation across the site and have been used to design the GHX, summary of the conductivity test for the piles during the design stages in 2007 is given in Table 4.4.

Table 4.5 *Keyworth 2 - Conductivity Test - Pile Test Summary of Results July 2007*

Quantity	Start	End	Result	
Power into Test Hole	12189.0	12367.3	178.25 178252	kWh Wh
Test Duration	0	2642	2642 44.03	Minutes Hours
			4048.1	W
Flow Meter	99917334	99957861	40527.00 40527000	m ³ l
Flow Rate			15339.52	L / min
Test Hole Depth			26	m
Slope Straight Line Portion			4.711	
Conductivity			1.315	W / m K
Density			1.2	Kg / m ³
Specific heat capacity			0.190	kJ / kg K
Thermal diffusivity			0.049	m ² / day
Margin of Error			0.002	+/- W / m K

4.4.3 Dry Air Cooler

**Figure 4.20** *Dry Air Cooler AlfaBlue BDDT902D*

As shown in Figure 4.5 above the GSHP system at K2 uses AlfaBlue series dry air cooler (DAC) model number *BDDT902D* which is a wide range of heavy-duty dry coolers. Dry coolers are used for cooling down condenser fluid in air conditioning and refrigeration installations. The DAC was employed as a safety device to protect the heat pump from operating outside its safe envelope. It is designed to operate by rejecting heat only in the event that the temperature of the water returning from the ground loop exceeds 38 °C; the control

system enables the DAC shunt pump which is positioned in the loop supplying the DAC and circulates the water to the already enabled DAC. The DAC has its own internal PID based control system which controls the temperature of the water leaving the DAC to 22 °C. The rating point data from manufacturer's catalogue for AlfaBlue BDDT902D are shown in Table 4.4.

Table 4.6 *DAC BDDT902D rating details*

Model	Alfablue BDDT902D
Capacity (kW)	300
Fluid	Propylene glycol
Air Temperature in/out (°C)	30/40.7
Fluid Temperature in/out (°C)	44/37
Fluid pressure drop (kPa)	94
Fluid Flow Rate (l/s)	44.27
Freezing point (°C)	-7.1
Air Flow (m³/hr)	89540
Rotation Speed (rpm)	700
Total Nominal Power (W)	10000
Total Nominal Current (A)	17.2
Number of Fans	4
Fan diameter (mm)	910
Sound Power Level (dB)	90

4.4.4 Circulating Pumps

The GSHP system uses four circulating pumps connected to secondary circuits fed from the primary GSHP low loss header. This provides either heating or cooling water to the services systems. The secondary pumps distribute the low pressure hot water (LPHW) or chilled water (CHW) over four systems supplying the roof mounted AHUs and floor local controls. There are a total of seven AHUs, three AHUs serving the North (AHU 1 - 3), three AHUs serving the South (AHU 4 - 6) and one serving the Back Pack areas (AHU 7).

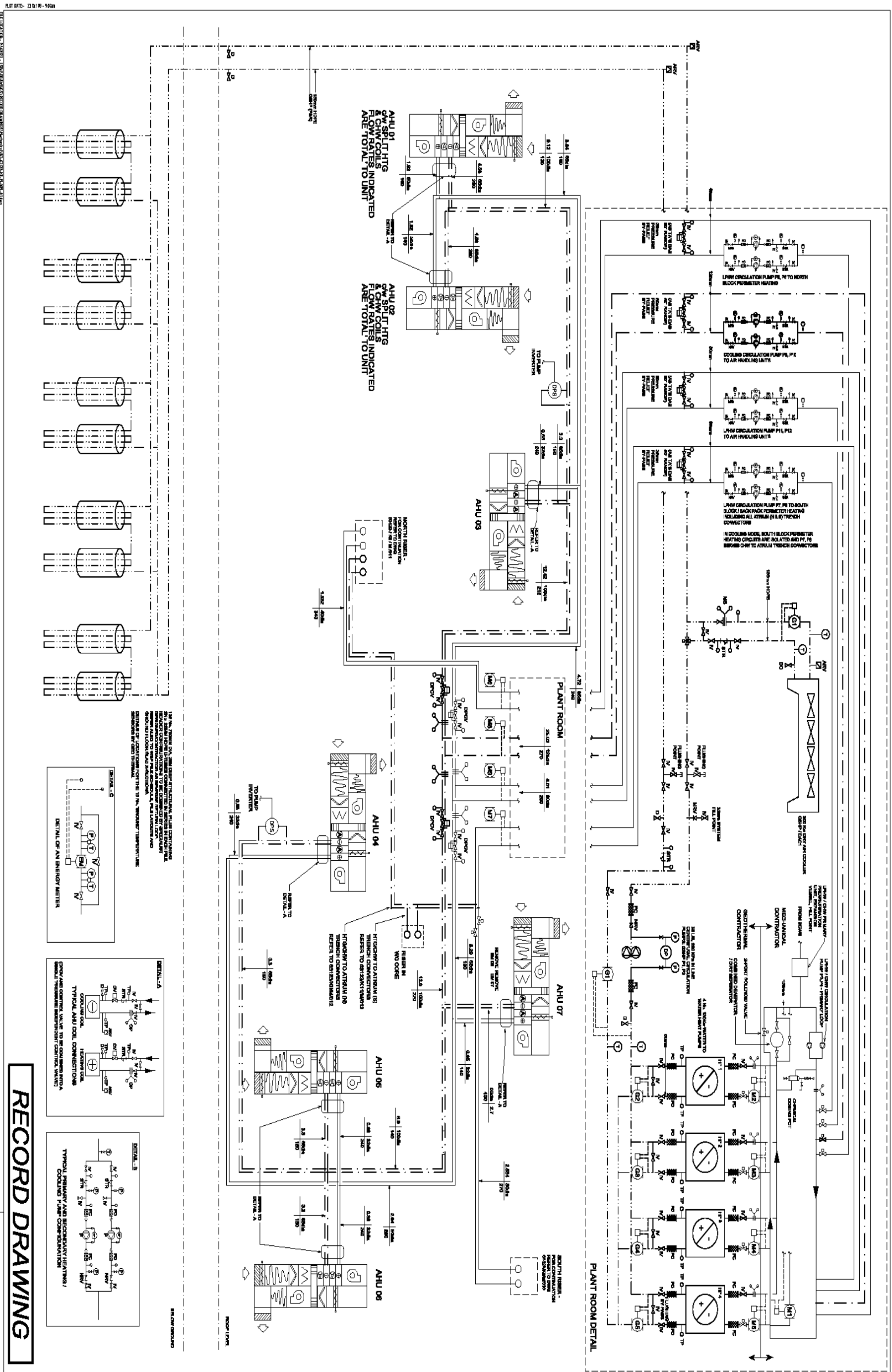


Figure 4.21 Detailed Schematic of the GSHP System

NO	15	RECORD PUMP
REV		DESCRIPTION
PROJ	LS	SOUTHERN
DATE	30.11.07	J.A.S.
SCALE	1:1	WTS@A1
FILE	RCY	FILE
HEAT	HE	IN
RC	RC	IN
DATE	11/11/09	REF

01 SCALE FROM 11

4.5 Current Control Strategies

This section describes the current control strategy of the GSHP system and the Honeywell Tridium integration system, a building management system (BMS) installed at LSBU's K2 building. The system comprises of main controllers utilising the Tridium Niagara platform which provides integration with various other industry standard protocols such as, Bacnet, LonWorks, ModBus and M-Bus. Communications between the BMS and the GSHP control panel is via the Tridium Niagara network over IP where the BMS is able to read all HP system values including flow and return main temperatures.

The BMS at LSBU K2 is used to control the ventilation and secondary water systems for the building. The system does not allow for simultaneous heating and cooling. The BMS graphical interface provides a graphical view of the GSHP system, including start stop signals for heating and cooling demand as well as alarm monitoring.

4.5.1 GSHP System Control of Cooling Mode

The GSHP system is enabled by the BMS in cooling mode when the outside air temperature is above 18 °C for a minimum period of 1 hour. The additional stages of the system are listed below.

- i. The GSHP System is enabled by the BMS to run in cooling mode
- ii. North perimeter heating pumps 5 and 6 are disabled from running
- iii. South perimeter pumps 7 and 8 are allowed to run in cooling mode with south flow and return isolating valves commanded shut
- iv. AHU CHW Pumps 9 and 10 are commanded to run
- v. AHU LTHW Pumps 11 and 12 are disabled from running
- vi. Geothermal Primary Pumps 3 and 4 are enabled to run

4.5.2 GSHP System Control of Heating Mode

The GSHP system is enabled by the BMS in heating mode when the outside air is below 14 °C for a minimum period of 1 hour. The GSHP system is also enabled in heating mode under an optimisation routine or during the 3rd stage frost protection. The additional stages of the system are listed below.

- i. The GSHP System is enabled to run in heating mode
- ii. North perimeter heating pumps 5 and 6 are enabled to run

- iii. South perimeter pumps 7 and 8 are enabled to run in heating mode with South flow and return isolating valves commanded open
- iv. AHU CHW Pumps 9 and 10 are disabled from running
- v. AHU LTHW Pumps 11 and 12 are commanded to run
- vi. Geothermal Primary Pumps 3 and 4 are enabled to run

4.5.3 GSHP System Dead band Mode

For an outside air temperature between 14 °C and 18 °C the GSHP system is set in dead band period and will not be required to provide either heating or cooling to the secondary systems. The only form of heating that could occur during this period is via the thermal wheels within the AHU's. Figure 4.7 illustrates the control strategy mechanisms when the GSHP system is operating in cooling, heating and dead band modes.

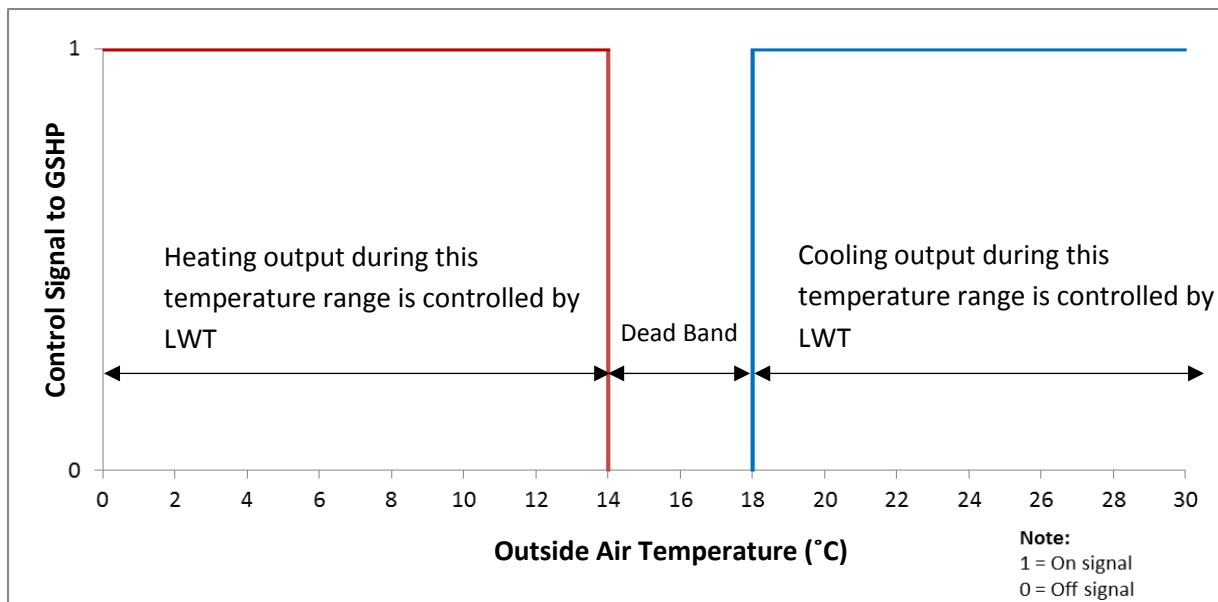


Figure 4.22 Diagram of the control mechanisms of GSHP in cooling and heating modes

4.5.4 Heat Pump Control

The HPs enabled signal is derived from the BMS which is based on both outside air temperature and on occupancy time schedules. The GSHP system controls the stages of the HPs in sequence to maintain the desired temperatures of either chilled water of 12 °C flow and 18 °C return or hot water of 50 °C flow and 40 °C return. This sequencing is achieved using a Biased Proportional Integral Derivative type controller output. The HPs are duty cycled to ensure equal run time on each HP and are sequenced by the FX40 controller. When

there is a demand for heating or cooling from the BMS, then the FX40 controller enables the lead HP which opens the load and source side isolation valves of that HP.

The FX40 HP controller also rotates the lead and lag HPs and the two compressors per HP are also rotated every 100 hours of operation. The flow rates required for the EKW130 HPs are 7 l / s minimum and of 9 l / s maximum per HP. The HP has an alarm output which is energised on refrigerant temperatures, source temperatures ground loop exceeding the required set-points and also includes flow sensors on the load and source side to protect the HP if no flow. All HP faults, temperatures and condition are transmitted to the BMS via the BACNet over IP interface.

4.6 Instrumentation and Monitoring System

4.6.1 Data Logging System

The building has extensive heat and electricity sub-metering to enable performance monitoring and evaluation at the individual zone levels. A Building Energy Management System (BEMS) has been configured to enable rapid data acquisition for all the key services and energy meters, retrievable from a web-based system. The Workplace Footprint Tracker (WFT), which is a Management Information System (MIS) is used to monitor the energy efficiency of the building's equipment and energy usage. The energy generation and consumption, carbon and cost savings are provided online as an Internet service. Usage and generation data for electricity is collected on half hourly basis from new smart meters that have been installed at CEREB. The meters communicate with the WFT via radio mesh networks and GPRS links. Other electricity usage, generation and sensor data for the rest of the building is collected from the BMS via a BACNet over an IP backbone (Ethernet) interface. The meter and sensor collected readings are stored in a database and processed to visualize consumption and gains in kWh, £ and CO₂e. The visualization is presented on configurable dashboards, which are available on the Web and can be displayed on strategically located screens to raise a public awareness.

4.6.2 Weather Station

The K2 building has its own electronically monitoring external weather station. The station is connected to devices which measure wind speed, sunshine duration, sun intensity, outside air temperature, humidity and rain fall quantity.

4.6.3 Temperature Measurement

In order to calculate the heating energy consumption of the building, temperature measurements are required at the inlet and outlet of both source and load sides of the HPs. The schematic in Figure 4.8 shows the different temperature measurement points for measuring the heat extracted from and dissipated to the ground. The figure also shows the positions of the heat metering equipment. Omega Pt100 platinum resistance temperature sensors have been used for the temperature measurements. Each of these sensors with high accuracy and repeatability contain a resistor that changes resistance as its temperature value varies. Platinum temperature sensors such as Pt 100 and Pt 500 sensors have resistances of 100 and 500 Ohms respectively at 0 °C. The higher the resistance rating of PRT the greater the sensitivity i.e. the change in resistance with temperature is larger for the resistance PRT. The Omega Pt100 DIN head sensors have 120 mm length and 6 mm diameter probes. The sensors are robust industrial types that are suited for plant rooms installation. The main challenges with temperature measurement include the correct positioning of the sensors to ensure good conductivity between the fluid carrying pipes and the temperature sensors whilst avoiding local temperature distortions through heating or cooling.

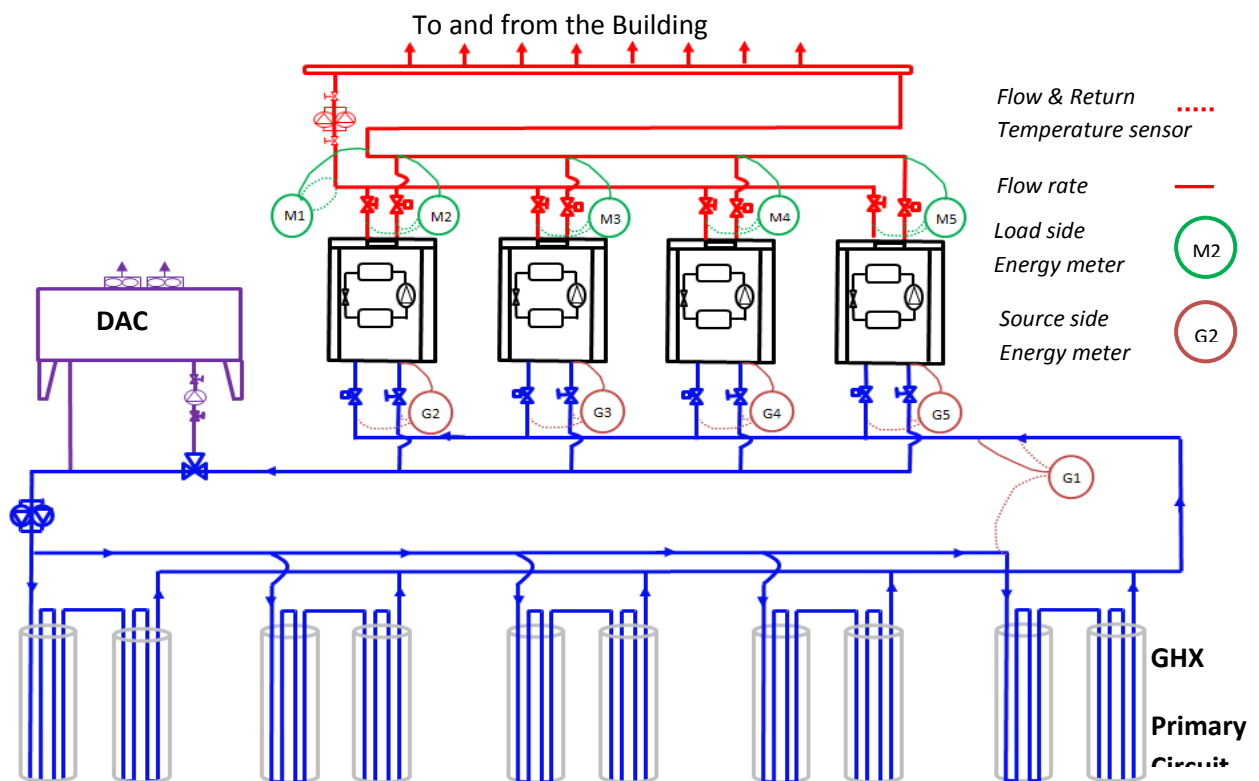


Figure 4.23 Schematic layout of the GSHP System with the location of sensors

4.6.4 Ground Temperature Measurement

Six of the 28 m deep piles have been equipped with 33 calibrated type T thermocouples at depths of 3 m, 14 m and 26 m to allow for close monitoring of the underground temperature distribution; this permits the study of both ground behavior and the effects of heating and cooling on the building's structure. The piles have diameters of approximately 750 mm. The installation also includes stress gauges to enable correlation of stress with ground temperature. One dummy thermopile was also monitored as a reference - case. The fully monitored GSHP system, which includes temperature sensing in the deep piles, is a unique research resource, and is an ideal facility for fully evaluating and optimising the performance of these systems. By measuring the temperatures around the piles it has been possible to gain understanding of the thermal charge and discharge characteristics of the system.

4.6.5 Flow Measurement

Six electromagnetic flowmeters were used on the load and source side of the GSHP system for all volumetric flow rate measurements. These flowmeters were designed exclusively to measure the flow and conductivity of electrically conductive liquid media. A magnetic field is applied to the metering tube, which results in a potential difference that is proportional to the flow velocity perpendicular to the flux lines. The specification for the Krohne OPTIFLUX 4100 Electromagnetic Flowmeter is given in Table 4.5.

Table 4.7 *Technical Data for Krohne OPTIFLUX 4000 Electromagnetic Flowmeter*

Temperature range	-40 °C to 140 °C
Velocity range	-12 to +12 m/s
Nominal diameter (DN)	2.5 to 1200 mm
Repeatability	±0.3 % of the measured value
Accuracy	± 0.3 % of the measured value

The sensors are positioned at carefully chosen locations on both the load and source side of the GSHP loops in accordance with the manufacturer's guidelines. Each flow meter is configured with respect to pipe thickness, pipe material and fluid properties. Figure 4.9 shows a photograph of an installed flowmeter and the meters positions are shown in Figure 4.8.



Figure 4.24 *Krohne OPTIFLUX 4100 Electromagnetic Flowmeter*

4.6.6 Electricity Consumption Measurement

Electricity is consumed by the four HPs, the DAC and the ground loop circulating pumps. Each HP has a dedicated electricity meter to monitor the input to the compressors. An Aidon 6000-series electricity meter as shown in Figure 4.10 is used to monitor the electricity use by the HPs. This 3-phase energy service device combines a meter, communication ability device and sensors and interfaces, with efficient data processing power for interpreting the signals.



Figure 4.25 *Aidon 6000-series electricity meter*

4.7 Summaries

Specifically, this chapter presented a detailed description of the K2 building, the main design objectives and construction considerations for CEREB and the K2 building. Some of the special design features for promoting energy efficiency and reducing the carbon emissions of the building were also discussed. The use of information systems, including advanced metering and the use of the BMS for the building and GSHP system control strategies, has also been presented.

Detailed description of the GSHP system, the different major components of the system i.e. heat pumps, energy piles, DAC and associated services are given. In addition the control strategy of the GSHP system, instrumentation and monitoring systems are also discussed.

The chapter has shown that the K2 building has an extensive heat and electricity sub-metering to enable performance monitoring and evaluation at the individual zone levels. A brief description of the instrumentation and monitoring system which enables rapid data acquisition for all the key services and energy meters has also been discussed.

Chapter 5

Commissioning of Apparatus & Investigation of Initial Results

5.1 Introduction

Chapter 4 described the GSHP system and the different major components of the system. This chapter presents a case study of the commissioning of the apparatus and investigation of the initial performance analysis of the GSHP system.

This chapter describes a range of installation challenges which were related to the flow meters, temperature sensors and heat metering units. This chapter identifies a number of problems in relation to the meters installation and the measurement of temperature. It also describes the process taken to overcome the difficulties and quantifies the associated errors.

In addition, this chapter specifically presents a validation of the historical data against manufacturer's data and an in depth analysis and evaluation of the monitored performance of the system. Subsequently, the reasons for the actual system performance variation have been identified.

Furthermore this chapter provides analysis of the potential CO₂ savings compared to other conventional heating technologies such as efficient gas fired boilers.

5.2 Initial Results and Commissioning

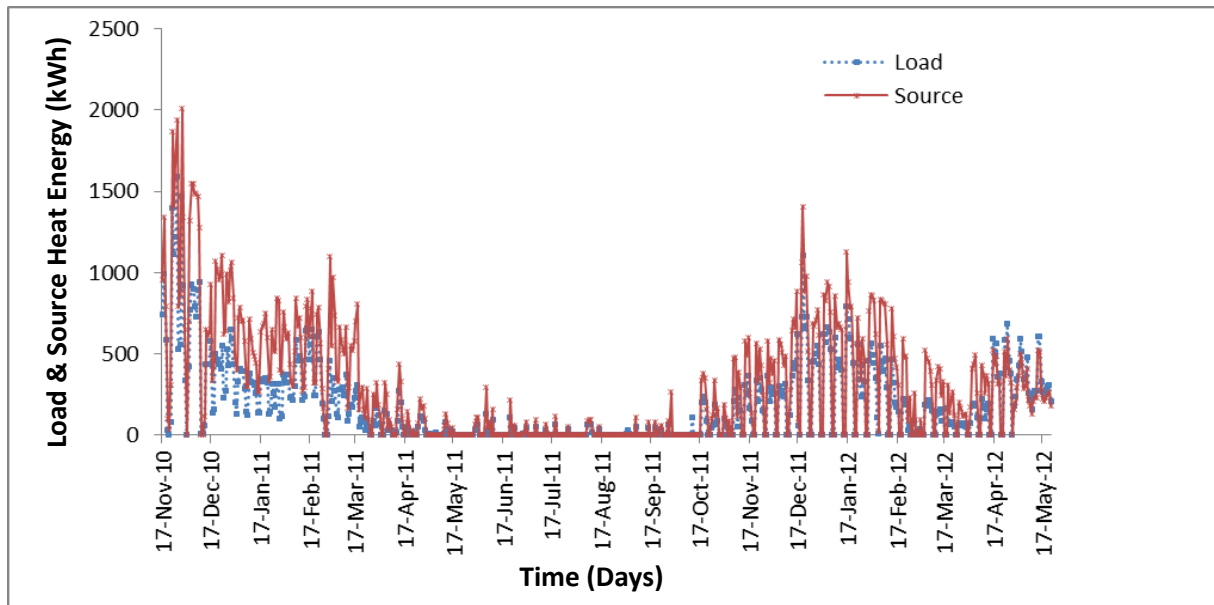


Figure 5.26 Comparison of load and source side heat energy

Figure 5.1 shows the initial results from the installation for load and source energy output from the GSHP system. As shown in Figure 5.1 it was noticed that when the load and source side energy were compared, the source side is much higher than the load side and this is impossible especially when the HP is running in heating mode. This anomaly had therefore led to an in-depth investigation of the different components of the heat metering system and these are discussed below in detail.

This section covers the detailed work carried out to investigate the range of installation errors within the complex heat metering and monitoring system in order to establish the long term practical performance of the GSHP installation. Incorrectly installed heat meters are a particularly important issue for a heat metering scheme designed to evaluate the performance of any heating technology since it's likely that they will bias the results.

5.2.1 Wrong Types of Heat Meter

At the beginning of the design stage the installers had specified and installed 5 of Metrима MF4 type heat meters on the source side and another 5 of SVM F4HC type heat meters on the load side. At a later stage it was identified that the heat meters installed on the source side could only register heating data but not cooling data and ultimately giving an accumulated false heat data reading. Consequently this required the re-commissioning of the system and

the adding of another additional 5 of new Landis Gyr T550 Ultraheat meters on the source side. However this intervention did not resolve the error associated with the source side being higher than the load side. Figure 5.2 illustrates the type of heat meters used in the installation.



Figure 5.27 Old and new types of heat meters used at K2

5.2.2 Heating Fluid Properties

The physical properties of the heating fluid are important for accurate measurement as they can affect flow meter measurements directly and also the calculation of measured heat consumption.

It was decided to run some more diagnostics to try and resolve the problems of lower load heat energy relative to the source heat energy. Having examined the schematic of the system thoroughly it was spotted that a temperature sensor had become dislodged from its designed position so that it is no longer correctly sensing the target temperature of the system. The temperature sensors were changed to the right location, however the problems of higher source side than the load side persisted. After conducting further investigation and speaking with the HP installers and heat meter suppliers it was established that the heat meters used in the installation were configured for a 25 % of ethylene glycol solution; however our system was designed / installed for a 32 % glycol content solution. The heat meters calculate the energy transfer by measuring the fluid flow and the difference between the supply and return temperature. In order to compensate for the change of density and specific heat with change of temperature the meters are pre-configured with built in heat coefficient factors and these heat coefficient factors are different according to the glycol type and content in the system. Incorrect concentration levels of the glycol on the system can lead to calculation errors.

Originally it was believed that the type of glycol substance used on the system was ethylene glycol hence all of the heat meters were specified for an ethylene glycol solution. However the type of glycol used in the system was neither ethylene nor propylene but a substance called CoolFlow FXC2 which is based on a proprietary blend of refined vegetable extracts. The physical and thermal property of this substance is different to ethylene and propylene glycol.

The addition of glycol will affect the physical properties of the heating fluid, including the specific heat capacity, density and viscosity. Theoretically, specific heat capacity and density affects all types of heat meters, with viscosity affecting vortex and turbine types of heat meters. Additional testing has also been carried out on glycol/water mixes to gauge the potential errors associated with using a heat meter calibrated for the wrong heat transfer fluid. This is discussed in section 5.3.

5.2.3 Temperature Sensors

Furthermore, a number of installation errors related to the temperature sensors have been discovered. It is a good practice when installing temperature sensors to give good thermal contact between the sensor and the pipe carrying the working fluid. A study by DECC (2014) has shown that a significant number of sites have heat meters with temperature sensors that are cable tied or taped to the outside of pipes or fitted using custom plumbing arrangements, rather than fitted inside the pipes to ensure the temperature sensor pocket is surrounded by flow. It was identified that some of the temperature sensors were strapped to the outside of the pipe wall. This leaves the sensors exposed to the outside air temperature fluctuations; poor contact modifies the measured temperature relative to the actual heat carrier fluid temperature. The interference could be minimised by insulating the pipe properly however it is difficult to completely eliminate its effect and therefore it may still contribute to some errors associated with the fluid temperature measurement and therefore to the heat energy output. Measurement Point A in Figure 5.3 shows the temperature sensors strapped horizontally in line with the pipes. Measurement Point B illustrates temperature sensor inserted inside a sensor pocket which is the preferred way of measurement.

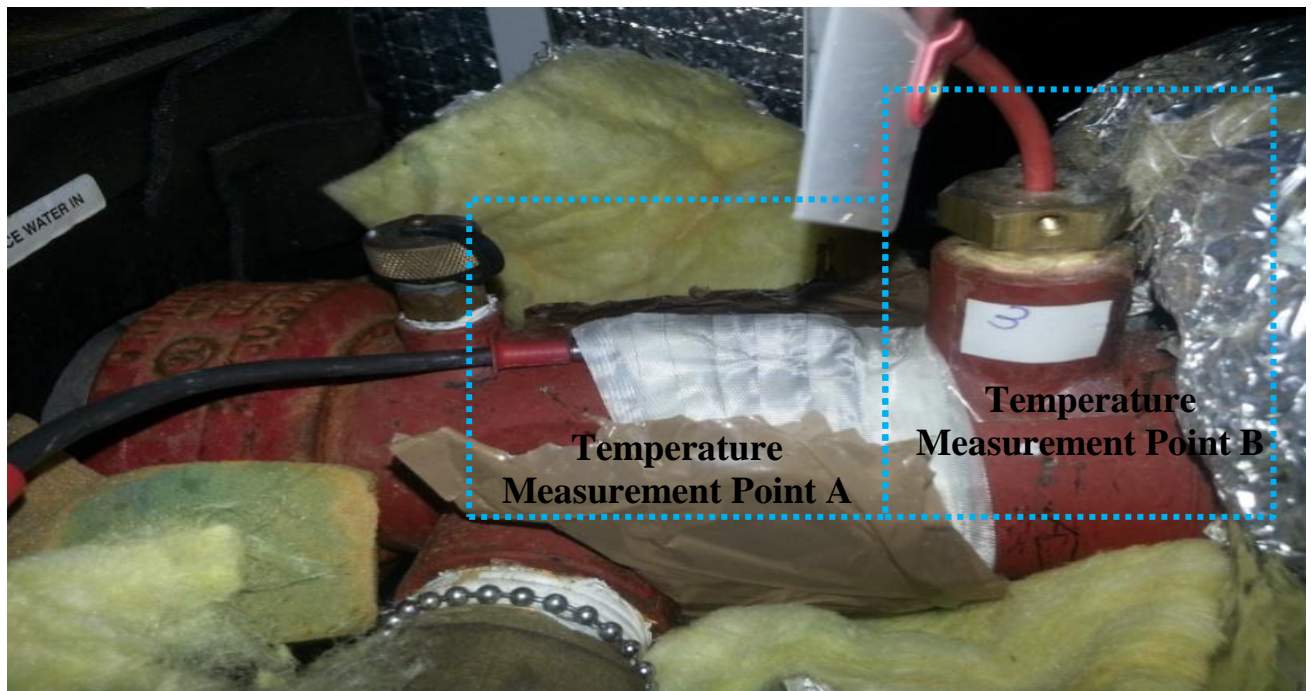


Figure 5.28 *Inserted and strapped temperature sensors*

The correct installation method for thermocouples is with the probes inserted inside sensor pockets with suitable thermal grease. Further investigation on the temperature sensors showed that the thermocouple sensor pockets were not deep enough within the pipes to ensure good thermal contact between the sensor and the heat carrier fluid. This introduces a gap between the fluid and the temperature sensor which creates a barrier for heat transfer and an accurate reading of the fluid temperature.

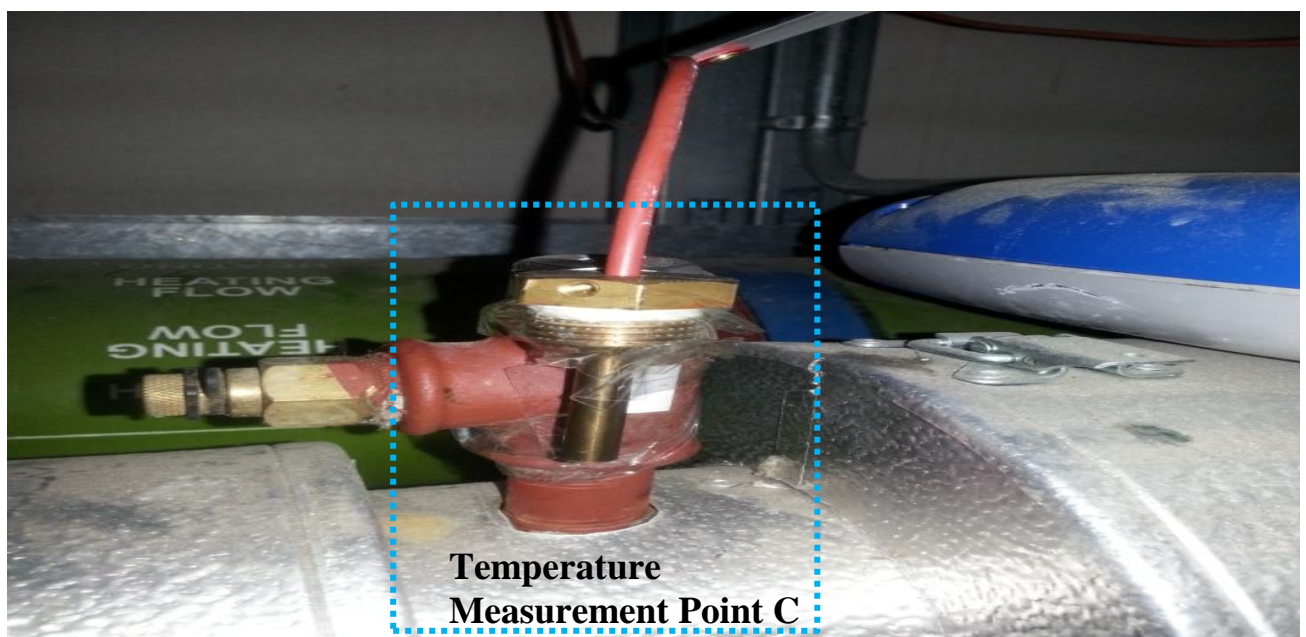


Figure 5.29 *A photographic image of short thermocouple pocket*

As can be seen in Figure 5.4, with Measurement Point C there is a very noticeable gap between the liquid circulating inside the pipe and the thermocouple's head. This consequently creates a delay and error between the actual fluid temperature value and the thermocouple's reading that are seen by the heat meter. A comparison has been made between a properly inserted thermocouple and one inserted into a short thermocouple pocket, to identify the potential errors associated with this anomaly and the results are provided in section 5.3.

5.3 Quantification of Identified Errors

This section provides the quantification of measurement errors resulting from the measurement difficulties and installation errors identified in the previous section.

5.3.1 Calculated Theoretical Error

An estimate of the effect of heat transfer fluid properties on the measurement of heat can be made based on standard heat transfer equations and the known properties of typical heat transfer fluids. The following example illustrates the theoretical error in measuring heat transfer resulting from a heat meter set up to measure a 25 % propylene glycol, 32 % glycol/water mix and a 32 % Thermox FXC2 water mix. Table 5.1 gives the properties of propylene glycol / water mix and 32 % Thermox FXC2 water mix.

Table 5.8 *Properties of Propylene Glycol and Thermox FXC2*

T (°C)	25 % Propylene Glycol		32 % Propylene Glycol		32 % Thermox FXC2		Error Comparing 25 % Propylene & 32 % FXC2 (%)	Error Comparing 32 % Propylene & 32 % FXC2 (%)
	ρ (kg/m ³)	C_p (kJ/kg.K)	ρ (kg/m ³)	C_p (kJ/kg.K)	ρ (kg/m ³)	C_p (kJ/kg.K)		
0	1028	3.91	1030	3.83	1040	3.81	1.4 %	0.4 %
10	1021	3.92	1028	3.83	1036	3.83	0.9 %	0.8 %
20	1019	3.93	1024	3.85	1031	3.85	0.9 %	0.7 %
40	1012	3.95	1015	3.9	1020	3.89	0.7 %	0.2 %
60	995	3.97	1005	3.91	1007	3.94	-0.4 %	1 %
80	980	3.98	995	3.92	993	3.98	-1.3 %	1.3 %

The effect of measuring pure water with a meter set up to measure a 32 % propylene glycol / water mix can be estimated based on the equation for heat:

$$Q = V \rho C_p \Delta T$$

Where:

Q = Heat output (kW)

V = Volumetric flow rate of heat transferring fluid (m^3 / s)

ρ = Density of heat transfer fluid (kg / m^3)

C_p = Specific heat capacity of heat transferring fluid ($\text{kJ} / \text{kg.K}$)

ΔT = The temperature difference between the flow and return (K)

Assumptions:

Heat flow measured for 1 hour

$V = 0.0068 \text{ m}^3/\text{s}$

$\Delta T = 10 \text{ K}$ at an average temperature of $45 \text{ }^\circ\text{C}$

From Table 5.1

$\rho.C_p \text{ 25 \%} = 1012 \times 3.95 = 3,997 \text{ kJ/m}^3.\text{K}$

$\rho.C_p \text{ 32 \% glycol} = 1015 \times 3.9 = 3,959 \text{ kJ/m}^3.\text{K}$

$\rho.C_p \text{ 32 \% Thermox FXC2} = 1020 \times 3.89 = 3,968 \text{ kJ/m}^3.\text{K}$

Assuming 25 % propylene glycol in the system the total heat consumption therefore is calculated to be 3,997 kWh. The GSHP system at LSBU was designed for 32 % Thermox FXC2. Using the characteristics for this fluid the total heat consumption is calculated to be 3,968 kWh. However, if the meter was set up for 32 % propylene glycol the actual consumption would be 3,959 kWh. Comparing the 25 % propylene glycol with 32 % propylene and 32 % FXC2 glycol mix there would be an approximate error between -1.3 % and 1.4 % in the system.

5.3.2 Temperature Sensors Installation

A further test was carried out on the installation of temperature probes to quantify the level of error attributed from the wrong installation of temperature sensors. Figure 5.5 illustrates the temperatures measured during experiments of (i) on the outside surface, (ii) with the temperature probes inserted correctly inside the thermocouple pocket with thermal grease and (iii) with the temperature probes half inserted inside the thermocouple pocket. Pipework and fittings were insulated with 100 mm thick Rockwool insulation to minimise effects of the environment.

It can be seen that both half inserted and surface strapped probes do not replicate the fully inserted probe well. This is particularly apparent under fluctuating conditions. Typically the

surface probe over estimates by around 1 K, whereas the half inserted probe over estimates by approximately 2.5 K. A temperature difference of 2.5 K is equivalent to approximately 25 % error in the heating output. The reason why the half inserted probe is performing much worse than the strapped probe is because the strapped probe is well insulated and the connection path to the ambient environment is around 300 mm. In contrast the connection path between the top of the pocket on the half inserted probe is around 100 mm.

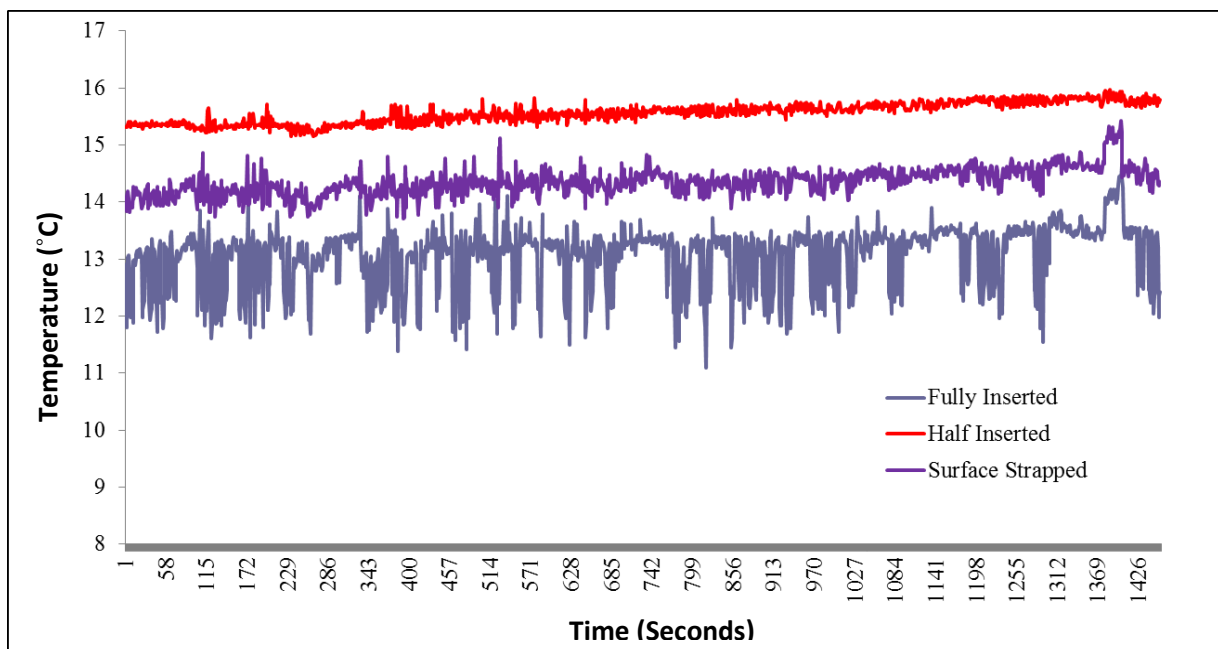


Figure 5.30 *Temperature measurement at different points of pipe*

Assuming that the fully inserted pocket measurement is correct, Figure 5.6 shows the errors in temperature difference recorded in experiment tests for two different temperature probe installations. Figure 5.6 shows that when the temperature probes are strapped on the outside surface of the pipe or half inserted into a pocket, a large temperature difference error of between +15 % to -40 % occurs compared to a fully inserted probe. AECOM (2013) has conducted a similar study to establish heat meter measurement errors and the result shows similar values to the above findings. The potential for this error is much greater on the load side because the temperature difference between load and ambient is much greater. This therefore is one of the key factors in which the results being incorrect. As a result long pockets were installed throughout and this corrected the source and sink load inversion shown in Figure 5.1.

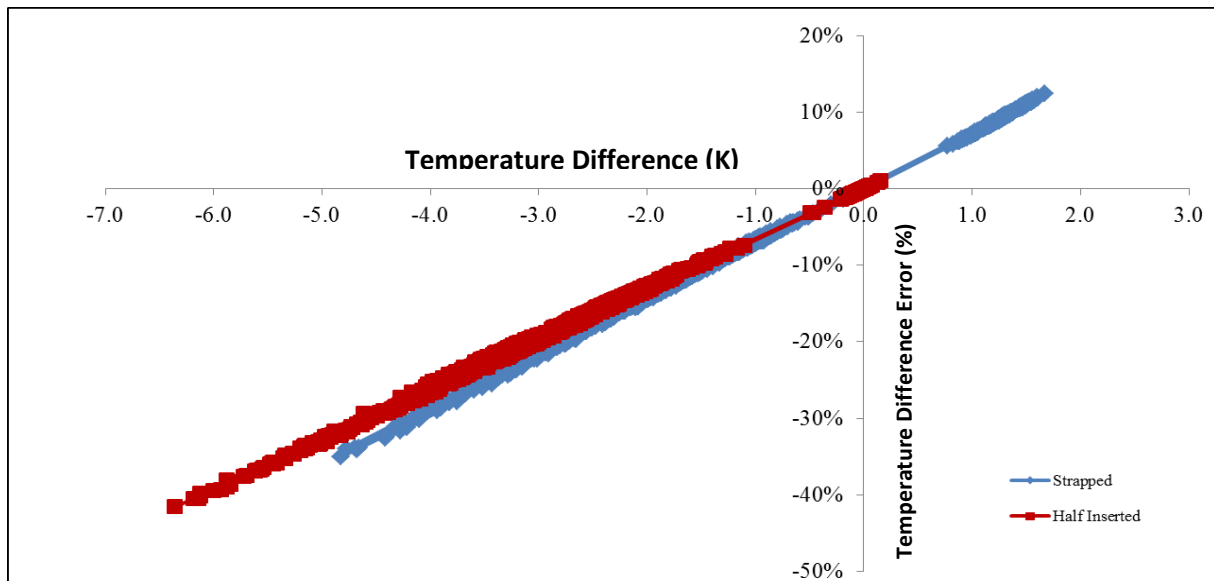


Figure 5.31 Errors due to incorrectly installed temperature probes compared to fully inserted

5.4 Investigation of the Performance of a Typical GSHP System

This section builds upon the previous initial results sections and specifically presents the validation of the experimental data as well as an in depth analysis and evaluation of the monitored performance data. This is used to understand the long term system performance. Detailed analysis of the results has identified the main factors resulting in variation in the actual HP performance.

5.4.1 Experimental Data Validation

In order to validate the historical performance data, heating season COP data has been collected between January and February 2014. Using linear regression analysis this data has been compared against manufacturer's performance data. As shown in Figure 5.7 this shows that nearly all of the experimental data is within 20 % of the manufacturer's data and this is mostly within the experimental error calculated in Chapter 7. According to the manufacturer, the specified COP values of the HPs are 4.9 and 5.6 at the full load design conditions in heating and cooling mode respectively.

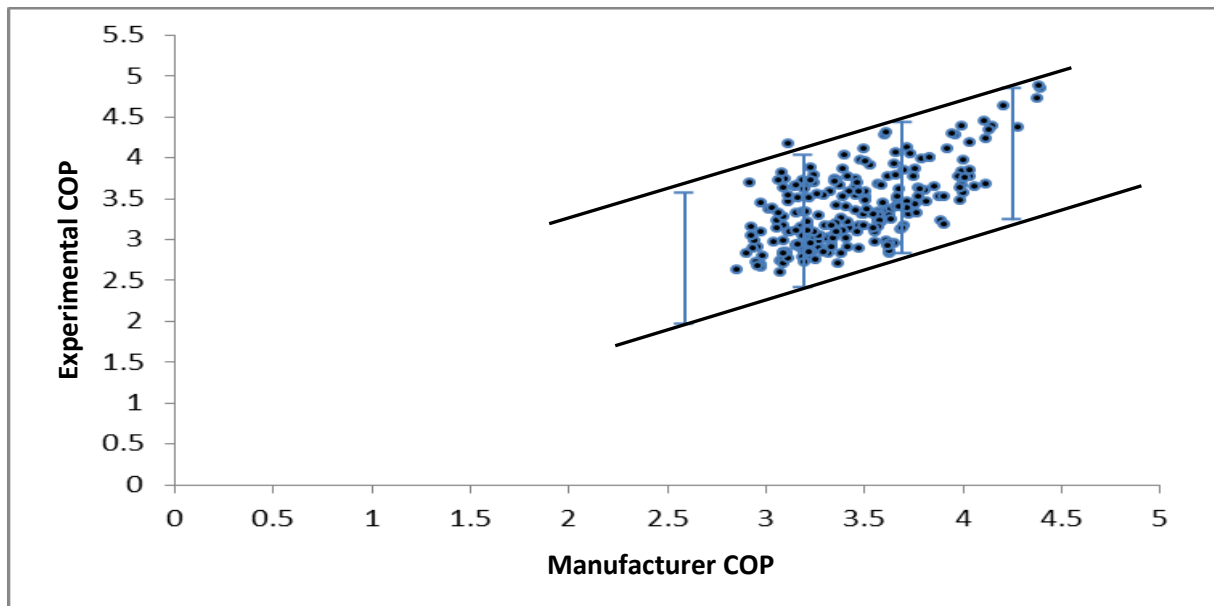


Figure 5.32 *Manufacturer and experimental COP correlation for heating*

Figure 5.8 presents a further validation of the variation in heating demand with external weather conditions expressed as daily heating degree days (HDD) using historic data from the LSBU weather station. HDD are used to estimate heating energy demand of the building. They are derived from measurements of the outside temperatures above which a building needs no heating. Figure 5.8 shows a good correlation with the monitored HP's heating output data and HDD. The degree of scatter for the correlation provides an indication of the reliability of the monitored historical data.

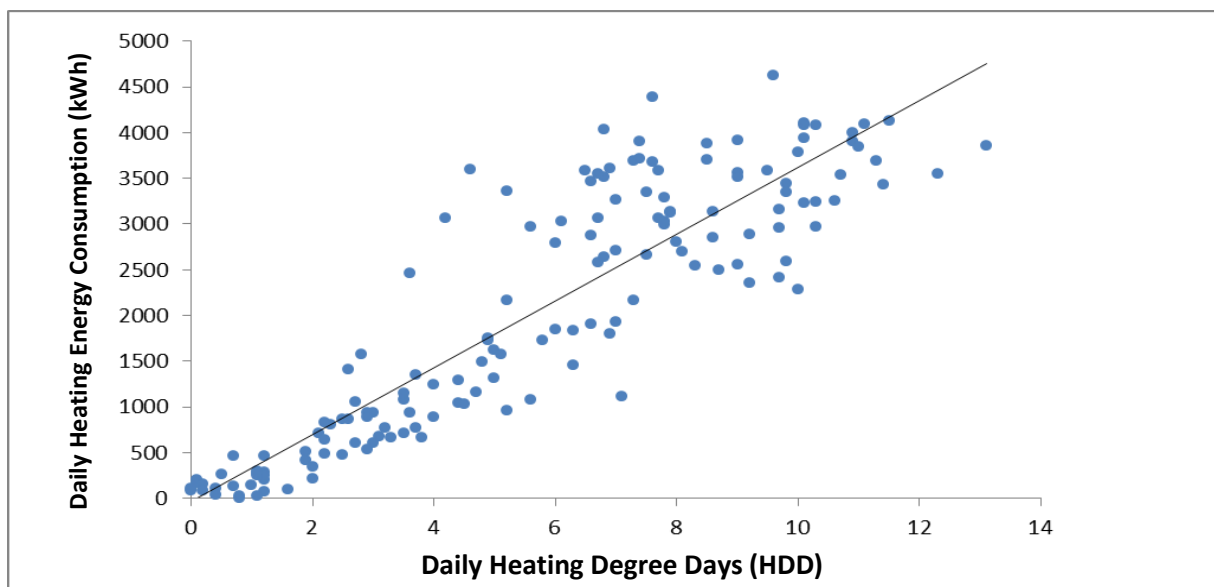


Figure 5.33 *Relationship of HP heat output to external weather conditions*

5.4.2 System Performance Measurement

System performance is calculated using the temperature difference between flow and return, the flow rate and the electricity input. These are combined to give Q_{HP} and COP. The COP indicates how much heat can be gained for a unit input of electrical energy. The unit COP is defined using the power consumption of the HP unit compressor where:

$$Q_{HP} = m C_p \Delta T \text{ [kW]} \quad (5.1)$$

$$\text{COP} = \frac{Q_{HP} \text{ [kW]}}{W_{HP} \text{ [kW]}} \quad (5.2)$$

Figure 5.9 presents the daily monitored heating load delivered to the building by HPs 1 and 3 between November 2013 and April 2014. HP 1 was operating at part load during this period, while HP 3 was operating at full load. The result shows that although HP 1 was operating at part load, the daily heat outputs of the two HPs are similar to each other.

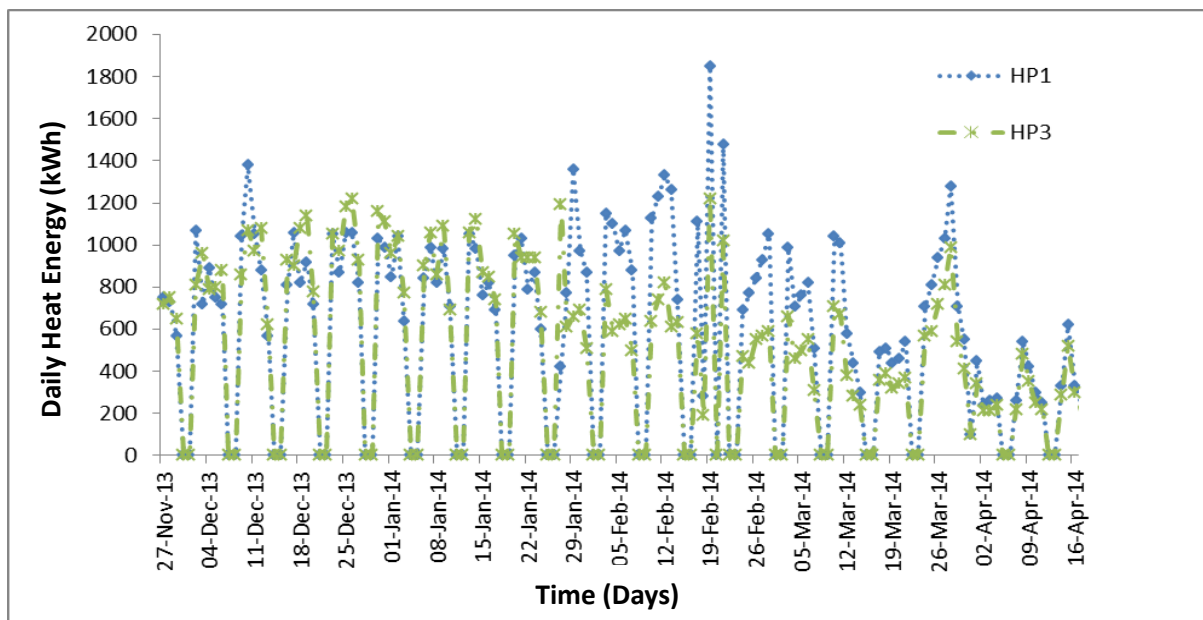


Figure 5.34 Daily building heat load profile

The daily heating and cooling COP values of HPs 1 and 3 during the 2013 / 2014 are shown in Figures 5.10 and 5.11. It can be noted that HP 1 has consistently higher COP values compared to HP 3. This can be attributed to HP1 running at part load. Fahlen (2012) has shown that it is advantageous to operate HPs at part load almost all the time in order to reduce the power utilization and improve the COP. The result shows that the part load COP of HP1 is higher than the full load COP of HP3 by an average of 37 %. The cooling COP is much higher than the heating COP; this is because the temperature lift in cooling mode is smaller compared to the larger temperature lift in heating mode.

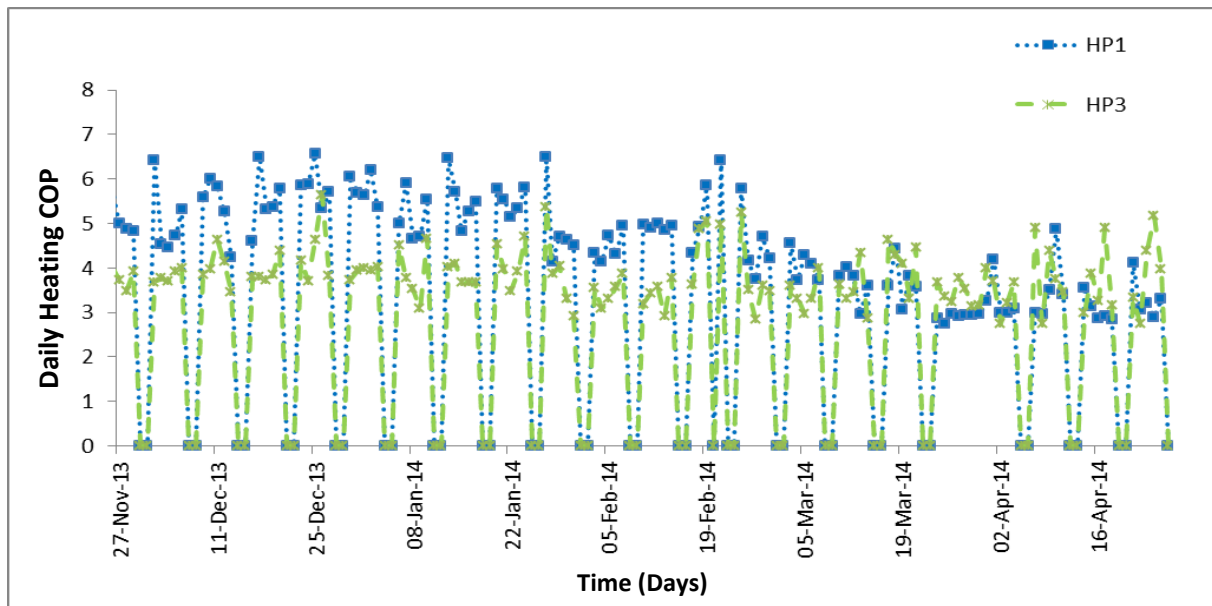


Figure 5.35 Daily heating COP

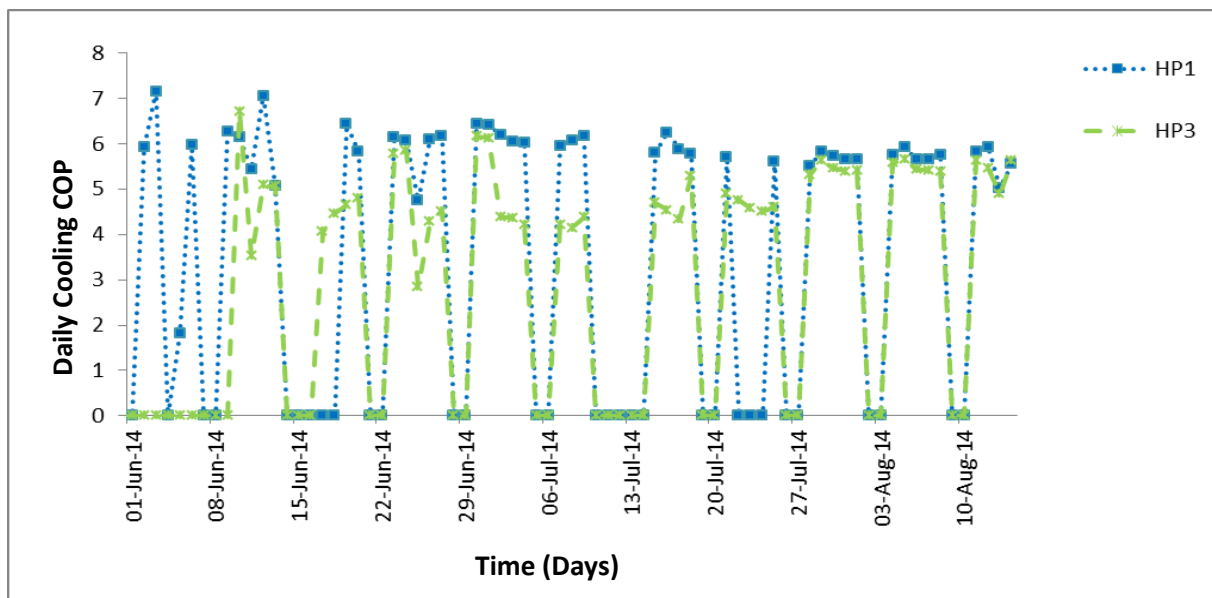


Figure 5.36 Daily cooling COP

At part load the difference between evaporator and condenser temperature decreases thereby increasing the Carnot COP and also improving the actual COP. The increase in evaporator temperature and decrease in condenser temperature at part load can be achieved if the compression ratio is reduced (giving higher evaporator pressure and a lower condenser pressure), so the compressor needs to do less work. This is illustrated using a vapour compression cycle on a pressure-enthalpy flow diagram in Figure 5.12.

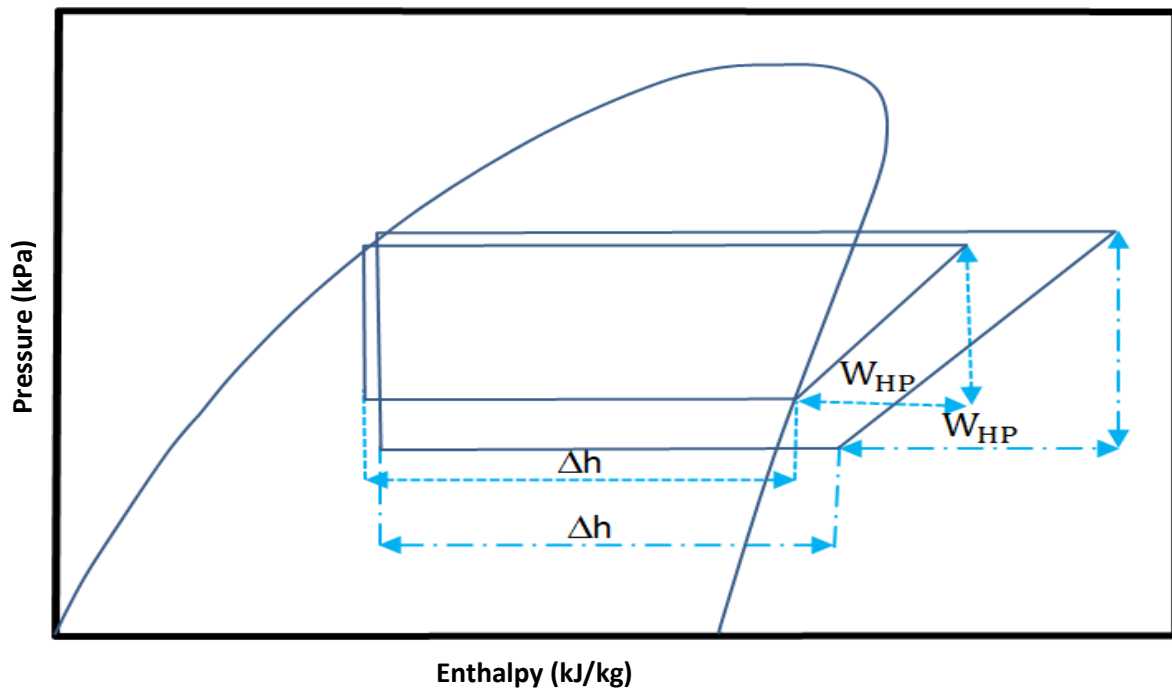


Figure 5.37 Vapour compression cycle on pressure–enthalpy chart

The daily monitored electricity consumption of HPs 1 and 3 during the heating operation periods is presented in Figure 5.13. As illustrated in Time Period A the result shows that between November 2013 and January 2014 the daily electricity used by HP 1, is nearly half that of HP 3. There are two compressors per HP and the very low electricity consumption for HP 1 can be attributed to the fact that only one compressor in HP 1 has been active during the operation periods. The other compressor was unavailable due to a fault. Time Period B shows both heat pumps running at full load with similar electricity consumption after the fault on the second compressor load has been rectified.

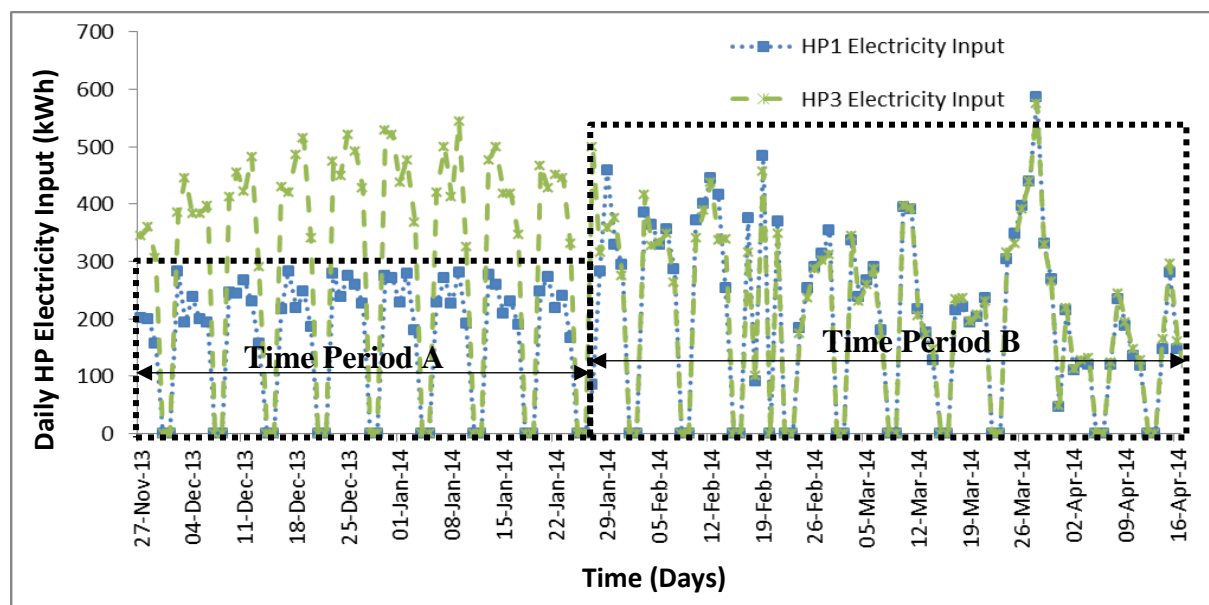


Figure 5.38 Daily electricity use by HPs

Figure 5.14 shows the total number of times that each HP has run per day between the periods of November 2013 and August 2014. The results demonstrate that HP 1 and 3 are duty cycled to ensure equal run time. The results show that although HP 1 was only operating at part load over this period, it still maintained an equal number of running hours compared with the HP 3 which had two compressors operating.

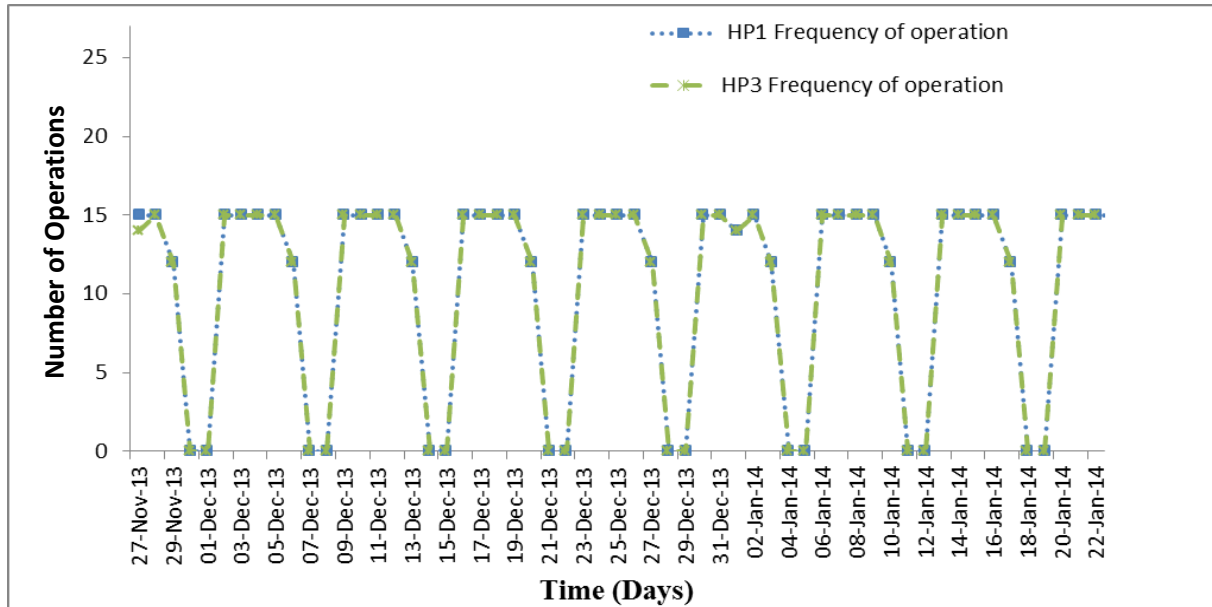


Figure 5.39 Number of running hours per day

5.4.3 Ground Temperature Variation

The performance of the GSHP system is intrinsically related to the ground and load temperatures. Further to the equations described in section 5.4.2 the reversible Carnot COP can also be calculated using the ground return temperature ($T_{\text{Source,in}}$) and temperature entering the building ($T_{\text{load,in}}$).

$$\text{Carnot COP} = \frac{T_{\text{load,in}}}{T_{\text{load,in}} - T_{\text{Source,in}}} \quad (5.3)$$

As well as monitoring the electricity consumption of the HPs the underground temperature profile at three different levels has also been monitored over the past four years. Monitoring the ground temperature distribution helps to identify the effects of (i) heat extraction, (ii) heat rejection and (iii) the long term operation of the GSHP system on the underground temperature variation. In addition the monitored underground temperature data has been used to validate the ground temperature prediction model discussed in detail in Chapter 6.

The relationship between daily ground temperature variation and performance of the HPs 1 and 3 is presented in Figure 5.15 the result shows the long term operation of the GSHP system in heating mode. As can be seen as winter progresses the overall ground temperature reduces with time. However the ground temperature and the COP of the system can also be seen to cyclically decrease and recover. This cyclic behaviour occurs between the weekday occupancy periods and the weekend when the building is unoccupied.

It is unavoidable that ground temperatures will change to some degree in response to extraction of heat from, or rejection of heat to, the ground. However, it is important to recognise that the ground is not an infinite source or sink of energy, and therefore excessive rates of heat extraction or rejection to the ground must be avoided. If excessive rates of heat extraction from or rejection to the ground are allowed for prolonged periods, then it is likely that significant changes in ground temperature will occur. Such ground temperature changes can have significant detrimental impact on the COP and therefore the overall system performance, as well as its large environmental impact. However one way of controlling the ground temperature reduction or depletion is to reject heat via a DAC when the ground and ambient temperatures favour this. The effect of heat rejection to the ground using the DAC and the effect of the DAC on the ground temperature variation is discussed in detail in Chapter 7.

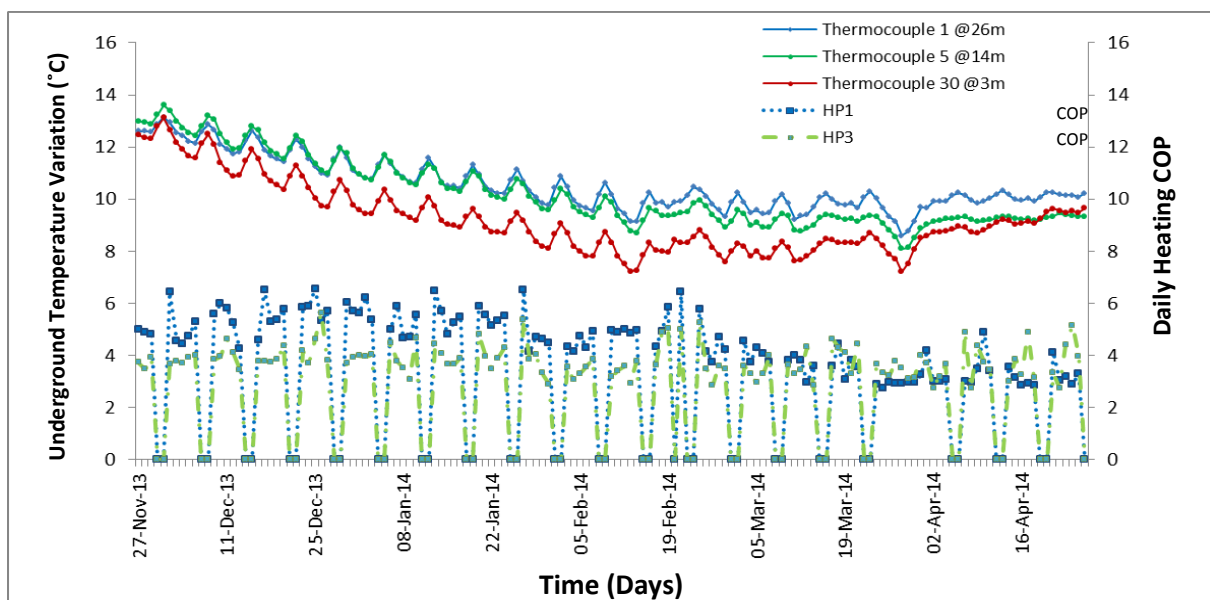


Figure 5.40 Daily COP and underground temperature variation at 3m, 14m and 26m

Figure 5.16 shows the cyclic ground temperature and COP variation in a shorter period. The result shows that between 13/01/2014 and 17/01/2014 the ground temperature reduces from 9.7 °C to 8.7 °C and for the same period the COP for HP 1 has also reduced from 6.4 to 5.5.

This shows a direct relationship between ground temperature variation and performance of the HPs.

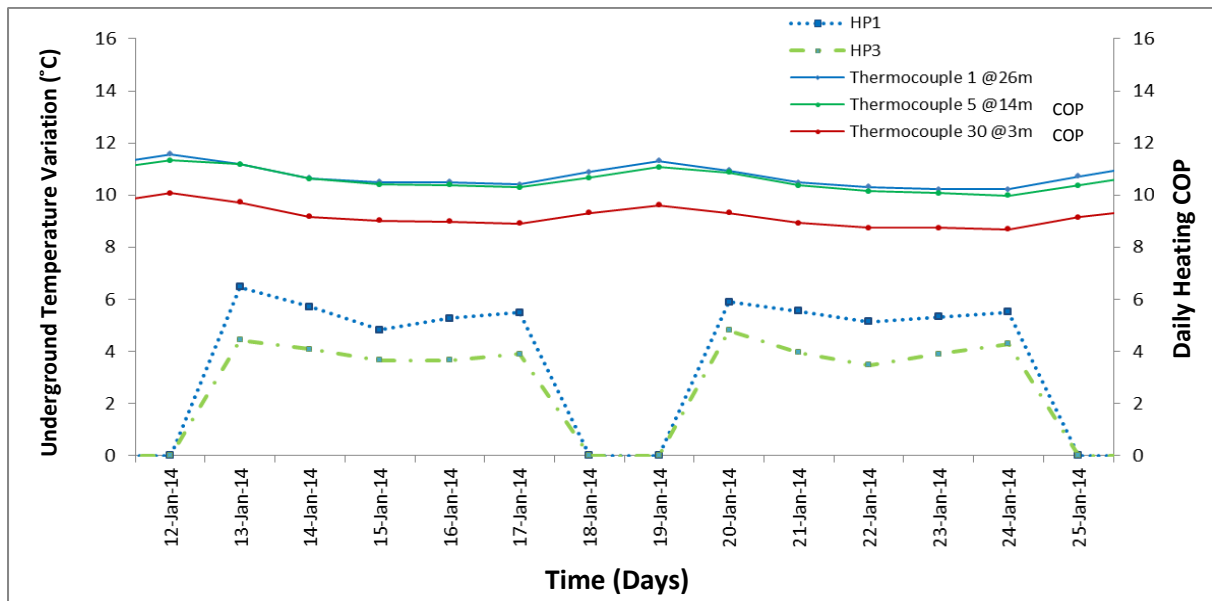


Figure 5.41 Daily COP and underground temperature variation at 3m, 14m and 26m

5.4.4 CO₂ Saving by the GSHP

An additional important advantage of GSHP systems is the possibility of saving CO₂ emissions compared to other commercial and domestic heating alternatives. A comparison has been made between the CO₂ emissions produced as a result of the electricity consumed by the HP, and the potential CO₂ emissions that would result from the use of other conventional heating methods such as GFB. The CO₂ emission saving was calculated as follows:

$$\text{CO}_2 \text{ emission from HP}[\text{kgCO}_2] = \text{ED}[\text{kWh}] \times 0.494 \left[\frac{\text{kgCO}_2}{\text{kWh}} \right] \quad (5.4)$$

Where ED is the energy input to the HPs. The CO₂ equivalent for a typical energy mix for heating was 0.184 kgCO₂/kWh. Hence, assuming an equivalent heating demand (HD), the CO₂ emission from GFB was determined using the following equation.

$$\text{CO}_2 \text{ emission from GFB}[\text{kgCO}_2] = \frac{\text{HD}}{\text{Boiler Efficiency}} [\text{kWh}] \times 0.184 \left[\frac{\text{kgCO}_2}{\text{kWh}} \right] \quad (5.5)$$

Using equations 5.4 and 5.5 the CO₂ savings by the GSHP system during the operation period was calculated as follows:

$$\text{Daily carbon savings [kg CO}_2\text{]} = \text{CO}_2 \text{ emission from GFB} - \text{CO}_2 \text{ emission from HP} \quad (5.6)$$

Equation 5.6 provides an appropriate average estimation of CO_{2e} savings attributed to the use of GSHP system. Figure 5.16 shows that due to the ground temperature reduction the COP of the system has reduced from 6.4 to 5.5. Therefore relating this COP reduction to CO₂ emissions using equation 5.6, approximately 79 kgCO_{2e} savings can be achieved by HP 1 at a COP of 6.4 compared to a CO_{2e} saving of 48 kgCO_{2e} at a COP of 5.5. Increasing the COP of the HP from 5.5 to 6.4 has therefore resulted in a CO_{2e} saving of approximately 40 %. This highlights the importance of achieving the highest possible COP for the HP in order to obtain the highest CO_{2e} savings.

5.5 Summaries

This chapter has described the commissioning of the experimental apparatus and investigation of initial results. It specifically described the process taken to investigate the difficulties and installation errors encountered during the installation and design stages of the GSHP system. A significant amount of time has been spent analysing and interpreting the data from the complex heat metering system and a substantial range of generic installation problems that the RACHP industry is currently facing have been identified. The work carried in this research has provided new practical insights into the operation of the GSHP and a real contribution to knowledge. The findings obtained from this chapter provide useful information for design and implementation of future GSHP systems in terms of improving energy efficiency as well as reducing costs. This chapter has identified that many of the temperature sensors were positioned and installed incorrectly. Incorrectly connected components or poorly sealed joints are another potential source of error, which can vary depending on the errors made.

This chapter further presented the validation of the experimental data as well as an in depth analysis and evaluation of the monitored performance data. Given the lack of availability of long term reliable HP data this study could be used in identifying some of the basic valuable information on heat measurement and consequently the long term GSHP performance in real life conditions. This chapter has shown that the performance of GSHP systems and their long term operational cost can be improved by operating the HPs at part load and with the use of a DAC.

This chapter has also looked at the benefits of utilising the GSHP for carbon savings compared to other commercial and domestic heating and/or cooling alternatives. The analysis has shown that low COP values could increase both cost and emissions compared to the use of a GFB, therefore it is important to ensure that the GSHP system is correctly installed and operating optimally with high COPs.

Chapter 6

Development of a Mathematical Model for Predicting Underground Temperature Distribution

6.1 Introduction

The critical literature review in Chapter 2 and the performance analysis in Chapter 5 have shown that the performance of the GSHP is highly dependent upon its interaction with the underground temperature distribution, and specifically the rate of heat extraction from and heat injection to the ground. There has been little work carried out to determine the relationship between the seasonal underground temperature variation and the performance of the GSHP system. Despite the importance of ground temperatures on performance, relatively little data has been published on disturbed underground temperature distributions. This is due to lack of experimental data and suitable mathematical models developed to investigate disturbed ground temperature.

This chapter presents detailed methods and approaches in the development of a novel mathematical model for predicting the seasonal disturbed underground temperature variation over time. This variation is caused by the seasonal operation of the GSHP system to extract heat from and inject heat to the ground. The novel model is a combination of two methods to calculate the dynamic disturbed ground temperature. This chapter therefore starts by discussing and describing the development and derivation of the first method which is a generic underground temperature model for estimating the annual variation of the daily average undisturbed ground temperature at different depths. Particularly the author has identified that the previous ground temperature model is only applicable to depths of up to

100 m. Consequently this model has been extended to include the effect of geothermal heat at depths beyond 100 m.

Subsequently this chapter provides the development and derivation of the second method, which gives the seasonal disturbed underground temperature variation over time. The model utilizes easily accessible data such as the annual daily average air temperatures, thermophysical properties of the ground and fluid temperatures to predict the seasonal underground temperatures depending on depth and time of year.

Furthermore this chapter provides validation of the mathematical model using long term historical underground temperature data obtained from the experimental apparatus described in Chapter 4. Finally it introduces a concept of a new optimisation control strategy based on the seasonal ground temperature variation.

6.2 Ground Temperature Prediction

The ground temperature fluctuates both annually and daily and is affected mainly by variations in air temperature, solar radiation and the effect of geothermal heat. This is termed undisturbed ground temperature variation. However, the ground temperature can also fluctuate both annually and daily, due to the effect of heat drawn from or added to the ground using the GSHP system. This is termed disturbed ground temperature variation. The undisturbed annual variation of the daily average ground temperature at different depths can be estimated using a sinusoidal function which is described in detail in section 6.2.1. Figure 6.1 below shows flow diagrams for the two scenarios of ground temperature variation i.e. with and without a GSHP installation. Mohamed et al. (2014) described that the ground temperature profile is characterized by three different zones: (i) surface zone (down to 1 m below the ground surface), (ii) shallow zone (from 1 m to 8 m), and (iii) deep zone in which the temperature remains almost constant throughout the year (below about 8 m).

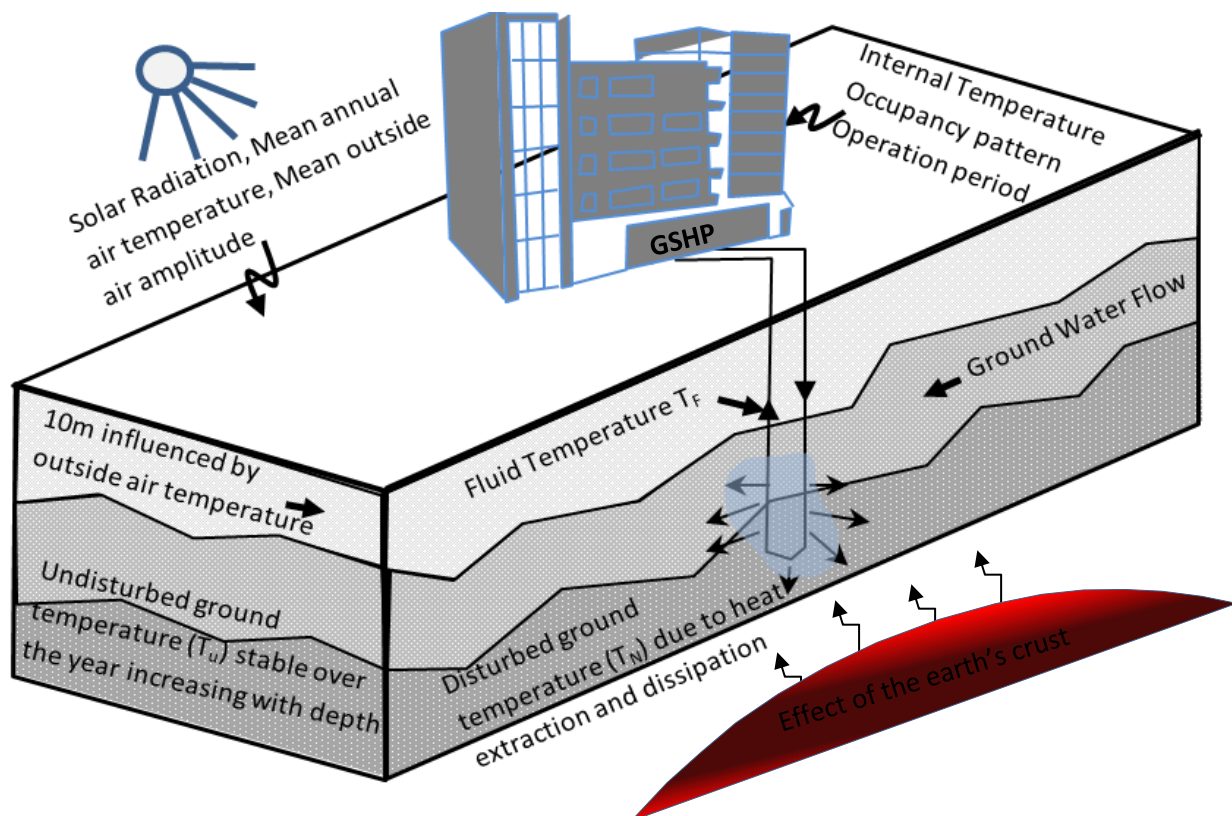


Figure 6.42 Flow diagram undisturbed and disturbed ground temperature pattern

6.2.1 Methods for Previous Models and Equations

In this section the development and derivation of the generic temperature model for estimating the annual variation of daily average undisturbed ground temperature at different depths is described. Subsequently in the second method of section 6.3, this generic model will be used as an input to develop and derive the mathematical model for predicting the disturbed ground temperature variation.

6.2.2 Undisturbed Ground Temperature Variations with Time and Depth

In order to derive the generic undisturbed ground temperature model, transient heat flow principles were used and certain simplifying assumptions were made in this study (Nagano, 2007; Esen and Inalli, 2009).

6.2.3 Assumptions

- The soil at site was clay, with a thermal conductivity (λ) of 1.3 W/ m K.
- T_m , the annual mean air temperature was assumed equal to the average ground temperature.

- Measurements of the ground temperature for 3.2 m, 14 m, and 26 m depth were obtained from the LSBU ground temperature monitoring system for hourly, daily and monthly average values for the last 4 years.
- Thermal diffusivity is constant, and assumed to be 0.083 m² / day
- The heat flow is one dimensional
- In all computations any interfacial resistance between the thermal probe and the bare soil has been neglected.

Using the above assumptions, the heat conduction equation can be used (Gao, 2008; Michopoulos et al. 2007).

$$\frac{\partial}{\partial t} T(z, t) = \alpha \frac{\partial^2}{\partial z^2} T(z, t) \quad (6.1)$$

Furthermore, assuming the transient period to be over, a steady state can be assumed to exist. Under these conditions the ground temperature fluctuates according to the mean yearly air temperature T_m if radiation effects and the geothermal temperature gradient are neglected. However, the amplitudes of the ground temperature fluctuations decrease with depth due to the thermal inertia of the ground.

A sinusoidal forcing function was used to represent the variations in heat transferred to the ground at the surface ($z = 0$). For this, a sinusoidal temperature function that fulfils the differential equation (6.1) but uses the corresponding boundary conditions derived by Hillel Gao (2008) involved the use of initial and appropriate boundary conditions to yield the following equation:

$$T(z, t) = T_m + A_z \eta e^{-\frac{z}{d}} \sin[\omega (t - \varepsilon) - \frac{z}{d}] \quad (6.2)$$

Where

$$d = \sqrt{\frac{2\alpha}{\omega}} = \sqrt{\frac{\alpha t}{\pi}} \quad (6.3)$$

$$\eta = \frac{1}{\sqrt{1+2k+2k^2}} \quad (6.4)$$

$$\varepsilon = \arctan \frac{k}{1+k} \quad (6.5)$$

$$k = \frac{\lambda}{hd} \quad (6.6)$$

$$\omega = \frac{2\pi}{t} \quad (6.7)$$

$T(z, t)$ (°C) is the ground temperature at time t and depth z .

T_m (°C) is the mean surface temperature.

ε (days) is the time lag needed for the surface ground temperature to reach T_m .

A_z (°C) is the amplitude of temperature wave at depth z .

d (m) is the damping depth.

t (s) is the period duration of temperature oscillation.

h (W / m² K) is the heat transfer coefficient from ground to air.

k is the hydraulic conductivity; permeability coefficient.

α (m² / s) is the thermal diffusivity.

ω is angular frequency of temperature oscillation.

η is the amplitude factor of the surface temperature.

6.2.4 My Contribution

The generic undisturbed ground temperature prediction model assumes that the ground temperature below 10 m is likely to remain constant at around 12 °C to 14 °C and that this ground temperature behaviour can be predicted using equation 6.2. However due to the effect of geothermal heat below depths of 100 m, the ground temperature is expected to increase by 2 °C to 3 °C for every 100 m and a linear relation between temperature and depth is observed, which is called thermal gradient (Fridleifsson et al., 2008). Below this depth equation 6.2 is modified by equation 6.10. Figure 6.2 shows that when predicting the underground temperature variation at different depths with time, the generic ground temperature prediction model assumes the underground temperature remains constant; this is illustrated in Zone A. Therefore the author has extended this generic formula to include the phenomenon effect of the earth's crust below 100 m which is shown in Figure 6.2 Zone B.

$$T(z, t) = T_m + A_z \eta e^{\frac{-z}{d}} \cos[\omega(t - \varepsilon) - \frac{z}{d}] + \sum_{n=100}^{\infty} \frac{2.5n}{100} \quad \text{For } 100 \leq n \leq \infty \quad (6.10)$$

Figure 6.2 illustrates the underground temperature distribution curves at different times (P).

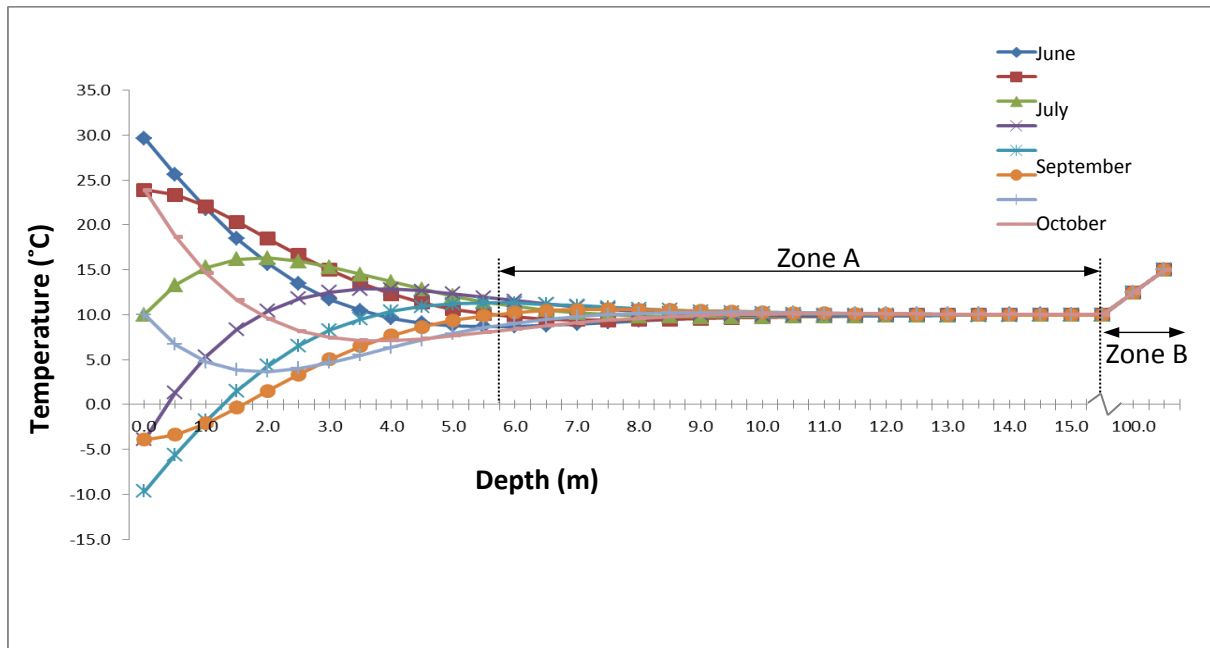


Figure 6.43 Undisturbed underground temperature distributions at different times

Figure 6.3 below demonstrates how the amplitude of the diurnal ground temperature wave is expected to decrease exponentially with increasing depth with the ground, assuming the thermal characteristics of the ground are considered constant with depth and time of day. It is evident that the amplitude of the surface temperature decreases by a factor ($\eta < 1$) in relation to the air temperature and, moreover, undergoes a time lag of ϵ .

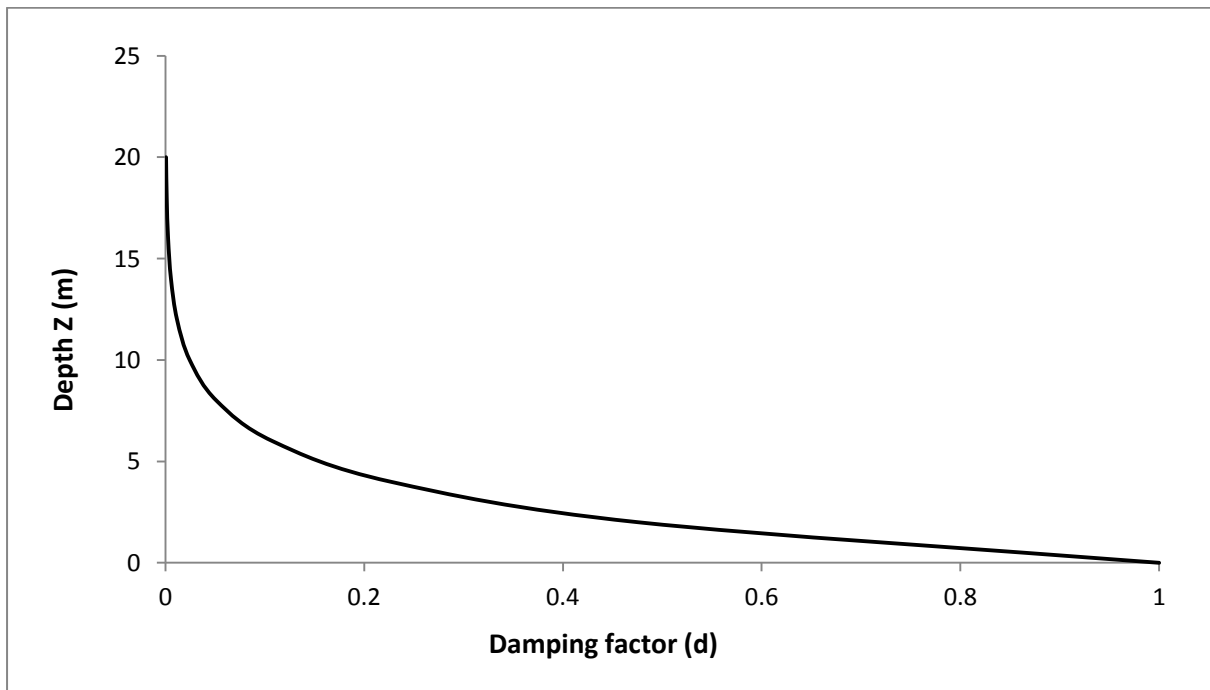


Figure 6.44 Depths against damping factor of the ground

6.3 Development of Mathematical Model for Disturbed Underground Temperature Distribution

Calculation of the temperature distribution in the ground resulting from heat extraction or heat dissipation from or into the ground is increasingly being demanded by local authorities. Such data is needed for system design parameters, evaluating the viability of GSHP schemes and environmental risk assessment. Of particular concern is the possible influence on adjacent ground properties and on the groundwater resulting from the long term operation of the GSHP system. GSHP systems use the ground whose temperature is not heavily dependent on the ambient temperature. Ground temperature can, however, increase or decrease over long periods of time because of the energy imbalance between the building's heating and cooling loads and such energy imbalance can degrade the HP's performance.

In this section, the development and derivation of a new mathematical model for predicting the disturbed underground temperature distribution pattern is described, in detail.

6.3.1 Methodology and Assumptions

This new mathematical model has been termed Seasonal Disturbed Ground Temperature Prediction (SDGTP). The mathematical model has been developed using the Finite Difference Method. It is used to predict the disturbed underground temperature variation due to the long term operation of the GSHP system.

When a heat extraction period commences at the start of operation of a HP, a sudden change in the temperature levels occur in the ground heat exchangers (GHX). Part of the heat that is absorbed by the circulating fluid is heat that is stored in the different materials inside the foundation of the building, e.g. pipe, groundwater and grouting. Consideration of these capacitive effects is important when studying the short term behaviour of these systems. However, this influence decreases as the GHX become more efficient, since the thermal resistances in the thermopiles are minimized and problems depend more and more on the thermal process in the ground itself.

For the transient response of the ground to heat pulses which occur during heat extraction periods that disturb the ground's temperature with a certain periodicity, it can be said that the

heat exchanged in the thermopiles is a function of time. This process is then superimposed onto the natural stationary temperature distribution that previously existed in the ground.

In the present model, the disturbed temperature at a given point within the ground is a superposition of two different mechanisms for estimating the disturbed seasonal ground temperature. T_N which takes account of the sudden change of ground temperature over time due to the system's fluid temperature and T_U which is the initial natural stationary temperature distribution that previously existed in the ground at $t = 0$. For the undisturbed ground temperature, the amplitude variation reduces to zero below a certain depth e.g. from around 10 m below the surface the effect of the outside temperature diminishes and effectively the ground temperature remains constant.

The effect of the GSHP system on the dynamics of the ground temperature variations can be simulated by considering an initial temperature T_U at $t = 0$, assuming a sudden temperature change T_N between the GHX element and the ground with which it is in contact. The temperature near the surface of the GHX will increase because of the fluid temperature change T_F , while the temperature far from the surface of the GHX is not affected and remains at the initial temperature T_U .

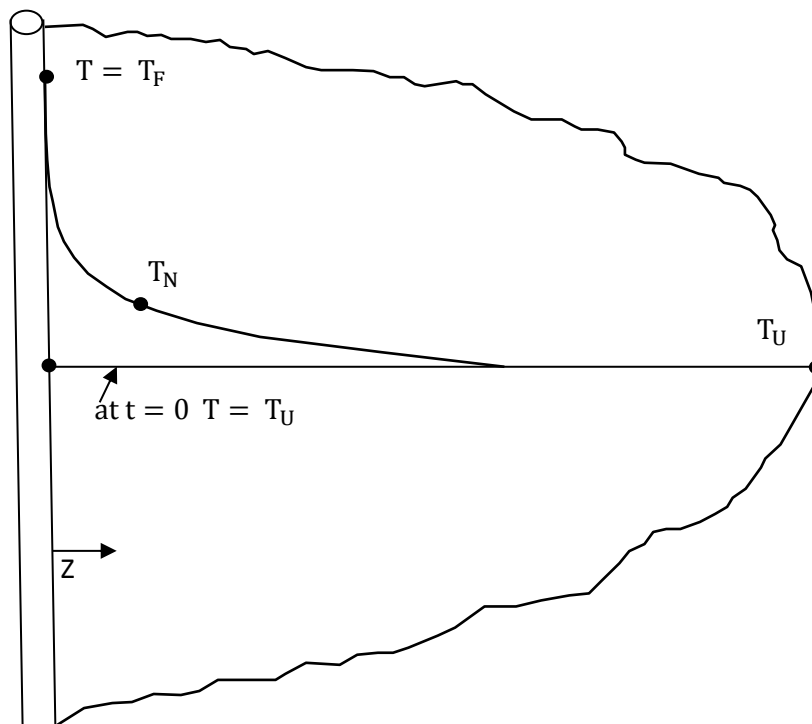


Figure 6.45 Physical model of the ground temperature change due to GSHP

The physical model of the problem is illustrated in Figure 6.4, and the governing equation for the temperature change problem and the corresponding initial and boundary conditions are (Incropera and DeWitt, 1996; Sachdeva, 2009):

$$\frac{\partial(\theta)}{\partial t} = \alpha \frac{\partial^2 \theta}{\partial z^2} \quad \text{Where } \theta = T_F - T_N \quad (6.11)$$

With the initial and boundary conditions

$$\theta = T_U - T_F = \theta_U \text{ at } t = 0 \text{ for all } z$$

$$\theta = T_U - T_U = 0 \text{ at } z = 0 \text{ for all } t > 0$$

$$\theta \rightarrow \theta_0 \text{ as } z \rightarrow \infty \text{ for all } t$$

The variation in temperature is dependent upon $\left[\frac{\alpha t}{z^2}\right]$

$$\theta = f\left[\frac{\alpha t}{z^2}\right]$$

If for convenience we define

$$\eta = \frac{z}{2\sqrt{\alpha t}} \text{ then equation (6.11) can be written as:}$$

$$\frac{\partial^2 \theta}{\partial \eta^2} + 2\eta \frac{\partial(\theta)}{\partial \eta} = 0 \quad (6.12)$$

With the transformed initial and boundary conditions as

$$\theta \rightarrow \theta_0 \text{ as } \eta \rightarrow \infty$$

$$\theta \rightarrow 0 \text{ as } \eta = 0 \text{ for } t \geq 0$$

Integration of Equation (6.12) gives:

$$\ln \frac{\partial(\theta)}{\partial \eta} = C_1 - \eta^2$$

Or

$$\frac{\partial(\theta)}{\partial \eta} = C_2 e^{-\eta^2}$$

With further integration yields

$$\theta = C_2 \int e^{(-\eta^2)} d\eta + C_3 \quad (6.13)$$

The integral in equation (6.12) cannot be solved analytically, but it can be tabulated as error function, defined as:

$$\text{erf}(z) = \frac{2}{\sqrt{\pi}} \int_0^z e^{(-\eta^2)} d\eta$$

In terms of error function, equation (6.13) can be written as:

$$\theta = \frac{C_2\sqrt{\pi}}{2} \operatorname{erf}(\eta) + C_3$$

The constants C_2 and C_3 can be found by applying the initial and boundary conditions.

$$\theta \rightarrow 0 \text{ as } \eta \rightarrow 0 \text{ therefore } C_3 = 0$$

And

$$\theta = \theta_0 \text{ as } \eta \rightarrow \infty \text{ therefore } C_2 = \frac{2\theta_0}{\sqrt{\pi}}$$

$$\therefore \theta = \theta_0 \operatorname{erf}(\eta)$$

$$\text{Or } \frac{\theta}{\theta_0} = \frac{T_F - T_N}{T_F - T_U} = \operatorname{erf}(\eta)$$

$$\text{Or } \frac{T_F - T_N}{T_F - T_U} = \operatorname{erf}(\eta) = \operatorname{erf}\left(\frac{\operatorname{LN}\left(\frac{T_F}{T_U}\right)}{2\sqrt{\alpha t}}\right)$$

$$T_N = T_F - (T_F - T_U) \operatorname{erf}\left(\frac{\operatorname{LN}\left(\frac{T_F}{T_U}\right)}{2\sqrt{\alpha t}}\right) \quad (6.14)$$

Equation 6.14 is used in the model to calculate new values of T_N for each time step. In the heat extraction mode, the fluid is heated as it travels through the GHX channels and the temperature rises between different points when the fluid travels down and upwards and thus can be accounted for by T_{Load} which is given by equation 6.15. Clearly the heat transfer between the fluid and the surrounding ground depends on many factors such as: the thermophysical properties of the ground, the heat exchanger, the geometrical arrangement of the GHX pipes, the convective heat transfer on the circulating secondary fluid sides, and on the thermal properties of the filling material of the piles.

$$T_{\text{Load}} = \left(\frac{T_F - T_U}{\operatorname{LN}\left(\frac{T_F}{T_U}\right)}\right) \quad (6.15)$$

The ground temperature distribution pattern due to the disturbance of GSHP installation T_d can then be estimated by averaging the T_{Load} and the newly calculated temperature T_N .

$$T_d = 0.5 \left[T_F - (T_F - T_U) \operatorname{erf} \left(\frac{\operatorname{LN} \left(\frac{T_F}{T_U} \right)}{2\sqrt{\alpha t}} \right) + \left(\frac{T_F - T_U}{\operatorname{LN} \left(\frac{T_F}{T_U} \right)} \right) \right] \quad (6.16)$$

Figure 6.5 presents a complete flowchart diagram for the mathematical prediction model.

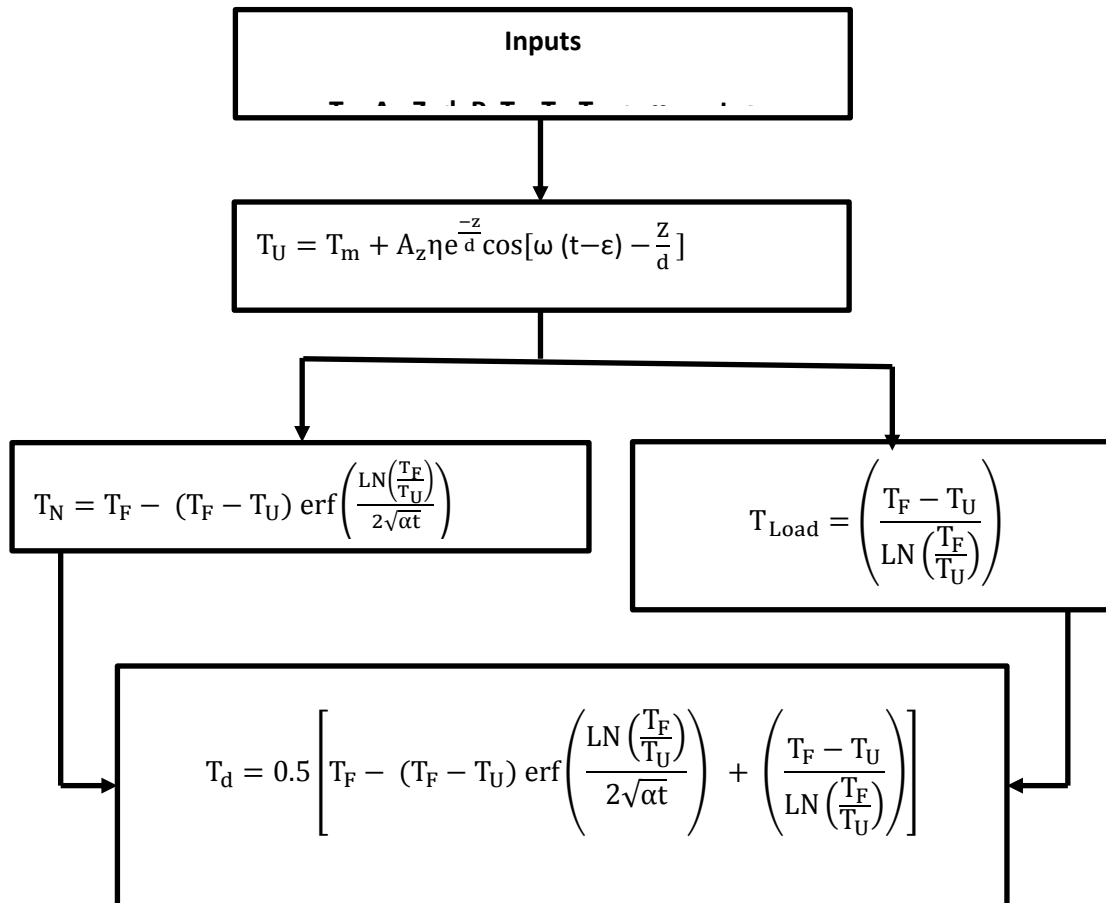


Figure 6.46 Flowchart of the model methodology of disturbed ground temperature

Using the predicted temperature T_d calculated using equation 6.16, the monthly underground temperature variation at 26 m was predicted and the temperature profile within the ground has been plotted in Figure 6.6. For a given site with vertical heat exchangers installed, the ground tends to behave differently from a site without heat exchangers. This is due to the fact that fluid will be constantly circulated throughout the year in order to balance the annual heating and cooling demand of the building. Consequently this will affect the pattern of the underground temperature distribution. The difference between disturbed and undisturbed ground temperature patterns can be seen by comparing Figures 6.2 and 6.6. The cyclic

ground variation due to the effect of the seasonal heat extraction and heat dissipation on the underground temperature profile is clearly shown in Figure 6.6, i.e. the underground temperature falls as the heating season progresses, and then increases when the GSHP system is operating in cooling mode.

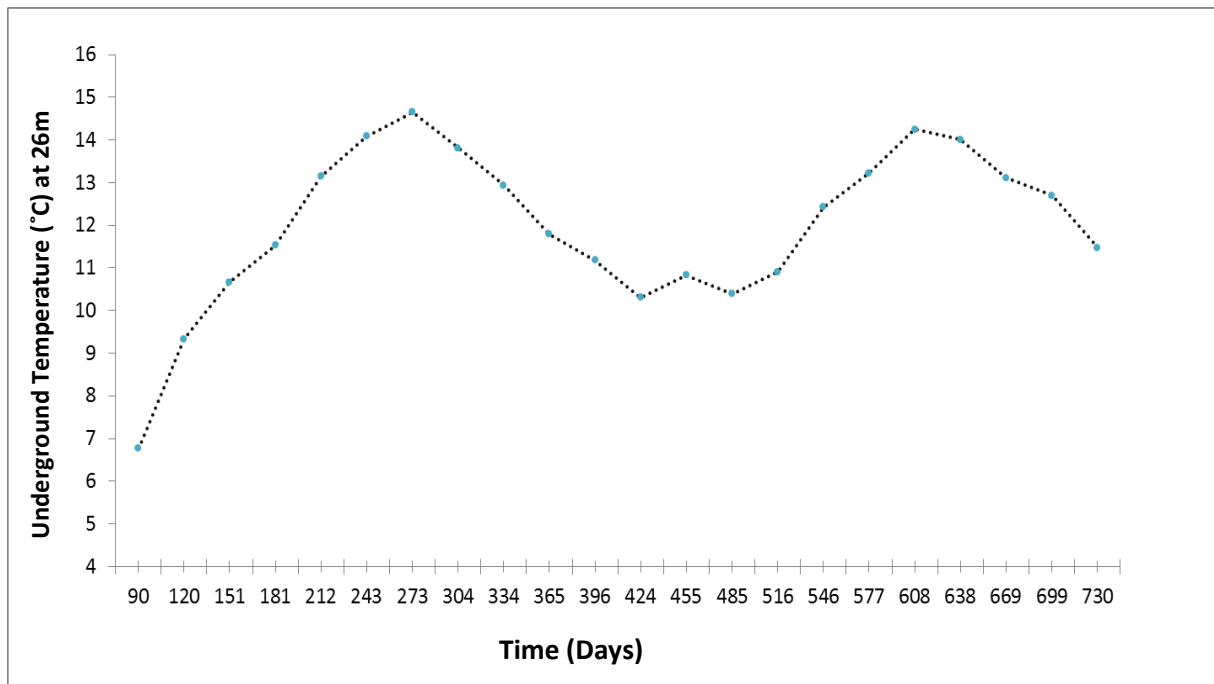


Figure 6.47 Monthly predicted disturbed underground temperature distribution at 26 m

The benefits of establishing the seasonal ground temperature range at which the ground temperature fluctuates is that it helps to understand the dynamics of the underground temperature variation with and without a GSHP installation. This information can also be used to formulate a relationship between the underground temperature variation and the system performance as discussed in Chapter 5. One of the governing factors for the performance of a GSHP system is the adequate availability of heat in the ground; therefore the SDGTP model enables the user to effectively monitor and control the underground temperature variation, by controlling the rate of heat extraction and rejection from and to the ground.

6.4 Ground Temperature Measurement

In order to validate the SDGTP mathematical model, long term historical temperature data has been used. Examples of the long term historical data are shown in Figures 6.7 and 6.8 below. Air and ground temperatures generally exhibit a diurnal cycle. Figure 6.7 displays the seasonal outside air temperature at London South Bank University between January 2010 and

December 2013. The air temperature data were acquired using commercial T-type thermocouples with Teflon coating connected to a data logger. It can be seen that the annual variation in the air temperature is approximately sinusoidal, but that obvious year to year differences exist.

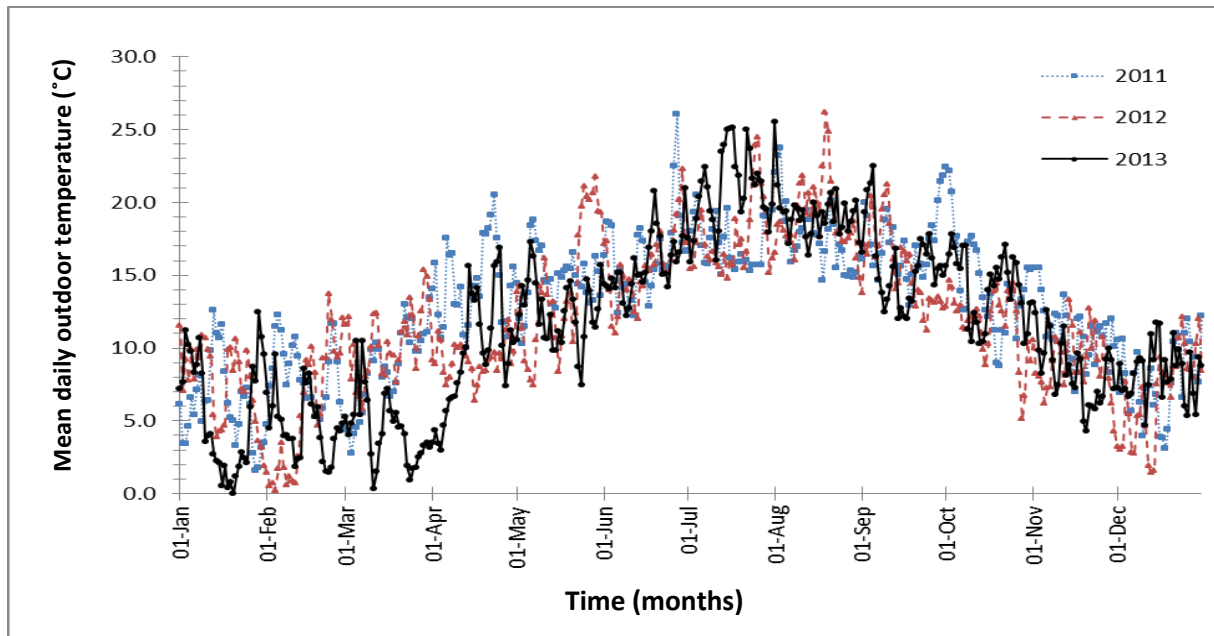


Figure 6.48 Mean daily outdoor air temperature variation in London

Figure 6.8 presents an example of underground temperature measurements carried out with thermocouples at different points along the U-pipe GHX. These historical underground temperatures were measured using 32 thermocouples over the period of August 2010 to August 2013. The figure shows the temperature variation over three years of the GSHP operation as well as the effect of load shifting in winter and summer to ground temperature variation.

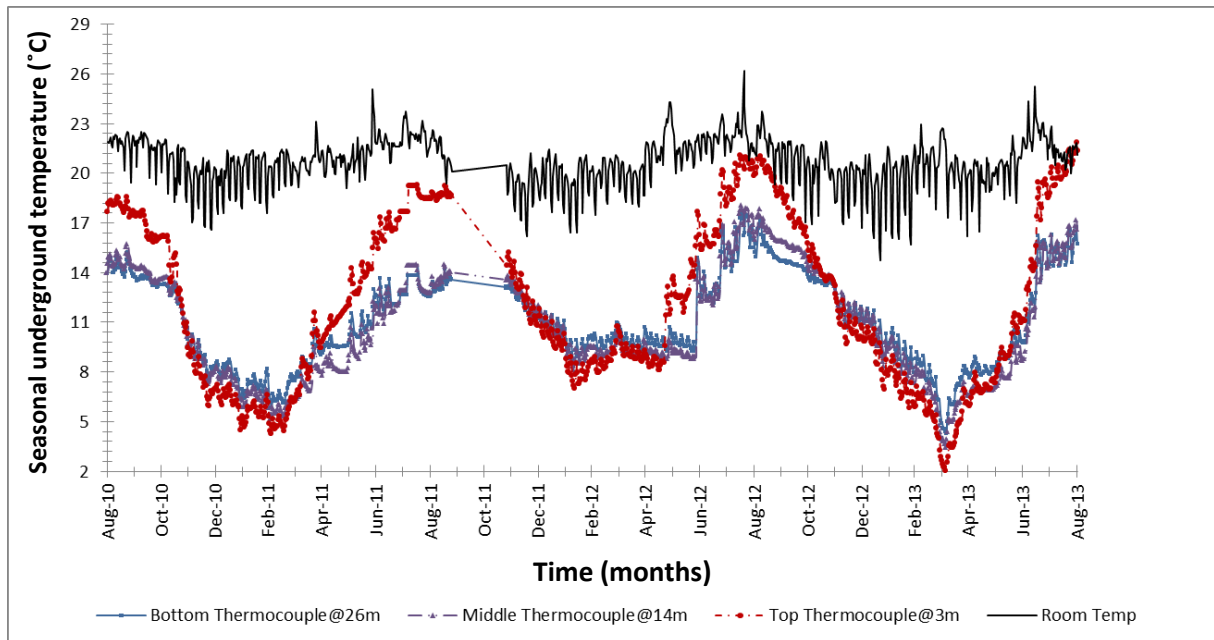


Figure 6.49 Seasonal ground temperature variations during HP operation

Over the two heating and cooling seasons Figure 6.8 shows that the underground temperature between August 2011 and February 2012 started at about 20 °C, which was higher than the ground temperature in the same month the previous year (2010) i.e. 18 °C. However between 25 September 2012 and 11 October 2012 heat was injected to the ground constantly, which ultimately enabled the ground temperature to recover and remain warmer than the previous year throughout the heating season. The bottom and middle thermocouples are lower in August 2011 than the previous year. The duration of each HP cycle will vary according to the outdoor temperature and the building energy demand.

The graph also shows that in the first winter (2010 – 2011) heat was extracted at a greater rate from the ground, particularly in January and February 2010, which were colder months than their counterparts in the following year. The temperature in the period October 2012 to March 2013 show significantly lower ground temperature than the previous year. The 2013 winter was longer compared to the other two previous winters. This may have long term ramifications for seasonal COP values. It is apparent that the heat distribution in the thermopile varies according to the building demand and how often the heat is added. However, the ground water movement is also important in facilitating the ground recovery rate characteristic. One interesting phenomena that can be seen in Figure 6.8 in relation to the top, middle and bottom thermocouples is that the rate of heat recovery at the three levels are different to each other. The bottom thermocouple recovers faster than the middle and top

levels. This characteristic can only be accounted for by the influence of ground water movement.

6.5 Model Validation

The mathematical model developed by the author in section 6.3 was validated against the above historical measured underground temperature data obtained from the GSHP system installation at LSBU's K2 building. To allow close monitoring of the underground temperature distribution, and also to investigate the effects of heating and cooling on the building's structure, seven of the 28 m deep piles were equipped with thermocouples at three different depths of 3.2 m, 14 m and 26 m. These effects are shown in Figure 6.8. The piles have diameters of approximately 750 mm. The installation also includes stress gauges to allow correlation of stress versus ground temperature. One dummy thermopile is also being monitored as a reference-case.

Acquiring the historical underground temperature data has required continues monitoring and recording of hourly ground temperature data for the K2 building for the last 4 years (2010 – 2014). The building has extensive heat and electricity sub-metering to enable performance monitoring and evaluation at the level of individual zones. Both the historic and current data obtained using the K2 GSHP system has been stored in the Building Energy Management System (BEMS). The BEMS has been configured to enable rapid data acquisition for all of the key services and energy meters within the building. The results are retrievable from a web-based system and the BEMS is also linked to monitoring and targeting software, available on the web.

The historical underground data has been recorded in three different formats. For validation and analysis purposes, a method of exporting and extracting the data using a Microsoft Excel spreadsheet model has been developed in order to minimize reliability issues. This was developed using Excel worksheet functions incorporating Visual Basic code. The worksheet is linked to a separate database containing the value for the heat energy delivered to the building, the thermal energy extracted by the GSHP from the ground, the thermal energy injected into the ground; the electricity consumption of the GSHP and the ground temperatures. The spreadsheet model has been programmed to search for certain parameters such as temperatures, electricity input, in the database and perform calculations of, the COP of the GSHP, as well as energy savings using the GSHP compared with a conventional

method of heating (i.e. gas fired boiler) and carbon savings. It can also display the output of the calculations on a daily, weekly, monthly or yearly basis.

Figure 6.9 shows a comparison of the model predicted and actual measured historical underground temperature at 26 m depth. A comparison between the predicted mathematical model and the historical measured underground temperature data obtained from the LSBU's K2 building shows a good level of agreement with the actual measured temperature data. Figure 6.9 illustrates for an annual cycle; at depth of 26 m, the average maximum percentage of error was estimated to be approximately $\pm 7\%$. Although that the model results are an approximate and depend on the theoretical approach and assumptions employed, the estimated errors are generally within an acceptable range for the purposes of calculation of heating and cooling design parameters and can substantially reduce the need for detailed site surveys.

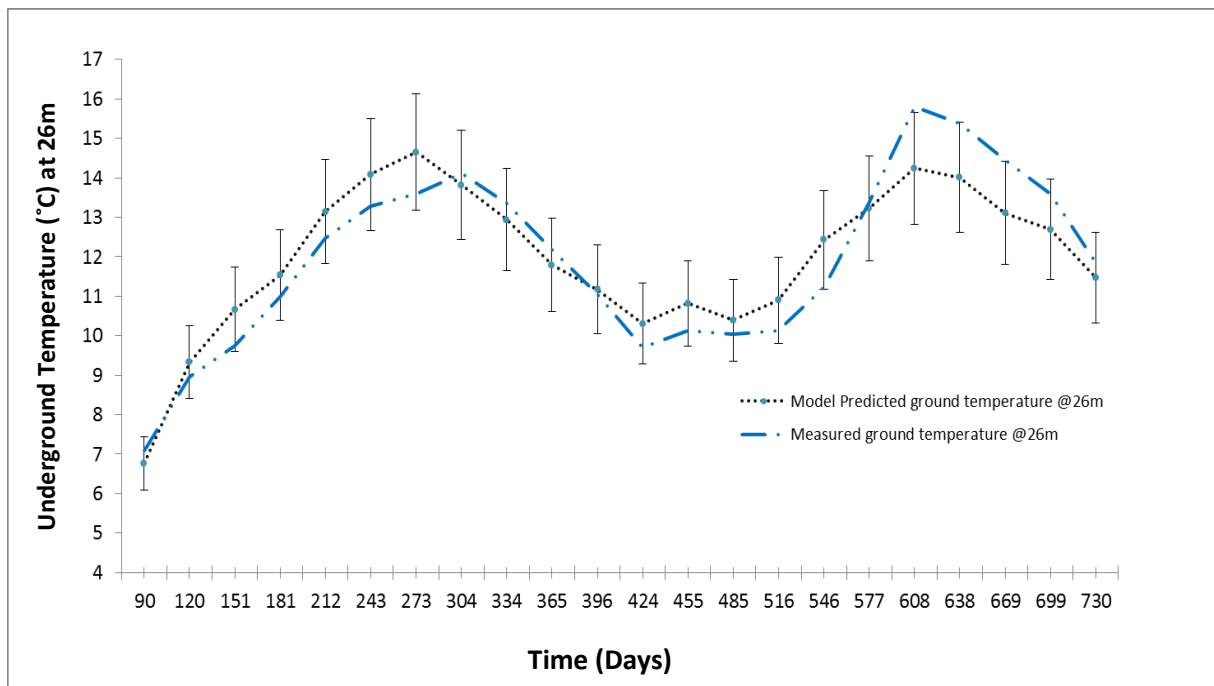


Figure 6.50 Comparison of model predicted and measured disturbed ground temperature at 26 m

As the long term data for ground temperatures and soil characterizations are not available in many parts of the world, the model developed in this study could be used to help reduce economic and technical risks for designers and project decision makers in applications involving shallow subsurface heat exchange, such as that investigated here.

6.6 Optimisation Based Control Strategy

In sections 6.2 and 6.3 above the mathematical model developed for estimating the seasonal underground temperature variation has been described. The model has also been validated against historical measured underground temperature data. In this section a simple concept of optimisation of control strategy is discussed to improve the performance of the GSHP system at LSBU's K2 building. This is based on the model's predicted underground temperature. The main advantage of this control method is that it provides adequate control for (i) monitoring, (ii) planning the use and (iii) operating the GSHP system. The underground temperature range could be a useful tool for making predictive decisions which could influence not only the energy consumption of the GSHP system specifically but also the building's occupancy energy demand behaviour.

It is important to recognise that the ground is not an infinite source or sink of energy, in that prolonged periods of heat extraction can lead to a worst case scenario of the ground temperature dropping to 0 °C or in a very rare occasion there is the possibility that the ground temperature could freeze. When the ground temperature decreases or increases to extreme limits, the ground may reach a point of saturation, where heat can neither be extracted nor be injected from or to the ground. This ground temperature change will result in deterioration in the system's performance and large environmental impacts.

The historical underground temperature data for the past four years as shown in Figure 6.8 illustrated that typically the underground temperature variation range was between 2 °C and 20 °C. The fact that the underground temperature is being monitored in the present case means that the information can easily be analysed and utilised by the predictive control system which uses predicted underground temperature variation provided by the model. In addition the graphical output of the underground temperature variation at different depths with time is displayed using a display mechanism to identify the effective periods and season in which the GSHP system can operate efficiently based on the displayed underground temperatures. This display mechanism is shown in Figure 6.10. In order to optimise the system's performance the predictive control can also be used to limit either the rate of heat extraction from the ground or the rate of heat dissipation into the ground. This could also help

to identify when to run the system in either monovalent or bivalent modes depending on the predicted ground temperature.

The historical ground temperature can also be used to serve as a benchmark for (i) making interventions and (ii) planning and controlling the running hours. Figure 6.10 below shows user interface, data display, and the calculated results from predicting the performance of the system, and the measured results from monitoring the ground temperature change over time. Thus when the ground temperature gauge is showing at different levels this information can then be used to switch a DAC to reject more heat to the ground, monitor, plan, control and operate the GSHP system accordingly.

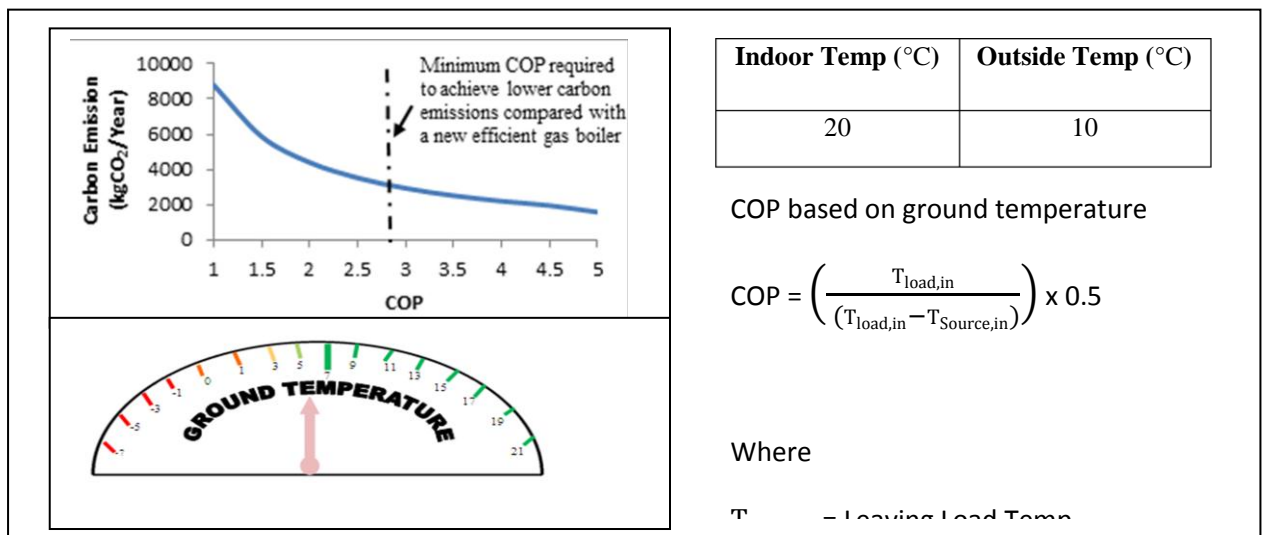


Figure 6.51 Control Strategy based on the ground temperature.

As a general rule, for every 1 °C ground temperature reduction the COP of the system typically reduces by 3 % and this effect can be easily identified from this control system. The user interface in Figure 6.10 also provides additional information on the carbon emissions emitted based on the COP of the system and the level of COP a GSHP would have to achieve a lower carbon emissions compared with a new efficient gas fired boiler. The graph in the user interface can be used to indicate the carbon emissions of the technology in comparison with a gas fired boiler. The graph shows the carbon emissions reduction with increasing COP. HPs must achieve a minimum COP of 2.9 before achieving overall energy savings. Note that even with COPs of 2.9 the carbon footprint of HPs will be higher than the gas fired boiler, this simple predictive control mechanism can nevertheless be used to indicate performance volatility.

Table 6.9 *Control strategies based on predicted ground temperature*

Ground Temp range (°C)	Status	Strategy
<3	HP running inefficiently	Either switch off the system or select bivalent alternate operation
3 – 5	Warning	Change over point between monovalent and bivalent mode.
>5	Normal	No action needed

Chapter 7 has demonstrated that significant carbon, cost and energy savings can be made by monitoring and controlling the underground temperature distribution using a DAC. Table 6.1 provides the user an opportunity and platform for making quick decisions, based on the predicted underground temperatures. Such information is useful, as the ground temperature profile of any site can be used to predict the approximate range of COP values for a given GSHP system. A particular concern for locations with colder ground temperatures is that the low temperatures can lead to lower fluid return temperatures from the ground and the effect of this is that the HP will be unable to achieve the manufacturer's specified COP.

6.7 Summaries

This chapter has presented the development and derivation methods of both the generic ground temperature prediction model for undisturbed ground temperature conditions and also the novel mathematical model for predicting the disturbed ground temperature caused by the seasonal rate of heat extraction or rejection from and into the ground.

This chapter has provided the validation process and the additional errors that are associated with the validation of the model against the actual recorded historical underground temperature data. It has been shown that the SDGTP model gives good agreement with the recorded data predicting daily mean disturbed underground temperatures. More specifically, a comparison of the field measured data and predicted temperature results indicated that the mathematical model developed could be used to predict the disturbed underground temperature profiles with sufficient accuracy for the purposes of engineering calculations for use in residential and commercial buildings. This could be used in heating and cooling system design and many other applications.

This chapter has also looked at an optimization based control strategy. The control strategy is applied by using temperature data predicted by the SDGTP model to assist the user in making critical decisions for optimising the performance of the system. The control strategy is one of the key components of any GSHP system. GSHP heating systems are complex to control because of swings in the daily and seasonal demands and required temperature adjustment for thermal comfort.

Chapter 7

Development of an Empirical TRNSYS Model of a GSHP System

7.1 Introduction

The critical literature review has shown that the performance of GSHP systems is intrinsically related to the ground and load temperatures. It is unavoidable that ground temperatures will change to some degree in response to extraction of heat from, or rejection of heat to, the ground. However, it is important to recognise that the ground is not an infinite source or sink of energy, and that excessively large net rates of heat extraction or rejection to the ground must be avoided. If excessive rates of heat extraction from, or rejection to, the ground are allowed for prolonged periods, then it is likely that significant changes in ground temperature will occur. Such ground temperature changes can have significant detrimental impact on the COP and therefore the overall system performance, as well as its environmental impact. However one way of controlling the ground temperature change is to reject heat via a DAC when the ground and ambient temperatures favour this.

This chapter investigates the use of a DAC to reduce the level of ground temperature saturation by rejecting heat selectively via the DAC. DACs are often fitted to GSHP systems to reject heat during extreme conditions to protect the system, rather than improve performance. Opportunities exist to control the performance of the GSHP using a DAC. However these control systems are not reported in the literature.

This chapter presents the description of the GSHP system and its operation, the simulation setup, the GSHP system and the different components used to build an empirical GSHP TRNSYS model.

This chapter also provides investigation of the potential to reduce the level of thermal saturation using a DAC as described above. In this investigation, an empirical Transient System Simulation (TRNSYS) model has been developed and used to investigate the control algorithms so as to identify the optimal operation and control strategies for the GSHP system for enhancing the system efficiency.

Specifically, this chapter investigates the effect of using a DAC in conjunction with a GSHP system. This includes investigating the (i) heat rejection, (ii) energy input to the GSHP system, fan and circulation pumps, (iii) COP and (iv) the ground temperature, using the experimental facility detailed in Chapter 5 as a case study.

7.2 Description of the System and Its Operation

The proposed system employs the existing LSBU's GSHP installation and components but operates it differently to how it was originally configured. The GSHP system within the K2 building at LSBU uses four WaterFurnace EKW130 reversible HP units. Each has a nominal capacity of 120 kW for heating and 125 kW for cooling. The heat is transferred from and to the ground through a closed loop system with the aid of 159 vertical energy piles which are built into the foundations of the structure and bored into the London clay. The building's heating and cooling demand is fully met by the GSHP system. The source-side of the system consists of energy piles and header pipes to which the HPs add or extract heat using a heat transfer fluid which is pumped and exchanges energy between the building and the ground.

The original system utilised a DAC designed to operate when the heat sink temperatures were either too high or too low. The DAC was therefore employed as a safety device to protect the GSHP system from operating outside its safe envelope. In the proposed system the DAC was used tactically to improve the efficiency and performance of the heat pump and therefore system. The system simulated is shown in Figure 7.1 below. This shows the system controlled to provide heat rejection via the DAC rather than the ground loop to achieve the best COP. This relies on the principle that heat pump efficiency or COP is affected

significantly by its temperature lift with a 1K reduction giving typically a 3 % rise in COP. The DAC can therefore be employed selectively when it will produce more favourable heat sink temperatures (and therefore higher COP) compared to those generated by the ground sink. The proposed system has the potential to save energy, however should not require additional components compared to the existing system, although it will be controlled differently. The performance improvement of the proposed system is investigated in detail in section 7.5.

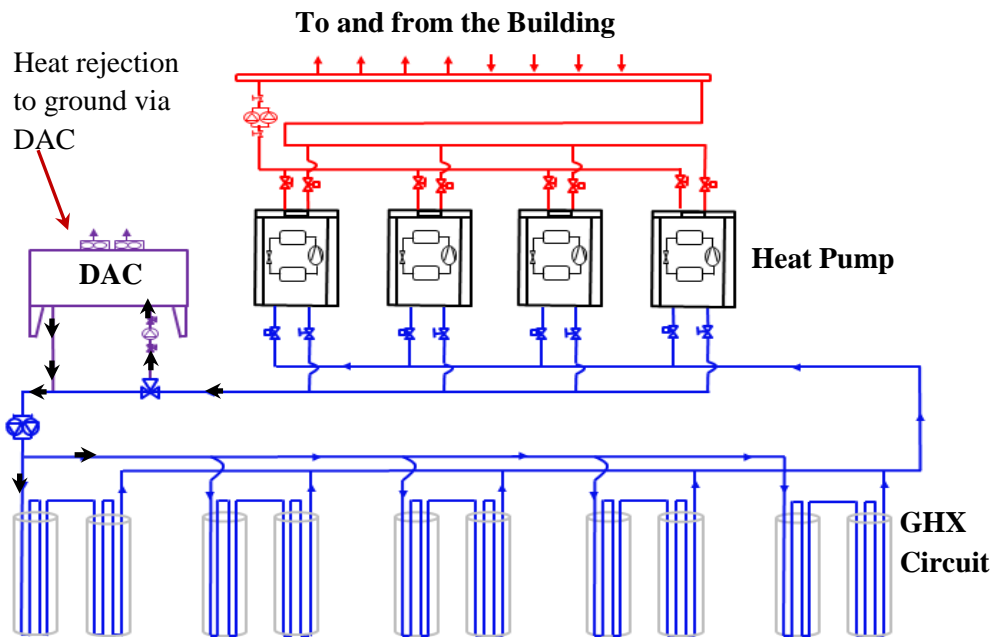


Figure 7.52 Schematic of the system simulated.

7.3 The Simulation Setup

The following section presents a description of the operation of the different components of the system which is replicated by interconnecting a set of models. In order to simulate the experimental observations, a model has been built using the TRNSYS 17 simulation software (TRNSYS, 2010). This allows the construction of a GSHP system simulator that closely resembles and simulates the actual GSHP installation. The main parts of the GSHP system that have been used in building the model are: the ground heat exchanger (Type 557), the HP model (Type 668), the circulating pumps (Type 110), simulated building load (Type 682), DAC (Type 511), tempering valve (Type 11) and tee piece (Type 11). These are described below. The system model which is used in this study is shown in Figure 7.2 below.

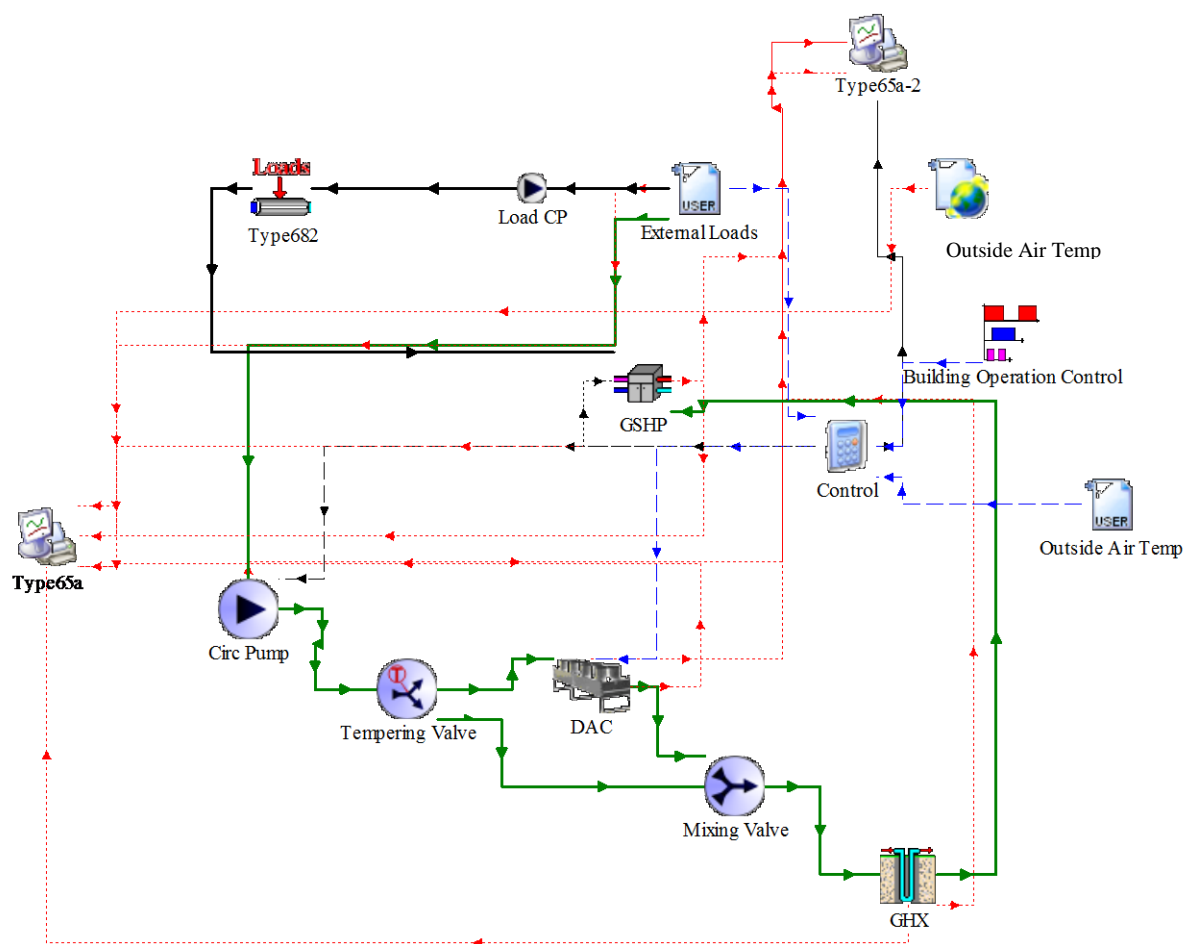


Figure 7.53 Schematics of the DAC simulation setup connected to GSHP system

7.3.1 Ground Heat Exchanger

The GHX model calculates the temperature of the surrounding ground from three parts; a global temperature, a local solution, and a steady-flux solution. The global and local problems are solved with the use of an explicit finite-difference method. The steady-flux solution is obtained analytically. The resulting temperature is then calculated using superposition methods.

The GHX component (Type 557a) was set up with the appropriate geometrical configuration and relevant ground thermal properties some of which were derived from the thermal response testing carried out in the GSHP design stage. In this model 159 energy piles were simulated each as a set of equal vertical U-tube heat exchangers which thermally interact with the ground. This GHX model is most commonly used in GSHP applications. A heat carrier fluid is circulated through the GHX and either rejects heat to, or absorbs heat from the ground depending on the temperatures of the heat carrier fluid and the ground.

7.3.2 Heat Pump Model

The HP model uses catalogue data readily available from HP manufacturers for the performance measurement related to the HP that is being simulated. At the heart of the component are two data files: a file containing cooling performance data, and a file containing heating performance data. Both data files provide capacity and power draw of the HP whether in heating or cooling mode as functions of entering source fluid temperature and entering load fluid temperature. These establish the performance envelope of the HP over a range of ground source side temperatures and a range of load side temperatures.

The data used to build this HP model were obtained from the manufacturer WaterFurnace. The Type668 HP is equipped with two control signals, one for heating and one for cooling. However, heating mode takes precedence over cooling mode. If the heating and cooling control signals are both ON, the model will ignore the cooling control signal and will operate in heating mode.

The HP's COP in heating mode is given by equation 7.1.

$$\text{COP} = \frac{Q_{\text{HP}}}{W_{\text{HP}}} \quad (7.1)$$

The amount of energy absorbed from the source fluid stream in heating mode is given by equation 7.2

$$Q_{\text{absorbed}} = Q_{\text{HP}} - W_{\text{HP heating}} \quad (7.2)$$

The outlet temperatures of the two liquid streams can then be calculated using equations 7.3 and 7.4.

$$T_{\text{Source,out}} = T_{\text{source,in}} - \frac{Q_{\text{absorbed}}}{m_{\text{source}}C_{p \text{ source}}} \quad (7.3)$$

$$T_{\text{load,out}} = T_{\text{load,in}} - \frac{Q_{\text{HP}}}{m_{\text{load}}C_{p \text{ load}}} \quad (7.4)$$

The HP's COP in cooling mode is given by equation 7.5.

$$\text{COP} = \frac{Q_{\text{HP}}}{W_{\text{HP}}} \quad (7.5)$$

The amount of energy rejected by the source fluid stream in cooling mode is given by equation 7.6

$$Q_{\text{rejected}} = Q_{\text{HP cooling}} + W_{\text{HP Cooling}} \quad (7.6)$$

The outlet temperatures of the two liquid streams can then be calculated using equations 7.7 and 7.8.

$$T_{\text{Source,out}} = T_{\text{source,in}} + \frac{Q_{\text{rejected}}}{m_{\text{source}}C_{p \text{ source}}} \quad (7.7)$$

$$T_{\text{load,out}} = T_{\text{load,in}} + \frac{Q_{\text{HP cooling}}}{m_{\text{load}} C_{p \text{ load}}} \quad (7.8)$$

7.3.3 Circulation Pumps

There are two circulation pumps in the GSHP system. In reality each pump represents a series of pumps; Type110 models a variable speed pump that is able to maintain any outlet mass flow rate between zero and a rated value. The circulation pumps are rated at 15 kW. The mass flow rate of the pump varies linearly with control signal setting. Pump electricity consumption, however, is modeled using a polynomial equation based upon the Bernoulli's principles. Pump starting and stopping characteristics are not modeled, nor are pressure drop effects. As with most pumps and fans in TRNSYS, Type110 takes mass flow rate as an input but ignores the value except in order to perform mass balance checks. Type110 sets the downstream flow rate based on its rated flow rate parameter and the current value of its control signal input.

7.3.4 Load imposed on a liquid stream

Often in simulating an HVAC system, the heating and cooling loads on the building have already been determined, either by measurement or through the use of another simulation program and yet the simulation task at hand is to model the effect of these loads upon the system. This component allows for there to be an interaction between such pre-calculated loads and the HVAC system by imposing the load upon a liquid flowing through a device.

Type682 can be thought of as an interaction point between a building load and the liquid working fluid in an HVAC system. Mathematically, the user provides the flow rate, specific heat, and temperature of liquid at a point in the system loop. The building loads are added to, or subtracted from that liquid, resulting in an outlet temperature just past the interaction point therefore the outlet temperatures of the liquid streams can then be calculated using equation 7.9. Q_{HP} is a variable load which was obtained from the experimental data and fed into TRNSYS using a DAT file.

$$T_{\text{out}} = T_{\text{in}} + \frac{Q_{\text{HP}}}{m C_p} \quad (7.9)$$

7.3.5 DAC

Type511 models a dry fluid cooler; a device used to cool a liquid stream by blowing air across coils containing the liquid. This model assumes that the device can be modeled as a single-pass, cross-flow heat exchanger; which is typically how these devices are constructed.

7.3.6 Tempering valve

The use of pipe or duct 'tee-pieces', mixers, and diverters, which are subject to external control, is often necessary in thermal systems. This component has ten modes of operation. Modes 1 through 5 are normally used for fluids with only one important property, such as temperature. Modes 6 through 10 are for fluids, such as moist air, with two important properties, such as temperature and humidity. This valve allows the system to be controlled in response to temperature of the fluid leaving the heat pump. This instance of the Type11b model uses mode 4 or mode 5 to model a temperature controlled liquid flow diverter. In mode 4 the entire flow stream is sent through outlet 1 when $T_h < T_i$. In mode 5, the entire flow stream is sent through outlet 2 under these circumstances.

7.3.7 Tee piece

This instance of the Type11h model uses modes 1 and 6 to simulate the function of a tee-piece that completely mixes two inlet streams of the same fluid at different temperatures and or humidities. This instance of the Type11h model uses mode 1 to model a tee piece in which two inlet liquid streams are mixed together into a single liquid outlet stream.

7.4 Model Validation

The developed empirical TRNSYS model was validated using experimental data from London South Bank University's actual GSHP system installation. For validation of the model, several tests have been conducted, the various physical components of the system have been kept as close to reality as possible. A comparison between model predicted and independently determined COP values for both the actual and predicted test shows a good agreement. Figure 7.3 shows that a maximum deviation of about $\pm 7\%$ is observed.

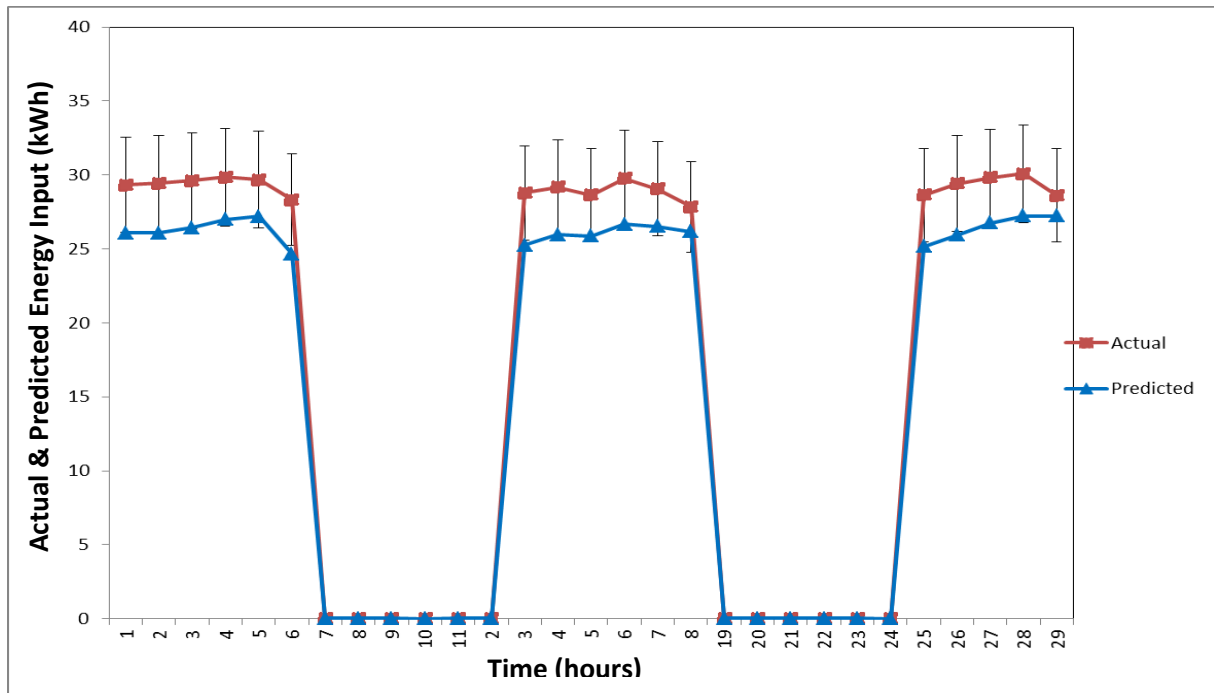


Figure 7.55 Comparison of model prediction and experimental data of energy input

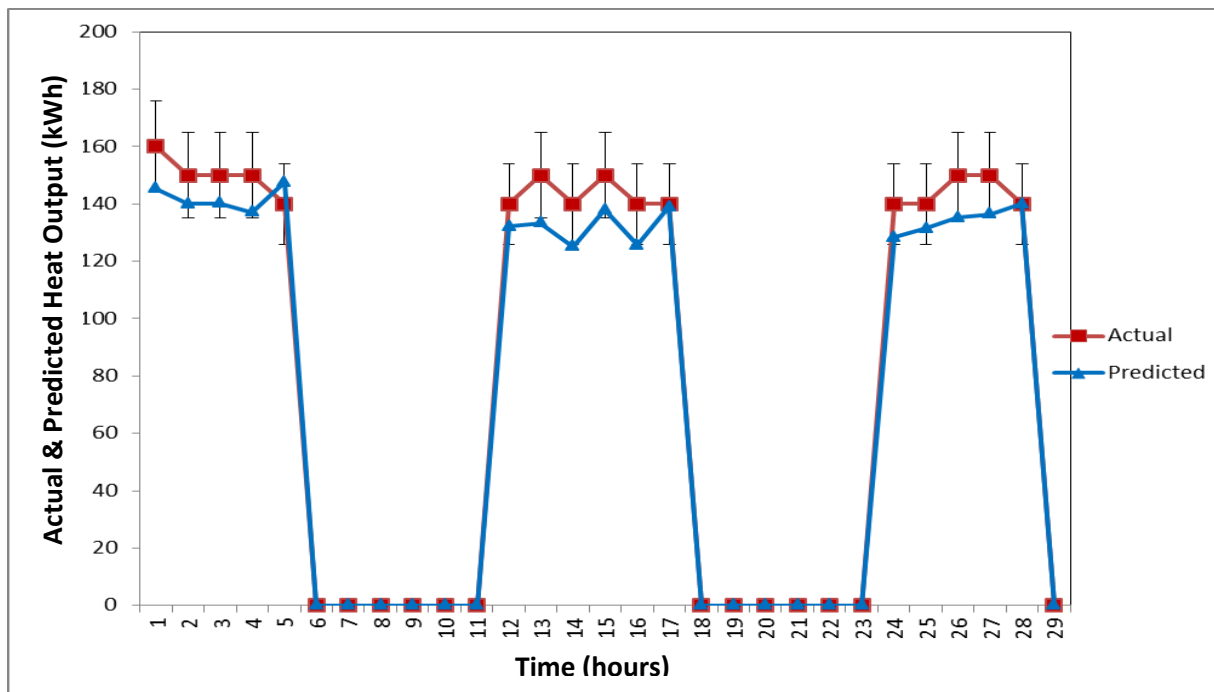


Figure 7.56 Comparison of model prediction and experimental data of heat output

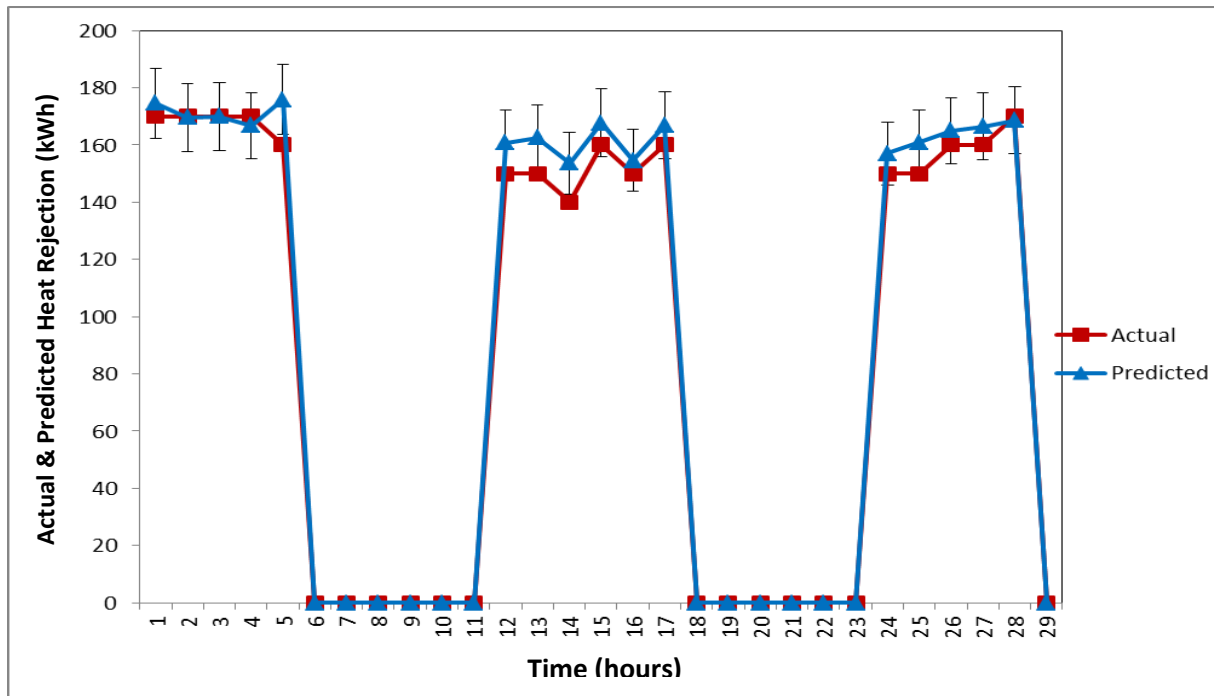


Figure 7.57 Comparison of model prediction and experimental data of heat rejection

7.4.1 Sensitivity Analysis

A sensitivity analysis has been performed to evaluate the influence of a number of input parameters that cannot be determined exactly, but estimated with some uncertainty. The term input parameters refers here to parameters that are not estimated. In addition the duration of the test and experimental measurement errors impact on the results, so a sensitivity analysis is performed. A summary of the sources of uncertainties and their effect on the estimation of energy input to the compressor, rate of heat extraction and rejection and COP of the system is given in Table 7.1. The uncertainty in the input parameters has a corresponding uncertainty in the predicted COP. A total of 22 % experimental uncertainty error has been determined, refer to Appendix B for full calculation details. As this is much greater than the difference between model and actual experiment as detailed in Appendix B, this indicates that the model is a reliable simulation tool.

Table 7.10 Summary of primary sources of uncertainties

Measurement	Meter	Uncertainty
Heat meter	Landis and Gyr T550	± 3 %
Temperature sensors Pt500	Kamstrup	± 0.3 %
Flow meter	KROHNE	± 0.3 %
Power Measurement	Aidon series 6000	± 1.5 %

7.5 Investigating New Control Strategies Using DAC

As shown in table 7.2 a number of control strategies have been identified in order to investigate the effects of different control strategy approaches using the DAC.

Table 7.11 Different control strategy approaches using DAC

<p>Control Strategy 1 (CS1) The DAC is controlled based on the fluid flow temperature exiting the HP. When the DAC is on, then the fluid is cooled down using the DAC, otherwise the fluid bypasses the DAC and enters the ground.</p>	<p>Control Strategy 2 (CS2) The DAC is controlled based on fluid return temperature leaving the ground. When the DAC is on, then the fluid is cooled down using the DAC, otherwise the fluid bypasses the DAC and enters the ground.</p>
<p>Control Strategy 3 (CS3) This is free cooling option; the DAC is controlled based on the difference between fluid return temperature leaving the ground and outside air temperature. When the DAC is on, then the fluid is cooled down using the DAC, otherwise the fluid bypasses the DAC and enters the ground. The fluid returning from the ground bypasses the HP and enters the building.</p>	<p>Control Strategy 4 (CS4) In this control strategy there is an option of cooling the fluid either on fluid flow temperature exiting the heat pump or on fluid return temperature leaving the ground, otherwise the fluid bypasses the DAC and enters the ground or the HP.</p>
	<p>Control Strategy 5 (CS5) The DAC is controlled based on the ground temperature and ambient air temperature, when the ground temperature reaches a certain value then the DAC can either be used to reject heat to the ground or the fluid bypasses the ground and enters the heat pump.</p>

The normal control strategy for the GSHP system is to operate the DAC only in the event that the temperature of the water returning from the ground loop exceeds 38 °C. The control system enables the DAC shunt pump which is positioned in the loop supplying the DAC and circulates the water to the already enabled DAC. The DAC has its own internal PID based control system which controls the temperature of the water leaving the DAC to 22 °C. The DAC is connected to the GSHP loop through a three-way valve. There are only two positions available for this valve. The valve can be controlled to either direct water through the DAC or let water bypass the DAC.

From the list of control strategies given in table 7.2 CS1 and CS2 were favoured because of its applicability and as the control procedures do not involve difficult algorithms and therefore can easily be simulated. These two control strategies were therefore investigated by simulation.

The existing system model was reconfigured to reject heat into the ground to ease ground saturation which has consequences on the performance of the system. Therefore having built and established a validated empirical TRNSYS system model the opportunity was taken to investigate the effects of different control strategy approaches using the DAC on HP performance and ground temperature variation. Control strategies utilized in this study define when and how the DAC circuit, circulation pumps and the HP should be turned on or off. A flow diagram of the investigated control strategies is shown below in Figure 7.7 and the building's operational hours are summarised below in table 7.3.

Table 7.12 *Zone Occupancy Period*

Period	Occupancy Start Time	Occupancy End Time
Monday – Thursday	8:00	21:00
Friday	8:00	19:00
Saturday	9:00	12:00
Sunday	9:00	12:00

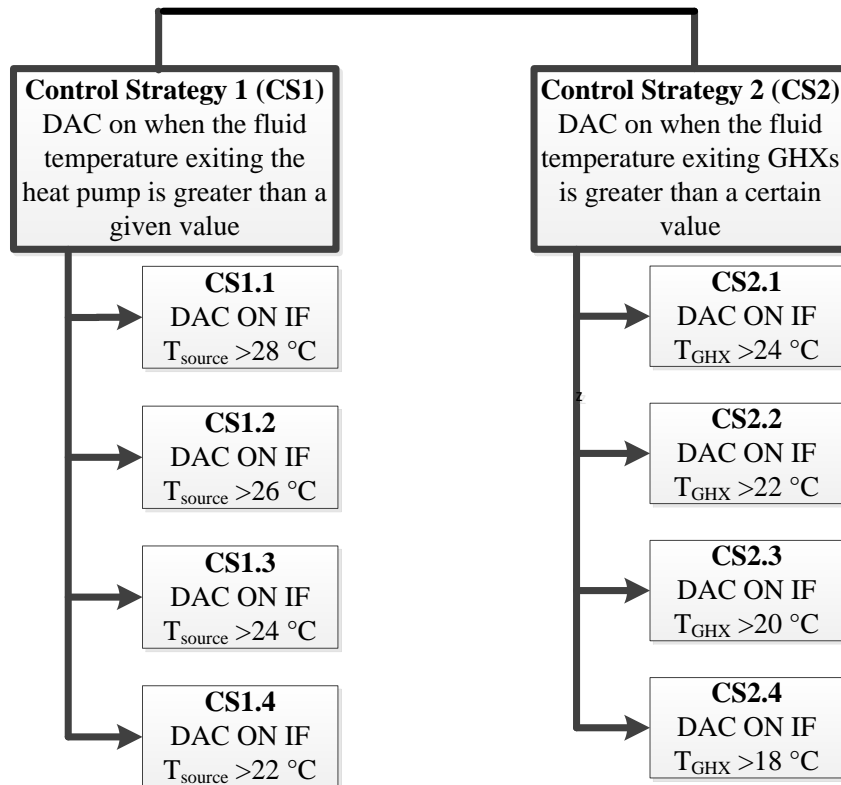


Figure 7.58 Flow diagram of the control strategies

The control strategies above are tailored based on the building's occupancy period as shown in table 7.3 and outside air temperature. This defines the control signal which indicates when the unit should be on or off in the cooling mode. Assuming that the building is occupied 13 hours every day except weekends, the time control signal function for a whole week would be as shown in Figure 7.8, where 1 is on-signal and 0 is off-signal. It is useful to highlight that this signal is the operating signal of the complete GSHP system. Additional model assumptions and inputs are also listed in table 7.4.

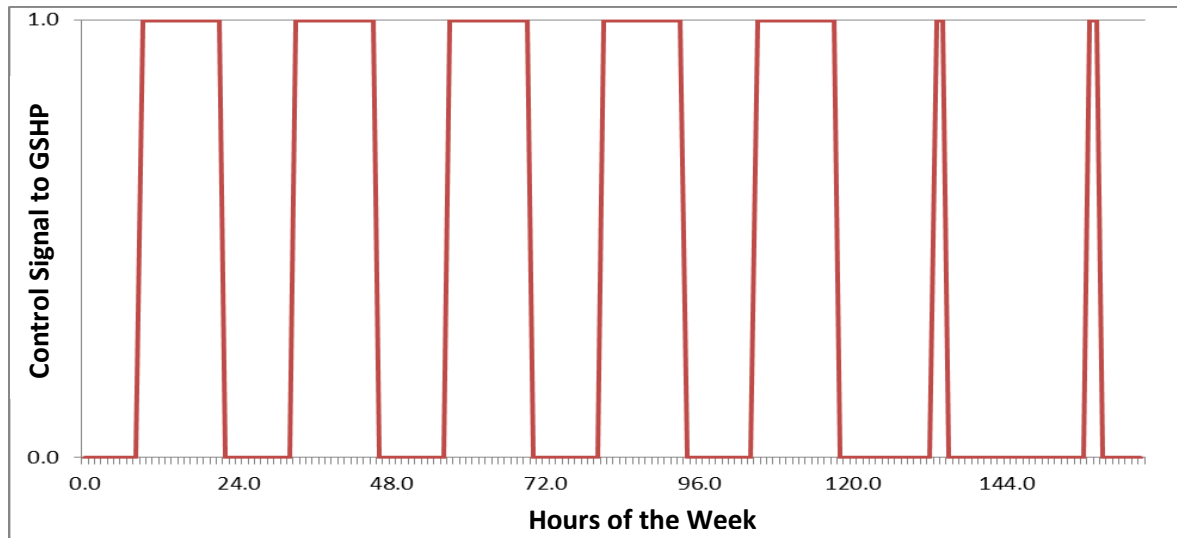


Figure 7.59 Weekly control signal to the GSHP

Table 7.13 List of model inputs and assumptions

List of Model Inputs and Assumptions
Occupancy period 13 hours every day except weekends
Historical outside air temperature (OAT)
Flow and return fluid temperatures on both source and load side of the system
Heating and cooling performance data of the heat pump model
Heat pump and Circulation pumps to operate in heating mode if the OAT > 18 °C
Heat pump and Circulation pumps to operate in heating mode if the OAT < 14 °C

7.5.1 Control Strategy 1

Figure 7.9 shows a schematic of the empirical GSHP system model used for investigating control strategy 1 (CS1). CS1 sets DAC on when the fluid temperature exiting HP is greater than a given value. Different desired outlet fluid temperatures of 22 °C, 24 °C, 26 °C and 28 °C are examined and hence the normal operating condition of the system has been compared to these four different scenarios to investigate the impact of running the DAC at different temperature set points. In these comparisons the following parameters have been investigated:

- Energy consumption of the system which is made up of the HP, circulation pump and fan energy inputs.
- COP of the system.
- Ground temperature variation
- Running frequency operation of the HP, circulation pump and fan.

These results are presented on the following sections 7.5.1.1 to 7.5.1.7 and compared against the normal control strategy.

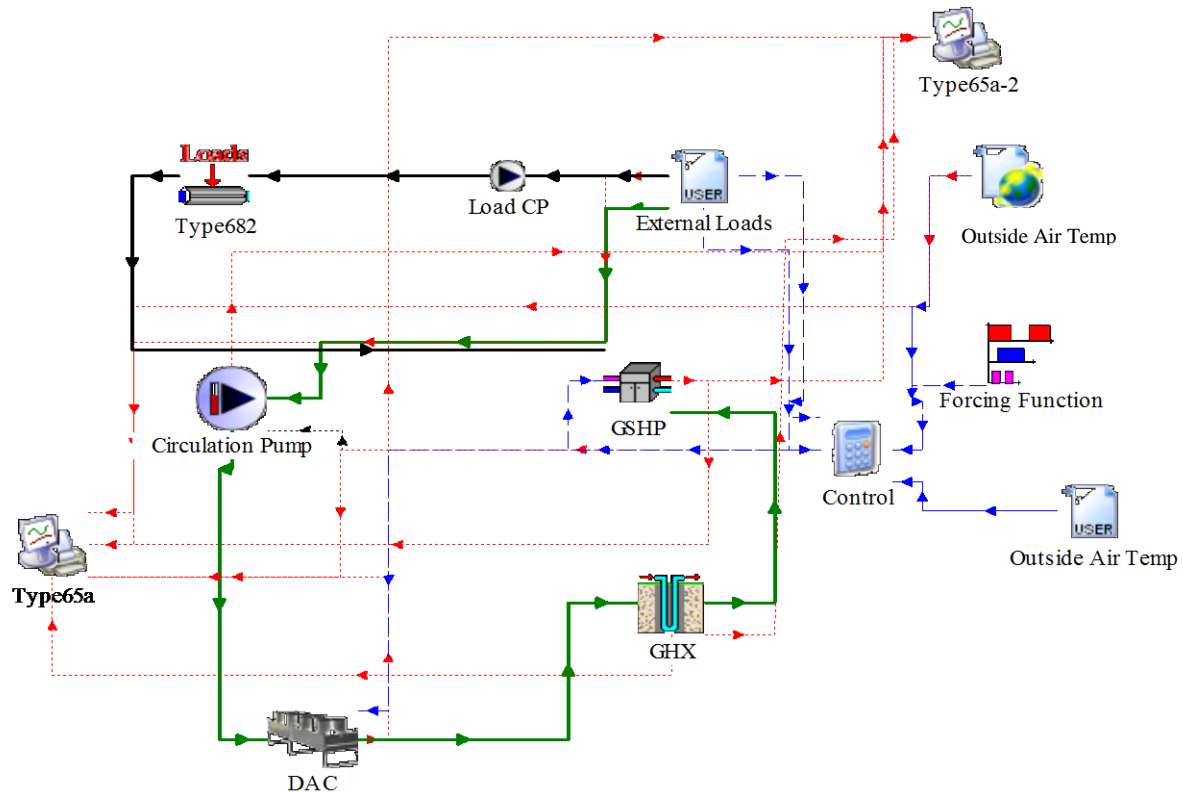


Figure 7.60 Schematic of the GSHP system model for Control Strategy 1

7.5.1.1 Effect of DAC on COP

The cooling COP value of the GSHP system under different temperature set points is illustrated in Figure 7.10. It can be noted that at the beginning of the season between April and June 2013 the COP values for all the four set temperature scenarios were very close to each other. This is when the DAC is not running and this is labelled Time Period A. In Time Period B the DAC is operating partially or fully between the periods of June to October 2013 and there is a variation in COP between the options. These COP differences are purely because the DAC has been utilised in lowering the leaving fluid temperature from the HP by rejecting the heat back to the ground at a lower temperature compared to the normal operating leaving fluid temperature.

It is clear that the GSHP's COP value decreases continuously with increasing set point temperature. For the first year's operation of the GSHP system, the COP values for cooling are highest for the lowest set point temperature.

Compared to the normal operating scenario in which the COP value for cooling is 5.2, CS1 with a temperature set point control of 22 °C achieves a higher cooling COP of 6.2 which is 19.2 % higher than the normal operating scenario.

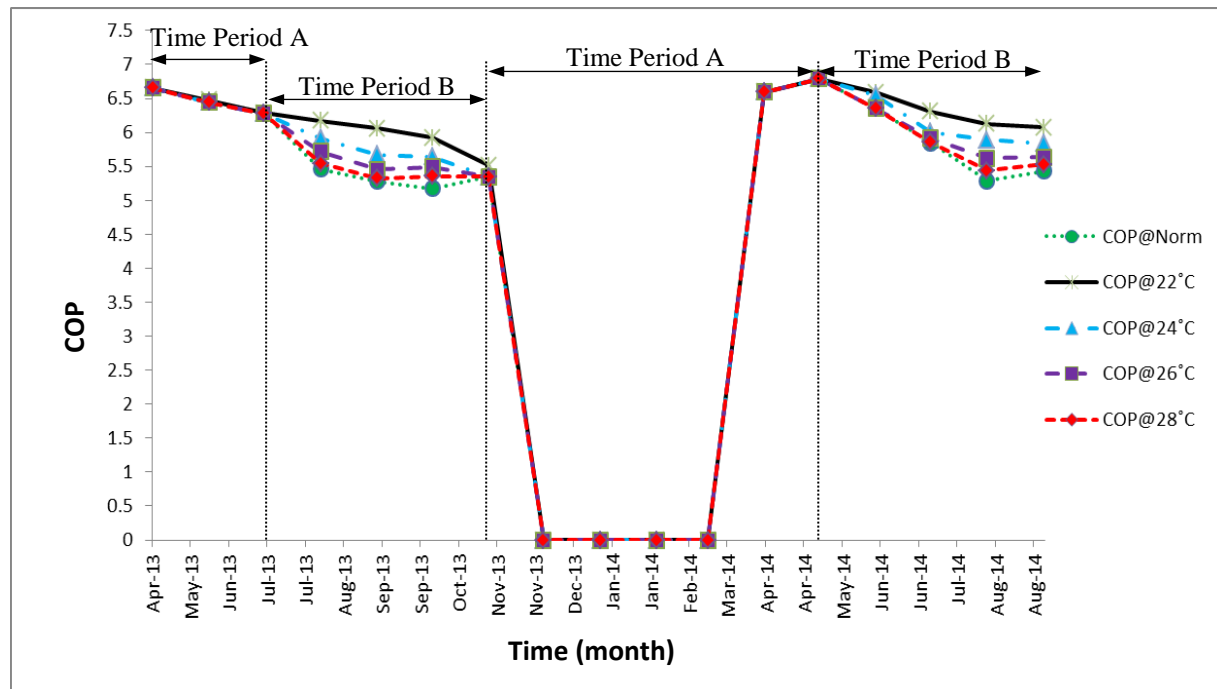


Figure 7.61 Average monthly system COP CSI

7.5.1.2 Effect of DAC on Ground Temperature

As well as investigating the effect of operating period of the DAC on the performance of the system, the effect on the ground temperature was also investigated. The simulation results of ground temperature for 1 year's operation are presented in Figure 7.11. The results show that the four different set point operation temperatures of the DAC leads to differences in the ground temperature variation when the set point temperature varies. In Time Period A when the DAC is not operating at the beginning of the cooling season the ground temperature is similar and hence varying the different set points has no effect at all. Therefore the ground temperature for all scenarios remains constant. However in Time Period B the temperature variation between the scenarios becomes clear that the more the DAC is running the lower the ground temperature variation is. The highest ground temperature after 1 year's operation in cooling mode is 23 °C for normal operation period, compared to 20 °C for the lowest set point temperature which is 15 % lower than the normal operation. This impacted on COP and this can be seen clearly in Figure 7.10 above.

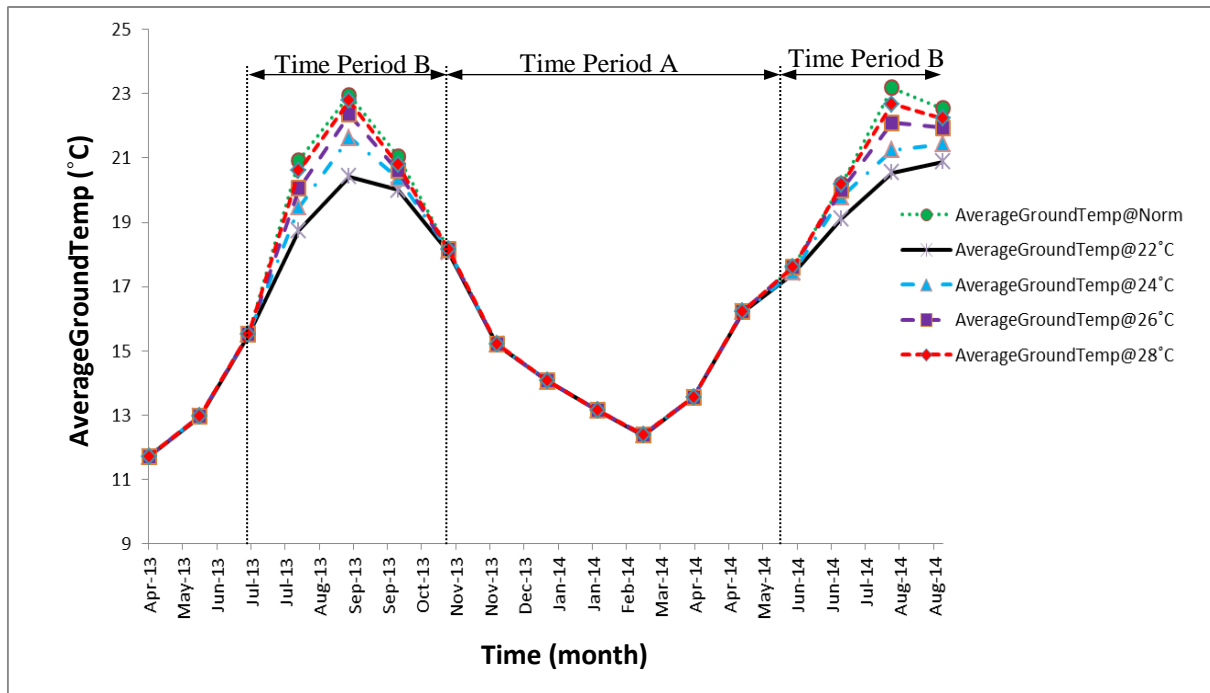


Figure 7.62 Monthly ground temperature variations CSI

With the decrease of average ground temperature around the GHX, the temperature difference between the ground and the circulated heat carrier fluid decreases, this phenomena has both advantages and disadvantages on the system. Although this incremental temperature change improves the COP value during cooling season, however it also reduces the COP value of the system in heating season.

7.5.1.3 Fan, Pump & Heat Pump Running Frequency of Operation

Figure 7.12 shows the number of times the HP, circulation pump and fan for the DAC has operated between the periods of April 2013 and August 2014. As expected the running operation frequency increases with decreasing temperature set points. The figure shows that the highest number of running hours was recorded on the months of July 2013 and July 2014.

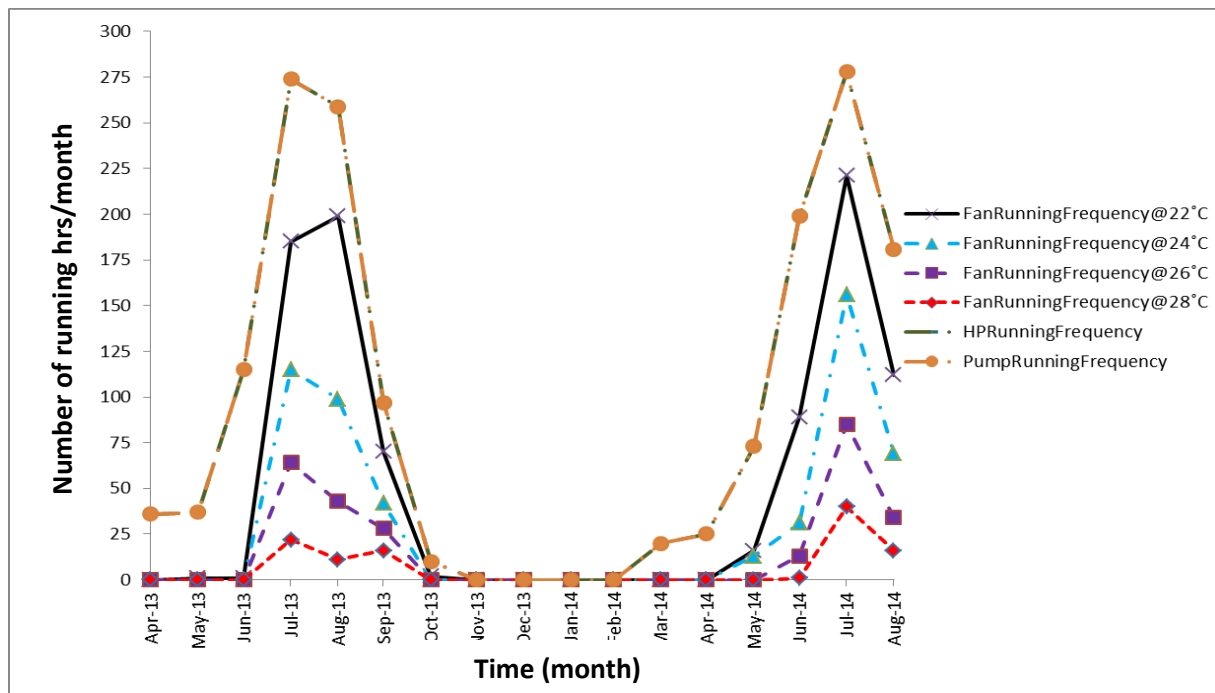


Figure 7.63 Annual fan, pump and HP running frequency of operation CS1

7.5.1.4 Effect of DAC on Heat Pump Energy Consumption

The total monthly HP energy consumption for scenarios CS1.1, CS1.2, CS1.3 and CS1.4 is presented in Figure 7.13. The operation cycle of the DAC can determine whether the GSHP system consumes more energy, compared to a GSHP system without a DAC. Figure 7.13 shows that between the periods of April 2013 and August 2014 the highest energy consumption of the HP were 7923 kWh and 7669 kWh respectively. This has occurred both when the system was running without the aid of the DAC and also when the DAC was controlled at the highest set point temperature of 28 °C. These dynamics can be shown clearly in Figure 7.13 during Time Period B. Time Period A shows that when the DAC is off, the output of the four set points remain unchanged. Time Period B shows when the DAC was operating at different set points, this zone also highlights the benefits of reducing the ground temperature as shown in Figure 7.11 to the energy input of the system. Reducing the ground temperature helps to reduce the temperature difference between the GHX leaving temperature and HP leaving temperature and hence increasing COP of the system.

Similarly the lowest energy consumption of the system during the transition period to heating mode was 267 kWh. In Time Period B between the periods of July and September 2013, comparisons of the four scenarios revealed that the energy consumption of the system has

decreased by 8 % when the lowest control set point of 22 °C (CS1.4) was compared to the normal operating conditions of the system.

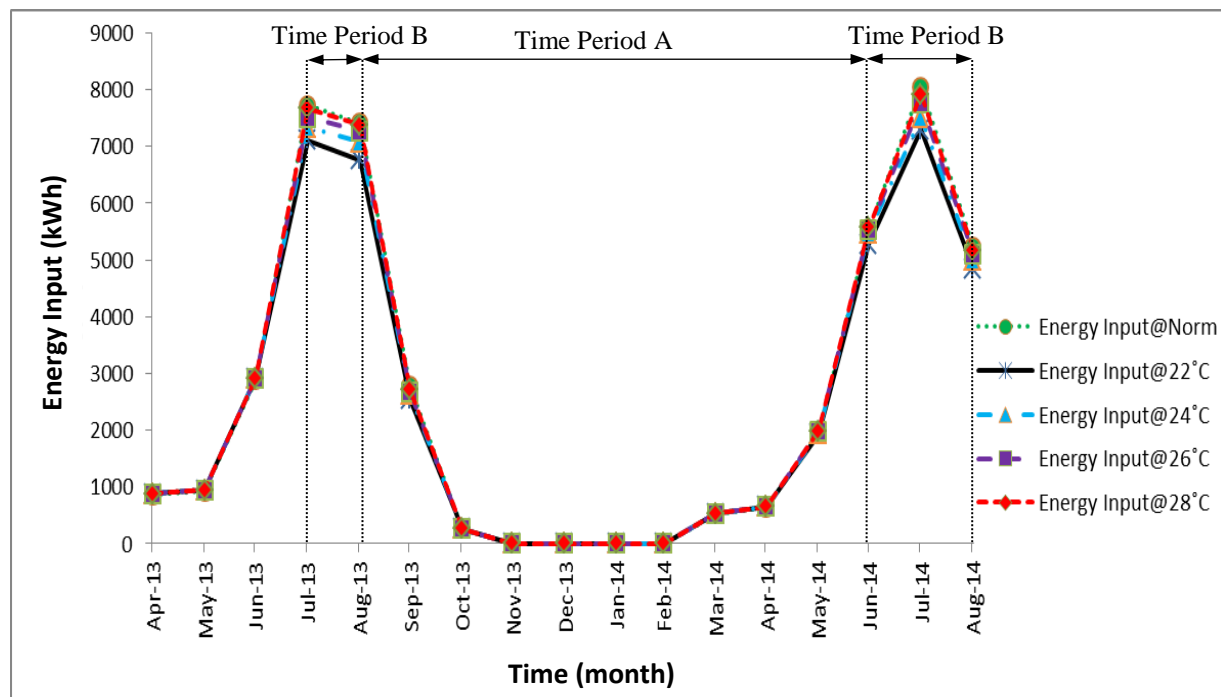


Figure 7.64 Monthly HP energy consumption CSI

7.5.1.5 Monthly Fan Energy Consumption

One inevitable fact is that lowering the loop temperature in the summer will increase the DAC energy consumption. There is a trade-off between the heat pump cooling COP and the DAC fan energy. However, as shown in Figure 7.15, since the energy consumption of the DAC is less than 10 % of the entire GSHP system energy consumption, it is still possible to achieve large amount of energy savings through the DAC control optimization.

Figure 7.14 shows total monthly fan energy consumption of the DAC and the graph shows that the highest fan energy consumption was 1105 kWh at the lowest set point temperature and the lowest fan energy consumption was 55 kWh when the set point temperature was at its highest. The fan energy consumption decreases with increasing the set point temperatures.

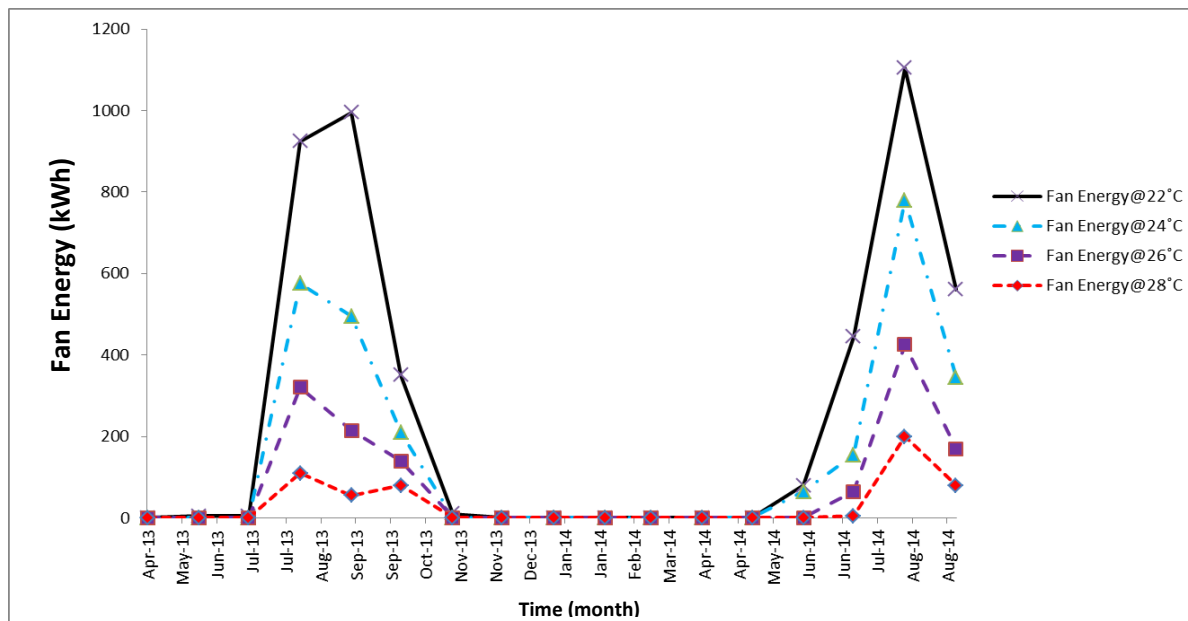


Figure 7.65 Monthly fan energy consumption CSI

7.5.1.6 Proportion of Energy Utilisation

Figure 7.15 below shows the overall proportion of energy utilisation of the HP, circulation pump and the fan. It shows that the compressor is responsible for 72 % of the annual electricity usage of the whole system followed by the circulation pumps which utilises 20 % of the total energy input of the system. The 9 % energy input of the DAC is relatively small in comparison to the compressor's energy input.

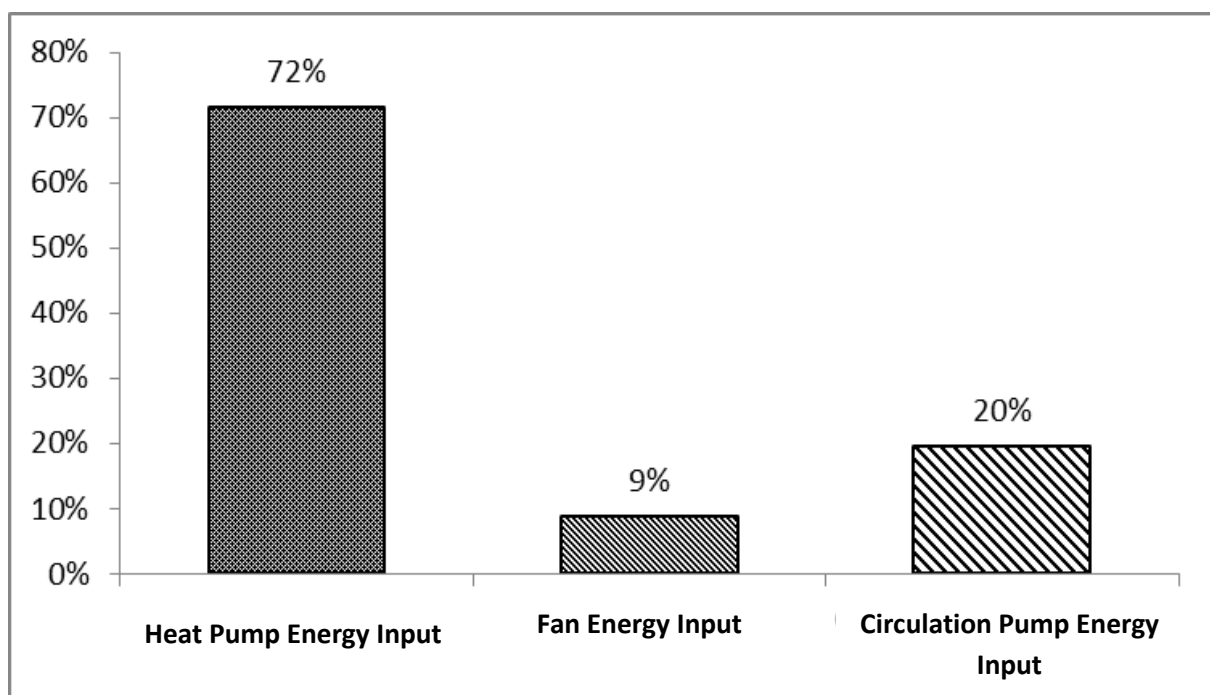


Figure 7.66 Proportion of energy utilisation of HP, circulation pump and fan CSI

7.5.1.7 Economics of The Control Strategy 1

In this section the financial and CO₂ emission savings of each strategy have been compared to the normal operation of the system. Figure 7.16 shows the additional monthly CO₂ emission savings (kgCO₂e) that can be achieved by implementing the different temperature control set points. The graph shows that in July 2014 a maximum CO₂ emission saving of 420 kgCO₂ was achieved. Relating this to Figures 7.10 and 7.11 this is also the point at which the highest COP and lowest ground temperature was recorded. Notably this has occurred at the lowest temperature set point of 22 °C. Moreover the lowest CO₂ emission saving was approximately 20 kgCO₂ and this has occurred at the highest temperature set point of 28 °C.

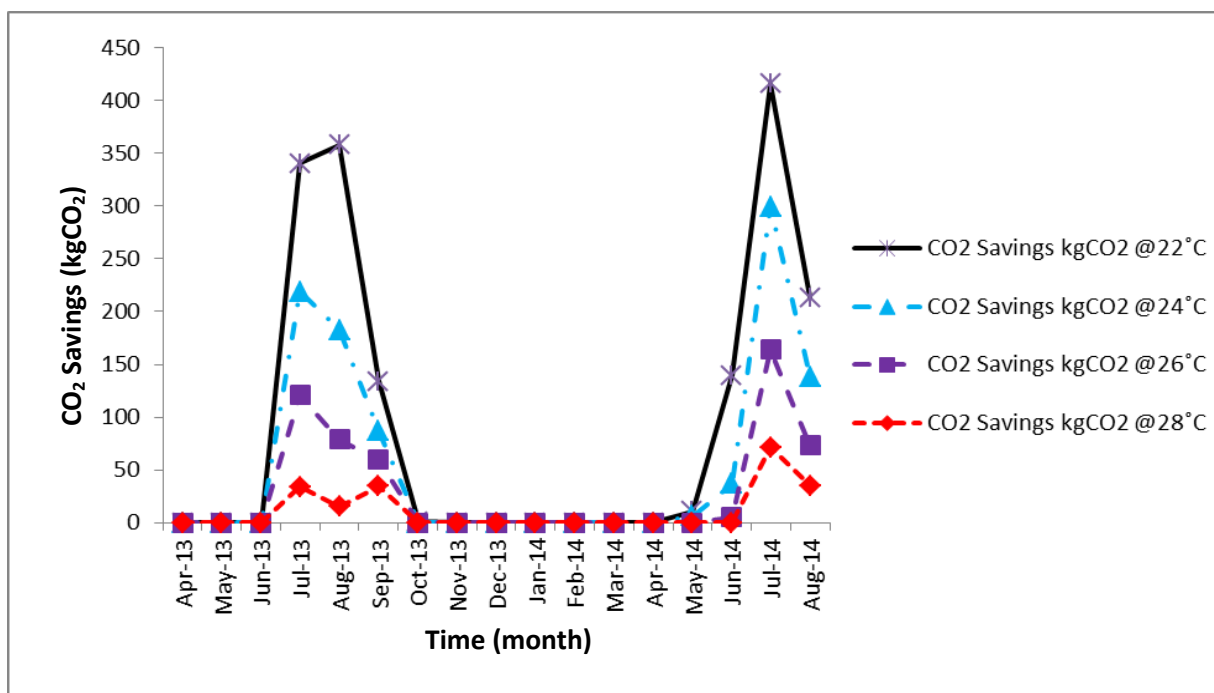


Figure 7.67 Monthly CO₂ emission savings from different control strategy CS1

Specifically Figure 7.17 shows the potential additional cost savings that can be made from the different temperature set points in comparison to the normal system operation. Figure 7.17 also shows that in the month July 2014 a maximum cost saving of £110 was achieved utilising the lowest temperature set point of 22 °C. Furthermore the lowest cost saving on the same month was approximately £20 and this has occurred at the highest temperature set point of 28 °C. The lowest temperature set point can achieve cost savings of approximately 18 % compared to the highest temperature set point.

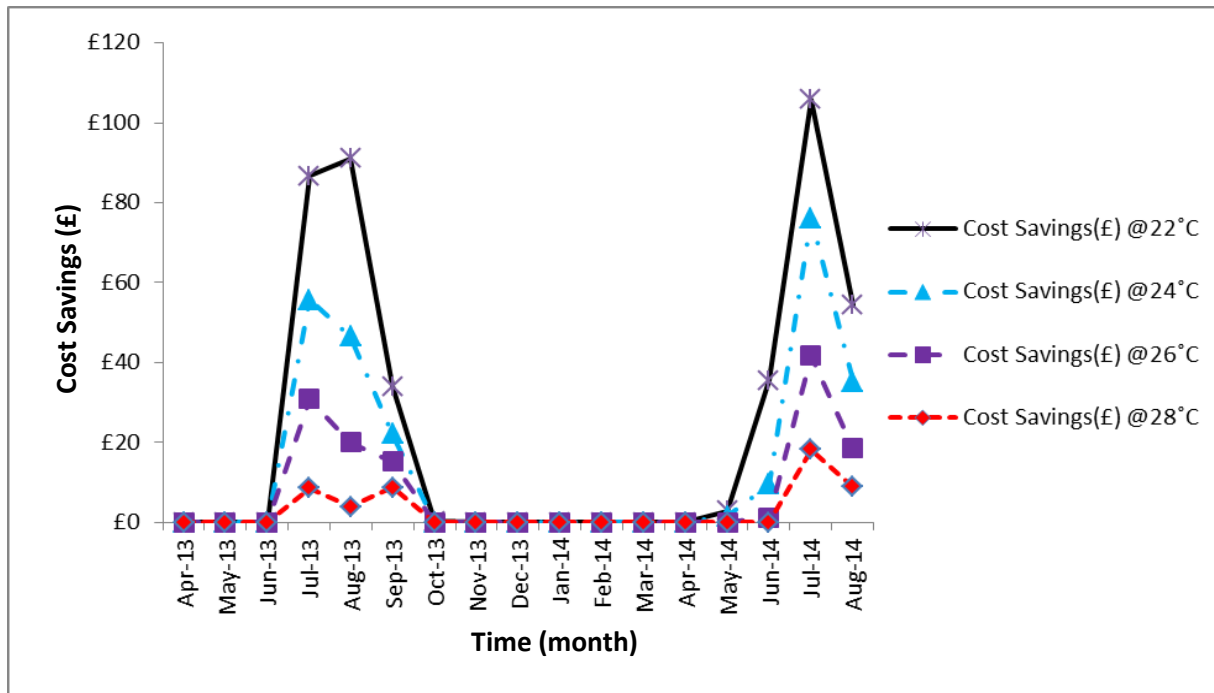


Figure 7.68 Monthly cost savings from different control strategy CS1

7.5.2 Control Strategy 2

Similar to CS1, Control Strategy 2 (CS2) shown in Figure 7.18 investigates the effect of controlling the return water temperature from the GHX and activates the DAC when the fluid temperature exiting the GHX is greater than a certain value. The normal operating conditions of the system have been compared to four different scenarios with desired GHX outlet temperatures of (CS2.1 = 18, CS2.2 = 20, CS2.3 = 22, and CS2.4 = 24 °C). In these comparisons the following parameters have been investigated:

- Energy consumption of the system which is made up of HP, circulation pump and fan energy inputs.
- COP of the system.
- Ground temperature variation
- Running frequency operation of the HP, circulation pump and fan.

These results are presented on the following sections 7.5.2.1 to 7.5.2.7 and compared against the normal control strategy.

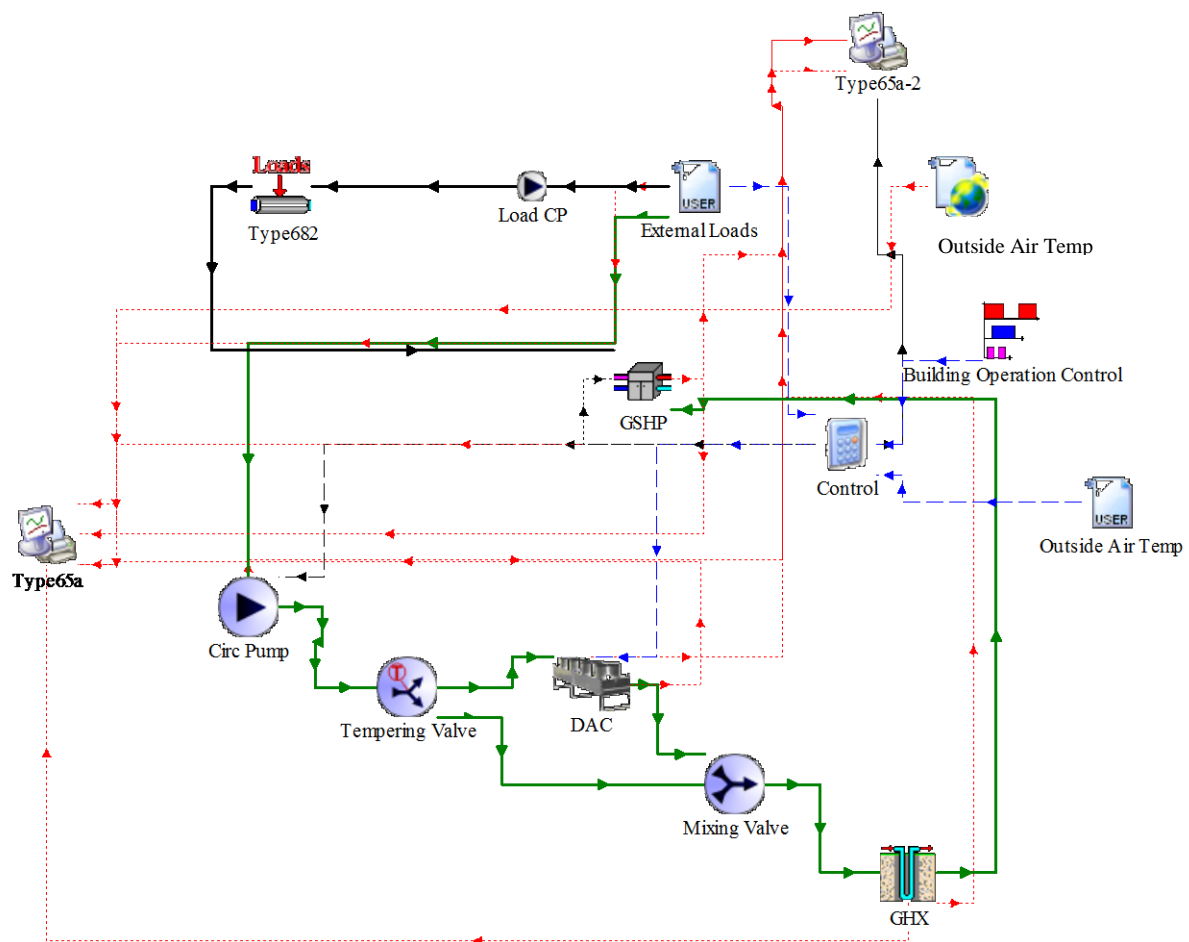


Figure 7.69 Schematics of the GSHP system model for CS2

7.5.2.1 Effect of DAC on COP

Figure 7.19 presents the cooling COP value of the GSHP system under different temperature set points. The result shows that at the beginning of the season, between April and June 2013, the COP values for all the four set temperature scenarios were very close to each other. Similar to CS1 Time Period A illustrates the period when the DAC is not operating. In Time Period B the DAC is operating partially or fully between the periods of June 2013 and November 2014. The result indicates that the COP varies with the operation period and the different control temperature set point scenarios. The DAC monitors the return temperature from the GHX in order to maintain the temperature of the heat carrier fluid entering the HP. The ground temperature is maintained by rejecting the heat back to the ground at a lower temperature compared to normal operating fluid temperature. This heat rejection to the ground therefore results in COP variation with time.

The lowest cooling COP in the normal operating conditions is approximately 5 while setting the temperature set point control to 18 °C achieves a higher cooling COP of 6.5 which is 23 % higher compared to the normal operating condition.

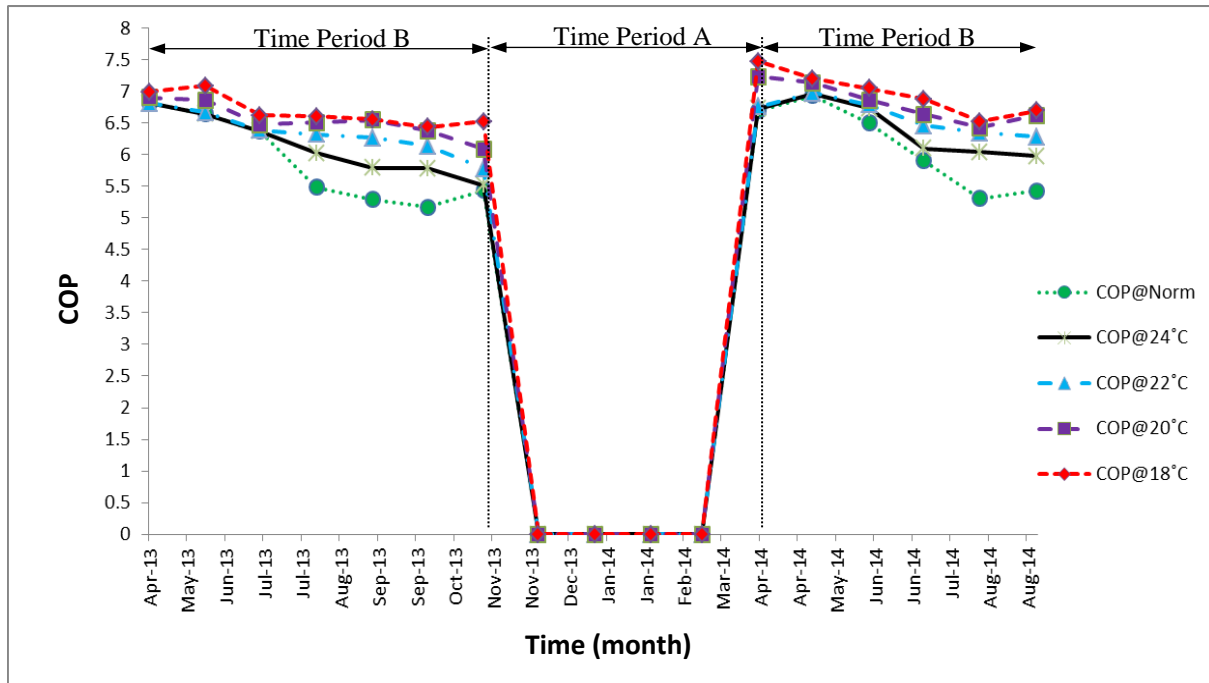


Figure 7.70 Average monthly system COP CS2

7.5.2.2 Effect of DAC on Ground Temperature

Figure 7.20 presents the annual ground temperature variation due to heat extraction and rejection attributed from operating the GSHP system and the DAC. As suggested in CS1 the results indicate that the four different set point operation temperatures of the DAC results in real differences in the ground temperature variation when the set point temperature varies. In Time Period A when the DAC is not operating, at the beginning of the heating season there is very little ground temperature change and hence varying the ground temperature set points has no effect at all. Therefore the ground temperature for all scenarios remains constant. However in Time Period B the temperature variation between the scenarios becomes clear that the more the DAC is running the higher the ground temperature variation becomes. In Time Period B there can be seen some irregularity in the pattern at which the rate of the four set point scenarios are reducing. This can be explained by looking at the running frequency of operation in Figure 7.21. Lower temperature set point results in lower ground temperature variation compared to the normal operating condition.

The ground temperature reaches approximately 23 °C during the normal cooling operating mode, compared to 19.7 °C for CS2.4 which is 14 % lower than the normal operation.

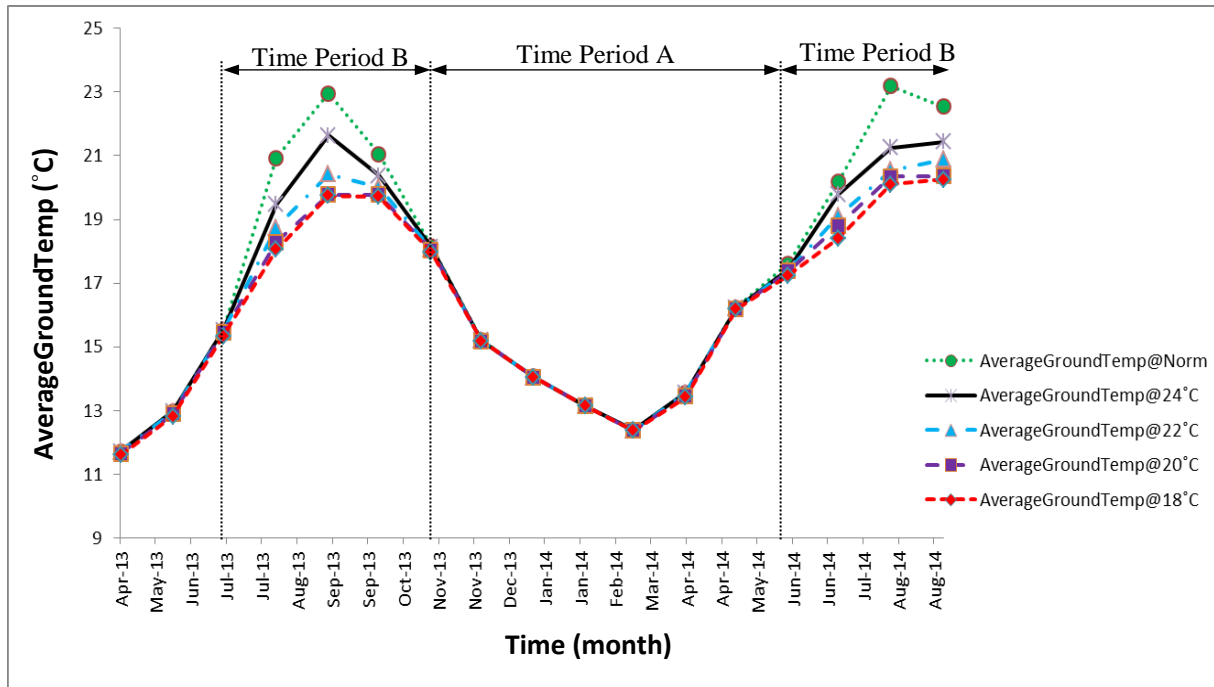


Figure 7.71 Monthly ground temperature variations CS2

7.5.2.3 Fan, Pump & Heat Pump Running Frequency of Operation

Figure 7.21 shows the number of times the HP, circulation pump and fan for the DAC has operated between the periods of April 2013 and August 2014. As expected similar to CS1 the running operation frequency increases with decreasing temperature set points. The figure shows that the highest number of running hours of 278 and 181 was recorded for the HPs on the month of July 2013 and July 2014.

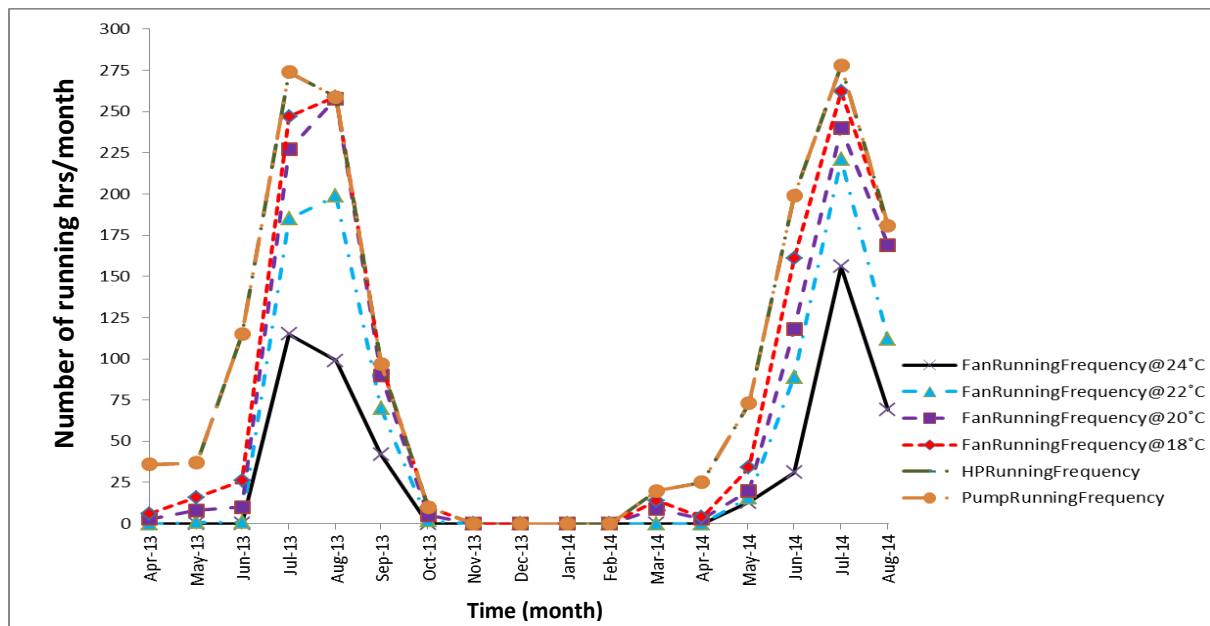


Figure 7.72 Annual fan, pump and HP running frequency of operation CS2

7.5.2.4 Effect of DAC on Heat Pump Energy Consumption

Figure 7.22 shows the monthly energy input to the HP under the four different temperature set point scenarios. The results show that between the periods of April 2013 and August 2014 the highest energy consumption of the HP was 7372 kWh and 8053 kWh respectively. Illustrated in Figure 7.22 Time Period B the highest energy input occurred at both when the system was operating without the aid of the DAC and also when the DAC was controlled at the highest set point temperature of 24 °C. Time Period A shows the period when the DAC is off. Time Period B shows that when the DAC was operating at different temperature set points, this highlights the benefits of reducing the ground temperature as shown in Figure 7.20 to the energy input of the system. Reducing the ground temperature helps to reduce the temperature difference between the GHX leaving fluid temperature and HP leaving fluid temperature and hence increasing COP of the system.

Similarly the lowest energy consumption of the system during the transition period to heating mode was 232 kWh. In Time Period B between the periods of July and September 2013, comparisons of the four scenarios revealed that the energy consumption of the system has decreased by 13 % when CS2.4 was compared to the normal operating conditions of the system.

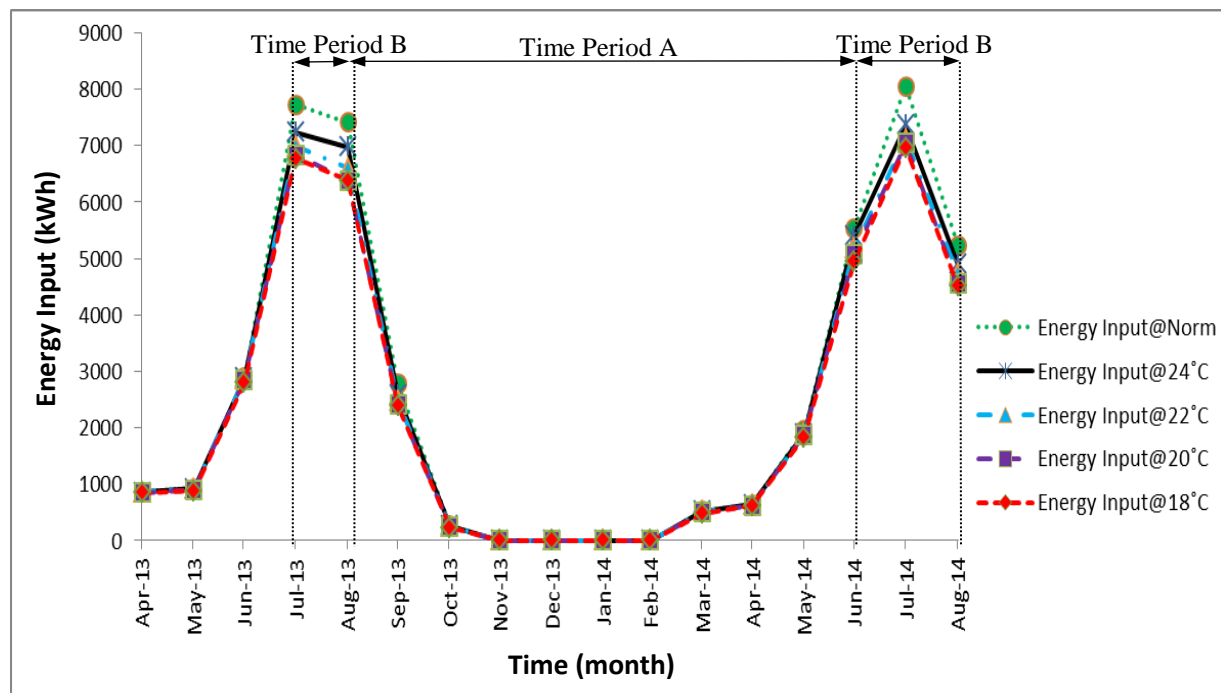


Figure 7.73 Monthly HP energy consumption CS2

7.5.2.5 Monthly Fan Energy Consumption

Figure 7.23 shows total monthly fan energy consumption of the DAC. The result shows that the highest fan energy consumption was 1310 kWh at the lowest set point temperature and the lowest fan energy consumption was 575 kWh when the set point temperature was at its highest. The fan energy consumption decreases with increasing the set point temperatures.

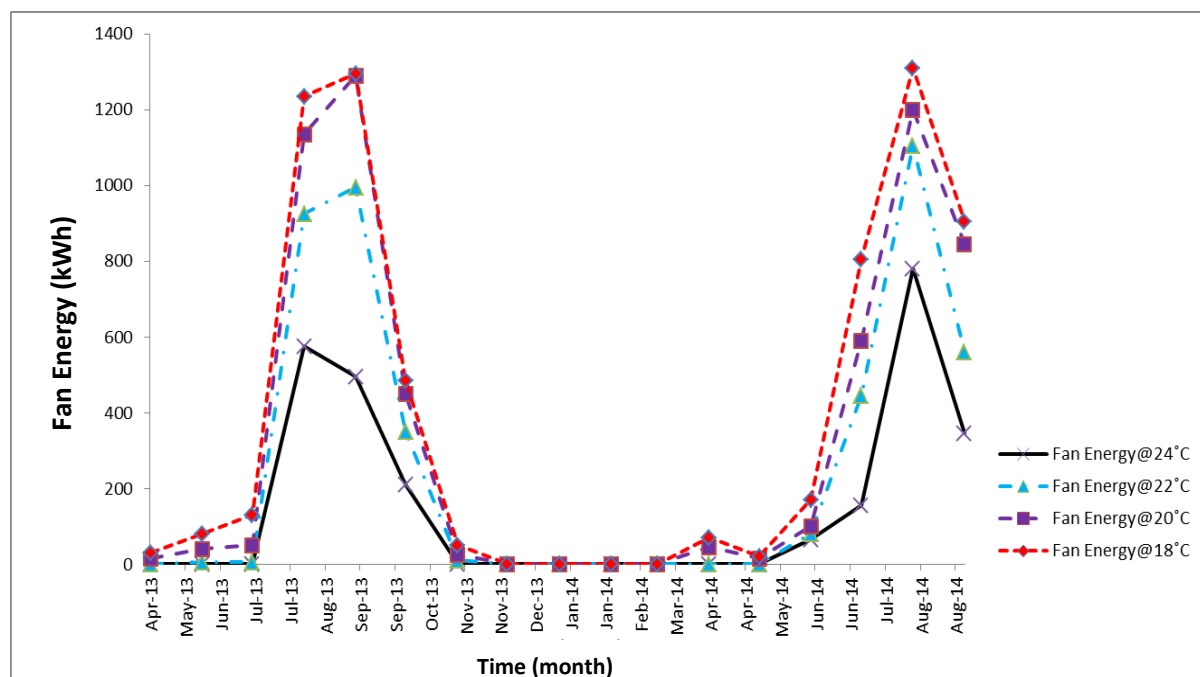


Figure 7.74 Monthly fan energy consumption CS2

7.5.2.6 Economics of The Control Strategy 2

As discussed above in CS1 in this section the financial and CO₂ emission savings of each temperature set point scenarios of CS2 have also been compared to the normal operating condition of the system. Figure 7.24 shows the additional monthly CO₂ emission savings (kgCO₂e) that can be achieved by implementing the different temperature control set points. The graph shows that in July 2014 a maximum CO₂ emission saving of approximately 600 kgCO₂ was achieved. Relating this to Figures 7.19 and 7.20 this is also the point at which the highest COP and highest ground temperature was recorded. Similar to CS1 this has occurred at the lowest temperature set point of 18 °C. Moreover the lowest CO₂ emission saving was approximately 280 kgCO₂ and this has occurred at the highest temperature set point of 24 °C. As can be seen the lowest temperature set point can produce a saving of approximately 55 % compared to the highest temperature set point.

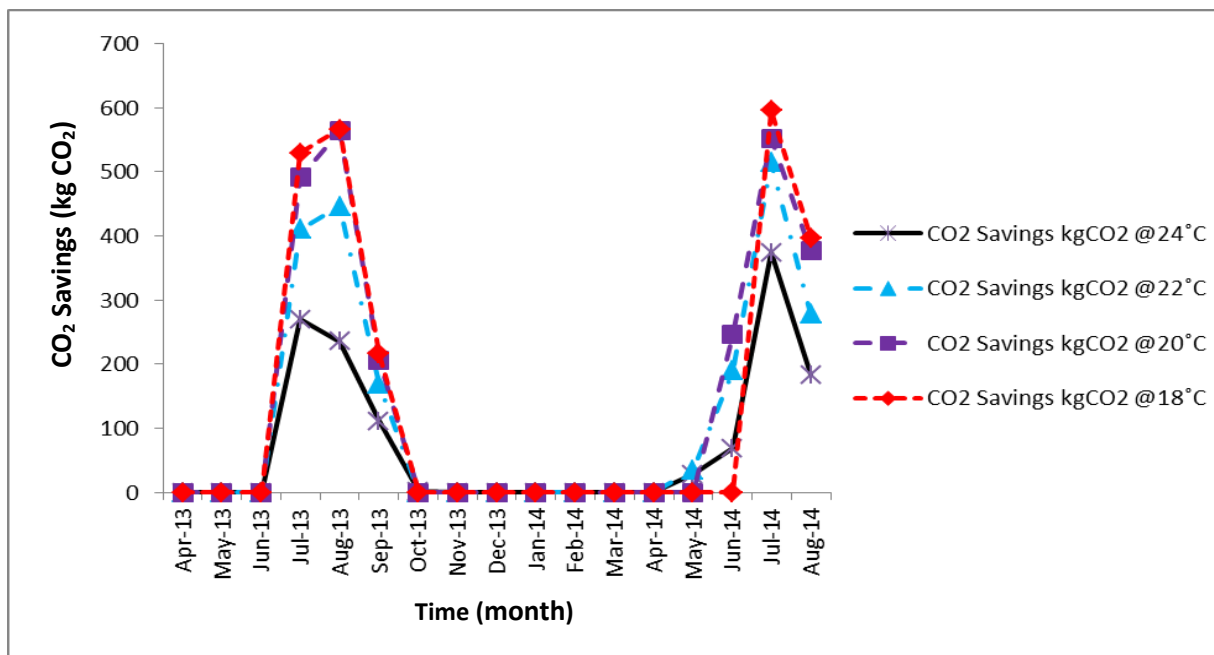


Figure 7.75 Monthly CO₂ emission savings from different control strategy CS2

In addition the results in Figure 7.25 present the potential additional cost savings that can be made from the different temperature set points in comparison to the normal operating condition of the system. Figure 7.25 also shows that in the month July 2014 a maximum cost saving of £150 was achieved using the lowest temperature set point of 18 °C. Furthermore the lowest cost saving on the same month was approximately £60 and this has occurred at the highest temperature set point of 24 °C. The lowest temperature set point can achieve cost savings of approximately 60 % compared to the highest temperature set point.

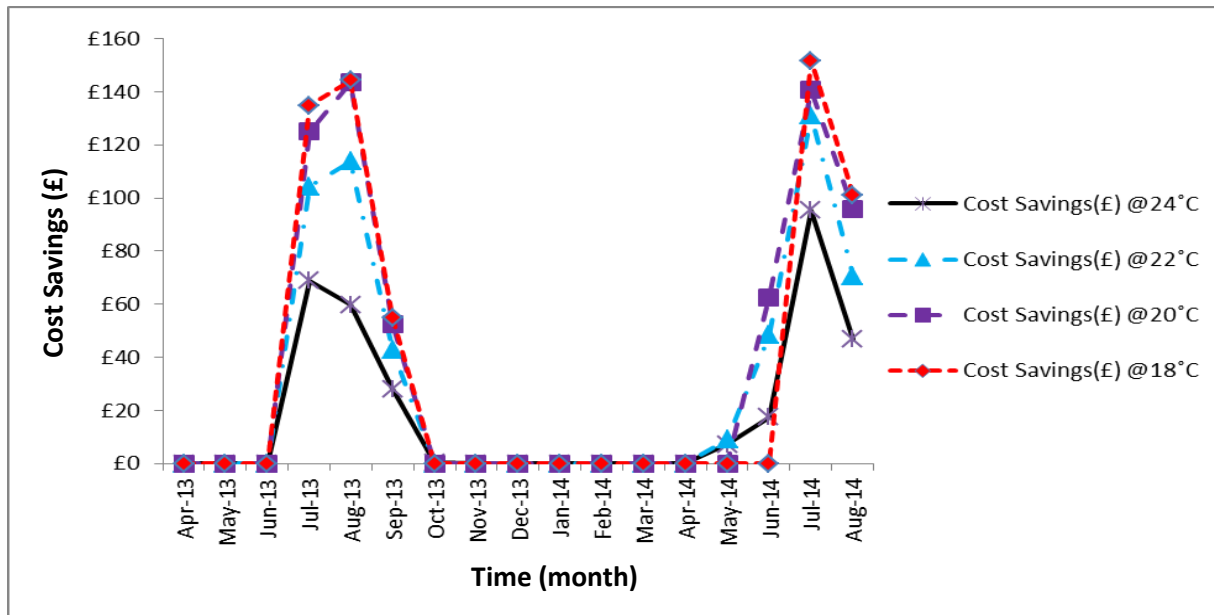


Figure 7.76 Monthly cost savings from different control strategy CS2

Figure 7.26 shows a summary of both the control strategies investigated in this chapter compared to the normal control strategy. The results show that it is beneficial to utilise a DAC for (i) HP energy input saving, (ii) optimising the performance of the GSHP system and (iii) to reduce the level of ground temperature saturation by rejecting heat selectively via the DAC. From the result it is evident that CS2 is favourable.

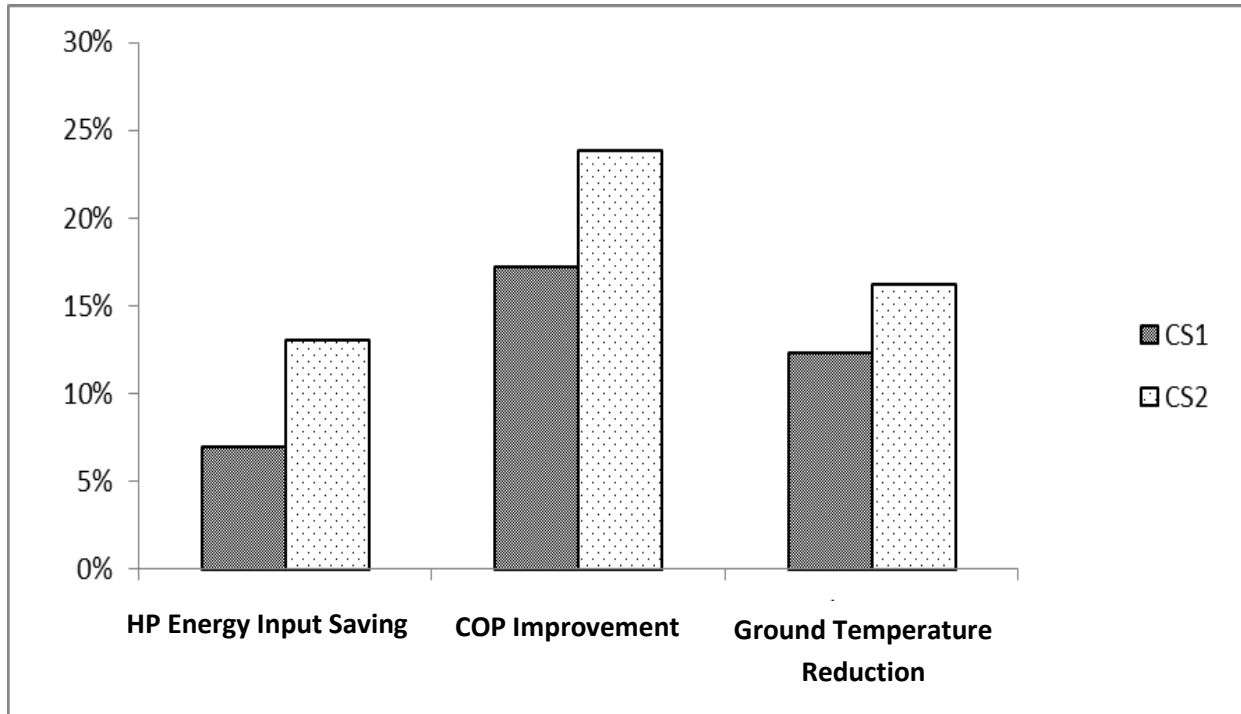


Figure 7.77 Comparisons of CS1 and CS2

7.6 Summaries

This chapter has provided a description of the new DAC aided GSHP system and operation of the different components of the TRNSYS simulation setup. This chapter further presented the validation of the TRNSYS model against historical experimental data from LSBU's actual GSHP system installation.

This chapter has presented a novel investigation of different control strategies for the GSHP system optimization during the net cooling period to a university building. The investigation has focused on the effect of a DAC on heat rejection to the ground, COP of the system, ground temperature variation and minimization of electric power consumption of the compressor and circulation pump.

This chapter has shown that by utilising and controlling a DAC using different temperature set points, a significant reduction to GSHP operating cost, the electric power consumption and an improvement to performance of the system could be achieved.

This chapter has identified that the lowest temperature set point control is the best of the examined so as to regulate the DAC's operation in the GSHP system. A comparison of these four basic scenarios illustrated that there are significant cost and carbon savings that can be made and all new control strategies achieve a better regulation to system operation which leads to an extra reduction in the energy consumption, carbon and cost savings. These remarks can be used as guidance to future GSHP designers.

This chapter has also looked at the benefits of utilising the DAC to cost and carbon savings, and identified that although the above carbon and cost savings are marginally low and do not substantiate the benefits or advantages of installing the DAC, these savings however are achieved purely from evaluating the different temperature set point control strategies. Nevertheless substantial savings can be made when the DAC is compared to other alternative technologies.

Chapter 8

Conclusions & Scope for Further Work

8.1 Introduction

This chapter describes the conclusions taken from

- i. The literature review.
- ii. The detailed background and description of the K2 building and CEREB, including the GSHP system, control strategy and the instrumentation and monitoring systems.
- iii. The commissioning of apparatus and initial results,
- iv. The development of a mathematical model for predicting underground temperature distribution and
- v. The development of an empirical TRNSYS model of a GSHP system to investigate the effect of using a DAC on heat rejection, energy input to the GSHP system, fan and circulation pumps, COP and finally the ground temperature.

This chapter concludes with a look at what further work should be performed to continue the progress in this field of research.

8.2 Conclusions from the Literature Review

Developments in HP technology have resulted in well proven technology in many countries that are efficient, reliable, environmentally beneficial, cost effective and socially acceptable. The literature review has shown that GSHP systems have been found to have great potential as an aid in tackling climate challenges and meeting legislation requirements by facilitating the abatement of additional CO₂ emissions resulting from the use of GSHP systems in comparison to conventional commercial and domestic heating and/or cooling alternatives.

In theory, GSHP systems can work efficiently if properly designed and operated. However, in practice the performance of these systems is dependent on a range of different parameters and issues. There has been very little published data on the performance of installed GSHP systems in the UK until recently. The literature review has given a comprehensive description of expected HP performance and performance metrics. It identified how GSHP systems performs in practice using a range of recently published monitored system COP data such as the EST field trial phase 1 and 2 reports.

The literature review has investigated the different components and parameters affecting the performance of the system. It covered an extensive collection of literature, looking at the design parameters affecting system's performance and operational experiences of GSHP systems. Identifying and understanding the relevant dynamics of groundwater effects and impact of ground temperature variation, control, climate conditions, site history, complex ground thermal properties, have huge effect to the vital energy piles and the GSHP performance.

Furthermore the literature review has shown that there are concerns that the use of GSHPs for extracting heat for a longer period could lead to a reduction of COP over time, and other complications. Opportunities exist to address the effect of seasonal imbalances of heat extracted versus heat returned to the ground by the GSHP system. The literature review has shown that by developing models for investigating performance of GSHP systems based on seasonal or daily underground temperature variations as well as predicting energy demand of the building it is possible to optimise the performance of the system.

8.3 Conclusions from the CEREB Life Laboratory Experiment

Specifically, Chapter 4 presented a detailed description of the K2 building, the main design objectives and construction process for CEREB and the K2 building. Some of the special design features for promoting energy efficiency and reducing the carbon emissions of the building are also discussed. The use of information systems, including advanced metering and the use of the BMS for the building and GSHP system control strategies, has also been presented.

Detailed description of the GSHP system, the different major components of the system i.e. heat pumps, energy piles, DAC and associated services are given. In addition the control strategy of the GSHP system, instrumentation and monitoring systems are also discussed.

The chapter has shown that the K2 building has an extensive heat and electricity sub-metering to enable performance monitoring and evaluation at the individual zone levels. A brief description of the instrumentation and monitoring system which enables rapid data acquisition for all the key services and energy meters has also been discussed.

8.4 Conclusions from the Commissioning of Apparatus and Investigation of Initial Results

Chapter 5 has described the commissioning of the experimental apparatus and investigation of initial results. It specifically described the process taken to investigate the difficulties and installation errors encountered during the installation and design stages of the GSHP system. A significant amount of time has been spent analysing and interpreting the data from the complex heat metering system and a substantial range of generic installation problems that the RACHP industry is currently facing have been identified. The work carried in this research has provided new practical insights into the operation of the GSHP systems and a real contribution to knowledge. The findings obtained from this chapter provide useful information for design and implementation of future GSHP systems in terms of improving energy efficiency as well as reducing costs. This chapter has identified that many of the temperature sensors were positioned and installed incorrectly. Incorrectly connected components or poorly sealed joints are another potential source of error, which can vary depending on the errors made.

This chapter further presented the validation of the experimental data as well as an in depth analysis and evaluation of the monitored performance data. Given the lack of availability of long term reliable HP data this study could be used in identifying some of the basic valuable information on heat measurement and consequently the long term GSHP performance in real life conditions. This chapter has shown that the performance of GSHP systems and their long term operational cost can be improved by operating the HPs at part load and with the use of a DAC.

This chapter has also looked at the benefits of utilising the GSHP systems for carbon savings compared to other commercial and domestic heating and/or cooling alternatives. The analysis has shown that low COP values could increase both cost and emissions compared to the use of a GFB, therefore it is important to ensure that the GSHP system is correctly installed and operating optimally with high COPs.

8.5 Conclusions from the Development of a Mathematical Model for Predicting Underground Temperature Distribution

Chapter 6 has presented the development and derivation methods of both the generic ground temperature prediction model for undisturbed ground temperature conditions and also the novel mathematical model for predicting the disturbed ground temperature caused by the seasonal rate of heat extraction or rejection from and into the ground.

This chapter has provided the validation process and the additional errors that are associated with the validation of the model against the actual recorded historical underground temperature data. It has been shown the SDGTP model gives good agreement with the recorded data predicting daily mean disturbed underground temperatures. More specifically, a comparison of the field measured data and predicted temperature results indicated that the mathematical model developed could be used to predict the disturbed underground temperature profiles with sufficient accuracy for the purposes of engineering calculations for use in residential and commercial buildings. This could be used in heating and cooling system design and many other applications.

This chapter has also looked at an optimization based control strategy. The control strategy is applied by using temperature data predicted by the SDGTP model to assist the user in making critical decisions for optimising the performance of the system. The control strategy is one of the key components of any GSHP system. GSHP heating systems are complex to control because of swings in the daily and seasonal demands and required temperature adjustment for thermal comfort.

8.6 Conclusions from the Development of an Empirical TRNSYS Model of a GSHP System

Chapter 7 has provided a description of the new DAC aided GSHP system and operation of the different components of the TRNSYS simulation setup. This chapter further presented the validation of the TRNSYS model against historical experimental data from LSBU's actual GSHP system installation.

This chapter has presented a novel investigation of different control strategies for the GSHP system optimization during the net cooling period to a university building. The investigation has focused on the effect of a DAC on heat rejection to the ground, COP of the system, ground temperature variation and minimization of electric power consumption of the compressor and circulation pump.

This chapter has shown that by utilising and controlling a DAC using different temperature set points, a significant reduction to GSHP operating cost, the electric power consumption and an improvement to performance of the system could be achieved. However, it is difficult to claim that this is the most economically beneficial scenario, not only because the heating period is not examined but, also because the investment and maintaining cost have not been considered in unit selection.

This chapter has identified that the lowest temperature set point control is the best of the examined so as to regulate the DAC's operation in the GSHP system. A comparison of these four basic scenarios illustrated that there are significant cost and carbon savings that can be made and all new control strategies achieve a better regulation to system operation which leads to an extra reduction in the energy consumption, carbon and cost savings. These remarks can be used as guidance to future GSHP designers.

This chapter has also looked at the benefits of utilising the DAC to cost and carbon savings, and identified that although the above carbon and cost savings are marginal low and do not substantiate the benefits or advantages of installing the DAC, these savings however are achieved purely from evaluating the different temperature set point control strategies. Nevertheless substantial savings can be made when the DAC is compared to other alternative technologies.

8.7 Scope for Further Work

8.7.1 Development of Theoretical Model for Estimating Seasonal Heat Energy

(Petrol tank/ ground charging and discharging)

While some evidence regarding the price sensitivity of heating and cooling demand has accumulated in recent years to our knowledge no one has provided any evidence concerning the relationship between the availability of seasonal heat energy reservoir and elasticity of demand.

Measurement of this elasticity is complicated by the presence of two offsetting effects; the building occupancy behaviour and the rate of heat extraction and dissipation has on availability the amount of heat left in the petrol tank. On the one hand an increase in seasonal ground temperature can be expected to optimise the systems performance through its effect on heat energy consumption per hour extracted. On the other hand improved performance reduces the marginal and average cost of the system, carbon savings and thereby leads to reduced consumption by encouraging the occupants to monitor, control and plans carefully to drive their petrol tank effectively. Opportunity exists to fully optimise the performance of the GSHP system by developing a theoretical model for estimating the seasonal heat reservoir availability, behaviour and use.

8.7.2 Optimisation of Ground Source Heat Pumps with Predictive Behavioural Control

There has been little work on the possibility of using inter-seasonal storage of energy in the ground using GSHPs. There has been even less research carried out on the control systems for storing/recovering energy from a long term store in relation to occupancy patterns and behaviour. An investigation is required to determine opportunities for a novel predictive GSHP control systems to effectively utilise inter-seasonal storage of energy in the ground using GSHPs.

Nearly half the energy consumed in the UK is used in buildings mostly for heating, cooling, and lighting. Inter-seasonal storage is able to offer a significant reduction in consumption of fossil fuels for heating and cooling in the move towards a low carbon economy by saving surplus energy in summer and returning it in winter. Using a Building Management System

(BMS) it should be possible to maximise savings and GSHP efficiency by matching the optimum system operation to the building demand, as dictated by the occupants. This will entail an entirely novel control based on heat stored (and rate of charge/discharge), system coefficient of performance (COP), fuel tank and occupant expectation of thermal comfort. Bringing these three aspects together into a single effective control will require a multi-disciplinary approach.

8.7.3 Control Strategy Based on DAC

Chapter 7 explored two different control strategies using the DAC for improving the performance of the GSHP system, there is further scope for investigating the impact of running the DAC based on alternative scenarios, for example controlling the GSHP system on the temperature difference between the fluid temperature leaving heat pump and outside air temperature exceeding a desired temperature set point value, this will provide significant opportunity to identify the impact of the control to the following parameters:

- Heat rejection to ground
- Energy consumption of the system which is made up of heat pump, circulation pumps energy and fan energy inputs.
- COP of the system.
- Ground temperature variation
- Running frequency operation of the heat pump, circulation pump and fan.

8.7.4 Investigating Heat Transfer Enhancement of Energy Piles using PCM

A recent area of research has focused on the potential for heating and cooling to be provided by thermally active foundations. The GSHP installation at LSBU employs 159 energy piles for extracting and injecting heat to the ground. Six of the 28 m deep piles have been equipped with 33 calibrated type T thermocouples at depths of 3 m, 14 m and 26 m to allow close monitoring of the underground temperature distribution. In addition to the thermocouples installing a phase change material (PCM) in the building foundation piles will further aid an understanding of the complex heat transfer process around the energy piles. This will permit a novel investigation of both the ground behavior and the effects of heating and cooling on the building's structure. The installation also includes stress gauges to enable correlation of stress with ground temperature. One dummy thermopile was also monitored as a reference-case. Including PCM temperature sensing in the deep piles, is a unique research resource, and

is an ideal facility for fully evaluating and optimizing the performance of the GSHP systems. As discussed in Chapter 6 by measuring the temperatures around the piles it has been possible to gain understanding of the thermal charge and discharge characteristics of the system.

8.8 Novelty and Contribution to Science

The novelty and contribution to science from this work is:

- The better understanding of the effect of ground temperature variation over time and its effect on the system's performance.
- The development of new measurement methods for assessing system performance.
- The use of ground temperature in the prediction and control of system performance, together with an analysis of the effects of specific interventions or control methodologies.
- The development of a novel mathematical model for predicting disturbed ground temperature.
- The development of a novel GSHP model using TRNSYS.
- The development and investigation of novel control strategies using DAC.

References

- Adam, D. and Markiewicz, R. (2009). Energy from earth-coupled structures, foundations, tunnels and sewers, *Géotechnique* 3 (59), pp. 229–236.
- AECOM. (2013). An Investigation into Heat Meter Measurement Errors. AECOM, Hertfordshire, UK.
- Allan, M.L. and Philippacopoulos, A.J. (1999). Groundwater protection issues with geothermal heat pumps, *Geothermal Resources Council Transactions* 23.
- Anderson, B.R., Chapman, P.F., Cutland, N.G., Dickson, C.M., Doran, S.M. and Henderson, G. (2008). BREDEM-8 Model Description, BR439 (ed) BRE Press: Watford, UK.
- Badescu, V. (2007). Economic aspects of using ground thermal energy for passive house heating, *Renewable Energy* 6 (32), pp. 895–903.
- Boennec, O. (2008). Shallow ground energy systems, *Proceedings of the Institution of Civil Engineers, Energy EN2* (161), pp. 57–61.
- Bourne-Webb, P., Amatya, B., Soga, K., Amis, T., Davidson C., and Payne, P. (2009). Energy pile tests at Lambeth College, London: geotechnical and thermodynamic aspects of pile response to heat cycles, *Géotechnique* 59 (3) pp. 237–248.
- Brandl, H. (1998). Energy piles and diaphragm walls for heat transfer from and into the ground. In: Van Impe and Haegeman, *Deep foundations on bored and auger piles – BAP III*, Balkema, Rotterdam pp. 37–60.
- Brandl, H. (2006). Energy foundations and other thermo-active ground structures, *Géotechnique* (2) 56 pp 81–122.
- Carslaw, H.S. and Jaeger, J.C. (1947). *Conduction of heat in solids*. Oxford, U.K.: Clarendon Press.

Centre for Alternative Technology. Air source heat pumps. Machynlleth, Powys, Centre for Alternative Technology. (2010).

Clarke, B., Agab, A. and Nicholson, D. (2008). Model specification to determine thermal conductivity of soils, *Proceedings of the Institution of Civil Engineers, Geotechnical Engineering* 161 (3) pp. 161–168.

CIBSE Guide B (2005). Heating, ventilating, air conditioning and refrigeration, London: Chartered Institution of Building Services Engineers.

DEFRA and DECC, (2010). AEA Technology for the Department of Energy and Climate Change and the Department for Environment, Food and Rural Affairs: Guidelines to DEFRA/DECC's GHG conversion factors for company reporting, London, UK.

De Moel, M., Peter M., Abdelmalek, B., Rao M., JingLiang O. (2010). Technological advances and applications of geothermal energy pile foundations and their feasibility in Australia Review Article *Renewable and Sustainable Energy Reviews*, 14 (9) pp 2683-2696.

Deerman, J.D. and Kavanaugh, S.P. (1991). Simulation of vertical U-tube ground coupled heat pump systems using the cylindrical heat source solution. *ASHRAE Transactions* 97 pp 287–295.

Del Col, D., Azzolin, M., Benassi, G., Mantovan, M. (2014). Experimental analysis of optimal operation mode of a ground source heat pump system *Energy Procedia*, 45, pp. 1354–1363.

Department of Energy and Climate Change, (DECC) (2009). The UK Supply Curve for Renewable Heat, London, UK.

Department of Energy and Climate Change (DECC) (2014). Preliminary data from the RHPP heat pump metering programme.

Diao, N., Li, Q., and Fang, Z. (2004). Heat transfer in ground heat exchangers with ground water advection, *International Journal of Thermal Sciences* 43 (12) pp. 1203–1211.

Ecofys (2013). Heat Pump Implementation Scenarios until 2030, Germany.

Ecuity Consulting LLP (2012). 6.8 million Heat Pumps by 2030: From Vision to Reality. Solihull, UK.

- Elias, E.A., Cichota, R., Torriani, H.H., (2004). Analytical soil-temperature model: correction for temporal variation of daily amplitude. *Soil Sci. Soc. Am. J.* 68 (3), 784–788.
- Energy Saving Trust (2008). *Domestic Heating Systems Ranked by Carbon Emission*: London, UK.
- Energy Saving Trust (2010). *Getting Warmer: A Field Trial of Heat Pumps*, London UK, 2010.
- Energy Saving Trust (2013). *The heat is on: heat pump field trials phase 2*, London UK, August 2013.
- EnergyPlus Energy Simulation Software, U.S. Department of Energy-DOE, Available online: <<http://apps1.eere.energy.gov/buildings/energyplus/>>[accessed 24.08.13].
- Eskilson P. (1987). Thermal analysis of heat extraction boreholes, Doctoral Thesis. Department of mathematical physics and building technology, Lund, Sweden: University of Lund.
- Esen, H. and Inalli, M. (2009). In-situ thermal response test for ground source heat pump system in Elazığ, Turkey, *Energy and Buildings* 41 (4) pp. 395–401.
- European Heat Pump Association and Delta Energy & Environment (2013). *European Best Practice in Building Successful Heat Pump Markets, Unleashing the Opportunity*: Joint publication. Available online: <http://www.ehpa.org/media/studies-and-reports/> [accessed 20.05.14].
- Fahlén, P. (2012). Capacity control of heat pumps. *Rehva European HVAC Journal* <http://www.rehva.eu/en/rehva-european-hvac-journal>, 2012-10, (REHVA.) Brussels, Belgium
- Florides, G. and Kalogirou, S. (2007). Ground heat exchangers—a review of systems models and applications, *Renewable Energy* 32 (15) pp. 2461–2478.
- Fridleifsson, I.B., Bertani, R., Huenges, E., Lund, J.W., Ragnarsson, A., Rybach, L., Hohmeyer, O., Trittin, T., 2008. The possible role and contribution of geothermal energy to the mitigation of climate change, *Scoping Meeting on Renewable Energy Sources*, Luebeck, Germany, pp. 59-80.

- Fritsche U.R. and Schmidt K. (2007). Global emission model of integrated systems (GEMIS) manual. Darmstadt: Institute for Applied Ecology. <http://www.iinas.org/gemis.html>. [24/01.2013].
- Gao, J. (2008a). Thermal performance and ground temperature of vertical pile-foundation heat exchangers: a case study, *Applied Thermal Engineering* 28 (17) pp. 2295–2304.
- Gao, J. (2008b). Numerical and experimental assessment of thermal performance of vertical energy piles: an application, *Applied Energy* 85 (10) pp. 901–910.
- Geothermal International (2013), Heat pump designers and installers, available online from: <http://www.gienergy.net/> .
- Hamada, Y., Saitoh, H., Nakamura, M., Kubota, H. and Ochifuji, K. (2007). Field performance of an energy pile system for space heating, *Energy and Buildings* 39 (5) pp. 517–524.
- Hanqing, W., Chunhua, H., Zhiqiang, L., Guangfa, T., Yingyun, L. and Zhiyong, W. (2006) Dynamic evaluation of thermal comfort environment of air-conditioned buildings, *Building and Environment*, 41 (2005) pp1522–1529. China: 19 April 2005.
- Healy, P.F. and Ugursal, V.I. (1997). Performance and economic feasibility of ground source heat pumps in cold climate, *International Journal of Energy Research* 21 (10) pp. 857–870.
- Hellstrom, G. (1989). *Duct ground heat storage model: Manual for computer code*. Lund, Sweden: University of Lund, Department of Mathematical Physics.
- Hellstrom, G. (1991a). *Ground heat storage: Thermal analysis of duct storage system, Part I Theory*. Lund, Sweden: University of Lund, Department of Mathematical Physics.
- Hellstrom, G. (1991b). *Bedrock heat store in Lulea: Numerical simulations 1983–1988*. Lund, Sweden: University of Lund, Department of Mathematical Physics.
- Hepbasli, A. (2002). Performance evaluation of a vertical ground-source heat pump system in Izmir, Turkey, *International Journal of Energy Research* 26 (13) pp. 1121–1139.
- Hepbasli, A., Akdemir, O. and Hancioglu, E. (2003). Experimental study of a closed loop vertical ground source heat pump system, *Energy Conversion and Management* 44 (4) pp. 527–548.

- Huber A, Wetter M. (1997). Vertical borehole heat exchanger, EWS model Version 2.4 Model description and implementation in TRNSYS, ZTL-Luzern and Huber Energietechnik-Zürich, Switzerland, November 7, 1997.
- IEA Heat Pump Centre IEA (2010), Retrofit heat pumps for buildings: final report. IEA heat pump programme. Borås.
- IEA (2014), IEA HPP Annex 42: Heat Pumps in Smart Grids. Market overview United Kingdom. Delta Energy & Environment.
- Incropera, F. P., and DeWitt, D. P. (1996). Fundamentals of heat and mass transfer 4th Edition. New York: J. Wiley.
- Inalli, M. and Esen, H. (2004). Experimental thermal performance evaluation of a horizontal ground-source heat pump system, Applied Thermal Engineering 24 (14) pp.2219–2232.
- Ingersoll, L.D. and Plass, H.J. (1948). Theory of the ground pipe heat source for the heat pump, ASHVE Transactions 47 (7) pp. 339–348.
- Ingersoll, L.R., Zobel, O.J and Ingersoll, A.C (1954). *Heat conduction with engineering, geological and other applications*, New York: McGraw-Hill.
- Jones, B.W. (2002). Capabilities and limitations of thermal models for use in thermal Comfort standards, Energy and Buildings 1 (34) 653–659.
- Karl, O. (2008). Geothermal Heat Pumps, A guide for Planning & installing: London, UK, pp.15. ISBN 9781844074068.
- Kasuda, T., Achenbach, P.R., (1965). Earth temperature and thermal diffusivity at selected stations in the United States. ASHRAE Trans. 71 (Part 1).
- Katsunori, N., Takao, K. and Sayaka, T. (2006) Development of a design and performance prediction tool for the ground source heat pump system. s.l., Appl.Therm.Eng. 26 (14-15) pp 1578-1592.
- Katzenbach, R., Clauss, F. and Waberseck, T. (2007). Geothermal energy – sustainable and efficient energy supply and storage in urban areas, the sixth China Housing conference, Beijing, China.

- Kavanaugh, S. (1998). Ground source heat pumps, *ASHRAE Journal* 40 (10) pp. 5–15.
- Kavgic, M., Mavrogianni, A., Mumovic, D., Summerfield, A., Stevanovic, Z., Djurovic-Petrovic, M. (2010). A review of bottom-up building stock models for energy consumption in the residential sector. *Build. Environ.* 45, 1683–1697.
- Kizilkan O, Dincer I. (2015). Borehole thermal energy storage system for heating applications: thermodynamic performance assessment. *Energy Convers Manage* 2015; 90:53–61.
- Klein, S. (1996). *TRNSYS manual, a transient simulation program*. Madison: Solar Energy Engineering Laboratory. Madison: University of Wisconsin.
- Kline, S.J., and F.A. McClintock. (1953). *Describing Uncertainties in Single-Sample Experiments*. *Mechanical Engineering* 57(1): 62-6.
- Kurevija, T., Vulin, D., Krapec, V. (2012). Effect of borehole array geometry and thermal interferences on geothermal heat pump system *Energy Convers Manage*, 60, pp. 134–142.
- Lee, C.K. (2010). Dynamic performance of ground-source heat pumps fitted with frequency inverters for part-load control *Appl Energy*, 87, pp. 3507 – 3513.
- Lund, J.W., Freeston, D.H. and Boyd, T.L. (2010). Direct application of geothermal energy: 2005 Worldwide review. *Geothermics*; 34(6): pp691–727.
- Madani, H., Claesson, J., Lundqvist P., (2013). A descriptive and comparative analysis of three common control techniques for on/off controlled ground source heat pump (GSHP) system *Energy Build*, 65, pp. 1 – 9.
- Michopoulos, A., Bozis, D., Kikidis, P., Papakostas, K. and Kyriakis, N.A. (2007). Three-year's operation experience of a ground source heat pump system in Norther Greece, *Energy and Buildings* 39 (3) pp. 328–334.
- Mitsubishi Product Data. Available online:
http://www.intelligentenergysolutions.com/groundsourceheat-pumps_c65.aspx (Accessed on 21 October 2013).
- Mohamed, O., Parham, E., Messaoud, B., Zine, A. (2014). New correlations for the prediction of the undisturbed ground temperature, *Geothermics* 53 (2015) 379–384.

- Montagud, C., Corberán, J.M., Ruiz-Calvo, F. (2013). Experimental and modelling analysis of a ground source heat pump system. *Applied Energy*, 109: 328-336.
- Morino, K. and Oka, T. (1994). Study on heat exchanged in soil by circulating water in a steel pile, *Energy and Buildings* 21 (1) pp. 65–78.
- Morrison, G.L, Anderson, T. and Behnia, M. (2004). Seasonal performance rating of heat pump water heaters. *Solar Energy* 76 pp147–152.
- Montagud, C., Corberán, J.M., Ruiz-Calvo, F. (2013). Experimental and modelling analysis of a ground source heat pump system *Appl Energy*, 109, pp. 328–336.
- Nagano, K. (2007). *Energy pile system in new building of Sapporo City University in thermal energy storage for sustainable energy consumption*, Springer, Netherlands.
- NERA and AEA (2009). *The UK supply curve for renewable heat: Study for the Department of Energy and Climate Change*. London, NERA Economic Consulting.
- Nordman, R. (2012). *Seasonal performance factor and monitoring for heat pump systems in the building sector SEPEMO-build*, London, UK.
- Office of Gas and Electricity Markets Ofgem (2011). Decision letter: Revision of typical domestic consumption values (5 November 2010) Available online: <http://www.ofgem.gov.uk>.
- Ozgener, L. (2005). Energy and exergy analysis of geothermal district heating systems: an application, *Building and Environment* 40 (10) pp. 1309–1322.
- Ozgener, O. and Hepbasli, A. (2005). Experimental performance analysis of a solar Assisted ground-source heat pump greenhouse heating system, *Energy and Buildings* 37 (1) pp. 101–110.
- Pachauri, R.K., Reisinger, A. (2007). *Climate Change 2007: Synthesis Report. Contribution of Working Groups I, II and III to the Fourth Assessment Report of the Intergovernmental Panel on Climate Change*, IPCC: Geneva, Switzerland; pp. 301–320.

- Parisch, P., Mercker, O., Oberdorfer, P., Bertram, E., Tepe, R., Rockendorf, G. (2015). Short-term experiments with borehole heat exchangers and model validation in TRNSYS Renewable Energy, 74 (2015), pp. 471–477.
- Pollard, A.R. (2010). The Energy Performance of Heat Pump Water Heaters; Branz Study Report 237; Branz Ltd.: Judgeford, New Zealand.
- Popiel, C.O., Wojtkowiak J. and Biernacka, B. (2001). Measurements of temperature distribution in ground, Experimental Thermal and Fluid Science 25 (5) pp. 301–309.
- Preene, M. and Powrie, W. (2009). Ground energy systems: from analysis to geotechnical design, Géotechnique 3 (59) pp. 261–271.
- Rawlings, R (1999). A BSRIA Technical Note Ground Source Heat Pumps. BSRIA TN 18/99, s.l BSRIA (1999).
- Rees, S.W., Adjali, M.H., Zhou, Z., Davies, M. and Thomas, H.R. (2000). Ground heat transfer effects on the thermal performance of earth-contact structures Renewable & Sustainable Energy Reviews 4 (3) pp. 213–265.
- RETScreen 4, (2005). Ground-source heat pump project analysis chapter. In: Clean Energy Project Analysis: RETScreen Engineering & Cases Textbook. CanmetENERGY at Varennes, Natural Resources Canada, Canada.
- Roy, R., and Caird, S. et al. (2008). YIMBY Generation yes in my back yard! UK. Householders Pioneering Micro-Generation Heat. London, Energy Saving Trust.
- Sachdeva, R.C. (2009). Fundamentals of engineering heat and mass transfer. Tunbridge Wells: New Age Science.
- Sanaye, S. and Niroomand, B. (2009). Thermal-economic modelling and optimization of vertical ground-coupled heat pump, Energy Conversion and Management 4 (50), pp.1136–1147.
- Sanner, B. (2001). Shallow geothermal energy, Geo-heat center bulletin, Klamath Falls, OR, Geo-Heat Centre.
- Singh, H. and Muetze, A. et al (2010). Factors influencing the uptake of heat pump technology by the UK domestic sector. Renewable Energy 35(4): pp873-878.

- Signorelli, S., Kohl, T., (2004). Regional ground surface temperature mapping from meteorological data. *Global Planet. Change* 40, 267–284.
- Smerdon, J.E., Pollack, H., Cermak, V., John, W., Kresl, M., Safanda, J., Wehmiller, J.F., (2006). Daily, seasonal, and annual relationships between air and subsurface temperatures. *J. Geophys. Res.* 111 (D7), D07101.
- Tarnawski, V.R. and Leong, W.H. (1993). Computer analysis, design and simulation of horizontal ground heat exchangers, *International Journal of Energy Research* 17 (6) pp. 467–477.
- Tarnawski, V.R., Leong, W.H., Momose T. and Hamada, Y. (2009). Analysis of ground source heat pumps with horizontal ground heat exchangers for northern Japan, *Renewable Energy* 1 (34) pp.127–134.
- Tarnawski, V.R., Momose, T. and Leong, W.H. (2009). Assessing the impact of quartz content on the prediction of soil thermal conductivity, *Géotechnique* 59 (4) pp. 331–338.
- The Government's Standard Assessment Procedure for Energy Rating of Dwellings, Revision 3; BRE Press: Watford, UK, 2005.
- Thomas, H.R. and Rees, S.W. (2009). Measured and simulated heat transfer to foundation soils, *Géotechnique* 59 (4) pp. 365–375.
- Thomson. Kelvin W. (1882). *Mathematical and Physical Papers II*, cited by Ingersoll et al 1954 pp. 41.
- Thornton, J.W., McDowell, T.P., Shonder, J.A., Hughes, P.J., Pahud, D. and Hellstrom, G. (1997). Residential vertical geothermal heat pump system models: calibration to data. *ASHRAE Transactions* 103: pp660–674.
- TRNSYS, (2005). Version 16.A. Transient system simulation program solar energy engineering laboratory Madison: University of Wisconsin.
- UK Committee on Climate Change (2011). *The Renewable Energy Review*, London, UK.
- UK HM Government (2009). *The UK Renewable Energy Strategy*, London, UK.

UK Office of Climate Change OCC (2007). Household Emissions Project–Analysis Pack, London, UK.

US Environmental Protection Agency EPA (1997). A short primer and environmental guidance for geothermal heat pumps.

Van Wijk, W.R., (1963). Physics of Plant Environment. North-Holland Books, North-Holland Pub. Co, 382 pp., Netherlands.

Wang, H. and Qi, C. (2008). Performance study of underground thermal storage in a solar-ground coupled heat pump system for residential buildings, *Energy and Buildings* 40 (7) pp. 1278–1286.

Wu, W., You, T., Wang, B., Shi, W., Li X. (2014). Evaluation of ground source absorption heat pumps combined with borehole free cooling *Energy Convers Manage*, 79, pp. 334–343.

Yari, M. and Javani, N. (2007). Performance assessment of a horizontal-coil geothermal heat pump, *International Journal of Energy Research* 31 (3) pp. 288–299.

Zhao, L., Zhao, L.L., Zhang, Q., Ding, G.L. (2003). Theoretical and basic experimental analysis on load adjustment of geothermal heat pump systems *Energy Convers Manage*, 44, pp. 1 – 10.

Zoi, S. and Constantinos, R. (2012). Control Strategy for minimizing the electric power consumption of Hybrid Ground Source Heat Pump System. *Proceeding of ECOS JUNE 26-29, 2012, PERUGIA, ITALY*.

Appendix A

TRNSYS Deck File

Introduction

To conduct a simulation in TRNSYS, a file is created by the simulation studio which lists all of the simulation conditions, the Types used within the model, all of the connections made between Types and the initial conditions for each variable in each Type. This file, called the Deck file (input file) is then read in by the TRNSYS simulation engine, which takes processes the data within the Deck file and runs the simulation, and upon completion, an output file is created with the results of the simulation. A new Deck file is created for each simulation, outlining all of the simulation conditions. The following is an example of the deck file created by the TRNSYS model of the experimental set-up. The total simulation was set to last 12408 hours, at 60 s time steps.

VERSION 17

*** TRNSYS input file (deck) generated by TrnsysStudio

*** on Monday, February 29, 2016 at 12:39

*** from TrnsysStudio project: C:\Users\yebiyom2\Desktop\Attachments_201435\New
folder\Control\Jul11_Aug14\DAC Scenarios\DAC Scenario 2 LWT GHX\DAC Scenarios 2 OAT
V2.tpf

*** If you edit this file, use the File/Import TRNSYS Input File function in

*** TrnsysStudio to update the project.

*** If you have problems, questions or suggestions please contact your local

*** TRNSYS distributor or <mailto:software@cstb.fr>

*** Units

*** Control cards

* START, STOP and STEP

CONSTANTS 3

START=1

STOP=12408

STEP=1

* User defined CONSTANTS

EQUATIONS 4

DAY=INT(START/24)+1

N_DAYS=INT((STOP-START)/24.000001) + 1

N_WEEKS=INT((STOP-START)/168.000001) + 1

N_YEARS=INT((STOP-START)/8760.000001) + 1

SIMULATION START STOP STEP

TOLERANCES 0.001 0.001

LIMITS 50 1000000 50

DFQ 1

WIDTH 120

LIST

MAP

SOLVER 0 1 1

NAN_CHECK 0

OVERWRITE_CHECK 0

TIME_REPORT 0

EQSOLVER 0

* Model "GHX" (Type 557)

*

UNIT 10 TYPE 557 GHX

*\$UNIT_NAME GHX

*\$MODEL .\GHP Library (TESS)\Ground Heat Exchangers\Vertical U-Tubes\Standard\Type557a.tmf

*\$POSITION 605 653

*\$LAYER Main #

PARAMETERS 44

1000

26

4

159

0.375

10

10

10

4.68

1343

-1
0.016
0.0131
0.026
4.968
1.44
1.44
0
24480.000687
13
0
3.9
1025
0
0.5
0.0254
1.000001
5
40
5
0
0
30
10
90
10.8
13.3
240
1
4.644
1343
26
0
0
INPUTS 5
23,1
23,2
0,0
0,0
0,0

*** INITIAL INPUT VALUES

10 6.8 19 10.8 1

*-----

* Model "Load CP" (Type 3)

*

UNIT 15 TYPE 3 Load CP

*\$UNIT_NAME Load CP

*\$MODEL .\Hydronics\Pump - no Powercoefficients\TYPE3d.tmf

*\$POSITION 357 201

*\$LAYER Main #

PARAMETERS 4

```
136620.002747
4.190
107999.992009
0
INPUTS 3
20,3
0,0
0,0
*** INITIAL INPUT VALUES
30 30600 1.0
*-----
* Model "Type65a" (Type 65)
*
UNIT 28 TYPE 65      Type65a
*$UNIT_NAME Type65a
*$MODEL .\Output\Online Plotter\Online Plotter With File\TRNSYS-Supplied Units\Type65a.tmf
*$POSITION 37 431
*$LAYER Main #
PARAMETERS 12
10
10
0
30
0
30
1
10
0
78
2
0
INPUTS 20
19,1
10,3
20,2
On_Fluid
20,3
0,0
10,1
16,8
20,5
20,6
0,0
0,0
16,5
16,6
16,7
0,0
12,1
0,0
0,0
0,0
*** INITIAL INPUT VALUES
DAC_FluidO grd_ave Flui_Temp On_Fluid return Load_tmp_Flow Sourc_RTemp
```

```
gs_cop THCPL32 OAT load_flrt source_flrt hp_load hp_source HP Power
HP1Elec OAT2 load_flrt load_flrt
LABELS 3
"COP"
"COP"
"Graph 1"
*** External files
ASSIGN "G_glhepro.plt" 78
*|? What file should the online print to? |1000
*-----
* Model "Type682" (Type 682)
*
UNIT 22 TYPE 682    Type682
*$UNIT_NAME Type682
*$MODEL .\Loads and Structures (TESS)\Flowstream Loads\Other Fluids\Type682.tmf
*$POSITION 192 202
*$LAYER Main #
PARAMETERS 1
4.19
INPUTS 3
15,1
15,2
0,0
*** INITIAL INPUT VALUES
30 30600 0
*-----
* Model "GSHP" (Type 668)
*
UNIT 16 TYPE 668    GSHP
*$UNIT_NAME GSHP
*$MODEL .\HVAC Library (TESS)\Water-to-Water Heat Pump\Type668.tmf
*$POSITION 430 327
*$LAYER Main #
PARAMETERS 9
3.9
4.190
85
3
4
86
5
4
1
INPUTS 6
10,1
10,2
22,1
22,2
COP_24hr
0,0
*** INITIAL INPUT VALUES
0 0 0 1 0
*** External files
```

ASSIGN "C:\Users\yebiyom2\Desktop\Attachments_201435\EKW 130 - Cooling FullandPart Load Data.txt" 85

*|? Which file contains the cooling performance data? |1000

ASSIGN "C:\Users\yebiyom2\Desktop\Attachments_201435\EKW 130 - Heating FullandPart Load Data.txt" 86

*|? Which file contains the heating performance data? |1000

*-----

* Model "External Loads" (Type 9)

*

UNIT 20 TYPE 9 External Loads

*\$UNIT_NAME External Loads

*\$MODEL .\Utility\Data Readers\Generic Data Files\First Line is Simulation Start\Free Format\Type9a.tmf

*\$POSITION 467 201

*\$LAYER Main #

PARAMETERS 30

2

1

6

1

-1

1

0

0

-1

1

0

0

92

-1

*** External files

ASSIGN "C:\Users\yebiyom2\Desktop\Attachments_201435\New folder\Control\Jul11_Aug14\DAC Scenarios\Apr13Sept14V2.txt" 92

*|? Input file name |1000

*-----

* EQUATIONS "Equa-2"

*

EQUATIONS 7

On_Cool = GT([20,6],18)

On_Heat = LT([20,6],14)

Building_Control = On_Heat*[17,3]

COP_24hr = [17,3]*On_Cool

On_Fluid = GT([20,2],24)*On_Cool*[17,3]

OFF_Fluid = LT([20,2],22)*On_Cool*[17,3]

On_OAT = GT([20,6],18)

*\$UNIT_NAME Equa-2

*\$LAYER Main

*\$POSITION 563 367

*-----

* Model "Forcing Function" (Type 579)

*

UNIT 17 TYPE 579 Forcing Function

*\$UNIT_NAME Forcing Function

```
*$MODEL .\Utility Library (TESS)\Forcing Functions\Multi-Level Functions\2-Level
Function\Type579-2.tmf
*$POSITION 673 293
*$LAYER Main #
*$# Possible Uses:
*$# Temperature Setpoints in a House/Building
*$# Occupancy Patterns for a School
*$# Controller for Detailed Pumping Scheme
PARAMETERS 12
2
168
24
1
0.0
120
1
12
14
1
8
21
INPUTS 4
0,0
0,0
0,0
0,0
*** INITIAL INPUT VALUES
0.0 0 0 0
*-----
* Model "Outside Air Temp" (Type 9)
*
UNIT 21 TYPE 9      Outside Air Temp
*$UNIT_NAME Outside Air Temp
*$MODEL .\Utility\Data Readers\Generic Data Files\First Line is Simulation Start\Free
Format\Type9a.tmf
*$POSITION 739 408
*$LAYER Main #
PARAMETERS 74
2
1
17
1
-1
1
0
0
200
-1
*** External files
ASSIGN "C:\Users\yebiyom2\Desktop\Attachments_201435\OutsideAirTempTHCPL.dat" 200
*|? Input file name |1000
*-----
* Model "ext temp" (Type 15)
*
```

```
UNIT 12 TYPE 15      ext temp
*$UNIT_NAME ext temp
*$MODEL .\Weather Data Reading and Processing\Standard Format\Meteonorm Files
(TM2)\Type15-6.tmf
*$POSITION 638 201
*$LAYER Main #
PARAMETERS 9
6
201
3
0.2
0.7
1
1
0.0
0
*** External files
ASSIGN "C:\Users\yebiyom2\Desktop\Attachments_201435\GB-London-Weather-C-37790.tmf"
201
*|? Which file contains the Meteonorm weather data? |1000
*-----

* Model "Type65a-2" (Type 65)
*
UNIT 18 TYPE 65      Type65a-2
*$UNIT_NAME Type65a-2
*$MODEL .\Output\Online Plotter\Online Plotter With File\TRNSYS-Supplied Units\Type65a.tmf
*$POSITION 585 101
*$LAYER Main #
PARAMETERS 12
4
6
0.0
500000
0.0
100000
1
12
0
202
2
0
INPUTS 10
16,5
16,6
On_Fluid
0,0
16,7
16,8
10,3
27,3
19,4
0,0
*** INITIAL INPUT VALUES
```

Load Source On_Fluid Heat Elec Coefficient Ave_GndTemp Pump_Power Fan_Power
Elec

LABELS 3

"Temperatures"

"Heat transfer rates"

"Graph 1"

*** External files

ASSIGN "****.plt" 202

*|? What file should the online print to? |1000

*-----

* Model "DAC" (Type 511)

*

UNIT 19 TYPE 511 DAC

*\$UNIT_NAME DAC

*\$MODEL .\HVAC Library (TESS)\Dry Fluid Cooler\Type511.tmf

*\$POSITION 391 527

*\$LAYER Main #

*\$# DRY FLUID COOLER

PARAMETERS 12

1

44

37.799988

44269.999695

4.190

20

89539200

17999.998668

10.0

2

0.0

1

INPUTS 5

26,3

26,4

On_Fluid

On_Fluid

On_Fluid

*** INITIAL INPUT VALUES

10.0 6.8 22 1 22

*-----

* Model "Tempering Valve" (Type 11)

*

UNIT 26 TYPE 11 Tempering Valve

*\$UNIT_NAME Tempering Valve

*\$MODEL .\Hydronics\Tempering Valve\Other Fluids\Type11b.tmf

*\$POSITION 275 527

*\$LAYER Main #

PARAMETERS 2

5

10

INPUTS 4

27,1

27,2

0,0

```
0,0
*** INITIAL INPUT VALUES
20.0 24480.000687 24 100
*-----
* Model "Circ Pump" (Type 114)
*
UNIT 27 TYPE 114      Circ Pump
*$UNIT_NAME Circ Pump
*$MODEL .\Hydronics\Pumps\Single Speed\Type114.tmf
*$POSITION 168 474
*$LAYER Main #
*$# SINGLE-SPEED PUMP
PARAMETERS 4
24480.000687
3.9
53999.996005
0.0
INPUTS 5
20,2
0,0
COP_24hr
0,0
0,0
*** INITIAL INPUT VALUES
30 24480.000687 1 0.6 0.9
*-----
* Model "Mixing Valve" (Type 11)
*
UNIT 23 TYPE 11      Mixing Valve
*$UNIT_NAME Mixing Valve
*$MODEL .\Hydronics\Tee-Piece\Other Fluids\Type11h.tmf
*$POSITION 491 591
*$LAYER Water Loop #
PARAMETERS 1
1
INPUTS 4
19,1
19,2
26,1
26,2
*** INITIAL INPUT VALUES
20.0 24480.000687 20.0 24480.000687
*-----
END
```

Appendix B

Experimental Uncertainty and Error Analysis

Introduction

In order to properly evaluate the validity of any experimental result it is important to understand the relative effect of associated error. This section of the thesis describes the various error approximations for this study and their combined effect on the reported results.

The results presented throughout this thesis make use of significant figures in order to omit the need for continuous reference to the effects of error. For example, if a systematic accuracy error of $\pm 0.3\%$ was defined for a set of weighing scales, and the measured mass (digital scale to omit bias errors) was 148.06 g, then the reported measurement will be 148 g. With zero decimal places, 148 g implies that the true value lies somewhere between 147.5 g and 148.5 g, equivalent to ± 0.5 g or 0.3 % accuracy error.

B.1 Error Approximation Method

Error can broadly be considered in one of two categories; systematic error (limitations of the measurement equipment) and random, or bias error (the skill of the experimenter in reading the measurement equipment).

When considering error, it is also important to understand the difference between the terms precision and accuracy. The precision of a value is a measure of the reproducibility or repeatability of a result (reducing the standard deviation from the mean measured value).

Precision accounts for the repeatability of a measurement; however the deviation from the true value determines the accuracy of a measurement.

In most cases, the required result is dependent on two or more variables, each with associated errors to consider. In these instances, quadrature is used to provide the propagated error (Kline and McClintock, 1953). Considering two measured quantities, X and Y, with errors ΔX and ΔY respectively.

Where $Z = X + Y$ or $Z = X - Y$ then

$$\Delta Z = \sqrt{\Delta X^2 + \Delta Y^2} \quad (\text{B.1})$$

Where $Z = X \cdot Y$ or $Z = \frac{X}{Y}$ then

$$\Delta Z = Z \cdot \sqrt{\left(\frac{\Delta X}{X}\right)^2 + \left(\frac{\Delta Y}{Y}\right)^2} \quad (\text{B.2})$$

The propagated error for simple relations can be defined by equations (B.1) and (B.2). However the more general form, where $Z = f(X_1, X_2, \dots)$ is defined by equation (B.3).

$$\Delta Z = Z \cdot \sqrt{\left(\frac{\delta f(X_1, X_2, \dots)}{\delta X_1} \cdot \Delta X_1\right)^2 + \left(\frac{\delta f(X_1, X_2, \dots)}{\delta X_2} \cdot \Delta X_2\right)^2 + \dots} \quad (\text{B.3})$$

This propagated error analysis is applied to the thermal power equation, (B.4), used in the evaluation of the COP

$$Q_{\text{HP}} = \dot{m} C_p \Delta T \quad (\text{B.4})$$

$$\text{COP} = \frac{Q_{\text{HP}}}{W_{\text{HP}}} \quad (\text{B.5})$$

B.2 Experimental Error Evaluation

As the GSHP system at LSBU employed data-logging equipment the effects of the random bias errors associated with the skill of the experimenter in reading gauges etc. was not relevant to this error analysis. The various errors that must be considered are presented below.

B.2.1 Systematic Errors

The precision of the measurement equipment was experimentally validated. In the absence of the relevant certification, equipment accuracy was assessed using calibration methods. It is also important to consider the potential error in values obtained from data tables. Using the thermophysical properties for a given material from data-tables assumes that the material used in the experiment is identical. In most instances, experimentally validating the data-table values is impractical and systematic errors must be estimated. The heat meters calculate the energy transfer by measuring the fluid flow and the difference between the supply and return temperature. In order to compensate for the change of density and specific heat with change of temperature the meters are pre-configured with built in heat coefficient factors and these heat coefficient factors are different according to the glycol type and content in the system therefore a 2 % error is included.

The primary evaluation metric in this study is COP which is defined see equation (B.5) as the quotient of the HP heat output (Q_{HP}) and HP electricity input (W_{HP}). We must consider the HP heat output and the HP electricity input values separately in order to determine the overall error in COP. As COP values were primarily calculated from the experimental data collected, the error analysis described here is specific to the GSHP system at LSBU. In order to determine the error limits, the upper design point operating points were selected ($Q_{HP} = 142$ kW, $W_{HP} = 25$ W, COP= 5.6).

In order to assess the systematic error of temperature measurements, the specifications of the dataTaker DT500 data-logger were reviewed. The manufacturer (dataTaker) provided an accuracy of ± 0.25 %.

16 (2 sets of 8) Pt500 thermocouples were tested. The thermocouples were bound together and submerged into water at 30 °C, 40 °C, 50 °C and 60 °C to assess the precision and response time. A graph of one set of experimental results is shown in Figure B.1. The accuracy of the measurements was verified using a NEMA certified thermometer.

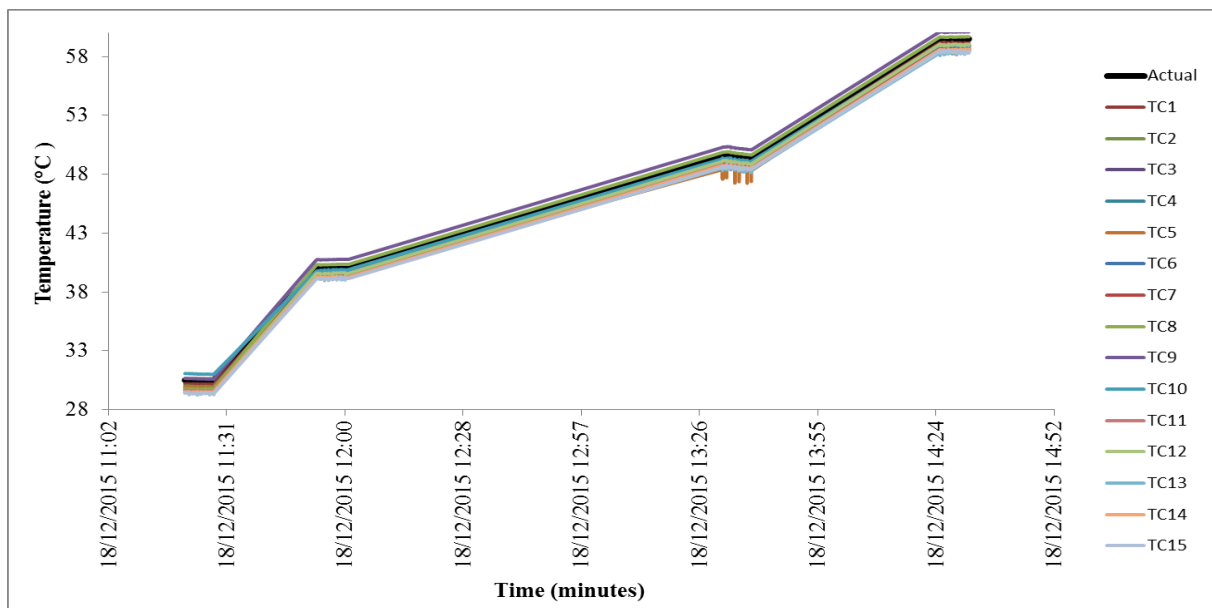


Figure B.78 Thermocouple calibration test

Figure B.2 shows the difference between the actual water temperature and the Pt500 thermocouples. The graph shows that as the water temperature increases the experimental error also increases. Temperature difference error of between 0.2 °C and 0.9 °C occurs when compared to the actual water temperature.

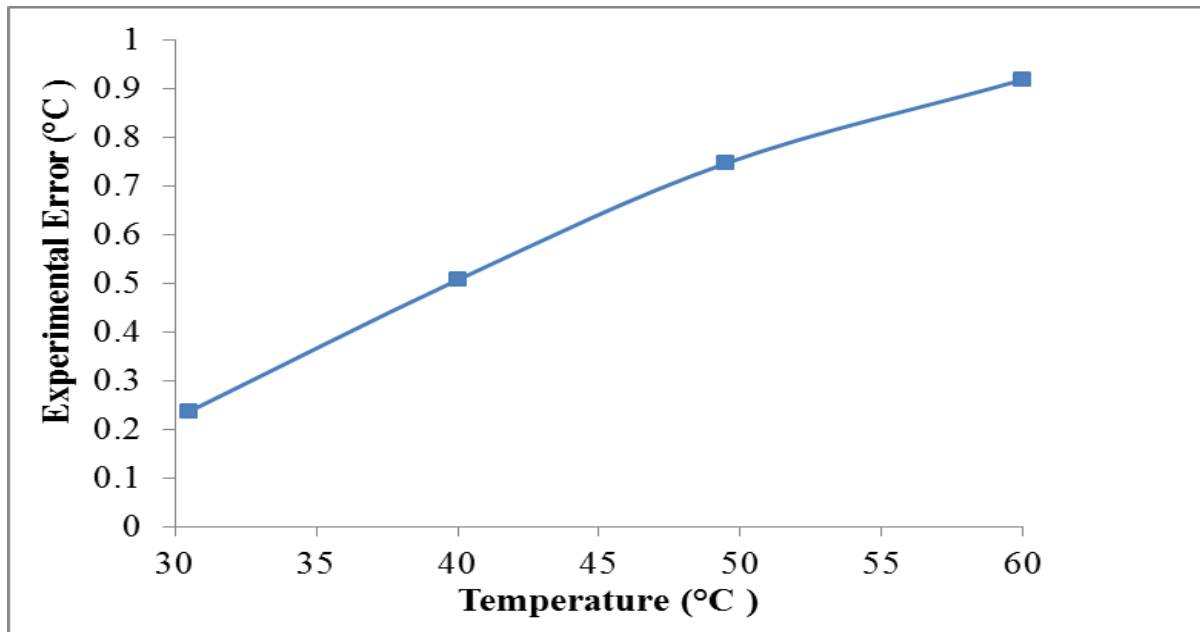


Figure B.79 Average experimental temperature difference error

Heat Output (Q_{HP}): The heat output is also estimated using equation (B.4). As the mass flow rate of the water could be measured using calibrated flow rate meter, and the time constant error of the data-logger was negligible, a systematic accuracy error of 1 % could be applied. Considering the specific heat capacity (C_p -water) of the water an accuracy of 2 % is estimated.

As previously discussed, the accuracy of temperature component of the Q_{HP} calculation has been experimentally validated as ± 0.8 °C. Using error propagation theory, 22 % accuracy can be calculated for Q_{HP} .

Further implementation of error propagation theory yields an accuracy error of 22 % in the COP. A summary of the component accuracies, relative percentages and propagated accuracies is presented in Table B.1.

Measurement	Type	Symbol	Units	Mean Value	Accuracy	Error evaluation method	Percentage
Flow meter	KROHNE	m	kg/s	6.80	0.003	0.3 % Calibrated scale	0.04 %
		Cp water	J/kg.K	4.186	0.084	2 % error on data table value	2 %
Temperature sensors Pt500	Kamstrup	ΔT	K	5	0.9	Experimentally validated	22 %
Heat meter	Landis and Gyr T550	Q_{HP}	kW	142	31.3	Propagated Error from 3 values above	22 %
Power Measurement	Aidon series 6000	W_{HP}	kW	25	0.375		1.5 % error on data table value
		COP	-	5.69	1.26	Total Propagated Error	22.1 %

Table B.14 Summary of propagated errors for the GSHP system

Appendix C

Experimental Against Manufacturer's Data Validation

Introduction

This appendix provides the methods used for validating the historical experimental data. As discussed in Chapter 5 in order to validate the historical performance data, the heating season COP data has been collected for January and February 2014. Using the linear regression analysis method this data has been compared against the manufacturer's performance data.

The GSHP system within the K2 building at LSBU uses four WaterFurnace EKW130 reversible HP units; the manufacturer's performance data for the EKW130 GSHP is obtained and is given in Table C.1.

Table C.15 *Manufacturer's Performance Data for EKW130*

ELT	EST	Load Flow		Source 6.8L/s						PD kPa	
		Flow	PD	Heating							
		L/s	Kpa	LLT	HC	kW	HE	COP	LST		
15.6	-1.1	6.8	21.4	20.2	127.6	22.8	105	5.6	-4.9	23.5	
		8.5	31.8	19.3	130.7	22.9	108	5.7	-5	23.5	
	4.4	6.8	21.4	20.8	144.6	23.7	121	6.1	0.1	22.8	
		8.5	31.8	19.8	148.2	23.9	124	6.2	-0.1	22.8	
	10	6.8	21.4	21.4	160.3	24.7	136	6.5	5.1	22.1	
		8.5	31.8	20.3	164.2	24.8	139	6.6	5	22.1	
	15.6	6.8	21.4	21.9	174.7	25.7	149	6.8	10.2	21.4	
		8.5	31.8	20.7	178.9	25.8	153	6.9	10	21.4	
	21.1	6.8	21.4	22.3	187.7	26.7	161	7.0	15.3	20.7	
		8.5	31.8	21.1	192.2	26.7	166	7.2	15.1	20.7	
	26.7	-1.1	6.8	20	31.1	123.7	28	95.7	4.4	-4.6	23.5
			8.5	30.1	30.3	126.7	28.2	98.5	4.5	-4.7	23.5
4.4		6.8	20	31.8	141.3	29.1	112	4.9	0.4	22.8	
		8.5	30.1	30.9	144.7	29.2	116	5.0	0.3	22.8	
10		6.8	20	32.4	157.2	30	127	5.2	5.4	22.1	
		8.5	30.1	31.3	161.1	30.2	131	5.3	5.3	22.1	
15.6		6.8	20	32.9	171.6	31	141	5.5	10.5	21.4	
		8.5	30.1	31.8	175.7	31.1	145	5.6	10.3	21.4	
21.1		6.8	20	33.3	184.3	31.9	152	5.8	15.6	20.7	
		8.5	30.1	32.1	188.8	32.1	157	5.9	15.4	20.7	
37.8		-1.1	6.8	18.6	42.1	119.7	35.4	84.3	3.4	-4.2	23.5
			8.5	28.3	41.3	122.6	35.5	87.1	3.5	-4.3	23.5
	4.4	6.8	18.6	42.7	136.4	36.2	100	3.8	0.8	22.8	
		8.5	28.3	41.8	139.8	36.4	103	3.8	0.7	22.8	
	10	6.8	18.6	43.3	151.7	36.9	115	4.1	5.8	22.1	
		8.5	28.3	42.3	155.4	37.1	118	4.2	5.7	22.1	
	15.6	6.8	18.6	43.8	165.5	37.7	128	4.4	10.9	21.4	
		8.5	28.3	42.7	169.5	37.9	132	4.5	10.8	21.4	
	21.1	6.8	18.6	44.2	177.9	38.5	139	4.6	16.1	20.7	
		8.5	28.3	43.1	182.2	38.6	144	4.7	15.9	20.7	
	48.9	-1.1	6.8	17.3	53	114.7	44.4	70.3	2.6	-3.7	23.5
			8.5	26.5	52.3	117.4	44.6	72.8	2.6	-3.7	23.5
4.4		6.8	17.3	53.6	128.9	44.9	84	2.9	1.4	22.8	
		8.5	26.5	52.7	132	45.1	86.9	2.9	1.3	22.8	
10		6.8	17.3	54	142.4	45.3	97.1	3.1	6.5	22.1	
		8.5	26.5	53.1	145.9	45.6	100	3.2	6.4	22.1	
15.6		6.8	17.3	54.5	155.3	45.8	110	3.4	11.6	21.4	
		8.5	26.5	53.5	159.1	46.1	113	3.5	11.5	21.4	
21.1		6.8	17.3	55	167.5	46.3	121	3.6	16.7	20.7	
		8.5	26.5	53.9	171.6	46.5	125	3.7	16.6	20.7	

The HP units are tested in accordance to BS EN 14511, the manufacturer's performance data is tested at the factory across a range of operational and test conditions such as, entering and exiting temperatures on the load and source sides as well as the heating and cooling capacity of the system. In order to compare this manufacturer's data to the actual performance data of our system, SPSS a statistical analysis software have been used to develop a linear relationship between the EST, LLT and the COP. Once the relationship has been established then this formulae has been used to interpolate the performance of the manufacturer's data in a range of flow and return temperatures.

The output from the SPSS analyses is given below.

Descriptive Statistics

	Mean	Std. Deviation	N
COP	3.5877	.65145	10
EST	10.0000	8.28841	10
LLT	48.6200	5.74298	10

Correlations

		COP	EST	LLT
Pearson Correlation	COP	1.000	.651	-.661
	EST	.651	1.000	.132
	LLT	-.661	.132	1.000
Sig. (1-tailed)	COP	.	.021	.019
	EST	.021	.	.358
	LLT	.019	.358	.
N	COP	10	10	10
	EST	10	10	10
	LLT	10	10	10

Variables Entered/Removed^a

Model	Variables Entered	Variables Removed	Method
1	LLT		Stepwise (Criteria: Probability-of-F- to-enter <= .050, Probability-of-F- to-remove >= .100).
2	EST		Stepwise (Criteria: Probability-of-F- to-enter <= .050, Probability-of-F- to-remove >= .100).

a. Dependent Variable: COP

Model Summary

Model	R	R Square	Adjusted R Square	Std. Error of the Estimate	Change Statistics				
					R Square Change	F Change	df1	df2	Sig. F Change
1	.661 ^a	.437	.367	.51835	.437	6.215	1	8	.037
2	.996 ^b	.992	.990	.06468	.555	506.744	1	7	.000

a. Predictors: (Constant), LLT

b. Predictors: (Constant), LLT, EST

ANOVA^a

Model		Sum of Squares	df	Mean Square	F	Sig.
1	Regression	1.670	1	1.670	6.215	.037 ^b
	Residual	2.150	8	.269		
	Total	3.819	9			
2	Regression	3.790	2	1.895	452.934	.000 ^c
	Residual	.029	7	.004		
	Total	3.819	9			

a. Dependent Variable: COP

b. Predictors: (Constant), LLT

c. Predictors: (Constant), LLT, EST

Coefficients^a

Model		Unstandardized Coefficients		Standardized Coefficients	t	Sig.	Correlations		
		B	Std. Error	Beta			Zero-order	Partial	Part
		1	(Constant)	7.235			1.472		4.915
	LLT	-.075	.030	-.661	-2.493	.037	-.661	-.661	-.661
2	(Constant)	7.192	.184		39.155	.000			
	LLT	-.086	.004	-.761	-22.782	.000	-.661	-.993	-.754
	EST	.059	.003	.752	22.511	.000	.651	.993	.745

a. Dependent Variable: COP

Excluded Variables^a

Model	Beta In	t	Sig.	Partial Correlation	Collinearity Statistics	
					Tolerance	
1	EST	.752 ^b	22.511	.000	.993	.982

a. Dependent Variable: COP

b. Predictors in the Model: (Constant), LLT

						COP = 0.059EST - 0.086LLT + 7.192							
	Living Source Temperature (LST)	Entering Source Temperature (EST)	Volume Flowrate (m ³ /hr)	Mass Flowrate (l/s)	Heat Output Q _{source} (kW)	Living Load Temperature (LLT)	Entering Load Temperature (ELT)	Volume Flow rate (m ³ /hr)	Mass Flowrate (l/s)	Heat Output Q _{load} (kW)	HP Electricity Input (kW)	Actual Performance data	Manufacturer's COP
01/01/2014 07:00	10.0	3.8	19.8	5.5	143.7	42.2	37.3	23.5	6.6	134.8	30.7	4.4	4.2
01/01/2014 08:00	9.6	3.9	20.3	5.7	135.5	46.9	42.4	23.4	6.6	123.2	37.2	3.3	3.7
01/01/2014 09:00	9.5	4.1	19.1	5.3	120.7	49.8	45.3	24.0	6.7	126.4	39.8	3.2	3.5
01/01/2014 10:00	9.5	4.2	20.7	5.8	128.4	51.5	47.0	24.0	6.7	126.4	41.7	3.0	3.3
01/01/2014 11:00	9.5	4.3	19.7	5.5	119.9	52.4	47.8	23.5	6.6	126.5	42.8	3.0	3.2
01/01/2014 14:00	9.6	3.8	20.1	5.6	136.5	47.6	43.1	23.9	6.7	125.9	36.0	3.5	3.7
01/01/2014 15:00	9.2	4.2	20.1	5.6	117.6	52.6	48.2	24.2	6.8	124.6	41.4	3.0	3.2
01/01/2014 17:00	9.1	4.3	19.8	5.5	111.3	52.5	48.2	23.8	6.7	119.8	42.9	2.8	3.2
01/01/2014 18:00	9.1	4.3	20.7	5.8	116.3	54.1	49.6	22.0	6.2	115.9	42.4	2.7	3.1
01/01/2014 19:00	9.2	4.0	22.2	6.2	135.1	51.9	47.5	21.4	6.0	110.2	37.7	2.9	3.3
01/01/2014 20:00	9.5	4.1	20.5	5.7	129.6	51.0	46.6	22.2	6.2	114.3	42.4	2.7	3.4
02/01/2014 07:00	9.8	3.7	18.3	5.1	130.7	42.6	37.9	23.1	6.5	127.1	28.6	4.4	4.1
02/01/2014 08:00	9.6	3.9	19.7	5.5	131.4	46.3	41.6	24.4	6.8	134.2	36.9	3.6	3.8
02/01/2014 09:00	9.4	3.9	20.3	5.7	130.7	48.1	43.4	23.6	6.6	129.8	38.8	3.3	3.6
02/01/2014 10:00	9.4	4.1	19.9	5.6	123.4	50.3	45.7	23.9	6.7	128.7	41.0	3.1	3.4
02/01/2014 11:00	9.2	4.2	19.5	5.5	114.1	52.4	48.1	24.1	6.7	121.3	41.4	2.9	3.2
02/01/2014 12:00	9.7	4.3	15.8	4.4	99.8	49.8	45.5	24.3	6.8	122.3	30.7	4.0	3.5
02/01/2014 17:00	9.7	4.5	14.7	4.1	89.5	46.2	41.9	20.4	5.7	102.7	25.7	4.0	3.8
02/01/2014 20:00	9.0	4.4	17.8	5.0	95.8	53.6	49.2	23.3	6.5	120.0	34.6	3.5	3.1
03/01/2014 07:00	10.0	4.0	19.7	5.5	138.4	45.9	41.2	23.3	6.5	128.2	32.0	4.0	3.8
03/01/2014 08:00	9.5	4.1	19.8	5.5	125.1	50.7	46.2	23.8	6.7	125.4	40.3	3.1	3.4
03/01/2014 09:00	9.4	4.2	19.6	5.5	119.3	52.2	47.7	23.5	6.6	123.8	42.4	2.9	3.3
03/01/2014 12:00	9.4	4.8	20.6	5.8	110.9	53.0	48.7	23.2	6.5	116.7	41.9	2.8	3.2
03/01/2014 13:00	9.2	4.1	20.8	5.8	124.1	52.9	48.4	22.6	6.3	119.0	41.4	2.9	3.2
03/01/2014 16:00	9.8	4.7	15.8	4.4	94.3	48.6	44.4	20.6	5.8	101.2	29.4	3.4	3.6
03/01/2014 17:00	9.8	4.5	14.5	4.1	89.9	50.2	45.9	20.2	5.7	101.7	28.8	3.5	3.5
06/01/2014 07:00	10.8	4.6	19.7	5.5	143.0	43.0	38.2	23.2	6.5	130.4	30.0	4.3	4.1
06/01/2014 08:00	10.5	4.7	20.2	5.7	137.1	46.6	41.8	24.0	6.7	134.8	37.5	3.6	3.8
06/01/2014 09:00	10.4	4.8	19.7	5.5	129.1	48.5	43.7	23.5	6.6	132.0	39.1	3.4	3.6
06/01/2014 10:00	10.0	4.6	19.9	5.6	125.8	50.2	45.7	23.7	6.6	124.8	40.4	3.1	3.5
06/01/2014 11:00	9.9	5.4	20.1	5.6	105.9	54.5	49.6	23.7	6.6	135.9	43.0	3.2	3.1
06/01/2014 13:00	10.6	5.1	21.8	6.1	140.3	48.4	41.5	21.0	5.9	169.6	43.1	3.9	3.7

07/01/2014 07:00	10.2	4.1	17.7	5.0	126.3	47.4	42.8	23.3	6.5	125.5	30.4	4.1	3.7
07/01/2014 08:00	10.0	4.6	20.1	5.6	127.0	52.7	48.3	24.4	6.8	125.6	41.4	3.0	3.2
07/01/2014 10:00	10.0	5.7	14.5	4.1	73.0	48.5	45.4	24.3	6.8	88.2	29.5	3.0	3.6
07/01/2014 11:00	9.6	4.6	19.9	5.6	116.4	52.9	48.3	24.0	6.7	129.2	42.2	3.1	3.2
07/01/2014 12:00	9.9	5.0	16.2	4.5	92.9	50.2	45.8	23.8	6.7	122.5	32.8	3.7	3.5
07/01/2014 16:00	10.1	4.9	13.5	3.8	82.2	48.7	44.4	20.2	5.7	101.6	23.8	4.3	3.6
07/01/2014 17:00	10.0	5.0	14.4	4.0	84.3	47.7	43.6	21.1	5.9	101.3	28.0	3.6	3.7
08/01/2014 07:00	9.9	3.8	17.7	5.0	126.3	44.4	39.7	23.1	6.5	127.1	29.6	4.3	4.0
08/01/2014 08:00	9.6	4.2	19.8	5.5	125.2	50.5	46.0	23.7	6.6	124.8	38.7	3.2	3.4
08/01/2014 09:00	9.6	4.5	19.8	5.5	118.2	53.5	49.0	23.8	6.7	125.4	42.8	2.9	3.2
08/01/2014 12:00	9.5	4.5	15.7	4.4	91.8	53.6	49.2	20.9	5.9	107.6	29.5	3.6	3.1
08/01/2014 13:00	9.5	4.5	17.8	5.0	104.2	53.9	49.7	21.2	5.9	104.2	33.7	3.1	3.1
08/01/2014 14:00	9.5	4.7	17.7	5.0	99.4	54.6	50.4	22.1	6.2	108.6	33.6	3.2	3.1
08/01/2014 17:00	10.0	5.0	16.4	4.6	96.0	46.5	42.4	21.9	6.1	105.1	29.0	3.6	3.8
08/01/2014 18:00	10.1	4.5	15.9	4.5	104.2	48.5	44.0	21.5	6.0	113.2	30.1	3.8	3.6
08/01/2014 19:00	9.8	4.3	15.8	4.4	101.7	50.2	45.8	21.8	6.1	112.3	30.8	3.6	3.5
08/01/2014 20:00	9.4	4.2	16.3	4.6	99.2	51.4	47.2	21.9	6.1	107.6	30.1	3.6	3.3
09/01/2014 01:00	10.2	8.0	8.9	2.5	22.9	55.6	51.5	10.6	3.0	50.9	15.1	3.4	3.0
09/01/2014 07:00	10.3	6.3	20.5	5.7	96.0	47.7	43.1	22.3	6.2	120.1	31.2	3.8	3.7
09/01/2014 08:00	9.9	5.8	21.0	5.9	100.8	48.4	42.1	23.0	6.4	169.6	39.4	4.3	3.6
09/01/2014 09:00	9.7	5.2	20.5	5.7	108.0	50.8	44.4	22.7	6.4	170.0	42.1	4.0	3.4
09/01/2014 16:00	9.8	6.7	14.2	4.0	51.5	46.8	43.0	22.4	6.3	99.7	26.4	3.8	3.7
09/01/2014 17:00	9.6	5.1	14.3	4.0	75.3	47.7	43.9	22.9	6.4	101.8	26.9	3.8	3.7
09/01/2014 20:00	8.9	3.8	19.8	5.5	118.2	52.4	47.9	23.7	6.6	124.8	39.4	3.2	3.2
10/01/2014 07:00	9.7	3.5	19.4	5.4	140.8	42.4	37.7	23.1	6.5	127.1	30.0	4.2	4.1
10/01/2014 08:00	9.4	3.7	19.8	5.5	132.1	46.3	41.9	23.8	6.7	122.5	36.9	3.3	3.8
10/01/2014 09:00	9.1	3.6	19.8	5.5	127.4	48.2	43.8	24.4	6.8	125.7	39.1	3.2	3.6
10/01/2014 10:00	9.1	3.9	20.0	5.6	121.7	51.4	47.0	23.9	6.7	123.1	40.9	3.0	3.3
10/01/2014 11:00	9.6	4.5	17.4	4.9	103.9	47.4	43.2	21.2	5.9	104.2	33.4	3.1	3.7
10/01/2014 13:00	9.3	5.7	17.8	5.0	75.0	46.6	41.3	20.1	5.6	124.6	30.8	4.0	3.7
10/01/2014 14:00	9.7	4.5	19.0	5.3	115.6	48.2	43.9	19.9	5.6	100.2	34.1	2.9	3.6
10/01/2014 15:00	9.5	4.5	15.1	4.2	88.4	49.4	45.1	20.3	5.7	102.1	29.0	3.5	3.5
10/01/2014 16:00	9.4	4.2	15.2	4.3	92.5	51.8	47.5	20.7	5.8	104.2	29.5	3.5	3.3
10/01/2014 17:00	9.2	4.3	16.2	4.5	92.9	53.3	49.1	20.6	5.8	101.2	30.5	3.3	3.2
13/01/2014 07:00	10.3	3.9	18.4	5.2	137.8	39.8	35.0	23.3	6.5	130.9	27.7	4.7	4.4

13/01/2014 08:00	10.2	4.0	19.6	5.5	142.2	43.7	38.9	23.6	6.6	132.6	35.2	3.8	4.0
13/01/2014 09:00	9.8	3.9	20.4	5.7	140.9	45.2	40.5	23.7	6.6	130.4	37.0	3.5	3.9
13/01/2014 10:00	9.7	4.0	19.2	5.4	128.1	47.7	43.0	23.8	6.7	130.9	38.5	3.4	3.7
13/01/2014 11:00	9.5	4.2	20.3	5.7	125.9	50.5	46.1	23.7	6.6	122.1	40.5	3.0	3.4
13/01/2014 12:00	9.6	4.5	19.8	5.5	118.2	53.5	49.1	24.3	6.8	125.1	42.9	2.9	3.2
13/01/2014 13:00	9.5	4.6	17.7	5.0	101.5	53.2	48.9	21.1	5.9	106.2	33.7	3.2	3.2
13/01/2014 14:00	9.7	4.4	14.6	4.1	90.6	51.2	46.7	20.8	5.8	109.5	29.4	3.7	3.4
13/01/2014 15:00	9.8	4.7	15.3	4.3	91.3	49.3	44.8	21.6	6.0	113.8	29.1	3.9	3.5
13/01/2014 16:00	10.0	5.6	16.6	4.6	85.5	47.5	43.2	20.9	5.9	105.2	33.2	3.2	3.7
13/01/2014 18:00	9.3	4.0	16.0	4.5	99.2	50.2	45.8	21.8	6.1	112.3	31.3	3.6	3.4
13/01/2014 19:00	9.0	3.9	19.5	5.5	116.4	51.8	47.3	23.7	6.6	124.8	41.8	3.0	3.3
14/01/2014 07:00	9.8	3.5	19.8	5.5	146.0	40.6	35.8	23.5	6.6	132.0	30.2	4.4	4.3
14/01/2014 08:00	9.4	3.3	19.9	5.6	142.1	42.9	38.3	23.9	6.7	128.7	35.2	3.7	4.1
14/01/2014 09:00	9.2	3.1	19.9	5.6	142.1	43.4	38.8	23.9	6.7	128.7	36.0	3.6	4.0
14/01/2014 10:00	9.0	3.1	20.0	5.6	138.1	44.4	39.8	23.8	6.7	128.1	36.4	3.5	3.9
14/01/2014 11:00	9.0	3.2	20.3	5.7	137.8	46.1	41.6	24.3	6.8	128.0	37.3	3.4	3.8
14/01/2014 12:00	8.8	3.4	20.0	5.6	126.4	48.2	43.7	23.8	6.7	125.3	38.8	3.2	3.6
14/01/2014 13:00	8.9	3.6	19.9	5.6	123.4	50.7	46.2	23.8	6.7	125.3	40.7	3.1	3.4
14/01/2014 14:00	8.9	3.9	20.0	5.6	117.0	53.0	48.5	23.8	6.7	125.4	42.7	2.9	3.2
14/01/2014 15:00	8.9	3.7	20.5	5.7	124.8	51.7	47.3	23.4	6.6	120.5	41.6	2.9	3.3
14/01/2014 16:00	9.1	3.6	20.7	5.8	133.3	49.5	45.1	23.4	6.6	120.5	41.6	2.9	3.5
14/01/2014 17:00	8.7	3.7	20.3	5.7	118.8	52.1	47.6	24.2	6.8	127.5	42.2	3.0	3.2
14/01/2014 18:00	8.6	3.5	19.9	5.6	118.8	51.9	47.5	23.8	6.7	122.5	43.0	2.9	3.2
14/01/2014 19:00	8.8	3.6	20.3	5.7	123.6	52.2	47.9	24.2	6.8	121.8	42.9	2.8	3.2
14/01/2014 20:00	8.5	3.6	19.9	5.6	114.1	52.3	48.1	23.8	6.7	117.0	42.9	2.7	3.2
15/01/2014 07:00	9.5	3.6	19.0	5.3	131.2	44.6	40.0	23.4	6.6	126.0	30.6	4.1	3.9
15/01/2014 08:00	9.4	4.2	19.7	5.5	119.9	51.7	47.1	23.6	6.6	127.1	40.0	3.2	3.3
15/01/2014 09:00	9.5	4.1	16.3	4.6	103.0	48.6	44.1	21.5	6.0	113.2	30.8	3.7	3.6
15/01/2014 10:00	9.7	4.3	16.8	4.7	106.2	47.8	44.1	22.3	6.2	96.6	32.7	3.0	3.7
15/01/2014 11:00	9.9	4.4	16.5	4.6	106.2	47.2	42.8	20.9	5.9	107.7	31.2	3.5	3.7
15/01/2014 12:00	9.7	4.3	17.7	5.0	111.9	48.1	43.7	21.5	6.0	110.7	33.7	3.3	3.6
15/01/2014 13:00	9.4	4.1	17.6	4.9	109.2	49.5	45.0	21.9	6.1	115.3	32.3	3.6	3.5
15/01/2014 14:00	9.4	4.1	14.6	4.1	90.6	50.8	46.6	21.0	5.9	103.2	28.2	3.7	3.4
15/01/2014 15:00	9.3	4.2	17.2	4.8	102.6	52.8	48.3	22.2	6.2	116.9	31.9	3.7	3.2
15/01/2014 16:00	9.2	4.3	15.4	4.3	88.3	52.9	48.6	21.6	6.0	108.7	29.2	3.7	3.2
15/01/2014 17:00	9.2	4.2	14.2	4.0	83.1	53.7	49.4	22.6	6.3	113.7	27.2	4.2	3.1
16/01/2014 07:00	9.4	3.9	19.8	5.5	127.4	46.4	41.8	23.1	6.5	124.4	32.2	3.9	3.8
16/01/2014 08:00	9.3	4.4	19.5	5.5	111.8	52.8	48.4	24.3	6.8	125.2	41.1	3.0	3.2
16/01/2014 09:00	9.3	4.2	21.7	6.1	129.5	50.7	46.2	21.1	5.9	111.1	39.2	2.8	3.4
16/01/2014 10:00	9.7	4.2	22.2	6.2	142.9	48.1	43.6	20.7	5.8	109.0	38.6	2.8	3.6
16/01/2014 15:00	9.6	4.4	17.4	4.9	105.9	48.7	44.3	20.5	5.7	105.6	31.6	3.3	3.6
16/01/2014 16:00	9.5	4.3	15.2	4.3	92.5	49.4	45.0	20.2	5.7	104.0	29.0	3.6	3.5
16/01/2014 17:00	9.3	4.1	17.7	5.0	107.7	50.7	46.3	20.4	5.7	105.0	32.3	3.3	3.4
16/01/2014 18:00	9.2	4.1	15.5	4.3	92.5	50.5	46.1	20.2	5.7	104.0	29.4	3.5	3.4
16/01/2014 19:00	9.0	3.9	17.3	4.8	103.3	50.8	46.5	20.5	5.7	103.2	32.3	3.2	3.4
16/01/2014 20:00	9.2	3.9	15.0	4.2	93.0	49.7	45.5	21.0	5.9	103.2	27.9	3.7	3.5
17/01/2014 07:00	9.4	3.4	19.6	5.5	137.7	43.5	38.9	22.9	6.4	123.3	31.0	4.0	4.0
17/01/2014 08:00	9.2	3.7	20.2	5.7	130.1	48.4	43.9	24.0	6.7	126.4	38.2	3.3	3.6
17/01/2014 09:00	9.0	3.8	19.7	5.5	119.9	51.0	46.6	23.4	6.6	120.5	41.0	2.9	3.3
17/01/2014 10:00	8.9	4.1	20.5	5.7	115.2	52.7	48.1	24.3	6.8	130.8	42.9	3.0	3.2

17/01/2014 11:00	8.7	4.0	19.7	5.5	108.4	53.5	49.2	23.7	6.6	119.3	42.4	2.8	3.1
17/01/2014 12:00	8.6	3.9	21.3	6.0	117.2	53.6	49.2	23.0	6.4	118.4	42.0	2.8	3.1
17/01/2014 13:00	8.9	4.0	20.8	5.8	119.3	53.8	49.4	22.4	6.3	115.3	41.8	2.8	3.1
17/01/2014 14:00	8.8	4.0	21.3	6.0	119.6	53.9	49.7	22.2	6.2	109.1	41.9	2.6	3.1
17/01/2014 16:00	8.9	3.8	14.3	4.0	85.4	53.1	48.9	19.9	5.6	97.8	26.7	3.7	3.2
20/01/2014 07:00	10.2	3.7	18.0	5.0	136.9	39.5	34.8	23.7	6.6	130.4	26.9	4.9	4.4
20/01/2014 08:00	9.7	3.5	19.6	5.5	142.2	42.4	37.8	23.7	6.6	127.6	34.7	3.7	4.1
20/01/2014 09:00	9.4	3.4	19.7	5.5	138.4	43.6	38.9	23.9	6.7	131.5	35.9	3.7	4.0
20/01/2014 10:00	9.5	3.6	19.7	5.5	136.0	45.8	41.2	23.8	6.7	128.1	37.0	3.5	3.8
20/01/2014 11:00	9.1	3.6	19.8	5.5	127.5	48.4	43.9	23.8	6.7	125.4	38.7	3.2	3.6
20/01/2014 12:00	9.4	4.1	20.2	5.7	125.3	52.0	47.6	24.4	6.8	125.6	41.2	3.1	3.3
20/01/2014 16:00	9.6	4.2	18.1	5.1	114.4	49.5	45.0	20.6	5.8	108.5	31.2	3.5	3.5
20/01/2014 18:00	9.6	4.0	21.2	5.9	139.0	48.0	43.4	22.2	6.2	119.5	41.8	2.9	3.6
20/01/2014 20:00	9.0	3.9	20.0	5.6	119.4	52.5	48.0	23.8	6.7	125.4	39.7	3.2	3.2
21/01/2014 07:00	9.6	3.5	18.3	5.1	130.6	41.3	36.4	23.2	6.5	133.1	28.7	4.6	4.2
21/01/2014 08:00	9.2	3.3	20.0	5.6	138.1	43.6	39.0	24.1	6.7	129.8	35.7	3.6	4.0
21/01/2014 09:00	9.2	3.1	20.0	5.6	142.8	44.7	40.3	23.1	6.5	118.9	36.8	3.2	3.9
21/01/2014 10:00	8.8	3.0	19.7	5.5	133.8	45.8	41.2	24.4	6.8	131.4	37.4	3.5	3.8
21/01/2014 11:00	8.7	3.2	19.7	5.5	126.8	48.1	43.5	23.5	6.6	126.5	38.5	3.3	3.6
21/01/2014 12:00	8.8	3.7	19.8	5.5	118.2	51.7	47.2	23.7	6.6	124.8	40.9	3.1	3.3
21/01/2014 13:00	8.8	3.7	16.6	4.6	99.1	50.6	46.2	21.1	5.9	108.7	31.8	3.4	3.4
21/01/2014 14:00	9.3	4.8	14.7	4.1	77.4	44.6	40.9	21.0	5.9	90.9	28.5	3.2	3.9
21/01/2014 19:00	8.5	3.9	19.9	5.6	107.1	53.2	48.7	23.6	6.6	124.3	40.3	3.1	3.1
21/01/2014 20:00	8.6	3.6	19.7	5.5	115.3	52.5	48.1	24.0	6.7	123.6	37.0	3.3	3.2
22/01/2014 07:00	9.1	3.4	19.0	5.3	126.8	43.4	38.6	23.4	6.6	131.5	30.0	4.4	4.0
22/01/2014 08:00	9.0	3.9	20.2	5.7	120.5	49.2	44.7	24.2	6.8	127.4	38.4	3.3	3.5
22/01/2014 09:00	8.9	3.8	18.4	5.2	109.9	51.0	46.8	22.5	6.3	110.6	34.9	3.2	3.3
22/01/2014 10:00	9.2	4.7	20.6	5.8	108.5	51.0	45.0	22.9	6.4	160.9	43.0	3.7	3.3
22/01/2014 11:00	8.8	3.8	20.8	5.8	121.7	53.7	49.2	23.2	6.5	122.2	42.9	2.9	3.1
22/01/2014 12:00	8.9	4.0	18.2	5.1	104.3	53.8	49.5	22.0	6.2	110.7	33.8	3.3	3.1
22/01/2014 13:00	8.9	3.8	15.7	4.4	93.7	52.2	47.8	21.7	6.1	111.8	28.8	3.9	3.2
22/01/2014 14:00	8.7	3.9	14.7	4.1	82.6	53.6	49.3	21.2	5.9	106.7	28.5	3.7	3.1
22/01/2014 15:00	8.7	4.0	14.8	4.1	81.4	53.8	49.5	20.6	5.8	103.7	27.2	3.8	3.1
22/01/2014 17:00	8.8	6.1	16.2	4.5	51.2	53.7	49.3	21.8	6.1	112.3	30.9	3.6	3.1
22/01/2014 20:00	9.2	6.7	10.7	3.0	31.3	44.1	40.8	20.0	5.6	77.2	18.0	4.3	3.9
23/01/2014 07:00	9.3	3.0	19.2	5.4	141.5	43.6	39.2	22.8	6.4	117.4	30.6	3.8	4.0
23/01/2014 08:00	8.9	3.2	19.5	5.5	130.1	48.1	43.7	24.1	6.7	124.1	38.3	3.2	3.6
23/01/2014 09:00	8.9	3.5	20.1	5.6	127.0	51.0	46.7	24.0	6.7	120.8	41.6	2.9	3.3
23/01/2014 11:00	8.7	3.7	19.7	5.5	115.3	52.9	48.4	23.0	6.4	121.1	39.0	3.1	3.2
23/01/2014 12:00	8.8	3.7	16.9	4.7	100.9	52.2	47.8	21.5	6.0	110.7	31.6	3.5	3.2
23/01/2014 13:00	8.7	3.7	18.3	5.1	107.1	51.9	47.5	20.8	5.8	107.1	34.6	3.1	3.2
23/01/2014 14:00	8.7	3.7	18.7	5.2	109.5	52.3	47.8	20.5	5.7	108.0	33.6	3.2	3.2
23/01/2014 15:00	8.7	3.9	22.4	6.3	125.8	53.7	49.3	20.4	5.7	105.0	38.8	2.7	3.1
23/01/2014 19:00	8.6	3.7	16.9	4.7	96.9	53.3	49.1	23.0	6.4	113.1	32.0	3.5	3.1
23/01/2014 20:00	8.6	3.6	16.1	4.5	94.2	51.8	47.5	22.8	6.4	114.8	30.3	3.8	3.2
24/01/2014 07:00	9.2	3.2	19.6	5.5	137.6	43.0	38.3	23.4	6.6	128.8	30.7	4.2	4.0
24/01/2014 08:00	8.7	3.4	19.5	5.5	121.0	48.9	44.3	23.5	6.6	126.5	38.3	3.3	3.5
24/01/2014 09:00	8.7	3.8	19.8	5.5	113.6	52.1	47.7	23.8	6.7	122.5	41.5	3.0	3.2

27/01/2014 19:00	8.5	3.9	17.7	5.0	95.3	54.2	49.2	20.7	5.8	121.1	35.8	3.4	3.0
27/01/2014 20:00	8.7	3.9	20.0	5.6	112.4	54.0	49.1	21.5	6.0	123.3	37.0	3.3	3.1
28/01/2014 07:00	9.3	3.5	19.7	5.5	133.7	45.5	40.3	20.9	5.9	127.2	31.8	4.0	3.8
28/01/2014 08:00	8.8	3.7	19.8	5.5	118.2	50.8	45.8	20.5	5.7	120.0	39.7	3.0	3.3
28/01/2014 10:00	8.9	4.8	23.3	6.5	111.8	52.0	45.4	18.3	5.1	141.3	38.3	3.7	3.2
28/01/2014 12:00	9.1	4.1	23.8	6.7	139.3	48.6	44.2	17.1	4.8	88.1	26.6	3.3	3.5
29/01/2014 07:00	8.3	3.2	17.7	5.0	105.7	52.1	47.4	19.8	5.5	108.9	32.6	3.3	3.2
29/01/2014 19:00	7.6	4.5	15.3	4.3	55.5	54.2	51.4	18.2	5.1	59.6	21.3	2.8	3.0
30/01/2014 07:00	8.0	2.9	18.7	5.2	111.6	51.1	46.4	19.8	5.5	108.9	33.1	3.3	3.3
30/01/2014 08:00	8.3	3.8	20.0	5.6	105.3	53.4	49.2	21.9	6.1	107.7	36.0	3.0	3.1
30/01/2014 13:00	7.8	6.0	22.1	6.2	46.5	48.1	43.9	18.8	5.3	92.4	27.4	3.4	3.5
30/01/2014 14:00	8.5	4.4	16.5	4.6	79.2	48.1	44.8	16.6	4.6	64.1	21.6	3.0	3.6
31/01/2014 07:00	8.1	3.4	19.8	5.5	108.9	55.0	50.5	20.0	5.6	105.3	35.3	3.0	2.9
31/01/2014 09:00	8.4	4.2	22.4	6.3	110.1	51.9	45.1	18.1	5.1	144.1	38.7	3.7	3.2
03/02/2014 07:00	8.6	3.6	18.6	5.2	108.9	50.6	45.6	20.2	5.7	118.2	31.8	3.7	3.3
03/02/2014 08:00	8.9	8.4	20.6	5.8	12.1	55.8	50.9	20.5	5.7	117.6	31.9	3.7	2.9
03/02/2014 12:00	8.6	5.9	14.0	3.9	44.2	51.6	49.4	20.2	5.7	52.0	14.6	3.6	3.3
03/02/2014 17:00	8.7	5.7	22.7	6.4	79.7	47.4	43.6	17.2	4.8	76.5	25.9	2.9	3.6
03/02/2014 18:00	8.3	8.0	17.1	4.8	6.0	55.3	51.3	18.1	5.1	84.7	27.8	3.0	2.9
03/02/2014 19:00	8.0	5.9	19.1	5.3	46.9	46.6	42.0	16.8	4.7	90.4	22.3	4.1	3.7
03/02/2014 20:00	8.4	3.3	18.5	5.2	110.4	49.8	45.2	17.7	5.0	95.3	28.0	3.4	3.4
04/02/2014 07:00	8.0	3.3	19.9	5.6	109.5	53.6	48.8	19.6	5.5	110.1	35.1	3.1	3.1
04/02/2014 08:00	8.1	3.6	21.0	5.9	110.6	54.6	49.9	19.1	5.3	105.0	39.1	2.7	3.0
04/02/2014 09:00	8.6	3.5	21.6	6.0	128.9	49.3	44.0	18.8	5.3	116.6	34.8	3.4	3.5
04/02/2014 10:00	7.8	3.4	21.2	5.9	109.2	54.7	50.0	18.8	5.3	103.4	37.9	2.7	2.9
04/02/2014 11:00	8.5	3.2	21.9	6.1	135.8	48.1	43.5	19.4	5.4	104.4	33.7	3.1	3.6
05/02/2014 09:00	8.4	3.5	22.2	6.2	127.3	52.0	47.4	18.7	5.2	100.7	35.3	2.9	3.2
05/02/2014 19:00	7.8	5.6	21.7	6.1	55.9	50.7	47.1	18.6	5.2	78.4	27.5	2.9	3.3
06/02/2014 16:00	7.6	3.1	22.6	6.3	119.0	53.5	48.8	18.2	5.1	100.1	33.8	3.0	3.0
06/02/2014 18:00	7.7	3.4	22.1	6.2	111.2	54.8	50.2	18.4	5.2	99.1	34.3	2.9	2.9
10/02/2014 07:00	8.6	3.4	19.0	5.3	115.6	49.8	44.7	19.7	5.5	117.6	31.2	3.8	3.4
10/02/2014 08:00	8.6	3.7	20.4	5.7	117.0	52.2	47.3	21.2	5.9	121.6	39.2	3.1	3.2
10/02/2014 15:00	8.6	3.2	19.9	5.6	125.8	46.6	41.8	16.9	4.7	94.9	30.3	3.1	3.7
10/02/2014 18:00	7.8	3.4	22.1	6.2	113.8	54.4	49.8	18.6	5.2	100.1	37.5	2.7	3.0
10/02/2014 20:00	7.7	3.1	22.3	6.2	120.0	52.7	48.1	19.1	5.3	102.8	37.1	2.8	3.1
11/02/2014 07:00	7.8	3.0	18.1	5.1	101.7	51.8	46.9	20.1	5.6	115.3	31.8	3.6	3.2
11/02/2014 20:00	6.9	2.7	21.9	6.1	107.6	55.2	50.6	18.4	5.2	99.1	37.7	2.6	2.9
12/02/2014 07:00	7.3	2.5	18.1	5.1	101.7	51.9	47.0	19.7	5.5	113.0	32.1	3.5	3.2
12/02/2014 13:00	7.9	2.7	16.6	4.6	101.0	48.3	43.8	17.7	5.0	93.2	23.5	4.0	3.5
12/02/2014 14:00	7.3	2.8	21.9	6.1	115.3	54.2	49.5	18.4	5.2	101.2	37.9	2.7	3.0
12/02/2014 15:00	7.7	3.2	22.6	6.3	119.0	46.8	42.0	17.8	5.0	100.0	34.3	2.9	3.6
13/02/2014 07:00	7.2	2.5	19.5	5.5	107.3	54.5	49.7	19.4	5.4	109.0	34.6	3.1	2.9
13/02/2014 09:00	7.2	2.6	15.5	4.3	83.4	52.9	48.4	18.2	5.1	95.9	25.7	3.7	3.1
13/02/2014 14:00	7.5	2.2	22.1	6.2	137.1	47.5	42.9	18.2	5.1	98.0	31.1	3.1	3.5
14/02/2014 07:00	7.1	2.6	19.6	5.5	103.2	53.9	49.3	19.9	5.6	107.2	34.7	3.1	3.0
14/02/2014 09:00	7.4	2.6	21.2	5.9	119.1	52.8	48.3	20.1	5.6	105.8	37.3	2.8	3.1
14/02/2014 10:00	7.4	2.8	21.4	6.0	115.2	48.0	41.9	19.6	5.5	139.9	34.0	4.1	3.5
14/02/2014 11:00	7.0	2.7	21.6	6.0	108.7	54.7	50.2	20.4	5.7	107.4	37.9	2.8	2.9
14/02/2014 12:00	7.4	2.3	22.0	6.2	131.3	48.0	43.3	19.4	5.4	106.8	33.6	3.2	3.5
14/02/2014 14:00	7.3	1.8	21.9	6.1	141.0	49.6	44.7	19.6	5.5	112.4	36.3	3.1	3.4

Appendix D

Ground Temperature Prediction

Introduction

This appendix provides daily and monthly historical ground temperature data used for validation of the novel disturbed underground temperature model discussed in Chapter 6 using long term historical underground temperature data obtained from the experimental apparatus described in Chapter 4.

Table D.16 Disturbed underground temperature distribution data

			Depth (m)				Monthly Fluid Temperature								
			0.0	3.0	14.0	26.0									
Month	Days	Cumulative Days	Undisturbed ground Temperature (T _u)				TLoad3	Tn ₂₆	Td26	TLoad3	Tn3	Td3	Measured Temperature at 3m	Measured Temperature at 26m	
Jan	31	31	3.0	8.4	8.1	8.0									5.0
Feb	28	59	3.9	7.4	8.1	8.0	5.1	6.4	7.2	6.8	6.2	7.4	6.8	5.7	8.1
Mar	31	90	6.5	8.0	8.0	8.0	5.3	6.6	7.0	6.8	6.6	7.1	6.8	5.2	7.5
Apr	30	120	10.0	14.1	8.0	8.0	13.1	10.3	8.3	9.3	13.6	8.4	11.0	8.7	8.7
May	31	151	13.6	19.6	8.0	8.0	15.6	11.4	9.9	10.7	17.6	10.0	13.8	11.1	9.4
Jun	30	181	16.1	24.7	8.0	8.0	16.8	11.9	11.2	11.5	20.5	11.2	15.9	14.0	10.3
Jul	31	212	17.0	30.8	8.0	8.0	20.3	13.2	13.1	13.1	25.2	13.1	19.1	16.8	11.5
Aug	31	243	16.0	34.0	8.0	8.0	21.5	13.6	14.5	14.1	27.3	14.5	20.9	18.7	12.4
Sep	30	273	13.4	34.6	7.9	8.0	21.7	13.7	15.6	14.7	27.7	15.6	21.6	19.0	12.7
Oct	31	304	9.8	29.8	7.9	8.0	17.2	12.0	15.6	13.8	22.9	15.6	19.3	18.9	13.3
Nov	30	334	6.4	24.0	7.9	8.0	13.2	10.4	15.5	12.9	18.1	15.5	16.8	15.7	13.0
Dec	31	365	3.8	17.9	7.9	8.0	10.0	9.0	14.6	11.8	13.5	14.6	14.1	12.5	12.2
Jan	31	396	3.0	14.0	7.9	8.0	9.2	8.6	13.8	11.2	11.4	13.8	12.6	10.2	11.3
Feb	28	424	3.9	11.4	7.9	8.0	8.0	8.0	12.6	10.3	9.6	12.6	11.1	8.0	10.2
Mar	31	455	6.5	13.3	8.0	8.0	10.5	9.2	12.5	10.8	11.8	12.5	12.1	8.9	10.2
Apr	30	485	10.0	14.4	8.0	8.0	9.3	8.6	12.1	10.4	11.7	12.1	11.9	9.2	10.1
May	31	516	13.6	19.7	8.0	8.0	11.6	9.7	12.1	10.9	15.3	12.1	13.7	9.7	10.0
Jun	30	546	16.1	28.0	8.0	8.0	17.3	12.1	12.8	12.4	22.2	12.8	17.5	13.6	11.2
Jul	31	577	17.0	32.9	8.0	8.0	19.1	12.8	13.7	13.2	25.4	13.7	19.5	16.8	12.4
Aug	31	608	16.0	36.7	8.0	8.0	21.4	13.6	14.9	14.2	28.4	14.9	21.6	20.0	14.4
Sep	30	638	13.4	35.1	8.1	8.0	19.1	12.8	15.3	14.0	26.3	15.3	20.8	20.0	14.4
Oct	31	669	9.8	29.6	8.1	8.0	14.6	11.0	15.3	13.1	21.2	15.3	18.2	17.3	13.9
Nov	30	699	6.4	25.0	8.1	8.0	12.9	10.3	15.1	12.7	18.3	15.1	16.7	14.2	13.4
Dec	31	730	3.8	18.4	8.1	8.0	9.5	8.7	14.2	11.5	13.5	14.2	13.8	10.9	12.1
Mean Yearly air Temp T _{mair} (°C)	Mean temperature Amplitude (A) (°C)	Period duration of temperature oscillation P (s)	t ₀	Thermal difusivity a (m ² /s)	damping depth	ω	Thermal Conductivity (α) W/m.K	Density (ρ) kg/m ³	Specific Heat Capacity (Cs) J/kg.K	k = λ/α√(PI/αP)	ξ = arctan(K/(1+K))	η = 1/sqrt(1+2k+2k ²)			
8	10	730	20	0.083	3.11	0.01	1.29	1025	3967	0.42	0.29	0.68			

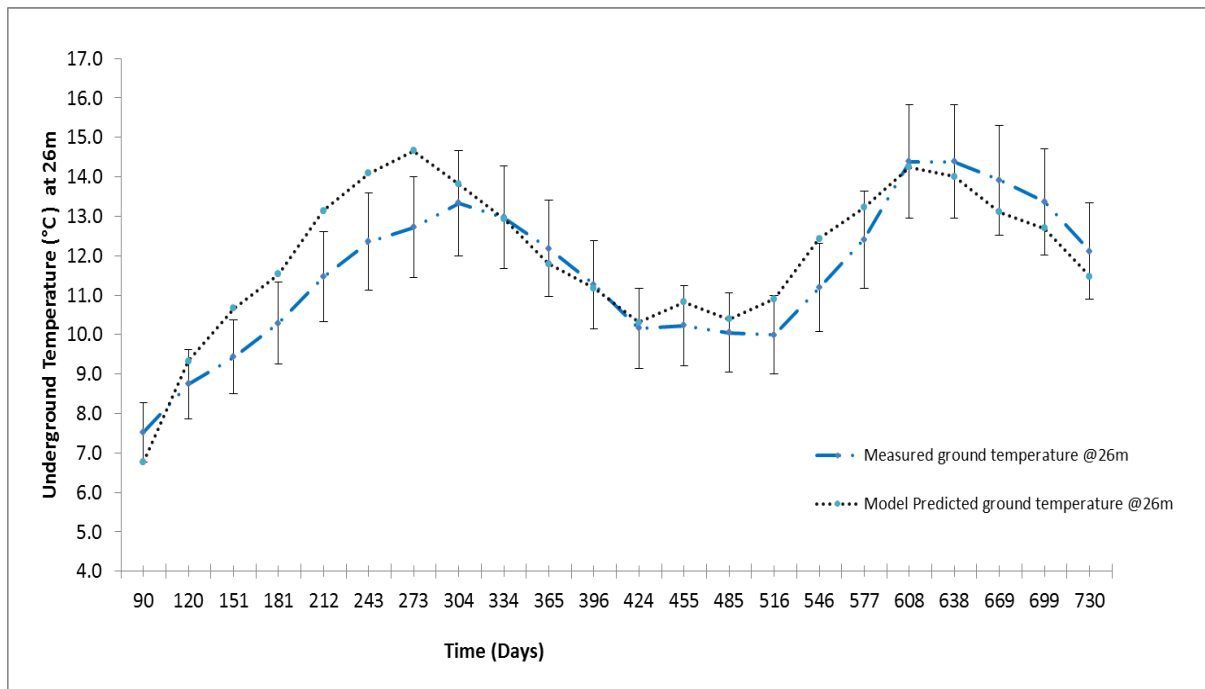


Figure D.80 Comparison of model predicted and measured underground temperature at 26 m

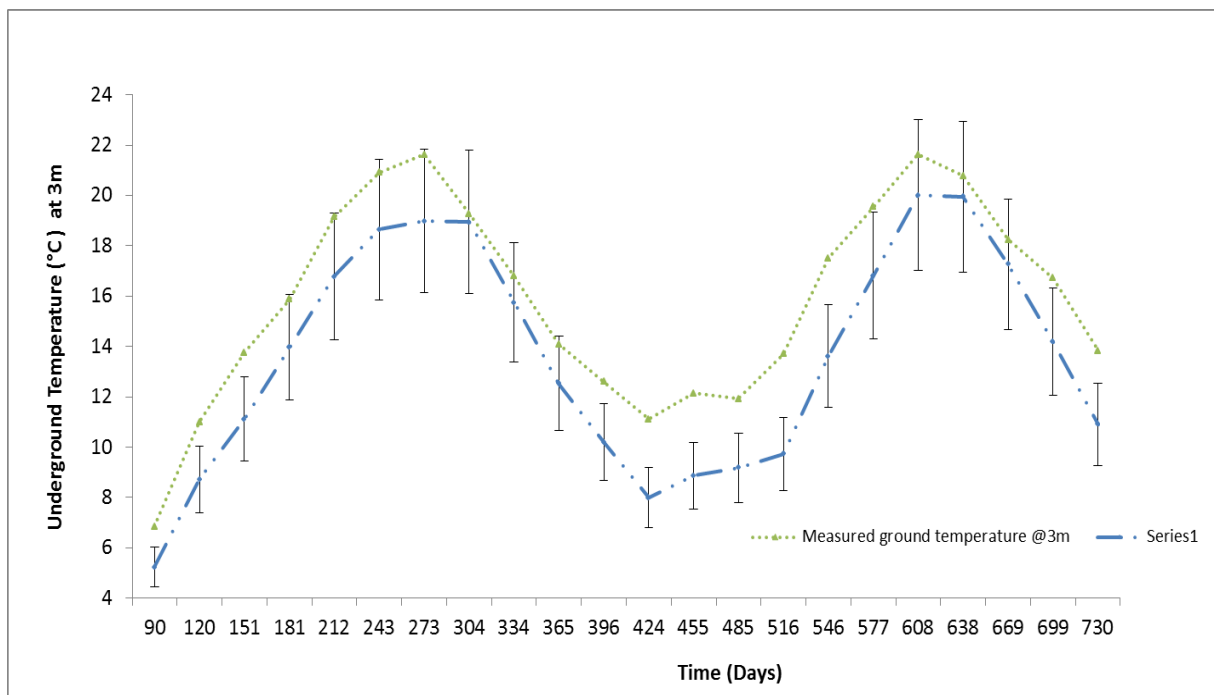


Figure D.81 Comparison of model predicted and measured underground temperature at 3 m

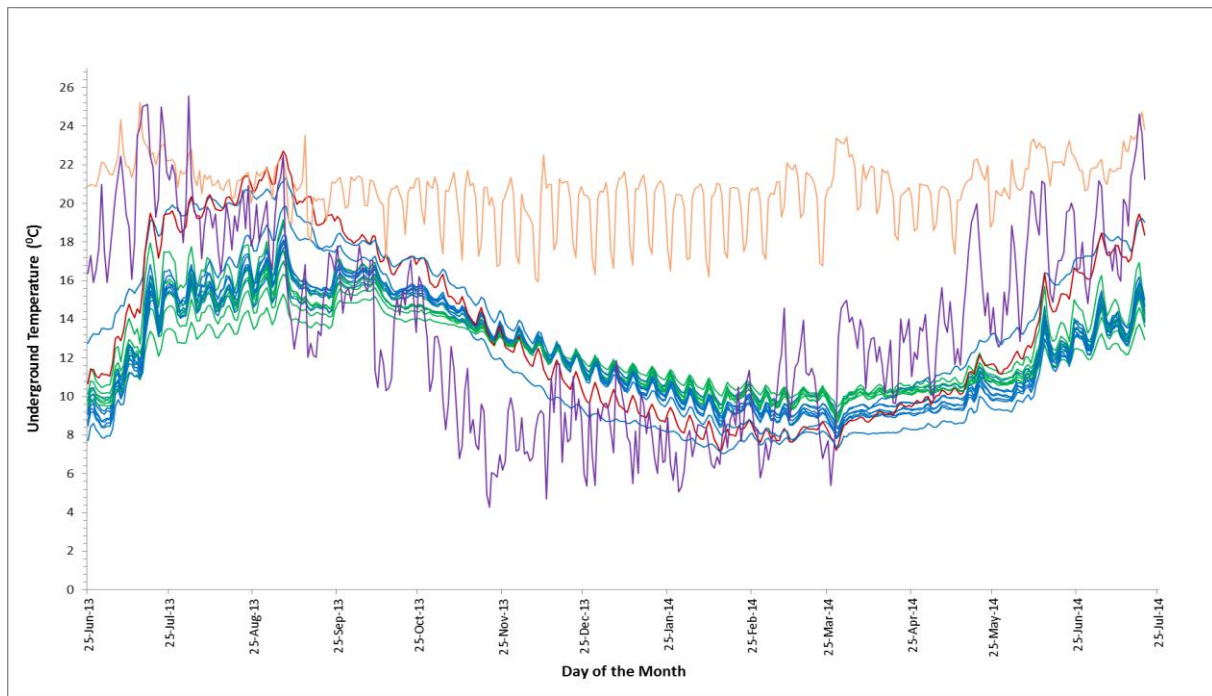


Figure D.82 Measured daily underground temperature distribution across 3 Levels

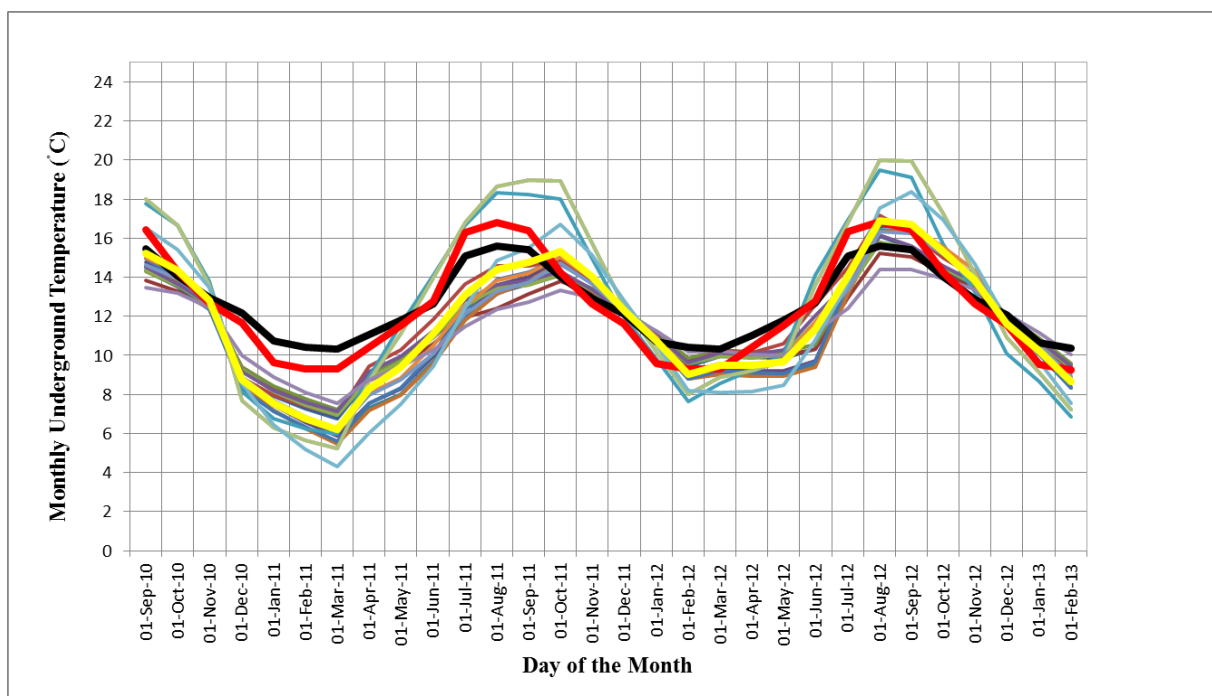


Figure D.83 Measured monthly underground temperature distribution across 3 Levels

Table D.17 Measured Monthly underground temperature data

Date	30-Sep-10	31-Oct-10	30-Nov-10	31-Dec-10	31-Jan-11	28-Feb-11	31-Mar-11	30-Apr-11	31-May-11	30-Jun-11	31-Jul-11	31-Aug-11	30-Sep-11	31-Oct-11	30-Nov-11	31-Dec-11	31-Jan-12	29-Feb-12	31-Mar-12	30-Apr-12	31-May-12	30-Jun-12	31-Jul-12	31-Aug-12	30-Sep-12	31-Oct-12	30-Nov-12	31-Dec-12	31-Jan-13	28-Feb-13
TCPL1	14.4	13.5	12.3	8.8	7.9	7.3	6.7	8.8	9.6	10.9	12.4	13.2	13.6	14.1	13.3	12.1	10.9	9.4	10.0	9.9	9.9	10.3	13.5	16.1	15.5	14.4	13.4	11.7	10.5	9.1
TCPL2	13.9	13.3	12.4	9.4	8.4	7.7	7.1	8.7	9.5	10.6	11.9	12.4	13.2	13.8	13.2	12.1	11.1	9.7	10.0	10.0	10.0	10.3	13.0	15.2	15.0	14.2	13.4	11.9	10.8	9.5
TCPL4	14.3	13.6	12.6	9.4	8.4	7.8	7.2	9.0	9.8	11.0	12.5	13.4	13.6	14.1	13.4	12.3	11.2	9.9	10.3	10.2	10.2	10.5	13.4	15.8	15.4	14.5	13.6	12.0	10.9	9.6
TCPL5	14.8	13.9	12.6	8.7	7.5	6.6	5.9	7.5	8.3	10.0	12.1	13.6	14.0	14.9	14.0	12.4	10.9	9.1	9.4	9.2	9.2	9.7	13.4	16.6	16.6	15.5	14.0	11.8	10.3	8.6
TCPL6	14.5	13.7	12.4	8.4	7.2	6.3	5.6	7.3	8.0	9.7	11.9	13.1	13.8	14.7	13.7	12.2	10.6	8.8	9.1	9.0	9.0	9.5	13.2	16.4	16.4	15.3	13.8	11.6	10.1	8.4
TCPL7	14.6	13.8	12.5	8.5	7.2	6.2	5.5	7.2	8.0	9.6	11.8	13.2	13.8	14.7	13.8	12.2	10.6	8.8	9.0	8.9	8.9	9.4	13.1	16.3	16.4	15.3	13.8	11.7	10.1	8.3
TCPL8	15.0	13.9	12.5	8.3	7.1	6.3	5.6	7.6	8.3	10.1	12.4	13.9	14.2	15.0	13.9	12.2	10.6	8.8	9.2	9.1	9.1	9.7	13.7	17.0	16.7	15.5	13.9	11.6	10.1	8.3
TCPL10	15.3	14.1	12.8	8.8	8.0	7.4	6.9	9.4	10.3	11.9	13.6	14.6	14.6	14.9	13.8	12.3	11.0	9.5	10.3	10.2	10.6	12.6	14.5	17.2	16.3	15.0	14.0	11.8	10.7	9.3
TCPL11	14.4	13.6	12.6	9.3	8.2	7.4	6.9	8.8	9.7	11.0	12.5	13.4	13.6	14.2	13.3	12.1	10.9	9.6	10.0	9.9	10.1	11.7	13.4	15.8	15.5	14.5	13.7	11.8	10.7	9.4
TCPL13	14.5	13.7	12.6	9.2	8.2	7.6	7.1	9.1	9.9	11.3	12.8	13.6	13.9	14.3	13.4	12.2	11.0	9.6	10.1	10.0	10.3	12.0	13.7	16.1	15.6	14.6	13.8	11.8	10.8	9.5
TCPL14	17.8	16.7	13.8	8.2	6.7	6.3	6.0	8.9	11.6	14.1	16.7	18.3	18.2	18.0	14.9	12.0	9.8	7.6	8.6	9.3	10.0	14.1	16.9	19.5	19.1	15.7	13.3	10.1	8.7	6.9
TCPL15	15.0	14.2	12.9	8.8	7.6	6.8	6.1	8.1	8.9	10.5	12.6	13.8	14.2	15.0	13.9	12.4	10.9	9.2	9.6	9.4	9.8	11.7	13.8	16.8	16.6	15.6	14.3	11.9	10.5	8.9
TCPL17	14.6	13.9	12.8	8.9	7.7	6.9	6.2	8.0	8.7	10.1	12.1	13.3	13.8	14.7	13.6	12.2	10.8	9.1	9.5	9.4	9.6	11.4	13.4	16.3	16.2	15.2	14.1	11.9	10.5	8.9
TCPL29	18.2	16.8	13.8	7.8	6.4	5.8	5.3	8.9	11.3	14.1	17.0	18.8	19.2	19.2	15.9	12.7	10.4	8.1	9.0	9.3	9.9	13.8	17.0	20.3	20.2	17.5	14.4	11.1	9.3	7.4
TCPL30	18.0	16.7	13.6	7.7	6.3	5.7	5.2	8.7	11.1	14.0	16.8	18.7	19.0	18.9	15.7	12.5	10.2	8.0	8.9	9.2	9.7	13.6	16.8	20.0	20.0	17.3	14.2	10.9	9.1	7.2
TCPL31	13.5	13.2	12.5	10.0	8.9	8.1	7.5	8.7	9.4	10.3	11.5	12.4	12.7	13.3	13.0	12.2	11.3	10.2	10.2	10.1	10.0	11.2	12.4	14.4	14.4	13.9	13.4	12.1	11.1	10.0
TCPL32	16.5	15.4	13.5	8.5	6.4	5.2	4.3	6.0	7.5	9.4	12.4	14.8	15.5	16.7	15.1	12.8	10.5	8.2	8.1	8.2	8.5	10.8	13.7	17.6	18.4	16.9	14.7	11.8	9.7	7.5
Total Average Gnd Temp	15.2	14.4	12.8	8.7	7.5	6.8	6.2	8.3	9.4	11.1	13.1	14.4	14.8	15.3	14.0	12.3	10.7	9.0	9.5	9.5	9.7	11.3	14.1	16.9	16.7	15.3	13.9	11.6	10.2	8.6
Mean Fluid Temp	16.4	14.3	12.7	11.7	9.6	9.3	9.3	10.4	11.5	12.8	16.3	16.8	16.4	14.3	12.7	11.6	9.6	9.3	9.3	10.4	11.5	12.8	16.3	16.8	16.4	14.3	12.6	11.6	9.6	9.3
Mean Monthly Outside Temp	16.0	12.6	7.7	2.1	6.2	8.2	8.5	14.5	14.8	16.4	17.2	17.7	17.0	14.5	11.4	7.9	7.6	5.9	10.3	9.4	14.2	15.6	17.5	19.1	15.6	11.7	8.8	7.0	5.5	4.6